VYSOKÉ UČENÍ TECHNICKÉ V BRNĚ
BRNO UNIVERSITY OF TECHNOLOGY

FAKULTA STROJNÍHO INŽENÝRSTVÍ
ÚSTAV STROJÍRENSKÉ TECHNOLOGIE

FACULTY OF MECHANICAL ENGINEERING
INSTITUTE OF MANUFACTURING TECHNOLOGY

MINIMUM QUANTITY LUBRICATION IN REAMING
MAZÁNÍ MALÝM MNOŽSTVÍM MAZIV PRO VYSTRUŽOVÁNÍ

DIPLOMOVÁ PRÁCE
DIPLOMA THESIS

AUTOR PRÁCE   **PAVEL MÜLLER**
AUTHOR

VEDOUCÍ PRÁCE   **doc. Ing. MIROSLAV PÍŠKA, CSc.**
SUPERVISORS   **Prof. LEONARDO DE CHIFFRE**

BRNO 2008

Vložit zadání v elektronické formě 1 strana (scan)

Vložit zadání v elektronické formě 2 strana (scan)

ABSTRACT

This master thesis deals with the development of a test procedure for cutting fluid performance in reaming and the application in testing MQL (minimum quantity lubrication). In this project the performance of insoluble oil has been investigated by varying cutting conditions and experimental setup. The tests were carried out on austenitic stainless steels using HSS reamers. Individual reaming operations were compared with respect to a number of evaluating parameters such as hole diameter, roundness, cylindricity, surface roughness, reaming thrust and reaming torque. For all mentioned measurands a detailed uncertainty budget was created. Furthermore, a new unconventional method of MQL delivery was proposed and realized.

Results show that reaming operations with cutting conditions $v_c=5$ $m·min^{-1}$, $f=0.21$ mm and $a_p=0.1$ mm performed the lowest scatter and uncertainty of the measurement and the process. For those reaming operations where the only change was in nozzle positioning setup, equivalent uncertainties for all measurands were observed. It was also investigated that using a reamer with smaller diameter resulted in poor surface finish with big scatter and uncertainty of the hole diameter. Reaming operation with increased cutting speed had a big impact on surface roughness and reaming torque uncertainties.

Test uncertainties were compared to those obtained in previous projects performed at DTU. It was found that no significant difference between uncertainties could be observed. However, care must be taken when evaluating the uncertainty since it contains both uncertainty of the measurement and uncertainty of the process itself. Moreover, it is associated with a loss of information regarding uncertainty contributors.

Key words
Reaming, lubrication, surface quality, measuring uncertainty.

ABSTRAKT

1.   Úvod

Již od počátku 20. století, kdy F. W. Taylor poprvé použil vodu ke chlazení obráběcího procesu a přišel k závěru zvýšení životnosti nástroje, byla k tomuto účelu použita velká variabilita řezných kapalin [1]. Obecnou specifickou funkcí řezné kapaliny je poskytnout mazání a chlazení k minimalizaci teploty, která vzniká mezi nástrojem a obrobkem, případně mezi třískou a nástrojem [1]. Za poslední desetiletí byl uskutečněn výzkum zaměřený na omezení spotřeby řezných kapalin ve výrobě. Je to z toho důvodu, že řezné kapaliny s sebou přináší i řadu nevýhod. Řezné kapaliny jsou ve většině případech náročné a drahé pro recyklaci, operátorovi stroje mohou způsobovat kožní a plicní problémy a znečišťují také životní prostředí. Dalším důvodem ke snížení množství řezných kapalin jsou vyšší náklady související s použitím těchto kapalin. Tyto náklady odpovídají zhruba 7-17% veškerých výrobních nákladů, ekologických problémů a dopadu na lidské zdraví [2].

Eliminací těchto kapalin dochází ke ztrátě jejich pozitivního účinku na obrábění, neboť řezná kapalina patří mezi důležité komponenty při obrábění. Jejich redukce či úplná eliminace by vedla ke zvýšení provozních teplot u těchto procesů, poklesu výkonu řezného nástroje, ztrátě rozměrové přesnosti a geometrie a kolísání tepelného chování stroje.

K tomu, aby došlo k minimalizaci použití řezných kapalin a byly splněny požadavky týkající se zdravého pracovního prostředí, slouží nová technologie tzv. mazání malým množstvím maziv (MQL). Opuštěním konvenčního chlazení a při použití nové technologie MQL se celkové náklady mouhou výrazně snížit [4].

Nicméně bylo dokázáno, že MQL patří v dnešním výrobním světě mezi důležité technologie, které jsou využívány v mnoha výrobních procesech. Kromě zlepšení efektivity výrobního procesu, přispívá tato technologie k ochraně dělníkova zdraví a životního prostředí [4]. Použitím MQL je možné dosáhnout efektivního mazání řezného procesu s použitím velmi malých částic maziva ve formě aerosolu. Výsledkem není pouze zvýšená produktivita v důsledku vyšších řezných rychlostí, ale také vyšší životnost nástroje a úspora nákladů na řezné kapaliny.

2.   MQL

MQL je nová technologie přívodu řezné kapaliny, při níž je přivedeno přesné množství maziva do místa řezu. Řezná kapalina je smíchána se stlačeným vzduchem a spolu tvoří směs, která se nazývá aerosol. MQL je charakterizována množstvím maziva menším než 80 ml/hodinu.

MQL rozlišuje dva způsoby přívodu aerosolu do pracovního místa a to: vnitřní přívod, kdy je vedení zabudované ve stroji (zařízení), a vnější přívod, kdy jsou trysky uchyceny na vnější straně stroje. Největší rozdíl mezi dvěma zmíněnými způsoby spočívá ve způsobu aplikace.

Vnitřní přívod aerosolu se prostřednictvím vřetene a nástroje v největší míře uplatňuje při vrtání, vystružování a řezání závitů s velkými l/d poměry. Tento způsob zajistí, že aerosol je nepřetržitě přítomen v blízkosti břitu nástroje. Zvláště vhodná je tato metoda při vrtání hlubokých děr s velkým l/d poměrem. Velikost částic je v rozmezí 0,5-5,0 μm.

Vnější přívod aerosolu je docílen pomocí trysek, které rozprašují aerosol na břit řezného nástroje z vnější strany. Uspořádání a pozice trysek mají velký vliv na drsnost povrchu. Tato metoda může být použita při obráběcích operacích jako jsou řezání pilou, frézování či soustružení. Při vrtání, vystružování a řezání závitů může být tato metoda použita při poměru l/d<3. Velikost částic je v rozmezí 15-40 μm.

Obě zmíněné metody se mohou dále dělit na *one channel supply*, kdy aerosol je tvořen před vřetenem a samostatné vedení slouží jako cesta pro tuto směs a *two channel supply*, kdy jsou mazivo a vzduch dodávány samostatně prostřednictvím vřetene. Směs maziva a vzduchu je pak přímo vytvořena před tím, než aerosol přichází do nástroje.

3.   Identifikace účinnostních veličin při vystružování

K vyhodnocení vlivu řezné kapaliny na řezné síly a kvalitu obrobeného povrchu bylo provedeno vyhodnocení účinnostních veličin při vystružování austenitické nerez oceli s využitím maziva. Byly použity dva výstružníky lišící se průměrem, při změněných řezných podmínkách při obrábění a změně nastavení trysek. Změna řezných podmínek se týkala změny řezné rychlosti, posuvu na otáčku, hloubky řezu a zpětné rychlosti vřeteníku z místa řezu. Pro kritérium jakosti byly použity následující parametry: přítlačná síla a kroutící moment při vystružování, průměr, kruhovitost a válcovitost vystružené díry, drsnost povrchu Ra. Byly vypočítány jak absolutní hodnoty, tak i experimentální směrodatné odchylky pro výše zmíněné vyhodnocující parametry. Byl vyhodnocen komplexní *uncertainty budget* pro všechny měřené veličiny. Je nutné věnovat velkou pozornost při vyhodnocování konvenčního parametru Ra, protože tento parametr zcela ztrácí informaci o daném profilu drsnosti povrchu.

4.   Experimentální aparatura

Testované obrobky byly z austenitické nerez oceli typu AISI 316L s již předhotovenou dírou o průměru 9,9 mm a dané geometrické přesnosti. Veškeré

experimenty byly provedeny na obráběcím centru CNC - konkrétně se jednalo o vertikální frézku Cincinnati Sabre 750. Výstružníky o průměrech 10,0 mm a 10,1 mm, které byly použity při obrábění, jsou z rychlořezné oceli s 5% obsahem ko-baltu. Výstružníky jsou opatřeny 6 drážkami uspořádanými do šroubovice. To-lerance výstružníku je ±0,003 mm. Nástrojový držák je pohyblivý. Experi-mentální aparatura se skládá z jednotky MQL pro vnější přívod aerosolu a je opatřena dvěma tryskami. Jedna z trysek je nasměrována shora pod úhlem 45° ve vzdálenosti 40 mm od osy obrobku, druhá tryska vede napříč dynamometrem, který je přímo spojen s přípravkem pro upnutí obrobku a je ve vzdálenosti 55 mm od spodní části obrobku. Jak již bylo zmíněno, daný dynamometr KISTLER typ 9271A slouží pro měření kroutícího momentu a přítlačné síly při vystružování. Signály jdoucí z dynamometru jsou konvertovány prostřednictvím dvou nábojových zesilovačů KIAG SWISS typ 5015 do napětí. Výstupní napětí těchto zesilovačů je digitalizováno s využitím PC s programem Labview 8.0. Pro měření průměru vystružené díry, kruhovitosti a válcovitosti bylo použito stroje CMM OMC 850 ZEISS. Průměr měřící sondy je 3 mm. Upínací přípravek pro uchycení obrobků se skládá ze tří hliníkových desek, mezi které jsou vloženy gumové kroužky. Po upnutí obrobků a sešroubování desek dochází k expanzi průměru kroužků a tudíž k pevnému sevření obrobků v upínacím přípravku. Upínací přípravek umožňuje uchycení až 40 obrobků najednou. Pro účel této dip-lomové práce bylo využito 15 libovolných úchytů. Drsnost obrobené plochy byla měřena pomocí dotykového přístroje TAYLOR HOBSON SUBTRONIC 3+, který je vybaven kluzným snímačem s poloměrem špičky 2 μm.

5.   Pracovní postup

Bylo vystruženo celkem šest sérií po 15 obrobcích a provedeno následné měření kvality obrobených ploch. Pro každou sérii bylo ze skupiny stejných obrobků náhodně odebráno 15 obrobků. Obrobek o rozměrech Ø29 mm x 15 mm měl již předhotovenou díru o průměru 9,9 mm. Jednotlivé vystružovací operace se lišily různými řeznými podmínkami při obrábění a aplikací dodávání maziva do místa řezu. Při jednotlivých obráběcích procesech došlo vždy pouze ke změně jednoho parametru. Průtok, tedy dodání aerosolu ve formě mlhy, byl u všech obráběcích operací konstantní, lišící se minimálně, a to jen v důsledku kolísání teploty v dílně. Geometrická přesnost vystružených děr (průměr, kruhovitost a válcovi-tost) byla měřena pomocí CMM. Průměr a kruhovitost byly měřeny ve čtyřech úrovních, ve vzdálenosti 3, 6, 9 a 12 mm od spodní plochy obrobku a v osmi místech kolem vnitřního obvodu obrobku na každé měřené úrovni. Tímto bylo docíleno vyhodnocení válcovitosti díry. Výše popsané měření bylo provedeno celkem pětkrát. Drsnost obrobené plochy byla měřena pomocí dotykového přístroje. Celkem bylo zaznamenáno 24 profilů pro každý obrobek, který byl měřen ve čtyřech bodech rozmístěných pod shodnými úhly (90°) kolem vnitřního

obvodu díry. Každé měření bylo třikrát opakováno. Dle naměřených hodnot byla posléze spočítána průměrná hodnota. Měření bylo provedeno ve dvou místech obrobku a sice: 2 mm od horní a 2 mm od spodní plochy obrobku po délce 4 mm a s použitím ISO filtrování 0,8 mm. Pro každý obrobek byla vypočítána průměrná hodnota kroutícího momentu a přítlačné síly při vystružování. Tyto průměrné hodnoty jsou odvozené ze záznamu, který je označen jako „rozpětí okna". Toto rozpětí okna je definováno jako vzdálenost mezi dvěma body, které jsou umístěny na stabilní části křivky při zohlednění poloviny času, který je potřebný pro vystružení dané díry. Proto se velikost rozpětí okna může lišit v závislosti na změně posuvové rychlosti.

6.   Diskuze

6.1   Jakost výrobku

Pojmem „jakost výrobku" se považuje jak geometrická přesnost, tak i povrchová topografie díry. K tomu, aby bylo docíleno spolehlivých výsledků, je vytvořen komplexní *uncertainty budget*. Při provádění experimentálních šetření je často zjištěno, že experimentální rozptyly výsledků mohou být veliké, jestliže tyto porovnáme s průměrnými hodnotami výsledků dílčích měření v návaznosti na změněných experimentálních podmínkách. Další chyby mohou nastat při vyhodnocování výsledků. Kvalita obrobené díry závisí do určité míry na podmínkách obrábění, jako jsou: řezná rychlost, posuv na otáčku a hloubka záběru ostří. Podmínky obrábění vykazují také odchylku od naprogramovaných hodnot, které nejsou konstatní během celého obráběcího procesu a mají proto vliv na nejistotu měření. Dalšími zdroji chyb jsou také teplota v dílně, teplota v laboratoři, druh obráběného materiálu, geometrie nástroje a obrobku, stroj atd.

6.2   Porovnání dosažených výsledků s výsledky dalších experimentálních testů provedených na DTU

Pro klasifikaci řezné kapaliny bylo provedeno porovnání dosažených výsledků a výsledků získaných v průběhu minulých let na Technické Univerzitě v Dánsku (DTU).

Pro vyhodnocení vlivu řezné kapaliny na řezné síly a kvalitu obrobeného povrchu dle [11] bylo při vystružování austenitické nerez oceli s využitím řezné kapaliny na bázi vody provedeno vyhodnocení účinnostních veličin a dosaženo následujících výsledků: hlavní rozdíl spočíval ve způsobu chlazení, kdy obrobky byly zcela ponořeny do nádoby s řeznou kapalinou. Tímto bylo docíleno vyšších hodnot přítlačné síly a kroutícího momentu, příliš velkého průměru díry a zhoršené drsnosti povrchu. Podmínky pro obrábění byly v_c=6 m·min^{-1}, f=0,4 mm a a_p=0,2 mm. Bylo také zjištěno, že vyšší hodnoty a_p zvyšují senzitivitu vůči řezné

kapalině. Další rozdíl může být spojen s různým postupem při měření daných veličin a strategie výpočtu nejistoty měření.

Byla provedena analýza opakovatelnosti a rozlišení dle [19] a [58]. Tyto dva parametry jsou vypočítány jak pro řezné síly, tak i pro vyhodnocení kvality obrobených ploch. Byl zaveden nový parametr relativního rozlišení σ/ρ, kde σ je směrodatná odchylka a ρ je variační rozpětí výsledků experimentu vyjádřeno v procentech průměrné hodnoty měřené veličiny. Kroutící moment je při vystružování dle [19] spojen s dobrou opakovatelností, relativním rozlišením, krátkým výrobním časem a z toho plynoucích nízkých nákladů na tento test. Toto je i případ tohoto projektu, který se vyznačuje výbornou opakovatelností naměřených hodnot a nízkým relativním rozlišením.

Při vystružování austenitické nerez oceli s využitím řezné kapaliny na bázi vody bylo při vyhodnocení vlivu řezné kapaliny na měřené veličiny dle [9] dosaženo velkého rozptylu hodnot výsledků. Při úběru materiálu (a_p=0,2 mm) měla řezná kapalina velký vliv na geometrickou přesnost a drsnost obrobené díry. Uvedené vlivy byly však sníženy při použití výstružníku s menším průměrem (a_p=0,05 mm). Tento projekt však potvrdil, že malý úběr materiálu vede ke zhoršení kvality díry. Aplikace řezné kapaliny je stejná jako v [11]. Nejistota měření (v tomto případě směrodatná odchylka) pro kroutící moment byla na základě šesti opakových měření v rozmezí 5-30%. Variační rozpětí výsledků testu bylo 40%. Výsledky byly více či méně totožné s výsledky dosažených v tomto projektu.

Při vystružování austenitické nerez oceli s využitím řezné kapaliny na bázi vody bylo v [8] pro vyhodnocení vlivu řezné kapaliny zjištěno, že volba řezné kapaliny má velký vliv na výslednou drsnost obrobené plochy. Bylo dosaženo opakovatelnosti 5-60% a relativní rozlišení 0,3-0,4. Nejistota měření u tohoto projektu se vykytuje v rozmezí 20-45% a relativní rozlišení testu je tak velké, že drsnost obrobené plochy je parametrem, který nemůže být použit pro posouzení dosažených výsledků.

7.   Výsledky a diskuze

7.1   Geometrická specifikace vystružené díry

K tomu, aby byla zajištěna shodnost všech obrobků s ohledem na geometrickou přesnost díry, byly obrobky změřeny pomocí CMM a byl proveden následný výpočet nejistoty měření. Pro kalkulaci nejistoty měření je postupováno podle ISO 15530-3 [55]. Toto zahrnuje nejistotu měření při kalibraci CMM, nejistotu měření při postupu práce, nejistotu měření ovlivněnou změnou teploty v laboratoři a systematickou chybou. Je předpokládáno normální rozdělení s pravděpodobností 95% (k=2) výskytu výsledku kolem jeho průměrné hodnoty. Výsledky pro geometrickou přesnost již předhotovených děr ukazují dobrou re-

produkovatelnost měření z pohledu vypočtených průměrných hodnot, získaných dle pracovního postupu. Při zohlednění nejistoty měření tyto výsledky prokazují velmi souhlasný průběh a dobrou opakovatelnost CMM. Kruhovitost a válcovitost děr společně s naměřenou nejistotou měření je menší než 5 μm, respektive menší než 10 μm. Pro výpočet nejistoty měření při vystružování musí být zohledněn fakt, že nejistota měření zahrnuje kromě nejistoty kalibrace, pracovního postupu a změny teploty, taktéž nejistotu rozptylu naměřených hodnot při vystružování celé série obrobků. Jak již bylo zmíněno, byl proveden celkový počet šesti vystružovacích operací. Výsledky jednotlivých operací jsou vůči sobě pochopitelně rozdílné z důvodu použití různých podmínek při obrábění či změněné aplikace maziva, avšak z pohledu vypočtených nejistot měření sobě odpovídají a všechny jsou v toleranci díry. Jedinou operací, která vykázala odlišný průběh je ta, při níž byl použit výstružník s menším průměrem, tedy menším úběrem materiálu.

7.2   Drsnost vystružené plochy

Stejně jako pro geometrickou přesnost díry, tak i pro drsnost vystružené díry, je nejdříve vypočítána nejistota měření pro již předhotovené díry. Je postupováno dle ISO 5436-2:2001 [56]. Toto zahrnuje nejistotu měření při kalibraci měřícího přístroje a nejistotu měření pracovního postupu. Je předpokládáno normální rozdělení s pravděpodobností 95% (k=2). Výsledky měření těchto děr společně s vypočítanými nejistotami vykazují drsnost povrchu pro všech 15 obrobků menší než 0,9 μm, což zaručuje velmi kvalitní opracování obrobků a kompatibilitu výsledků vůči sobě. Kalkulace těchto nejistot je provedena dle pracovního postupu. Pro jednotlivé výstružovací operace je při výpočtu nejistoty opět zohledněn rozptyl celé série obrobků, který je v tomto případě největším ukazatelem nejistoty. Výsledky jednotlivých operací se liší, ale jsou při zvažování vypočtených nejistot měření vůči sobě opět ve vzájemné kompatibilitě. Operace, kdy změnou byl zpětný posuv vřetene z místa řezu, vykazují stejně kvalitní obrobené plochy. Avšak při rychlém zpětném chodu vřetene zůstaly na obrobku viditelné stopy po výstružníku. Při malém úběru materiálu a při zvýšené řezné rychlosti došlo ke zhoršení povrchu obrobené plochy a také k nárůstu nejistoty měření pro obě tyto operace. Jako nejoptimálnější operace jsou považovány operace s menším posuvem na otáčku a menší řeznou rychlostí, které vykazují malou nejistotu měření. Obě tyto operace také dokazují, že nezáleží na způsobu aplikace aerosolu a to, když jsou obě trysky nasměrovány shora pod stejným úhlem a ve stejné vzdálenosti od osy obrobku nebo jedna z trysek je shora a druhá vede přes dynamometr a upínací přípravek.

7.3   Řezné síly při vystružování

Obecně se při výpočtu nejistoty měření u řezných sil počítá pouze s rozptylem naměřených hodnot. To ale není dostačující. Je proto zapotřebí počítat také s dalšími vlivy chyb. Nejistota měření pro přítlačnou sílu a moment při vystružování je kalkulována dle metody GUM [57]. Toho je docíleno první derivací výrazů vystihujících výpočet těchto řezných sil a násobením jejich vlastní nejistotou. Je předpokládáno opět normální rozdělení s pravděpodobností 95% (k=2). Kromě derivace všech členů vyskytujících se v daných výrazech je uvažováno a počítáno také s nejistotami způsobenými definicí rozpětí okna, teplotou, která přímo ovlivňuje průtok aerosolu a měřícím přístrojem pro detekci daných veličin. Kromě toho je počítáno také s rozptylem naměřených hodnot. Porovnáním operací, kdy změnou byl zpětný posuv vřetene z místa řezu, byla zjištěna dobrá reprodukovatelnost výsledků. Obě operace však vykazují příliš vysoké naměřené hodnoty obou veličin společně s vysokými nejistotami měření v porovnání s dalšími operacemi. Je také dokázáno, že použitím výstružníku s menším průměrem, došlo k výraznému poklesu řezných sil. To má ale za následek zvýšené hodnoty rozptylu naměřených hodnot. To je zejména způsobeno tím, že příliš malý úběr materiálu je citlivý na signál, který řezné síly vykazují při obrábění. Za optimální operaci je považována operace s menším posuvem na otáčku a menší řeznou rychlostí vykazující také malou nejistotu měření. Tato operace je charakterizována nastavením obou trysek shora, což zajišťuje snadnou manipulaci a aplikaci.

8.   Závěr

8.1   Shrnutí

Při vyhodnocování nejistoty měření je nutné dát pozor a vzít vždy v úvahu kromě rozptylu naměřených hodnot také veškeré možné zdroje chyb, které ovnivňují daný proces. Pro některé veličiny, jako jsou kroutící moment při vystružování a drsnost obrobené plochy, má rozptyl dat velký význam. Parametry, které mohou být použity pro klasifikaci řezné kapaliny při vystružování, jsou přítlačná síla a kroutící moment. Výsledky dokázaly, že dosažené výsledky řezných sil jsou spolehlivé a zaručující konzistentní charakterizaci mazacího účinku řezných kapalin. Měřením geometrie a drsnosti obrobených děr bylo dosaženo výsledků, které mohou být použity ve spojení s kontrolou kvality. Drsnost Ra obrobených ploch se pohybovala v rozmezí 0,70-0,85 μm, válcovitost pak v rozmezí 0,006-0,009 mm. Bylo zjištěno, že operace, při nichž bylo použito menšího úběru materiálu a vyšší řezné rychlosti, mají větší vliv na nejistotu měření pro měření drsnosti obrobené plochy a kroutícího momentu při vystružování. Porovnáním dvou operací, kdy došlo ke změně nastavení trysek

pro mazání, se dospělo k závěru, že aplikace nastavení trysek nemá vliv na kvalitu obrobené díry.

8.2 Doporučení pro praxi

Pro aplikaci tohoto testu existuje mnoho dalších variant. Jelikož je dle literatury pro vystružování nejvhodnější použít vnitřního přívodu maziva do místa řezu, je očekáváno také zlepšení kvality obrobené plochy a snížení rozptylu hodnot výsledků. K tomu, aby bylo tohle proveditelné, je ale nezbytné mít pro tuto aplikaci k dispozici CNC zařízení vybavené tímto systémem a speciálně vyrobené výstružníky. Další alternativou, jak zdokonalit tento proces, je použít výstružníků z cermetů, které mají vyšší tvrdost a tepelnou stálost a tudíž je možné použít vyšší řeznou rychlost a posuv na otáčku. Pro porovnání výsledků by bylo také vhodné změnit způsob chlazení a použít konvenčního chlazení a nebo vystružit díry bez chlazení, tj. za sucha.

Klíčová slova
Vystružování, mazání, kvalita plochy, nejistota měření.

REFERENCE

MÜLLER, Pavel. *Minimum Quantity Lubrication in Reaming: Diplomová práce.* Brno: Vysoké učení technické v Brně, Fakulta strojního inženýrství, 2008. 180 s., 4 přílohy. Vedoucí práce doc. Ing. Miroslav Píška, CSc. a Prof. Leonardo de Chiffre.

Statement

I declare that the present diploma thesis with its name Minimum Quantity Lubrication in Reaming was carried out only by me with the help of literature and sources stated in the reference list which is a part of this diploma thesis.

7.10.2008   ………………………………….

                                                PAVEL MÜLLER

Acknowledgement

LIST OF CONTENT

CHAPTER 1 - INTRODUCTION

1.1 Background of the project and state of art

Since the beginning of the 20th century, when F.W. Taylor used water for the first time to cool the machining process and concluded it in increased tool life, a large variety of cutting fluids has been used with this and other purposes. Generally, the specific function of cutting fluid in the machining process is to provide lubrication and cooling to minimize the heat produced between the surface of the workpiece and the tool and the contact area between the tool and the chip [1]. However, in the last decade a significant research has been made aiming of restricting the use of cutting fluids in the production. This is because cutting fluids bring several drawbacks. Cutting fluids most of the times are difficult and expensive to recycle, can cause skin and lung diseases to the machine operator and air pollution. Other reasons for decreasing the quantity of cutting fluids are the costs related to the fluids, which can be evaluated to be in range of 7 – 17% in the overall manufacturing costs, ecological issues and impact on human health [2] (see Fig. 1.1).

COST OF COOLANT MANAGEMENT

Tool cost
2~4%

Coolant
cost
7~17%

3~5 times higher cost,
compared with the
tool cost.
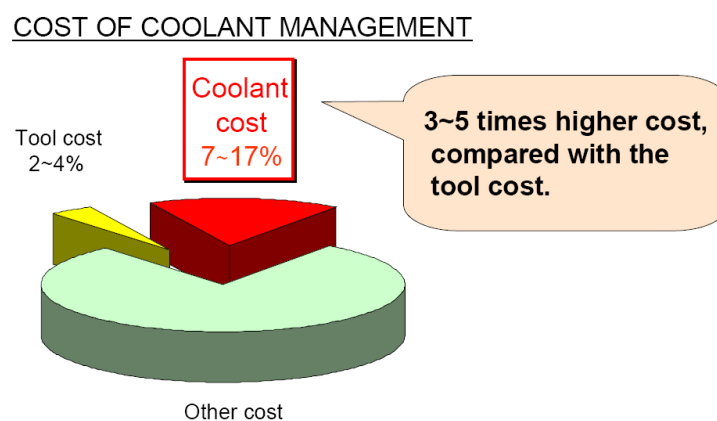
Other cost

Fig. 1.1 - Coolant percentage vs. other costs [3]

However, eliminating these fluids, their positive influence on machining is also lost, since cutting fluid is an important technological parameter in machining. Their reduction or even complete elimination could lead to increased temperatures in these processes, decline in cutting tool performance, loss of dimensional accuracy and geometry of the parts, and variation on the machine's thermal behavior [1].

In order to minimize the use of cutting fluids and to fulfill all the demands concerning health work environment, a new technology called minimum quantity lubrication

(MQL) is proposed. By abandoning conventional cooling lubricants and taking into account only the use of this new technology, costs can be reduced significantly [4].

It was however proved that MQL plays a paramount role in today's manufacturing world. This technology can be used in many manufacturing processes. Besides an improvement in the efficiency of the production process, such a technology change makes a contribution to the protection of labor and the environment [4]. By using MQL it is possible to achieve effective lubrication of the cutting process with extremely small quantities of oil in the form of aerosol. The result is not only higher productivity due to faster cutting speeds but also longer tool life and cost savings on cooling lubricants (see Fig. 1.2).
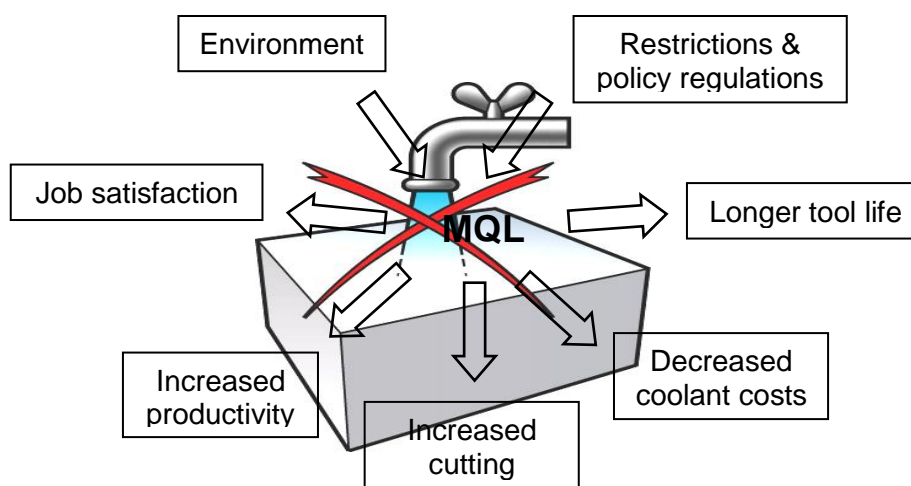
Fig. 1.2 - Benefits of MQL [5]

Machine tool makers and customers are calling for optimized MQL systems in terms of their response characteristics and metering accuracy. The implementation of these requirements permit shorter machining times, faster tool changes and less start-up related time and expenses. It was proved that when the new MQL systems are installed and optimized, these goals can be achieved [4]. Fig. 1.3 represents the costs per part vs. cutting speed in order to optimize and reach the best efficiency and productivity range.
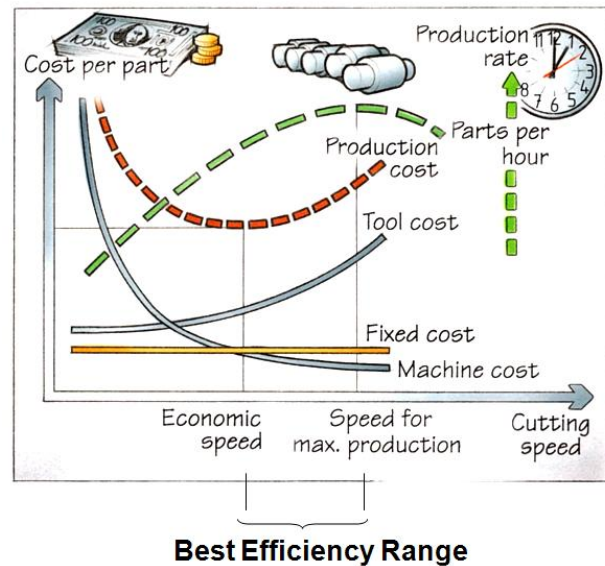
Fig. 1.3 - Productivity - cutting data and costs [6]

All of the components in the MQL systems must be very carefully coordinated in order to achieve the desired outcome, which should be optimal, both technologically and economically. Among such MQL system components belong tools, machine tool, different setting, fluids and equipment [4] (see Fig. 1.4).
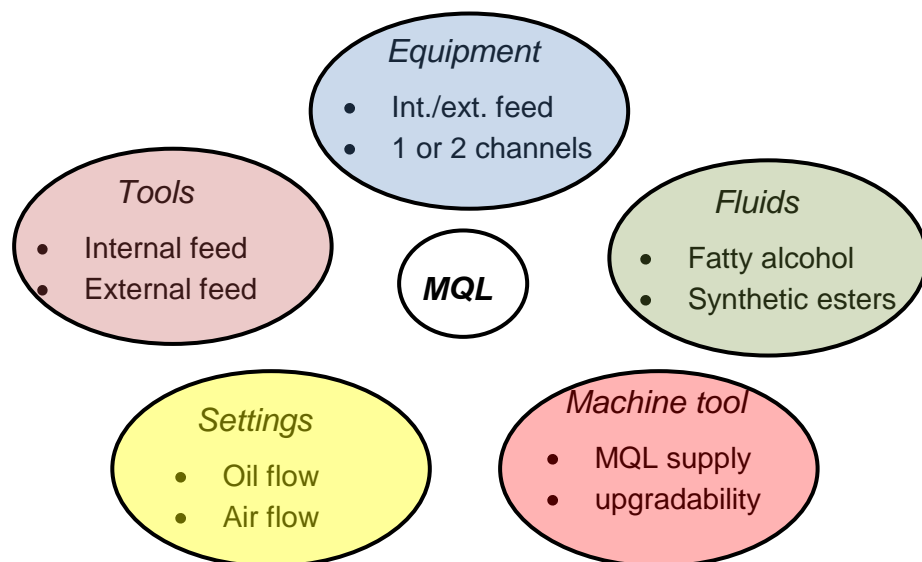
Fig. 1.4 – MQL components [4]

Minimum quantity lubrication for the purpose of this master thesis is used in connection with cutting fluid performance tests. Cutting fluid performance tests serve for

classification of cutting fluids with respect to different cutting processes. The different performance criteria can be tool life, product quality, cutting torque, chip evacuation, cutting power. The cutting fluid performance in terms of product quality and cutting torque and cutting thrust in reaming on austenitic stainless steel is considered in this work.

There have been a lot of tests developed at IPL (Department of Manufacturing Engineering and Management) at DTU (Technical University of Denmark) concerning material machinability, machine tool accuracy, cutting fluid efficiency and cutting fluid performance. Research projects on cutting fluid performance tests have been reported in [7][8][9][10][11][12][13][14][15][16][17][18][19][20][21][22].

An experimental investigation analyzing cutting fluid performance using MQL in reaming is considered for the purpose of this master thesis since it enables an evaluation and classification of the cutting fluids from many evaluation criteria point of view such as surface topography, hole dimensions, for error, cutting forces. It also offers the possibility of re-using the specimens for other reaming tests since the hole diameter can be still enlarged with bigger reamer diameter [10].

1.2   Organization of the work

This report includes 10 chapters starting with general introduction about the project (Chapter 1) and about cutting fluids and their impact to the environment, their functions, types, applications and lastly the application of using MQL (Chapter 2). All influence parameters on reaming process and criteria for cutting fluid performance are stated as well.

Furthermore this thesis informs about reaming as one of many cutting operations, its general specifications and its use for cutting fluid performance tests (Chapter 3).

A description of present cutting fluid performance test is stated (Chapter 4).

A development of a setup for MQL application with detailed description of all equipments is presented (Chapter 5), a development of a test procedure is created (Chapter 6).

Measurements of pilot holes (Chapter 7) and reamed holes (Chapter 8) are performed calculating the uncertainty budget for product hole quality assurance and reaming thrust and reaming torque.

Discussion concerning cutting fluid performance tests at DTU and consequent comparison with the results obtained in this thesis is held (Chapter 9).

Several conclusions and suggestions for further development are drawn at the end (Chapter 10).

CHAPTER 2 - CUTTING FLUIDS

2.1   Cutting fluid functions

Cutting fluids are also called coolants and lubricants. The term coolant was coined by researchers soon after F. W. Taylor reported that tool life could be improved by applying water. The term lubricant originated with the introduction of oils [23].

Fluids in machining processes play paramount role. They are mainly used for process optimization and can be commonly seen during material removal processes.

It has to be taken into account that different machining processes need to select and to use only cutting fluid suitable for a particular machining application. These criteria include surface finish, power consumption, tool life and tolerances. Cutting fluids need to be also non-corrosive to the equipment and to the workpiece being machined. The selection of the cutting fluid can be also influenced by other factors like fluid characteristics, workpiece material and machining operation.

The characteristic function of cutting fluids in the machining processes is to provide lubrication and cooling to minimize the heat produced in the cutting zone. The efficiency of the cutting fluid depends on its penetrating function into the chip-tool interface and creating a thin layer. Otherwise, loss of dimensional accuracy, geometry of the parts and roughness can result. The heat has its direct influence on tool life. When applying higher cutting speeds and feed in order to achieve higher material removal rates, cutting fluid has its irreplaceable function in carrying away the heat and thus increases tool life. The lubrication film with desired layer thickness is applied between the tool and the workpiece material in order to reduce friction between the tool and the chip and between the tool and the workpiece. With decreasing friction, power consumption of the machine also decreases. So when applying lubricants into the cutting processes one can expect decrease in friction and wear and thus increase of tool life and improved surface finish. Surface finish is therefore influenced by formation of the build-up edge (BUE) on the cutting tool and on workpiece itself. Another important characteristic of the cutting fluid is to transport chips and swarfs by flushing them away from the cutting area. This ability of the cutting fluid depends on its viscosity and its volume flow, the machining application and chip type formation.

A comparison can be made by comparing different machining processes with respect to their requirement for cooling and lubrication effect (see Fig 2.1).

	1	Grinding
	2	Sawing
	3	Turning
	4	Planning and shaping
	5	Milling
	6	Drilling
	7	Reaming
	8	High speed machining
Enhanced requirements for lubricating effect	9	Machining with profile tools
	10	Boring
	11	Deep hole drilling
	12	Thread cutting
	13	External threading
	14	Tapping
	15	External Broaching
	16	Inner Broaching

Enhanced requirements for cooling effect
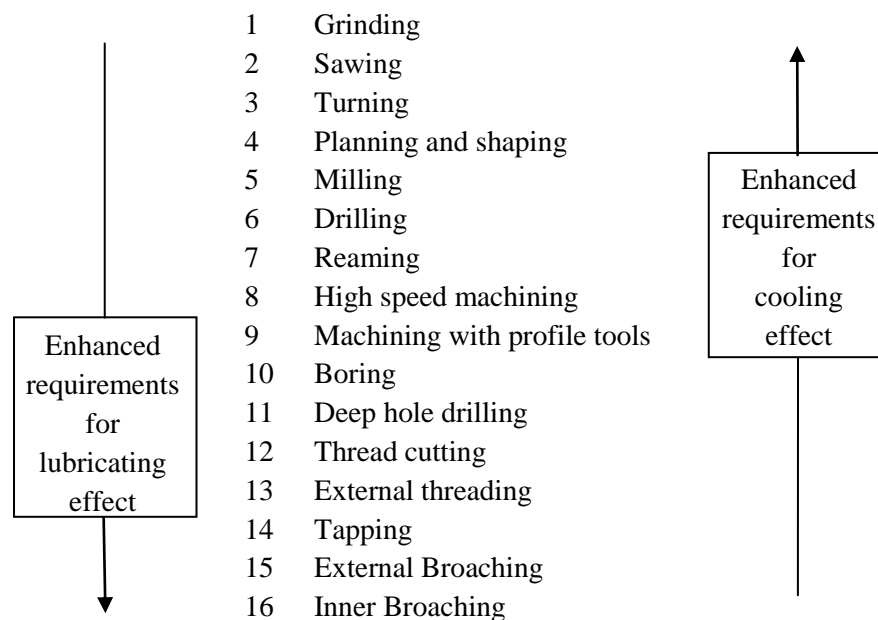
Fig. 2.1 – Cooling and lubrication requirements with respect to machining method [24]

2.2   Cutting fluid types

When selecting oil as a lubricant, the importance of its viscosity-temperature-pressure characteristics should be recognized. Low viscosity can have a significant insulting effect on friction and wear. Different functions of cutting fluids, whether primarily a lubricant or a coolant, must also be taken into account. Water-base cutting fluids are very effective coolants, but as lubricants are not as effective as oils [23].

Cutting fluids classification:

a) Straight oils (Insoluble oils = Neat oils)

These oils contain no water and are comprised of neat oil. Insoluble oils are used as lubricants. They are connected with low speed, low clearance operations requiring high quality surface finishes. They prevent the material from rusting; provide the longest tool life for a number of applications. Additives such as sulfur, chlorine or phosphorus improve the oil's wettability, which is the ability of the oil to coat the cutting tool, workpiece and metal fines. They also guard against microscopic welding. Disadvantages of straight oils include poor heat dissipating properties and creating of a mist and smoke [25].

b) Soluble oils (Water-soluble oils)

These emulsions and water-soluble oils are designed to cool and lubricate. These fluids prevent welding of the cutting tool and the workpiece surface, reduce abrasive wear of the tool at high temperatures, and prevent thermal distor-

tion caused by residual heat. They do not match the lubricity offered by straight oils. The presence of water makes soluble oils more susceptible to rust control problems. They also do create mist. [25].

c) Synthetic cutting fluids

Synthetic cutting fluids do not contain petroleum or mineral oil; they consist of chemical lubricants and rust inhibitors dissolved in water. Also functioning as coolants and lubricants, synthetic cutting fluids eliminate smoking, reduce misting, provide detergent action, and reduce oxidation. Consequently, the simple synthetics offer rust protection and good heat removal, but usually have very low lubricating ability. Synthetic cutting fluids are stable, provide effective cooling capacity at high machining speeds and feed rates. [25].

d) Semi-Synthetic cutting fluids

This class of cutting fluids contains small amounts of oil (5% to 30% in the concentrate) and may be formulated with fatty acids, sulfur, chlorine, and phosphorous to provide lubrication for higher speed and feed operations to medium and heavy operations. The same extreme-pressure agents that are added to insoluble oils may also be added to water-soluble oils. The presence of water in the soluble fluids can cause machine tools and parts to corrode. Consequently, nitrites, amines, and certain oils may be added to inhibit corrosion. [25].

2.3 Cutting fluid application

Correct application of the cutting fluid at the tool/workpiece interface is fundamental for the effective use of the fluid. Moreover, the method of application affects not only lubrication and cooling but also the efficiency in removing swarf and chips from the cutting operation.

Types of cutting fluid application:

1. Standard cooling: this type of cooling does not need any adjustment of the cooling delivery system. This system consists of a reservoir for cutting fluid, pump and distribution pipeline. Amount of the cutting fluid delivered to the cutting edge depends on the type of the pump and the flow coming out from the outlet hole [26].
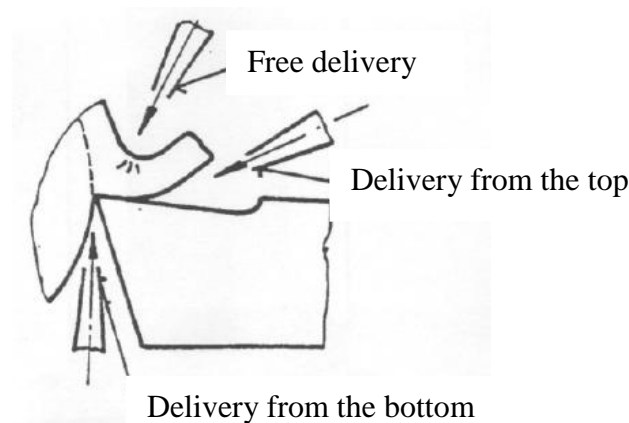
Fig. 2.2 – Standard cooling application [26]

2. <u>Pressurized</u>: during this type of cooling the cutting fluid is delivered to the cutting edge under a high pressure. The diameter of the outlet hole is of 0.3-1.0 mm and the pressure is of 0.3-3 MPa. The cutting fluid is delivered to the cutting edge from the bottom, directly to the cutting edge. This type of cooling is preferable where the created heat has unfavorable influence on tool life [26].

   Amount of the cutting fluid is in the range 0.5-2.0 l/min. One of disadvantages of this type of cooling is that the cutting fluid is spread out and forms mist [26].

3. <u>Flooding</u>: this type of cooling is a widely used method which promotes lubrication, cooling, chip removal and access to the cutting operation. The cutting fluid is applied via external nozzles situated near the cutting zone. Amount of cutting fluid applied varies from 1 to 2000 l/min depending on feed, speed and cutting tool material and geometry. There are special requirements on the pressure and amount of cutting fluid applied for different type of cutting operation [27].

4. <u>Misting</u>: this method is best suited to operations in which the cutting speed is high and the areas of cut are small. Mist application provides better tool life that dry cutting, provides enhanced cooling and lubrication during machining since there is a vaporization of the small oil particles. It also provides a means of applying fluids in otherwise inaccessible areas and provides better visibility of the cutting process. Heat removal is achieved in the way that expanding air contains cutting fluid droplets and therefore has higher ability to receive the heat. Care must be taken when misting cutting fluids to prevent excessive buildup in the air and tin the workplace [26][27].

5. <u>Inner cooling delivery</u>: this method enables enhanced cutting speeds for about 5-15%. During turning the cutting fluid delivery is performed via inserts. During drilling and hole making operations, this is achieved by delivering the cutting fluid

via ducts incorporated inside the machine tool, tool holder and tool directly to the cutting edge [26].

2.4 Minimum Quantity Lubrication (MQL)

2.4.1 MQL definition

Minimum Quantity Lubrication (MQL) is a machining method that delivers a precise amount of lubrication to the tool tip. The lubricant is mixed with compressed air and forms the desired air/oil aerosol mixture.

Definition by lubrication usage per hour:

Tab. 2.1 - Lubrication usage per hour [5]

0 ml/hour	Dry
< 80 ml/hour	Minimum Quantity Lubrication (MQL)
80 ml/hour → 2000 ml/hour	Minimum flow lubrication
> 2000 ml/hour	Flood lubrication

2.4.2 MQL principles

MQL technique is distinguished between internal supply of aerosol via ducts incorporated in the tool and external supply of aerosol via nozzles that are fitted on the machine from outside. The main difference between mentioned principles relies on the type of application.

Internal supply of aerosol via spindle and tool, see Fig. 2.3, is mostly applied in drilling, reaming and tapping operations with larger l/d ratios. This ensures that aerosol is constantly present very close to the cutting edge. Especially in deep-hole drilling with large l/d ratio this method is very useful. The droplet size range is 0.5 - 5µm [28].

External supply of aerosol is achieved via external nozzles; see Fig. 2.4, that spray aerosol on to the cutting edge from outside. The arrangement and positioning of the nozzles play a paramount role in surface quality. This method can be used in cutting operations like sawing, milling and turning. In machining operations such as drilling, reaming and tapping this method can be used in certain concern up to l/d ration < 3. The droplet size range is 15 - 40µm [28].
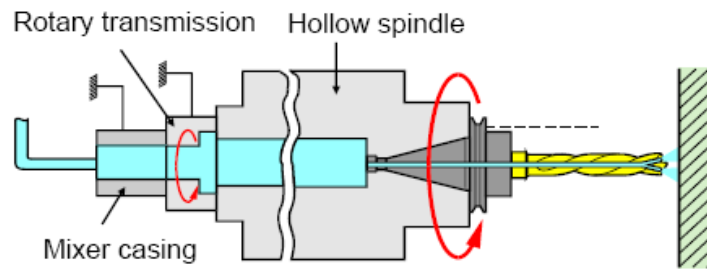
Fig. 2.3 – Internal MQL [29]
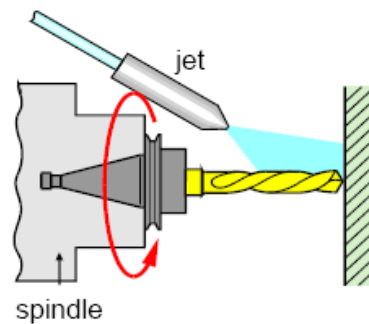
Fig. 2.4 – External MQL [29]

In internal supply a distinction is drawn between 1-channel and 2-channel systems:

a) **One channel supply** - the aerosol mixture is formed outside the spindle, and the single channel acts as a feed route for the mixture.

b) **Two channel supply** - oil and air are fed separately through the spindle. The air-oil mixture is then produced directly before aerosol comes to the tool.
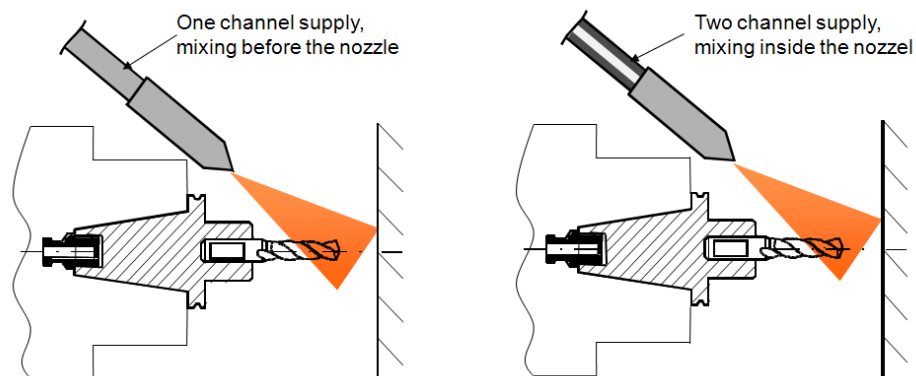
Fig. 2.5 – MQL application for external supply [29]
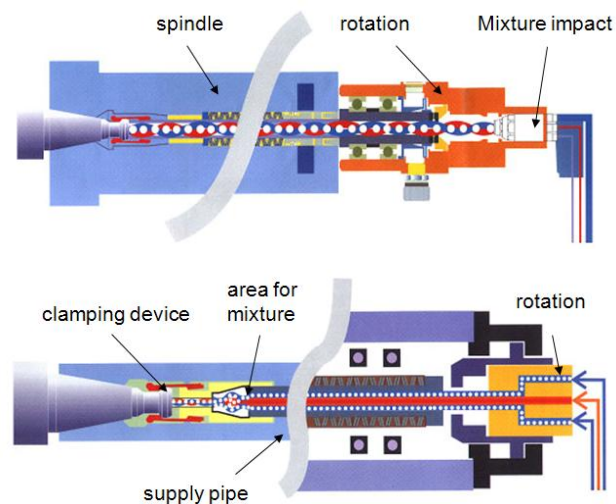
Fig. 2.6 – MQL supply through spindle [29]

One channel supply

The aerosol is produced in the equipment's reservoir and fed through the rotating spindle to the tool tip. The quantity of lubricant emerging at the tool in the form of aerosol depends on the system-defined ratio between lubricant and air quantity and on the existing line and duct cross sections of the aerosol transport path from the MQL unit all the way to the outlet hole on the tool [28]. The oil supplied is completely used up with no residue being left when the optimum setting is used. Thanks to small size of droplets there is hardly any inertia or rate of fall of these oil droplets. This makes it possible to incorporate complicated supply lines around corners to transport aerosol over a long distances so the oil droplets are fed efficiently to the tool's cutting edge.

When the following criterions are fulfilled, it is possible to quickly transport demand-defined quantities of oil to the effective location [28]:

- The aerosol feed should have the fewest possible changes in cross sections since some of the lubricant can be deposited at such places and thus hinder a delay-free supply of aerosol;
- There is also risk of aerosol condensation. If changes in the cross section cannot be avoided for design reasons, the transitions should be as streamlined as possible. A transition angle of < 150° is ideal;
- The aerosol line should be also kept as short as possible. The longer the aerosol line the greater the pressure and aerosol losses. Response times grow longer as well.

2.4.3 MQL benefits and advantages [30]

Advantages that MQL offers over coolant lubrication

- Higher productivity (shorter machining times as a result of higher cutting values);
- Less wear (the tool's service life is increased by as much as 300 %);
- Improved surface quality as a result of 100 % lubrication;
- Virtually dry process (chips, tool, working environment, no drag out losses);
- Health benefits (skin, respiratory tract);
- Eco-friendly (no waste disposal issues, no risk of water pollution);
- Clean environment (staff satisfaction & motivation, operational safety).

How can MQL affect an economy?

- Reduced cooling lubricant consumption:

  - cooling lubricant costs for traditional lubrication are approximately 3 to 4 times higher than the cost of the tools;

- Increased productivity:

  - shorter production times are one of the main outcomes in terms of costing. These savings result from the higher cutting values of MQL-compatible tools.

Whereby can MQL make higher cutting values possible?

The cutting values are higher than for wet processing by a factor of 1.5 - 4 depending on the machining procedure and materials. This is possible due to the fact that:

- The lubrication is more effective;
- Shorter contact times are better in terms of the thermal load;
- High cutting values with MQL permit narrower tolerances;
- Improved tools (carbide substrate, coating, geometry) are used.

How MQL makes longer tool life possible?

The use of MQL increases tool life travel by factors of 2 - 20 in comparison with wet machining due to the following reasons:

- Lubricant is applied exactly where it is needed;
- Full-flood lubrication results in thermal shock to the tool, instead MQL technology produces a more constant temperature range;

- It has also been discovered that MQL is easier on the tool, i.e. for thermal reasons less cutting force is required for the machining of cast metals than with traditional coolant machining;
- Tests have also revealed that with full-flood lubrication, the lubricant often fails to reach the place it is needed due to large particle diameters. In comparison, however, the smaller particles produced in the MQL process get much closer to the cutting edge thereby producing a better lubricating effect.

Why there is no overheating with MQL?

- Because of the higher cutting parameter settings, often 1.5 - 2 times higher, the resulting heat build-up in the chips can be dissipated very quickly. This is due to the increased rate of metal removal and the reduced tool/workpiece contact time

What are the benefits of MQL for health and working safety?

None of the following occurs with MQL:

- No noxious ingredients (fatty alcohols, natural ester oils);
- No skin irritation (contact eczema, allergic reactions);
- No respiratory tract irritation (headaches, bronchitis, cancer risk);
- No slippery floors - as is often the case with full-flood lubrication (oil or water-miscible cooling lubricant);
- No risk of bacterial contamination;
- No hazardous reaction products.

Which advantages offers a dry process over a wet process?

- The process is dry, therefore there are no costs for chip recycling (wet chips have to be dried before being recycled);
- With full-flood lubrication the cutting process is not visible;
- With dry machining, the entire process is visible. This is particularly advantageous during test runs or when setting up cutting processes. Broken tools can be identified more quickly.

2.4.4   Aerosol

While using MQL, finely dispersed droplets of oil within a stream of compressed air are applied as a lubricant. These droplets are produced in an aerosol reservoir within the machine and then delivered all the way through the MQL tubing to the cutting edge. Droplet size diameter range is from approximately 0.1 to 30 μm depending on

the way the aerosol is delivered (internally vs. externally). However, as soon as the aerosol is carried in tubing over long distances or through high-speed rotating tools, the physical effects and the forces that are applied to the aerosol need to be taken into account. Because of the little weight of the droplets they do not experience the centrifugal force within the rotating spindle. Therefore, the separation of the oil on its way towards the tool is minimized [31].

General properties of aerosol differ based on dissimilar properties of the air and the oil delivered to the cutting edge. As different input pressure, also different oil amount can be used to create aerosol. Property of the aerosol can be influenced by choosing different type of oil since every type of oil has different properties like viscosity and density.

2.5   Cutting tests

2.5.1   Introduction

There are different cutting processes used for cutting fluid performance evaluation and reaming is one of the many cutting operations that have been used for cutting fluid performance tests [11]. There are also many performance criteria according to which the cutting fluid performance can be classified (see Fig. 2.7).
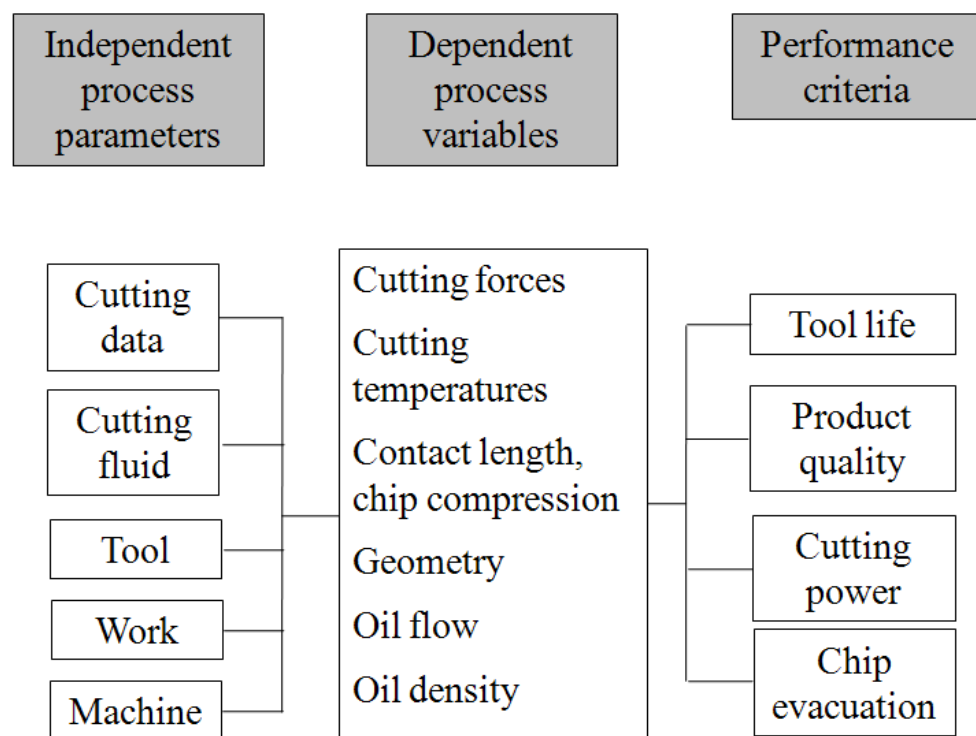
Fig. 2.7 – Test variables in machining (adopted from [32])

2.5.2   Parameter investigation

By investigating all influential parameters and their effect on evaluating parameter, a development of the test procedure is feasible. By performing this investigation it is possible to determine an acceptable tolerance for each parameter. These aspects will be extensively discussed in chapter 7 "Pilot hole quality measurement and uncertainty budget development" and chapter 8 "Reaming tests and uncertainty budget for reamed holes".

Development of the procedure for reaming torque evaluation and quality assurance are proposed and realized with respect to uncertainty calculations. Parameters that have an influence on reaming torque and product hole quality can be seen on following figures. Parameters that are investigated in the present thesis are marked with grey color. Parameters that are used for cutting fluid classification are marked with green color.
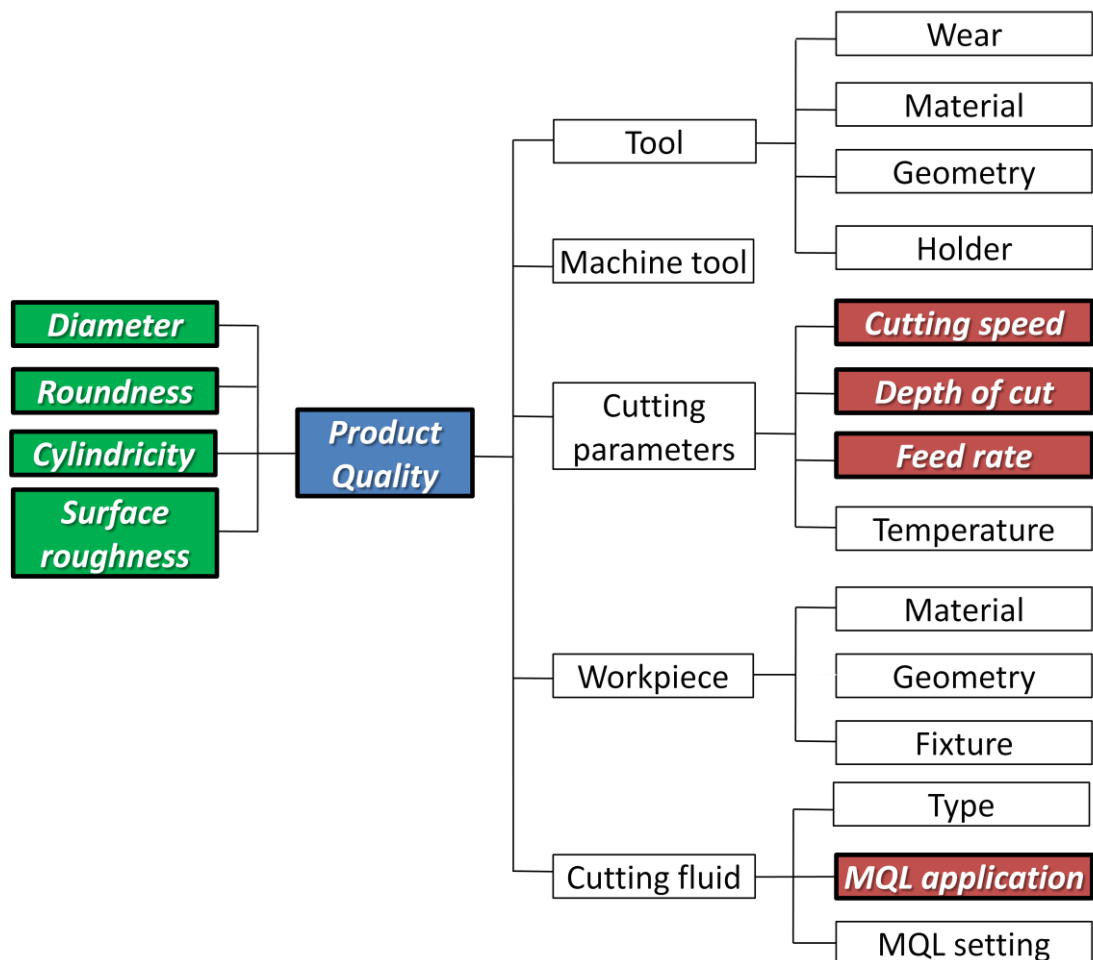
Fig. 2.8 – Influence parameters concerning product hole quality (adopted from [33])

Besides the parameters mentioned in Fig. 2.8 and Fig. 2.9, also the following parameters are discussed:

> › Measuring procedure;
> › Recording and data analysis;
> › Accuracy of the measurements performed by the operator.
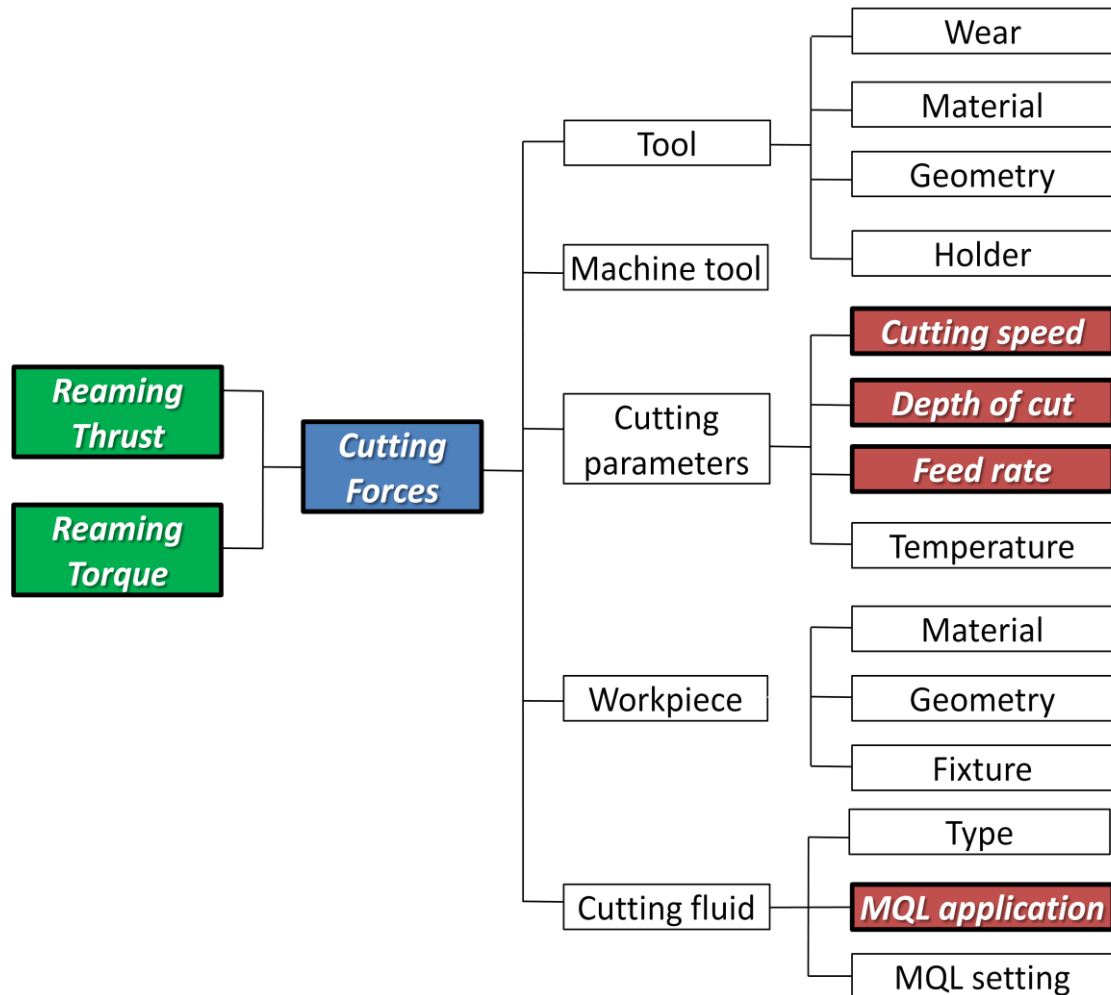
Fig. 2.9 – Influence parameters concerning reaming torque (adopted from [33])

All the above mentioned influence parameters have different impact on the hole quality and therefore some of these can be assessed and can be controlled.

2.5.3 Mechanical tests

Machining tests can either be based on direct measurements of the performance criteria, i.e. tool life, product quality and power consumption, or they can be indirect.

Examples of indirect metal cutting tests are the chip compression test, the contact length test, the oblique cut test, the drill penetration rate test, the drill torque test, the tapping torque test, the critical rake angle method, the threading speed test, the high-temperature drill thrust test, the cutting temperature test, the drill wear rate test, the lathe-turning test, the drill-fee rate-decrease test, and the vibration test and many others [9]. The main objective of these tests is to investigate the basic cutting fluid properties.

On the other hand, the direct testing of cutting fluids is preferred since direct cutting fluid evaluation results are obtained. In previous research works it was also experimentally proved that cutting fluid performance is sensible to the type of operation as well as to the performance criterion considered [12].

As mentioned above, there are many cutting fluid performance tests, indirect and direct, based on different evaluating performance criteria for certain machining operation. The cutting fluid performance in terms of product quality and cutting torque and cutting thrust in reaming is considered in this work.

CHAPTER 3 - REAMING

3.1   Introduction

Reaming belongs to common machining processes with its characteristic property of enlarging, smoothing and accurately sizing existing holes to tight tolerances. The characteristic hole quality depends on the reamer geometry, cutting conditions, application, stock removal, lubrication and the quality of the holes to be reamed. Reaming is considered as a second operation since the holes are first drilled and therefore reaming operation can be performed on the same type of machine as used for drilling.

Since stock removal is small and must be uniform in reaming, the starting holes (drilled or otherwise produced) must have relatively good roundness, straightness, and finish. Reamers tend to follow the existing centerline of the hole being reamed [19]. If insufficient stock removal is left in the hole before reaming, the reamer can show wear faster than normally and result in loss of diameter.
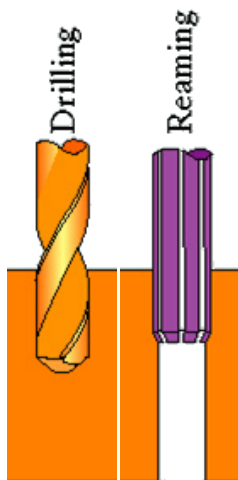
Fig. 3.1 – Drilling and reaming process [34]

3.2   Reamer specifications

3.2.1   Reamer geometry

Reamer consists of either parallel to the tool axis or in helix straight cutting edges (flutes) along the length of a cylindrical body. This provides evacuation of the chips from machined area. Each cutting edge is ground at a slight angle and with a slight undercut below the cutting edge [35].

Flutes on reamers can be straight, right-hand or left-hand spiral and or they can be expandable (on expansion reamers) that can be enlarged for regrinding [35].

Straight flutes are used on through holes in materials that do not form chips, such as cast iron, bronze and free-cutting brass. Straight-flute reamers should not be used on holes with interruptions [35].

Right-hand spirals pull chips out of the hole in blind-hole applications. The right-hand spiral provides a positive cutting action, which pulls the tool away from the spindle. Due to its aggressive flute geometry, a right-hand spiral may cut slightly oversize but it is effective in bridging interruptions and for reaming hard materials [35].

Left-hand spirals push chips ahead of the reamer and are effective for through holes. A left-hand spiral provides a negative cutting action, which pushes the tool back against the spindle. This type of reamer provides good size control and finish, and it is effective in bridging interruptions and handles hard materials [35].

Two most common types of reamers are hand and machine or chucking reamers. Machine reamers have a plain cylindrical or taper shank while hand reamers have a drive square and cylindrical shank. The main difference is the length of the cutting chamfer. It is about 1/4 of the flute length on hand reamers. The long cutting chamfer provides the reamer with excellent guidance but makes the reamer unsuitable for blind holes. Under certain circumstances, hand reamers can be used in machines [35].
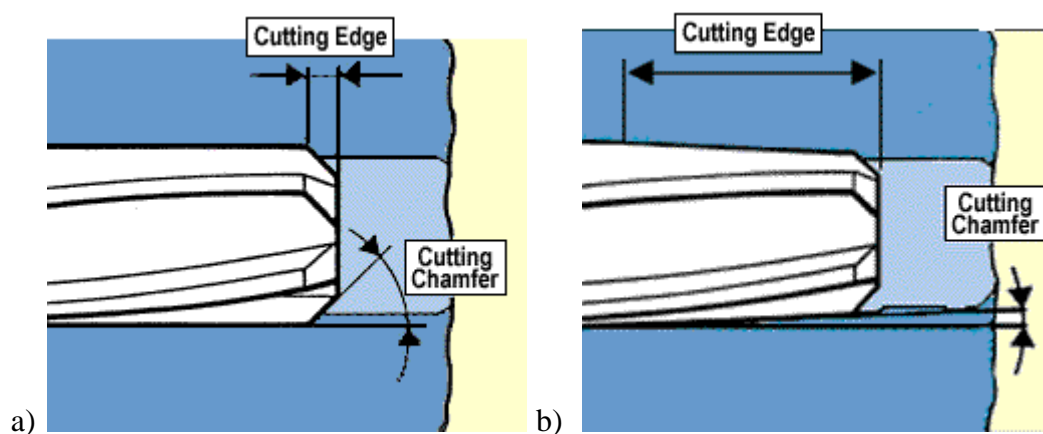

Fig. 3.2 – a) Machine Reamer; b) Hand Reamer [35]

Reamers must combine both hardness in the cutting edges, for long life, and toughness, so that the tool does not fail under the normal forces of use. They should only be used to remove small amounts of material. This ensures a long life for the reamer and a superior finish to the hole [35].
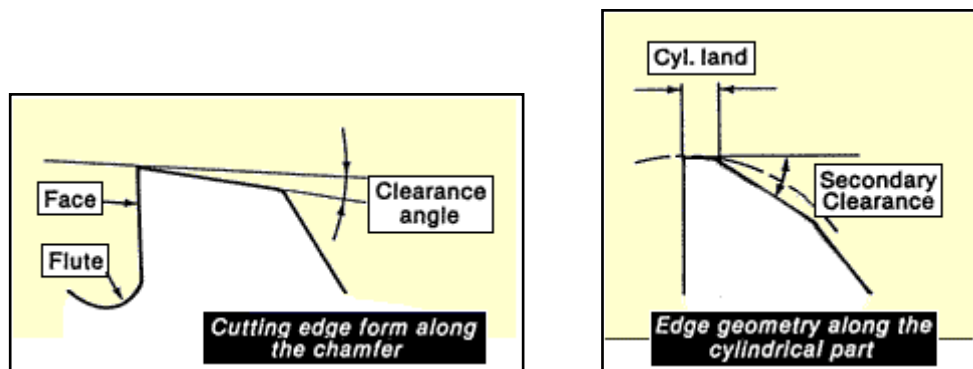
Fig. 3.3 – Cutting edge geometry [35]

The cutting chamfer at the end is usually around 45° for machine reamers while for hand reamers the angle is smaller. Along the flute length of the reamer a guiding or cylindrical land is ground followed by a secondary clearance angle. Here the land is critical as regards guiding the reamer and sizing the hole. For this reason the clearance is not extended up to the edge. A cylindrical ground land of a few thousands of an inch is left. On the cutting chamfer the cutting edge is ground to a point [35].
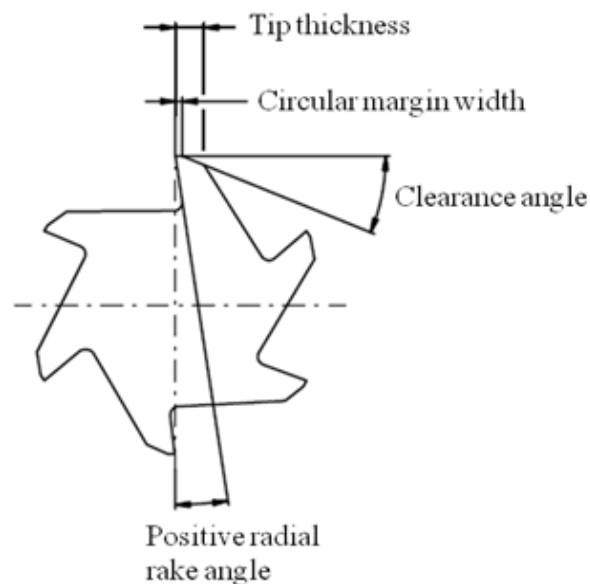
Fig. 3.4 – Reamer geometry (adopted from [34])

3.2.2   Reamer materials

Reamers are typically made from high-speed steel (HSS) or solid carbide (SC); they can be carbide-tipped (CT) with an alloy steel body or they can be made out of cermets [37].

High speed steel:

The term "high speed steel" was derived from the fact that it is capable of cutting metal at a much higher rate than carbon tool steel and continues to cut and retain its hardness. Tungsten is the major alloying element but it is also combined with molybdenum, vanadium and cobalt in varying amounts. Although replaced by cemented carbides for many applications it is still widely used for the manufacture of many cutting tools. HSS reamers, with a cutting-edge hardness between Rc 63 and Rc 67, or cobalt cutting tools are generally chosen for shorter production runs in non-ferrous materials and applications where machining conditions restrict the use of harder, more brittle substrates. These tools exhibit lower wear resistance and notably less heat resistance than carbide cutting tools. These types cutting tools are not recommended for applications involving hard or abrasive materials, or high cutting speeds [36][37].

Solid carbide and material:

SC reamers have cutting-edge hardness from Rc 77 to Rc 81, and work well for small diameters. These reamers exhibit better wear properties than HSS tools, and are extremely rigid. However, solid carbide is brittle, and that can lead to chipping or breakage if misused or mishandled. Carbide-tipped reamers excel in close-tolerance work. Typically, a carbide tip is brazed to a tough, hardened alloy-steel body [37].

Carbide-tipped material:

CT reamers stand up to abrasive and tough materials and handle high-production runs. Because carbide is highly wear resistant, CT reamers maintain accurate hole sizes and smooth finishes longer than HSS tools. In addition, total cost per reamed hole usually is lower with CT reamers because of higher speeds and feeds, consistent quality and longer tool life [37].

Cermets:

Other suitable materials for reamers are cermets. The word cermet is derived from terms CERamic and METal and therefore comprises abilities of both ceramic and metal, i.e. hardness of the ceramic and toughness of the metal. Cermets are basically sintered carbides with a hard phase formed by TiC+TiN [38].

The typical advantages of using cermets are their high wear resistance, low reactivity with most work materials (i.e. no significant BUE and cratering on the cutting edge) and long tool life. Because of their great properties they produce excellent surface finishes (even when dry machining), and maintain tight tolerances over their life span. Cermet reamers also perform high shape and diameter accuracy. Higher cutting speeds may be used with cermets, especially for semifinishing to finishing operations, because of their high wear resistance and therefore high productivity can be achieved. A typical structure of a cermet material can be seen in Fig. 3.5.
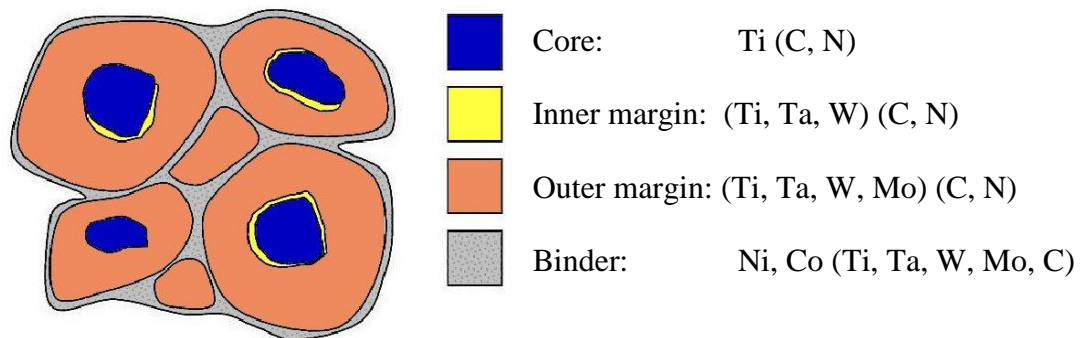
Fig. 3.5 – Cermet structure [39]

Choosing the most suitable type of reamer for a specific application depends on work-piece material, its condition and hardness, the number of holes to be finished, tolerance and finish requirements and tool cost.

3.2.3 Practical information concerning reamers [40]

Feed

In reaming, feeds are usually much higher than those used for drilling. The amount per feed may vary with the material. Generally it is recommended to start between 0.038 and 0.10 mm per flute per revolution. Too low feed may result in glazing, excessive wear, and occasionally, chatter. Too high feed tends to reduce the accuracy of the hole and may lower the quality of the finish. The basic idea is to use as high feed as possible and still to be able to produce the required accuracy and finish.

Stock removal

Insufficient stock for reaming may result in a burnishing rather than a cutting action. It is very difficult to generalize on this phase as it is closely related to the type of material the finish required, depth of hole, and chip capacity of the reamer. It is recommended to use the following material removal rate for different hole diameter:

a) Machine reamers: 6 mm hole → 0.20 mm, 12 mm hole → 0.30 mm, and 50 mm hole → 0.50 mm.

b) Hand reamers: stock allowances are much smaller because of the difficulty in hand forcing the reamer through greater stock. A common allowance is 0.003 inch to 0.005 inch.

Speed

The most efficient speed for machine reaming is closely connected to the type of material being reamed and the tolerance or finish required. Quite often the best speed is found to be around two-thirds the speed used for drilling the same material. When

close tolerances and high finishing are required it is usually necessary to finish the reaming at considerably lower speeds.

Chatter

In general, reamers do not work well when they chatter. Consequently, one primary consideration in selecting a speed is to stay low enough to eliminate chatter, and speeds must not be so high as to permit chatter. The presence of chatter while reaming has a very bad effect on reamer life and on the finish of the hole. Chatter may be the result of several causes, some of which are listed:

1. Excessive speed.
2. Too much clearance on reamer.
3. Insecure holding of work.
4. Excessive overhang of reamer in spindle.
5. Excessive looseness in floating holder.
6. Too light feed.

The parameters of cutting speed and feed rate control metal removal rate, hole quality and tool life. Any increase in these parameters generally increases metal removal rate, but decreases tool life. While an increase in either speed or feed has an equal effect on metal removal rate, an increase in speed usually has a larger effect in reducing tool life than an increase in feed rate.

3.2.4   Optimized reaming

For reaming operations, hardness of the workpiece has the greatest effect on machinability. Other significant factors include hole diameter, hole configuration (e.g., hole having keyways or other irregularities), hole length, amount of stock removed, type of fixturing, accuracy and finish requirements [41].

It is recommended to produce a chamfer around the hole before reaming in order to help the reamer maintain an accurate central position, obtain better surface finish during penetration and improve tool life. It is also recommended to perform the drilling and the reaming operation while the workpiece is clamped in the same position. If the workpiece has been removed after drilling and then clamped again for reaming, misalignment between the reamer and the hole center lines may occur. Therefore, it is recommended to leave a larger allowance for reaming [41].

For efficient operation, the amount of stock left in the hole for reaming must be sufficient to permit the reamer to cut at all times rather that to burnish the surface. Variations in the amount of stock to be removed can affect the finish size of the hole reamed. Removal of too much stock by reaming often causes oversize and rough holes [41].

In general applications, surface finish for reaming is expected to be in range <0.8; 3.2>, for some special applications the range can be extended for both better quality surface and worse quality surface as can be seen in Fig. 3.6.
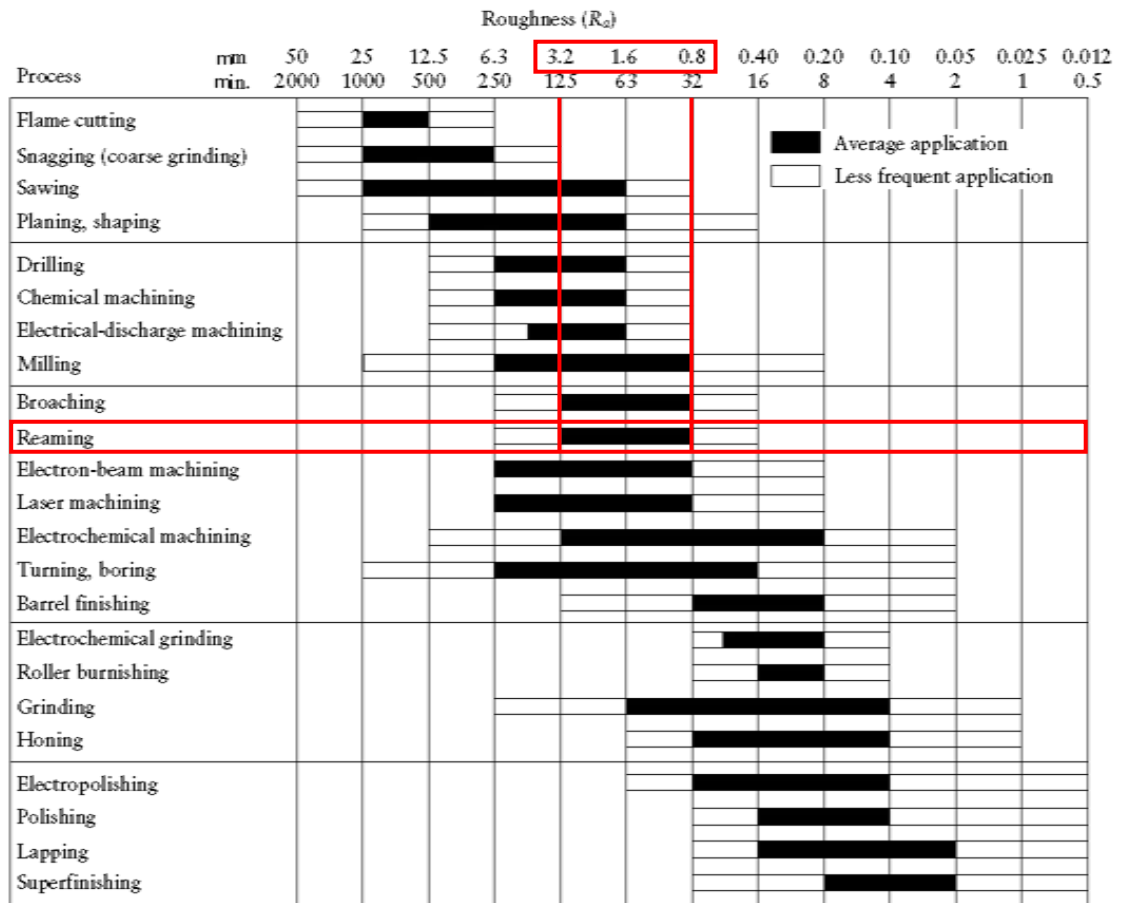
Fig. 3.6 – Surface roughness specification for all manufacturing processes [34]

In cases when an extremely precise and high surface hole quality is required, a semi-finish operation such as cored drill is used prior to the reaming operation.

3.2.5   Reaming Force and Reaming Torque calculation

In order to express a formula for reaming torque, some basics concerning chip thickness, chip width etc. has to be introduced. A simple drawing showing the area of removed material specifications can be seen in Fig 3.7.

Fig. 3.7 – Removed material specifications during reaming

In the specific case considered during this project, there were six cutting edges inte-racting with workpiece during the reaming operation, therefore:

$$f_Z = \frac{f}{z} \qquad \text{Eq. 3.1}$$

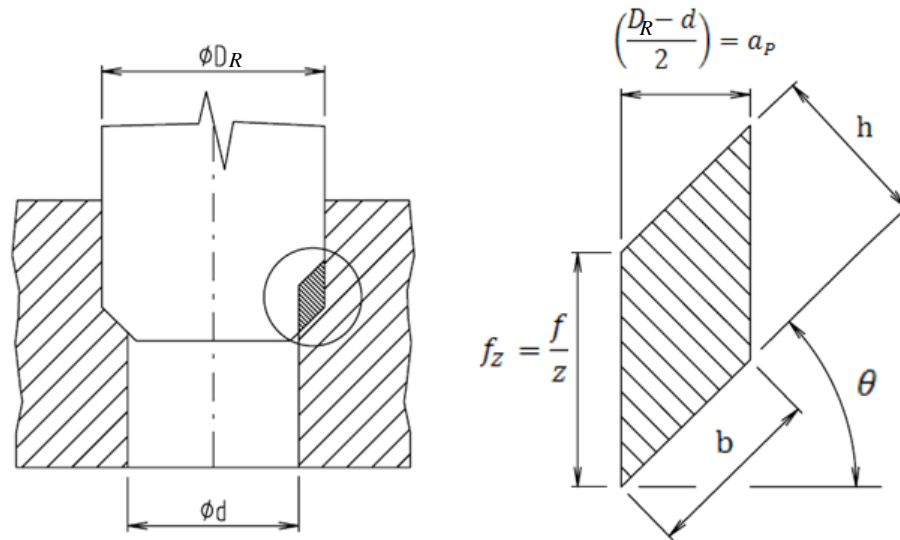$$b = \frac{D_R - d}{2 \cdot \cos\theta} \qquad \text{Eq. 3.2}$$

$$h = \frac{f}{6} \cdot \cos\theta \qquad \text{Eq. 3.3}$$

The nominal chip cross-section A_C removed by six cutting edges can be expressed as follows (see Fig. 3.7):

$$A_C = h \cdot b = \left(\frac{f}{6} \cdot \cos\theta\right) \cdot \left(\frac{D_R - d}{2 \cdot \cos\theta}\right) = \frac{f}{12} \cdot (D_R - d) \qquad \text{Eq. 3.4}$$

$$A_C = f_Z \cdot a_P = \frac{f}{12} \cdot (D_R - d) \qquad \text{Eq. 3.5}$$

The definition of the tangential reaming force F_C is:

$$F_C = k_C \cdot A_C \qquad \text{Eq. 3.6}$$

After inserting equation Eq. 3.4 (or Eq. 3.5) into Eq. 3.6 one can express the tangential reaming force as:

$$F_C = k_C \cdot \frac{f}{12} \cdot (D_R - d) \qquad\qquad \text{Eq. 3.7}$$

The reaming torque T is expressed as:

$$T = F_C \cdot r_A \qquad\qquad \text{Eq. 3.8}$$
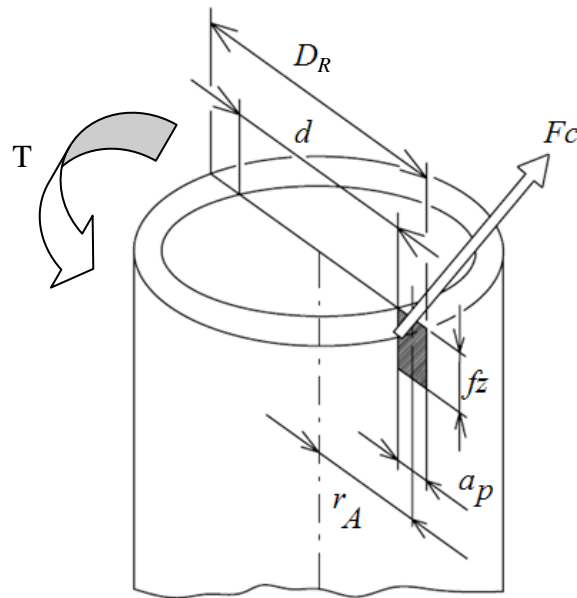
Fig. 3.8 – Tangential reaming force acting on the tool (adopted from [42])

Calculating the radius r_A as:

$$r_A = \frac{d}{2} + \frac{a_P}{2} = \frac{D_R + d}{4} \qquad\qquad \text{Eq. 3.9}$$

Then the final expression for reaming torque is:

$$T = \frac{k_C \cdot f \cdot (D_R^2 - d^2)}{48} \qquad\qquad \text{Eq. 3.10}$$

The reaming torque is the sum of the moments on each cutting edge (i.e. the product of the tangential reaming force and the radius from the centre where the tangential reaming force is acting).

The main factors affecting the reaming torque are the feed, the cut of depth and the work material.

There are other forces acting on the tool except the one causing reaming torque, see Fig. 3.9.

Fig. 3.9 – Force components acting on the tool (adopted from [42])

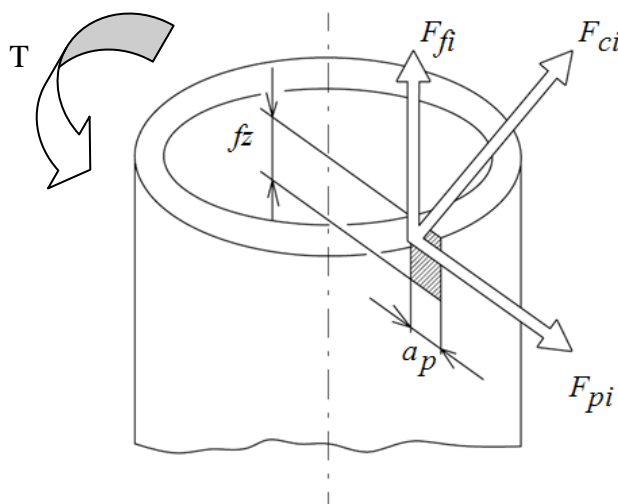The feed force is very important in reaming. It is the axial force acting on the reamer when penetrating into the workpiece. Applying an excessive axial feed force can negatively affect the hole quality and tool reliability. On the other hand, applying a sufficient feed force is important for the cutting action and also from productivity point of view [43].

3.3 Workpiece material

Work material that is used during the project was an austenitic stainless steel AISI 316 L. The workpiece specification can be found in Tab. 3.1. This kind of stainless steel belongs to low-carbon grade stainless steels which are non-magnetic steels. Such material is hard to machine due to its ductility, high strain hardening and low thermal conductivity. The austenitic steels are characterized by very good corrosion resistance, very good toughness and very good weldability [23]. Chips produced are long wiry chips, material can easily work harden if not machined with correct feeds.

Tab. 3.1 - Description of the test workpiece [44]

Test Workpiece Material								
Test Material	AISI 316 L Stainless Steel				Vickers Hardness		258.1 HV20	
Analysis	C	Si	Mn	P	Ni	Cr	Mo	S	N
	0.016	0.39	1.4	0.027	11.21	17.31	2.11	0.026	0.052

Stainless steels are alloyed steels with chrome content normally above 12%. Their classification can be seen in Fig. 3.10.
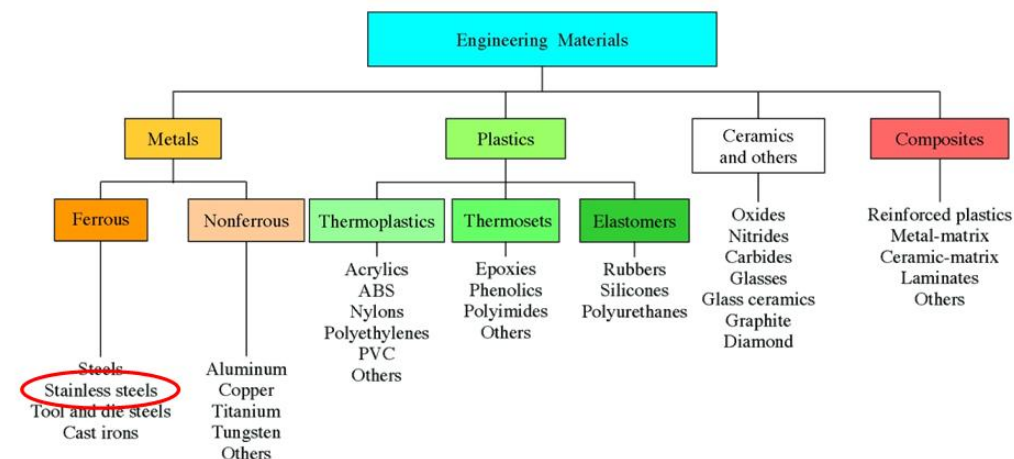

Fig. 3.10 – Workpiece material among other materials [34]

Furthermore stainless steels can be divided into six groups as can be seen in Tab. 3.2.

Tab. 3.2 – Composition ranges for different stainless steel categories [45]

Steel category	Composition (wt%)					Hardenable	Ferro-magnetism
	C	Cr	Ni	Mo	Others		
Martensitic	›0.10	11-14	0-1	-	V	Hardenable	Magnetic
	›0.17	16-18	0-2	0-2			
Martensitic-austenitic	‹0.10	12-18	4-6	1-2		Hardenable	Magnetic
Precipitation hardening		15-17	7-8	0-2	Al,	Hardenable	Magnetic
		12-17	4-8	0-2	Al,Cu,Ti,Nb		
Ferritic	‹0.08	12-19	0-5	‹5	Ti	Not hardenable	Magnetic
	‹0.25	24-28	-	-			
Ferritic-austenitic (duplex)	‹0.05	18-27	4-7	1-4	N, W	Not hardenable	Magnetic
Austenitic	‹0.08	16-30	8-35	0-7	N,Cu,Ti,Nb	Not hardenable	Non-magnetic

The alloying elements that are present in stainless steels have different effect on the properties of stainless steels. Chromium as an alloying element has the most significant influence on corrosion resistance of the stainless steels and promotes a ferritic structure. On the other hand, nickel promotes an austenitic structure and generally increases ductility and toughness.

De Long diagram

The nickel and the chromium equivalent provide information about the amount of the various structures in stainless steels. By entering the Ni-equivalent over the Cr-equivalent for stainless steel into a diagram according to De Long one is able to find the content of austenite and ferrite in the resulting microstructure [45].

The chromium and nickel equivalents can be calculated in the following way:

$$Chromium\ equivalent = \%Cr + 1.5\%Si + \%Mo$$
$$Nickel\ equivalent = \%Ni + 30(\%C + \%N) + 0.5(\%Mn + \%Cu + \%Co)$$
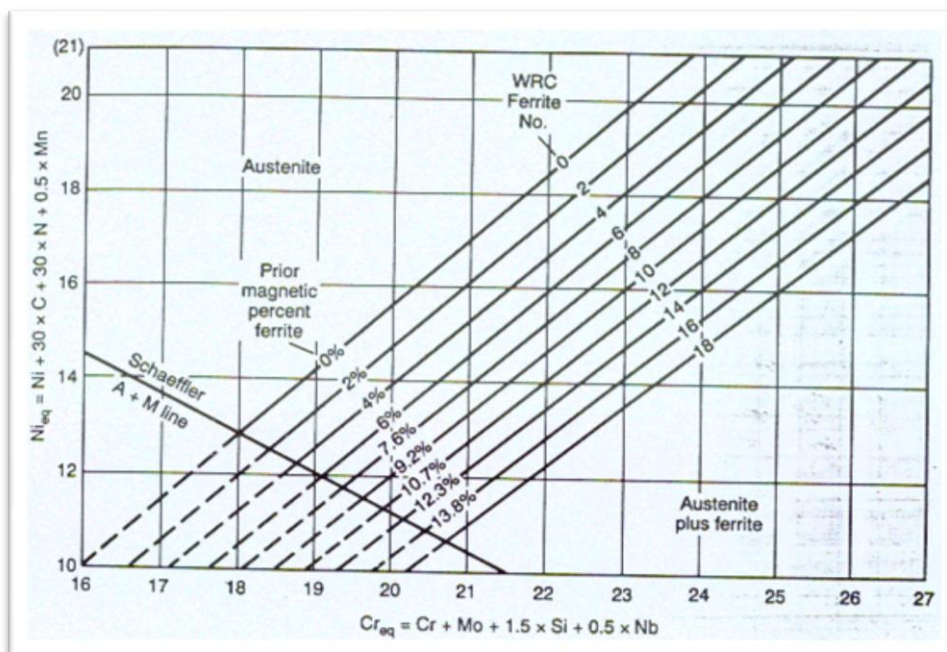
Fig. 3.11 – De Long diagram for stainless steel [46]

Machinability of stainless steels

Resistance against corrosion generally increases with increasing Cr-content. Other alloying elements like nickel and molybdenum change the structure and mechanical properties of the steel [47].

Stainless steels can be divided into the following groups [47]:

› Ferritic stainless steels – often have good strength. Good machinability.
› Martensitic stainless steel – relatively good machinability.
› *Austenitic stainless steel* – characterized by high coefficient of elongation.

› Austenitic-ferritic stainless steel – often called duplex stainless steel. These steels have low machinability.

Stainless steel materials are difficult to machine due to following properties [47]:

› Most stainless steel materials work harden during deformation. The hardening decreases rapidly with an increasing distance from the surface. Hardness values close to the machined surface can increase by up to 100% of the original hardness value if using the incorrect tool.
› Stainless steels are poor heat conductors, which leads to high cutting edge temperatures compared to steel.
› High toughness leads to high torque, which in turn results in a high work load.
› The materials have a tendency to smear the surface of the cutting tool.
› Chip breaking and swarf management problems, due to the high toughness of the stainless steel.

CHAPTER 4 - DESCRIPTION OF CUTTING FLU- ID PERFORMANCE TESTS

4.1   Introduction

In the following the description of cutting fluid performance tests including both cutting torque tests and product hole quality tests are presented. Both types of cutting fluid tests are defined and described together with experimental details.

4.2   Experimental details

4.2.1   Workpiece

The tested workpieces were austenitic stainless steel specimens with pre-manufactured hole (see dimension and geometry specification of the workpiece in Fig. 4.1).
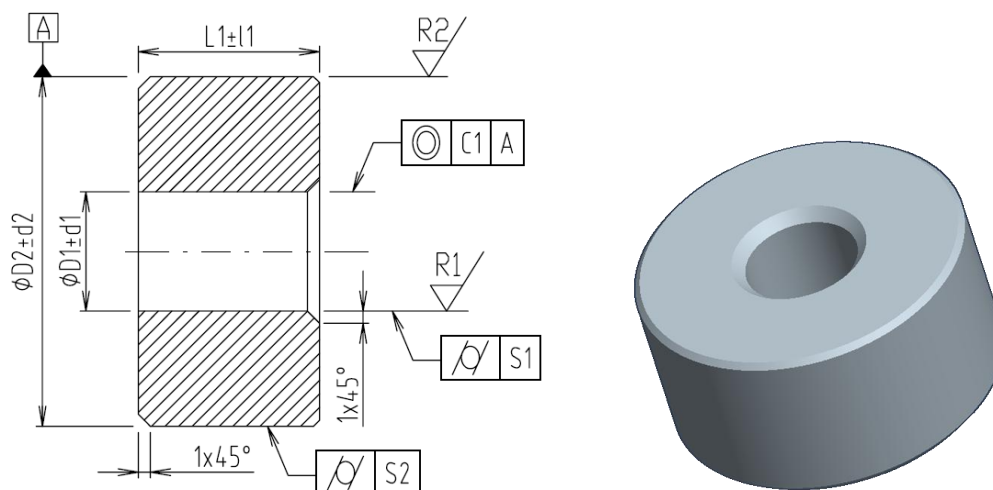
Fig. 4.1 - Test workpiece

Tab. 4.1 – Dimensions and geometry specification of the test workpiece [44]

D2	d2	D1	d1	L1	l1	R1	R2	S1	S2	C1
29 mm	+ 0.05 - 0.1	9.9 mm	± 5 µm	15 mm	± 0.05 mm	< 0.6 µm	< 5.0 µm	< 10 µm	< 10 µm	< 50 µm

4.2.2   Test equipment

All the reaming tests are carried out using a Cincinnati Sabre 750 CNC 7.5 kW vertical milling centre which is a computer numerical control (CNC) machine tool.

Fig. 4.2 - Cincinnati Sabre 750 CNC 7.5 kW

Reamers that are used for the tests are HSS-E COBALT 10.1 mm and 10.0 mm rea-mers with 5% of cobalt composition. This ensures a good combination of toughness and hardness. It has also a good machinability and wear resistance. Reamer specifica-tions are listed in Tab. 4.2.

Tab. 4.2 – Reamer specification [48]

Type	Magafor 600
Material	HSS-E COBALT
Shank	DIN 212-B
	NFE 66014
No. of flutes	6
Dimensions [mm]	
D	10.1
L	133 ± 1
l_1	$38 + 1$
l_2	99
d_2	10 h8
Reamer tolerance	± 0.003
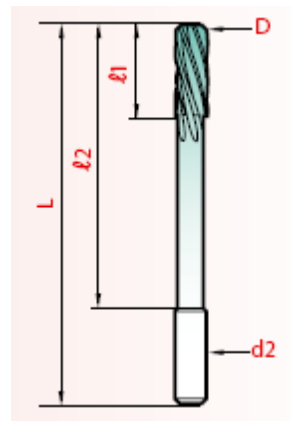
Tool holder: SK 40x10, Rohm - Germany

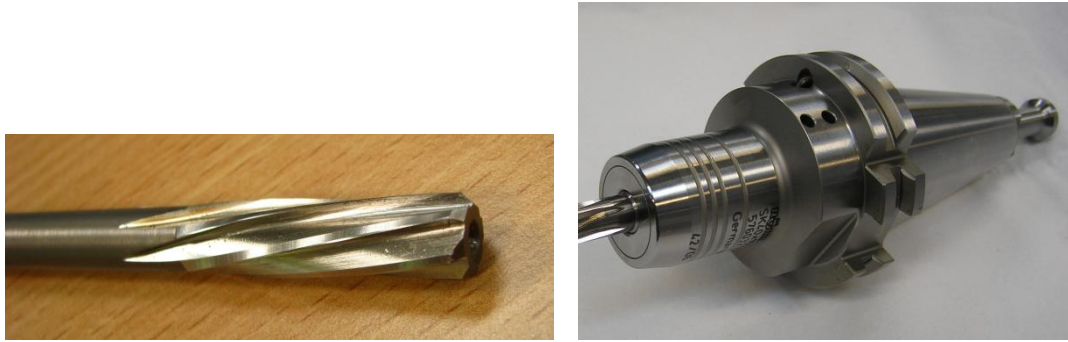Because the tool holder is a floating tool holder, it is not necessary to measure tool run-out.

Fig. 4.3 – a) HSS-E Cobalt reamer; b) Tool holder

Tab. 4.3 – HSS-E COBALT reamer composition [47]

Grade	Hardness	C %	W %	Mo %	Cr %	V %	Co %	ISO standard
M35	830-870	0.93	6.4	5.0	4.2	1.8	4.8	HSS-E

4.3   Equipment and additional features for product quality test

Product quality tests are based on measuring the shape of the workpiece which includes measurements of hole diameter, roundness and cylindricity, as well as measuring surface integrity. Further the test equipment is described.

4.3.1   Hole geometry

Hole geometry (diameter, roundness and cylindricity) is measured on a tactile coordinate measuring machine (CMM) OMC 850 ZEISS (see Fig. 4.4). The specimens are measured by 3 mm probe in diameter (see Fig. 4.5).

Fig. 4.4 - CMM - OMC 850 ZEISS   Fig. 4.5 – Measuring probe
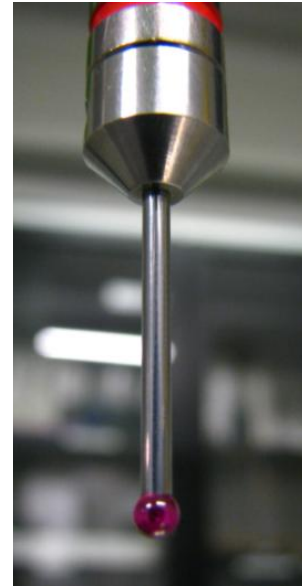
Fixture for holding the specimens was produced in the way that 40 specimens could be measured at a time (see Fig. 4.6). For the purpose of this master thesis, only 15 "holes" out of 40 are used. The fixture holds the specimens by means of o-rings compressed between three aluminum plates (see Fig. 4.7). The fixture also provides the clamping system for a 10 mm diameter reference ring.

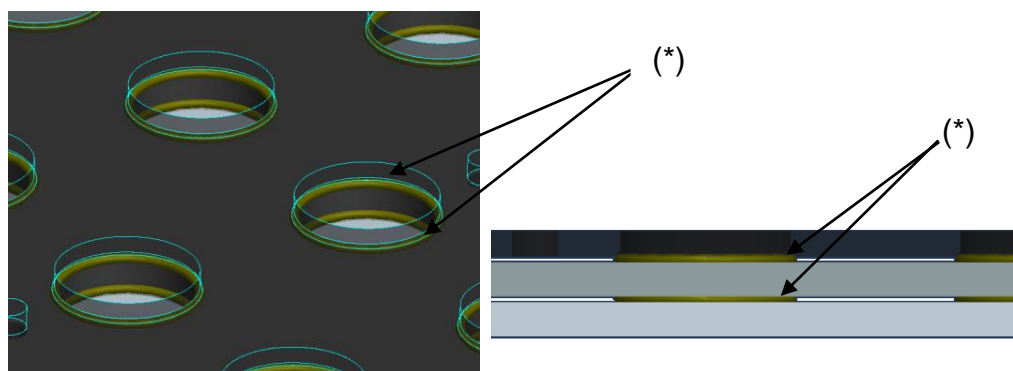Fig. 4.6 - Fixture clamped to the CMM table

Fig. 4.7 - Position of the O-rings (*) between three aluminum plates

4.3.2 Surface roughness

Surface roughness measurement is carried out using a stylus instrument TAYLOR-HOBSON SURTRONIC 3+ (see Fig. 4.8) provided with a skid pick-up and a 2 μm radius tip according to ISO 4287:1997 [49].

Fig. 4.8 - Stylus instrument with a skid pick-up and a tip

4.4 Equipment for reaming torque and reaming thrust test

Torque and thrust during cutting are measured on KISTLER dynamometer, Type 9271A; SN 76766 (see Fig. 4.9). Dynamometer is an integrated measuring system equipped with piezoelectric cells, whose output charges are converted into voltages through charge amplifiers - KIAG SWISS Type 5015 (see Fig. 4.10). The output voltages of the charge amplifiers are digitized using a PC with acquisition board and Labview 8.0 software.

Fig. 4.9 - Dynamometer with fixture

Fig. 4.10 - Charge amplifier

The fixture is designed in the way that when the pilot hole is produced in the centre of the specimen, the produced pilot hole will be as well in the centre of the dynamometer and thereby will give the lowest error from the dynamometer.

CHAPTER 5 – EXPERIMENTAL INVESTIGATION

5.1   Development of the setup for MQL application

A setup for MQL application is built up and can be seen in Fig. 5.1.
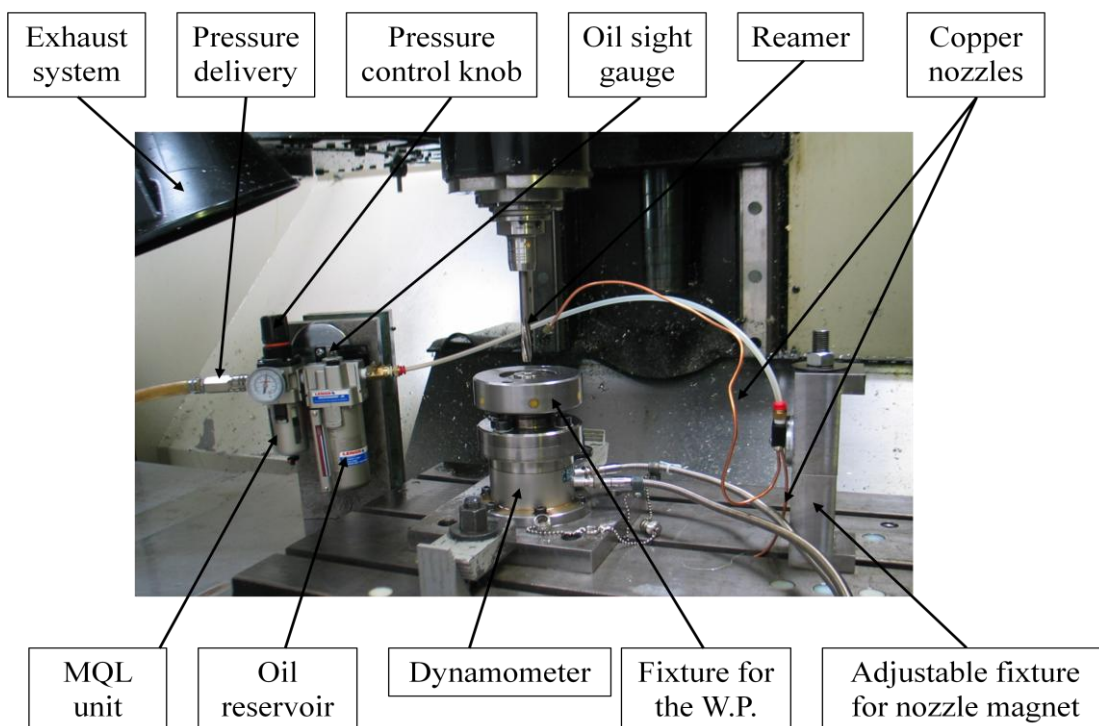

Fig. 5.1 - Experimental setup for MQL application

The way the oil is delivered in this MQL application can be described in the following steps:

- The air is delivered to the MQL system under pressure that is set on the pressure control knob;
- The air passes from the regulator to the fluid reservoir; and;
- A venturi type system pulls the oil up into the air stream;
- The mixture is fed down the tubing to the nozzles with rubber tips at the outlet.

It is shown that one of the nozzles is going through the dynamometer and the fixture from the bottom and the second nozzle is directed from the top under 45°. The distance between the tips of both nozzles and the workpiece is 40 mm and 55 mm respectively (see Fig. 5.2). Aerosol is sprayed through the rubber tips mounted at the end of the copper nozzles. The outlet hole diameter of the tips is 1 mm. This is measured when the air passes through the nozzles, otherwise the rubber tips are closed.
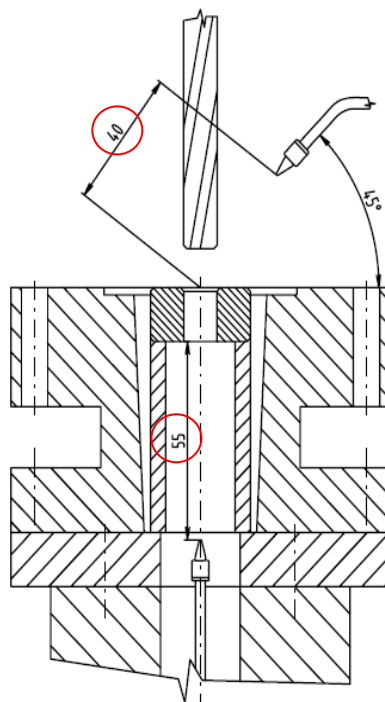
Fig. 5.2 – Nozzle positioning for a setup TB

5.2   Equipment for MQL

Fluid – test parameter

Oil that is used for the experiment is a LENOX LUBE C/Al cutting lubricant. It is an insoluble oil with viscosity of 26.02 cSt measured at 40°C.

Because the oil density is not specified in the characteristics list of the oil, it is measured using a density meter (DMA 4100, Anton Paar) at DTU facilities and is 823.2 kg·m^{-3} at 20°C. Because the aerosol flow rate depends on the oil viscosity, the density of the oil is measured also for other temperatures to see the trend between the density and temperature (see Fig. 5.9 in section 5.3).

Flow meter

Air flow is measured using Brooks flow meter, type 5853S with measuring range up to 100 l$_n$·min^{-1} and pressure 100 bar. The flow can be read on control unit, model 0152.

Fig. 5.3 - Flow meter

Fig. 5.4 - Control unit

MQL unit

MQL unit is a constant flow type spray. Both air and oil are dispensed continually until the air supply is shut off. According to the manual for the MQL unit, the system uses different amount of oil droplets that correspond to certain volume per hour depending on the air pressure set on the pressure control knob. This is experimentally disapproved, since no matter how big pressure is set; the system uses the same amount of droplets per time. Therefore all experiments are run under 6 bars.
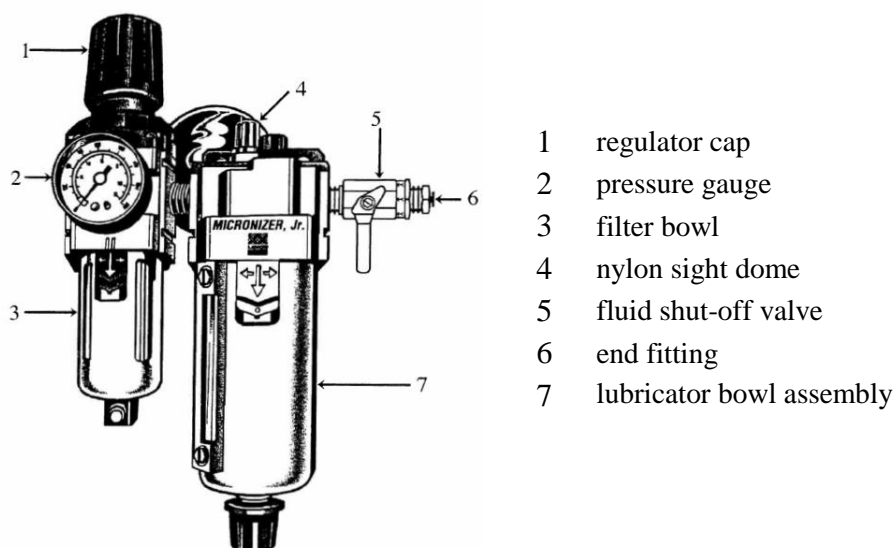

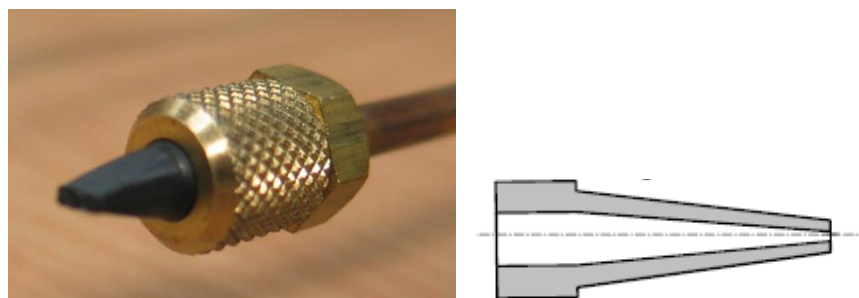| 1 | regulator cap |
2	pressure gauge
3	filter bowl
4	nylon sight dome
5	fluid shut-off valve
6	end fitting
7	lubricator bowl assembly

Fig. 5.5 - MQL unit [50]

Fig. 5.6 – Nozzle with rubber tip

Length of the copper pipes (nozzles) is 50 cm.

5.3   Measurement of the air/oil flow

Air flow is measured using Brooks flow meter type 5853S and a control unit type 0152. The procedure for air flow measurements is as follows:

- Firstly, the air is delivered to the flow meter under pressure that is controlled on MQL unit through which the air passes. This measurement is carried out without taking into account a setup for cutting (measuring setup 1), i.e. connection of the flow meter to the nozzles. Using this setup, five measurements in total are performed.

- Secondly, air flow measurement is performed in a so called "setup mode" (measuring setup 2), i.e. the air passes through MQL unit and flow meter and leads to the nozzles from where the air goes out. The measuring setup can be seen in Fig. 5.7.
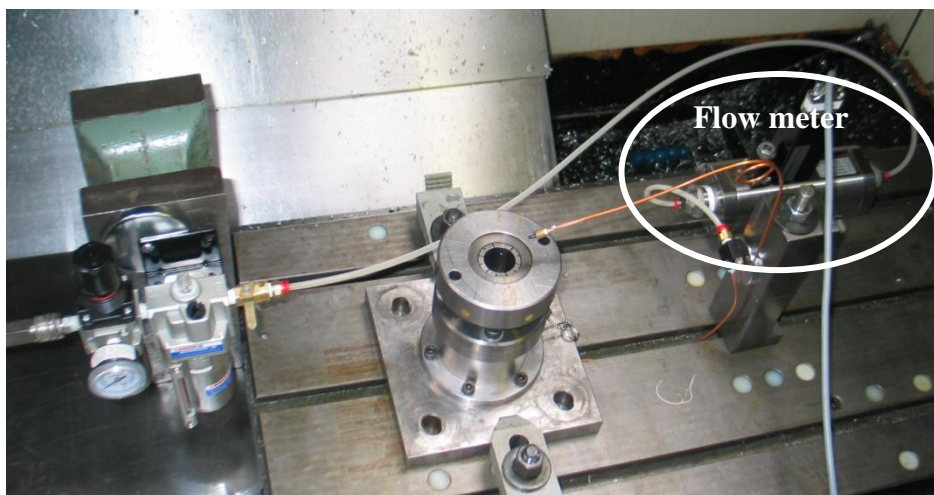

Fig. 5.7 – Air flow measurement setup

- Lastly, the flow meter is unmounted from the system since the measurement of oil flow is carried out. The weight of the oil is weight before and after it is used to check how much oil is used in 10 minute intervals. A setup of 6 and 9 droplets respectively is set on the control sight gauge of the MQL unit and the tests are carried out for different pressure setups ranging from 4 to 6 bar. As it is described in section 5.2, the pressure set on the MQL unit does not influence the oil usage when selected in the range <4; 6> bar on the pressure gauge.

The oil flow is then calculated using a single formula for mass flow, see Eq. 5.1:

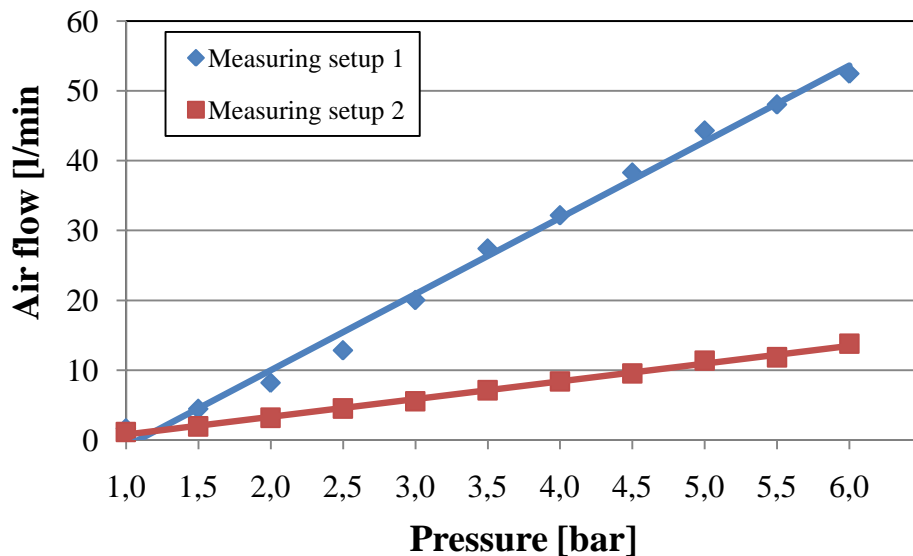$$Q = \frac{\dot{m}}{\rho}$$
<div align="right">Eq. 5.1</div>

Fig. 5.8 – Air flow measurement

Values in Fig. 5.8 are calculated as an average based on five measurements for air flow that is not in a "setup mode" and three measurements in a "setup mode". Because of the backpressure that is formed in the nozzles, results change considerably; this is obvious from Fig. 5.8. The backpressure is caused because of the reduction in diameter, going from the nylon tubing to the copper pipes and from copper pipes to the rubber tips.

There are two parameters that influence the oil usage. First parameter is a setup of number of droplets on the sight gauge. It is observed that with increasing number of droplets, the oil usage increases. The second parameter is the temperature in the workshop. With increased temperature in the workshop, the oil usage increases. This is due to the fact that when temperature increases, the oil viscosity and therefore also oil den-

sity decreases. This behavior can be seen in Fig. 5.9. The bars represent experimental standard deviation that is calculated based on 5 measurements for different pressure setups.

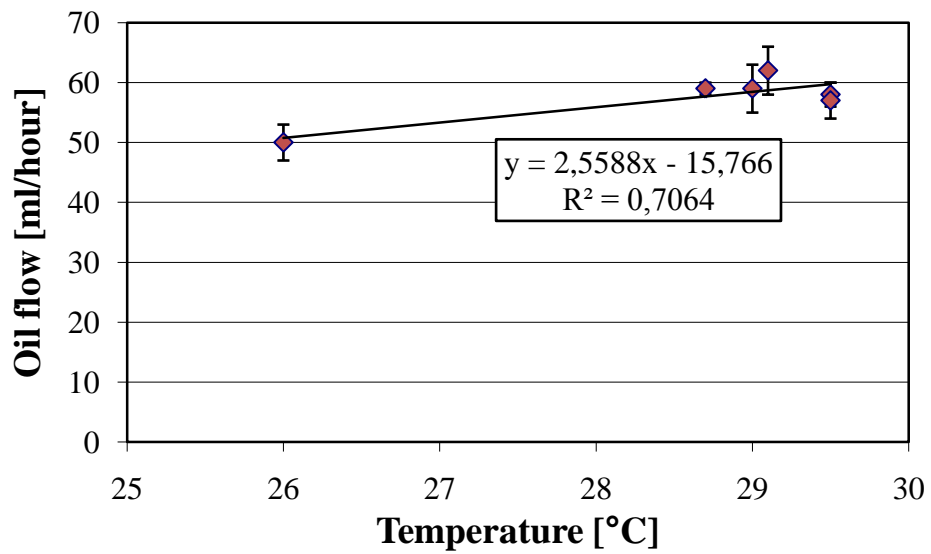The temperature difference of $\pm 1°C$ gives an oil flow variation of about ± 5 ml/hour.

Fig. 5.9 – Oil flow measurement for a setup with 9 droplets

CHAPTER 6 – DEVELOPMENT OF PRELIMINARY TEST PROCEDURE

6.1   Introduction

A preliminary test procedure is a test procedure developed to investigate the quality of the hole with respect to different measurands. Also a preliminary test procedure for reaming thrust and reaming torque is proposed.

6.2   Characterization of the measurands

6.2.1   Roundness and cylindricity specification

Roundness and cylindricity belongs to geometrical tolerances and are generally called "form". Both of them can be calculated on different mathematical principles which give different results. Roundness can be evaluated based on several mathematical methods like: Minimum Zone Centre, Minimum Circumscribed Circle, Maximum Inscribed Circle and Least Square Circle. The same evaluation methods are valid also for cylindricity [51].

There are several ways how to perform roundness measurement. There are easy measuring methods like using dial gauge or there are specially designed measuring instruments like rotating spindle and rotating table. Cylindricity is usually measured using CMM [51].

Generally there can be one measuring instrument that measures several geometrical features, for instance coordinate measuring machine. There are also specially designed measuring instruments that are intended just for one measurand, e.g. roundness tester for measuring the roundness [51].

According to ISO 1101 [52] a given form parameter has to be evaluated according to the minimum zone condition. Roundness is defined as a radial distance between two concentric circles and cylindricity as a radial distance between two concentric cylinders [51] (see Fig. 6.1).
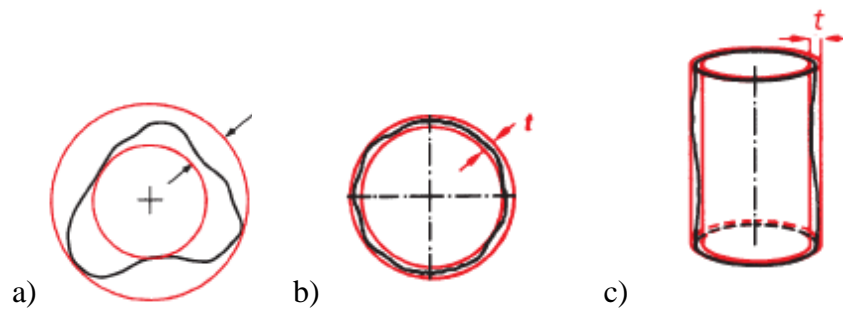
Fig. 6.1 – Definition of minimum zone circle (a), form error indication for roundness (b), form error indication for cylindricity (c) [53]

6.2.2 Surface roughness specification and calculation

Because the whole concept of surface topography is very complex, only basics concerning surface parameters, parameter calculation and measuring instrument will be presented.

According to [49] there are 14 parameters related to each of the three profiles (primary profile (P-profile), roughness profile (R-profile) and waviness profile (W-profile)) [51].

The most widely used quantification parameter in surface texture measurement is Ra (also called "arithmetic average roughness") and therefore it was selected during this project. Mathematically, Ra is the arithmetic average value of the profile departure from the mean line, within a sampling length and can be expressed in the following way:

$$Ra = \frac{1}{L} \cdot \int_0^L |Z(x)| dx \approx \frac{1}{n} \cdot \sum_{i=1}^n |y_i| \qquad \text{Eq. 6.1}$$

The schematic illustration of how the Ra is calculated can be seen in the following figure.
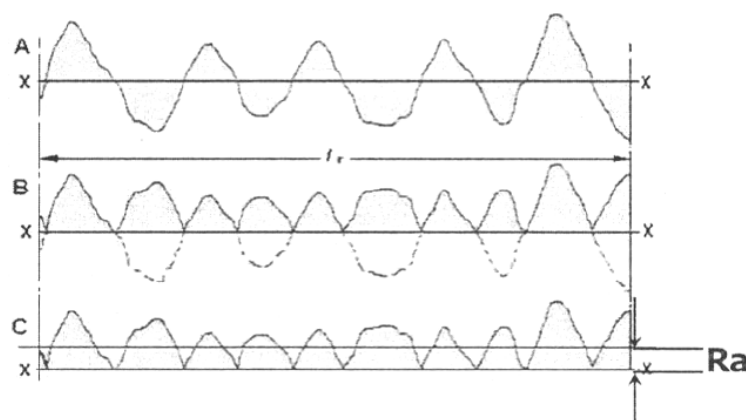

Fig. 6.2 – Schematic illustration of Ra evaluation [51]

One has to be careful when using a parameter Ra for evaluation of the surface roughness. This parameter tells us only the nominal value of the result; it does not say anything about the real profile of the measured surface.

Pick-up systems

First, with a datum system, this is a ground bar capable of measuring form waviness, surface finish, radius and angle. Second with a skid based datum system. The datum is established by resting a skid on to the surface being measured on [51].

a)   b)
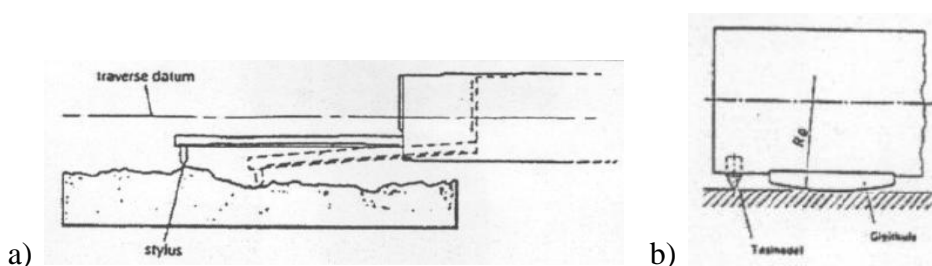
Fig. 6.3 – Stylus instruments with: a) stylus following the surface; b) skid [51]

6.3   Hole geometry

First of all, a CAD model of the fixture for holding the specimens is designed and created in ProEngineer and consequently transformed into Calypso software. Calypso software is a program for automatic motion of the CMM's probe.
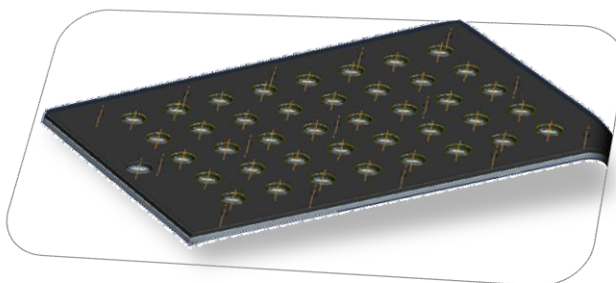
Fig. 6.4 – CAD model of the fixture

Secondly, the alignment is carried out and consists of a plane which is the top surface of the fixture and a 3D line which is defined by connecting axes of two cylinders.

Using Calypso software, 40 cylindrical features are created, representing 40 holes on the fixture. In this way, specimens can be placed at any position on the fixture. One

additional feature is created for measurements on reference ring (RR). In each hole, four features (i.e. circles), are created, representing positions where hole diameter, roundness and cylindricity are measured. This can be seen in Fig. 6.5 and Fig. 6.6.

For RR, only 3 circles are created at distance 3, 10 and 12 from top face of the workpiece.
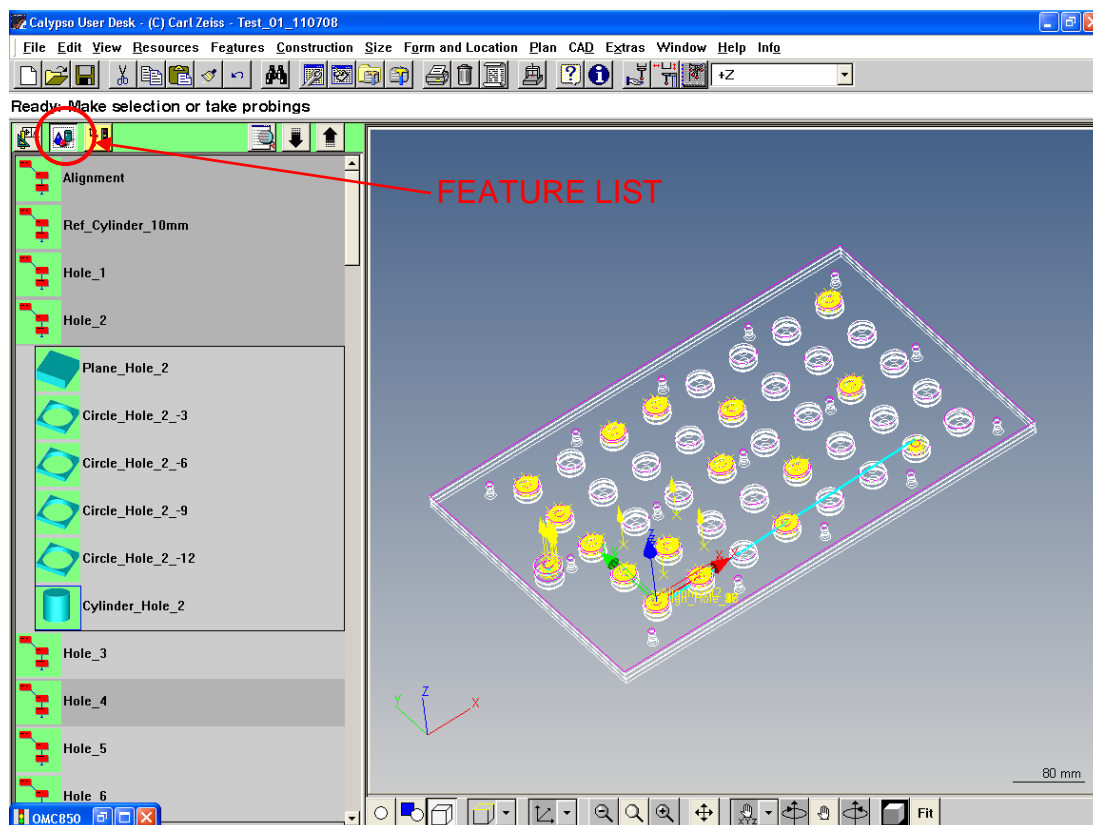
Fig. 6.5 – Calypso interface, selecting specimens from the feature list

By selecting the features (individual holes representing specimens) from the feature list, the program is automatically able to recognize where the specimens are to be measured. Changing an option from "features list" to "characteristic list" one is able to define individual geometrical specifications on the corresponding features (see Fig. 6.6). Roundness and diameter are measured on each circle feature and cylindricity is measured on a cylindrical feature which is defined and formed by corresponding circles placed at four levels on the workpiece.

From Fig. 6.5 one can notice that measurement begins by making the alignment and continue with measuring RR and lastly measuring specimens in the sequence of where they are placed on the fixture. After every measurement, geometrical tolerances are selected from the characteristic list (see Fig. 6.6) and the results are printed out.
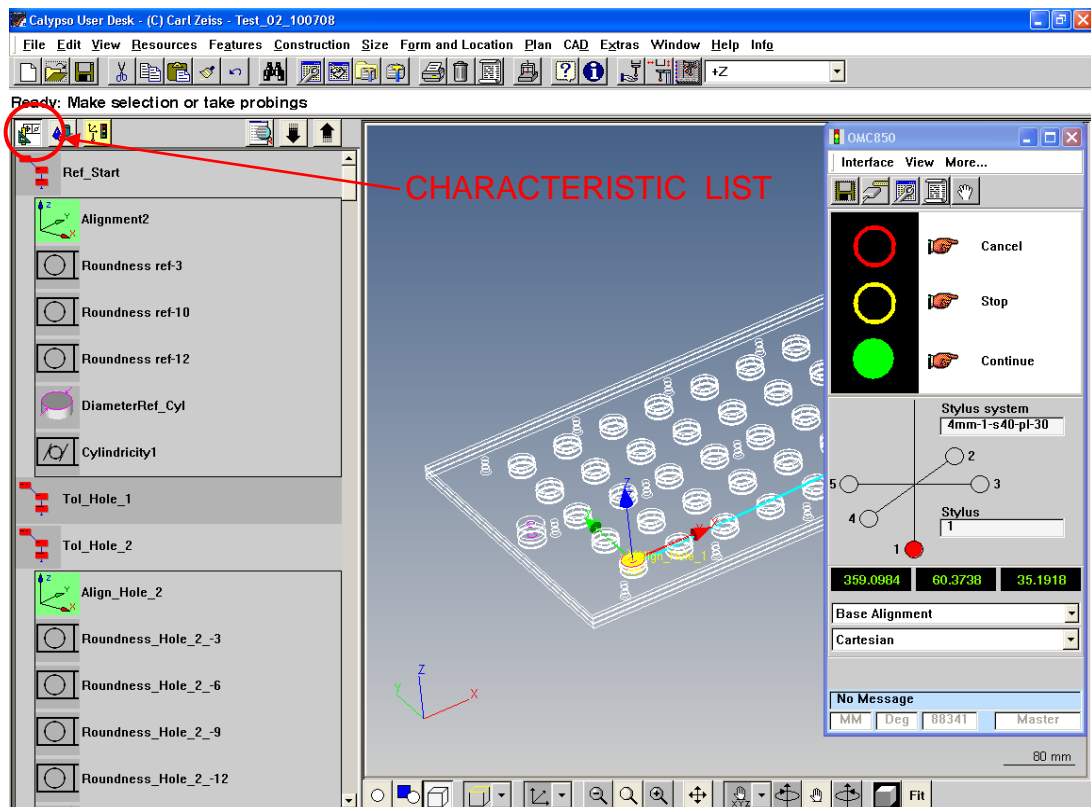
Fig. 6.6 – Calypso interface, defining of geometrical features from the characteristic list

Test procedure for geometrical specification using CMM:

- Specimens are measured at 4 levels, at distance 3, 6, 9 and 12 mm from the bottom face of the cylinder (see Fig. 6.7).
- 8 points are probed around the hole circumference at each level of the workpiece.
- A total of 32 points are probed per workpiece.
- Every test series (pilot or reamed holes) is measured five times.
- For each measured circle, a form error (roundness) is calculated.
- Based on 4-level strategy, a form error (cylindricity) is calculated.
- All three measurands (diameter, cylindricity and roundness) are calculated based on minimum zone method.
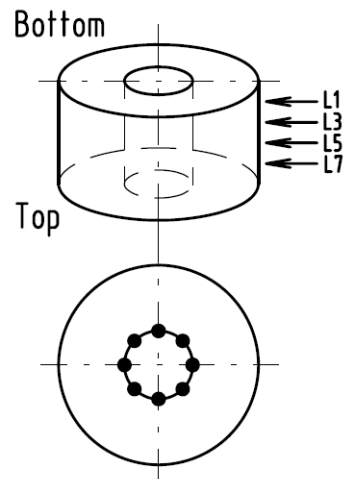
Fig. 6.7 – Measuring strategy on the workpiece

6.4 Surface roughness

24 profiles are recorded for each specimen, distributed at equal angles around the circumference, turning the workpiece 90° and repeating each measurement three times. The average value is then calculated. The measurement is performed at two positions on the workpiece over a length 4 mm and with 0.8 mm ISO filtering [54] as shown in Fig. 6.8, starting at position A and consequently measured at position B.
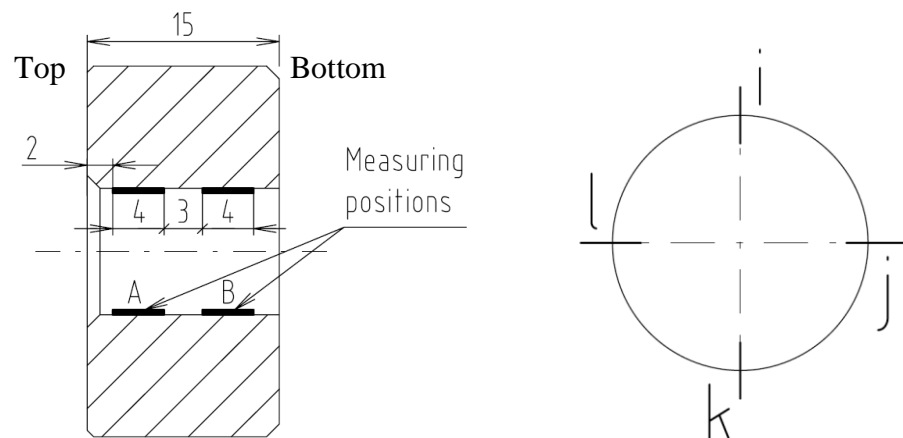
Fig. 6.8 - Surface roughness measurement positions

6.5 Thrust and Torque

For each reamed hole the average reaming thrust and reaming torque is calculated. The average reaming thrust and reaming torque are derived from the recording that is indicated in Fig. 6.9 as a window span. Window span is defined between two points that are placed around the part of the curve that is stable, taking into account half of the

time that the reamer interacts with the workpiece. This is influenced by the feed rate at which the reamer moves in z direction. This means, that if the feed increases, the time needed for the reamer to machine the workpiece is shortened. Therefore the window span, where the measurands are evaluated, is shortened as well, so that the average values are calculated from fewer points.

Reaming time is calculated according to the following formula:

$$t = \frac{L}{v_f}$$

Eq. 6.2

Fig. 6.9 – Window span for determination of the mean thrust and torque

CHAPTER 7 - PILOT HOLE QUALITY MEASU-REMENT AND UNCERTAINTY BUDGET DE-VELOPMENT

7.1   Pilot hole manufacturing quality

This chapter is concerned with metrological considerations in product quality measurements. By the term "product quality" both geometrical specifications and surface topography of the hole is denoted.

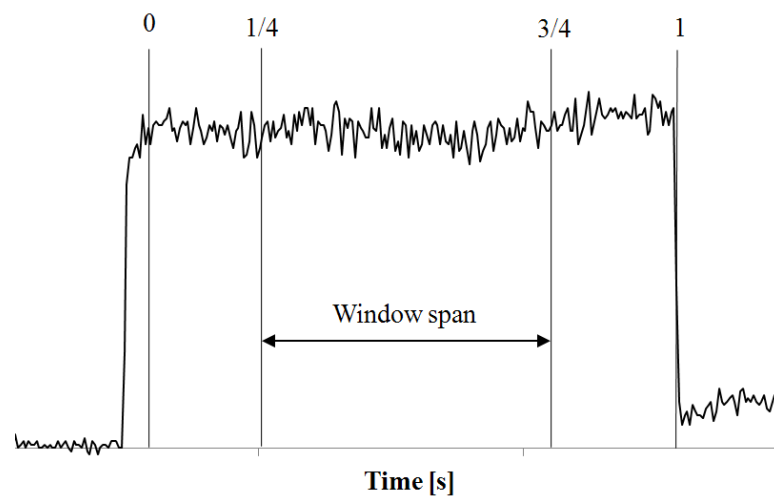In order to have reliable results, an uncertainty budget for both considerations is created.

When carrying out experimental investigations, it is often found that experimental dispersions can be rather large, when compared to the average values of results from a single experiment and to the variation due to different experimental conditions. Other source of error exists when performing data analysis. Since the hole product quality depends on cutting parameters such as cutting speed, feed rate and depth of cut into certain degree, they do present a deviation from the programmed values and are not constant during the cutting process, therefore resulting in an influence on measurement uncertainty. Other sources of variability are also associated with the process itself, e.g. temperature in the workshop, temperature in the laboratory, workpiece material, tool and workpiece geometry and alignment, machine etc. [11].

7.2   Geometrical specifications of pilot hole

Pilot hole measuring procedure for dimensional specification:

The procedure for hole geometry assurance includes five measurements in total and the measuring strategy as described in 6.3 is followed. Each measurement on CMM is different from each other (see Tab. 7.1). This is done for the purpose of estimating the measurement reproducibility.

Tab. 7.1 – Quality assurance measuring procedure for pilot holes

Test 1	15 specimens clamped in the fixture at random positions.
Test 2	The screws holding three aluminum plates together are released a bit to check whether such clamping and developed forces can release the compression of o-rings and thus move the workpiece while probing.
Test 3	The clamping fixtures holding the aluminum fixture is unmounted, the whole aluminum fixture is removed from its original position and is placed back at the same place.
Test 4	Specimens are randomly repositioned in the fixture.
Test 5	The same procedure as for *Test 4* is repeated.

Temperature during measurements remained constant during the whole measuring process, and is 20±1°C.

An uncertainty budget is created for geometrical specification (diameter - D, round-ness - R, cylindricity – C) of the pilot hole including uncertainty contributors related to the CMM machine.

Uncertainty calculation using ISO 15530-3 [55]:

ISO 15530-3 describes the procedure for uncertainty assessment consisting on carry-ing out repeated measurements on calibrated workpiece, with same conditions of ac-tual measurands and then calculating the uncertainty. The experimental method for uncertainty assessment is based on the substitution of the component to be provided with uncertainty estimation with a calibrated workpiece. The uncertainty of the pilot hole (U_{Hole}^P) is calculated in the following way:

$$U_{Hole}^P = k \cdot \sqrt{u_{cal}^2 + u_p^{P\,2} + u_w^{P\,2}} + |b'| \qquad \text{Eq. 7.1}$$

In the following sections uncertainty contributors are discussed.

7.2.1 Standard uncertainty of calibration u_{cal}

The calibration is performed on a high precision coordinate measuring machine CA-RAT.

Tab. 7.2 – Uncertainty of CMM on CARAT

	D	R	C
u_c	0.00035	0.00040	0.00040
u_p	0.00034	0.00051	0.00069
u_{cal}	0.00049	0.00065	0.00080
U_{cal} *(k=2)*	**0.0010**	**0.0013**	**0.0016**

Note: All values are in mm

7.2.2   Standard uncertainty u_p^P

Standard uncertainty u_p is divided into two uncertainty portions, performing experimental investigation based on varying measuring strategy and positioning specimens on different positions in the fixture. A maximum value out of both portions is then taken into account for uncertainty calculation.

Standard uncertainty u_{p1}^P is calculated experimentally measuring reference ring (RR) and pilot hole. Four experiments are performed for both types of rings, based on different measuring strategies as can be seen in Fig. 7.1. These strategies are based on varying number of levels and number of points which are probed around the hole circumference. A randomly chosen workpiece from the batch is selected and used for the experiment.
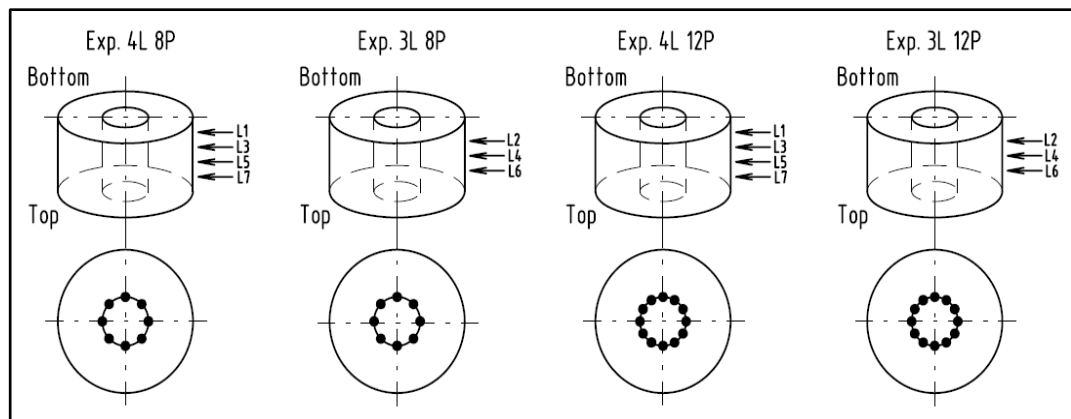

Fig. 7.1 – Measuring strategy for standard uncertainty u_{p1} uncertainty assessment

Tab. 7.3 - Results of the influence of strategy and machine on RR and pilot hole

RR	1	2	3	4	$u_{strategy}$	1	2	3	4	$u_{machine}$
D	10.0005	10.0005	10.0007	10.0007	0.00011	0.00016	0.00025	0.00022	0.00019	0.00025
R	0.0010	0.0012	0.0012	0.0012	0.00009	0.00030	0.00035	0.00029	0.00021	0.00035
C	0.0011	0.0012	0.0012	0.0012	0.00005	0.00026	0.00035	0.00023	0.00020	0.00035
Pilot hole	1	2	3	4	$u_{strategy}$	1	2	3	4	$u_{machine}$
D	9.9059	9.9057	9.9060	9.9058	0.00013	0.00034	0.00033	0.00035	0.00027	0.00035
R	0.0017	0.0013	0.0018	0.0016	0.00019	0.00021	0.00040	0.00038	0.00020	0.00040
C	0.0039	0.0026	0.0040	0.0032	0.00068	0.00013	0.00042	0.00036	0.00013	0.00042

Note:
- All values are in mm
- 1 - *4L 8P*; 2 - *3L 8P*, 3- *4L 12P*, 4 - *3L 12P*

Individual measurement data of present investigation can be found in the Appendix A (Tab. A.1 and Tab. A.2).

Based on these calculations, which are summarized in Tab. 7.3, it is possible to withdraw several conclusions regarding the measuring strategy. In particular:

- The influence of number of points on measuring strategy can be best seen when looking at results from measurements of roundness on RR. It is found that no matter whether 8 or 12 points are probed around the circumference, no deviation in results is observed.

- From a point of view of number of levels, there is no significant difference in the results looking at the results from measurements of cylindricity on RR. This means that choosing 3- or 4-level strategy does not play a role.

- Concerning the measurements on pilot hole, a difference in results is more clear. It can be observed that strategy *3L 8P* performs the best strategy for measurements since it gives the smallest uncertainty (i.e. smallest standard deviation).

- However measuring strategy used for evaluation of D, R and C for all pilot and reamed holes (*4L 8P*) gives more information about the hole profile since there is loss of information using measuring strategy *3L 8P*.

Maximum value $u_{p1}^{P} = \max(u_{strategy}, u_{machine})$ out of these uncertainty contributors for diameter, roundness and cylindricity is taken into account for further uncertainty evaluation.

Standard uncertainty u_{p2}^{P} investigates the influence of the workpiece positioning (*space accuracy*) in the fixture on different positions. Five specimens in total positioned on three different positions within the fixture are used for this investigation. Da-

ta from this measurement can be found in the Appendix A (Tab. A.4.1 and Tab. A.4.2).

Tab. 7.4 – Space accuracy results for standard uncertainty u_p^P assessment

	D	R	C
u_{p2}^P	0.00025	0.00020	0.00026

Note: All values are in mm

7.2.3   Standard uncertainty u_w^P

Calculation of temperature related uncertainty is performed for a maximum possible change in temperature ±1.0°C. This is based on the fact that the laboratory is an accredited laboratory with controlled temperature of 20°C. A contribution of a person being in the room when performing measurements has to be taken into account. A formula for diameter change taking into account a change in temperature ±1.0°C can be seen below.

$$u_w^P = \alpha \cdot \Delta T \cdot D \qquad\qquad \text{Eq. 7.2}$$

Tab. 7.5 – Diameter variation due to temperature difference for standard uncertainty u_w^P assessment

	RR	Pilot
D	0.11000	0.15851
R	0.00001	0.00003
C	0.00002	0.00008

Note: All values are in μm

Tab. 7.6 – Temperature expansion coefficients

α	α (10^{-6} m/m°C)
steel	11
austenitic SS (316)	16

7.2.4   Systematic error b'

Systematic error is calculated as a difference between the values from calibration certificate and measured values at three levels of the RR. Then the average values for diameter, roundness and cylindricity are calculated.

Tab. 7.7 – Systematic error results *b'*

	From calibration certificate		
Level	D	R	C
-3	10.0011	0.0015	0.0017
-10	10.0018	0.0012	0.0017
-12	10.0024	0.0005	0.0017
b	0.00117	0.00043	0.00056

Note: All values are in mm

7.2.5 Expanded combined uncertainty

Summarizing all above mentioned, one can calculate U_{Hole}^{P} uncertainty. An uncertainty budget including all uncertainty contributors can be seen in Tab. 7.8.

Tab. 7.8 – Uncertainty budget for pilot hole measurement on CMM

No.	Uncertainty component category	Uncertainty component	Symbol	Standard uncertainty [mm]		
				D	R	C
1	Reference	Uncertainty of calibration	u_{cal}	0.00049	0.00065	0.00080
2	Procedure	Uncertainty of strategy	u_p^P	0.00035	0.00040	0.00068
3	Environment	Temperature difference	u_w^P	1.6E-04	3.0E-08	7.7E-08
4	Systematic error		*b'*	0.00117	0.00043	0.00056

Standard combined uncertainty [mm]	u_{Hole}^{P}	0.00062	0.00076	0.00105
Coverage factor (for a confidence level of 95%)	k	2	2	2
Expanded combined uncertainty [mm]	U_{Hole}^{P}	**0.0024**	**0.0020**	**0.0027**

7.2.6 Pilot hole geometry measurement results and discussion

Data from the measurement of hole diameter, roundness and cylindricity can be found in the Appendix E on the CD attached to the report.

Following data are calculated on the basis of an average from 4-level measurement strategy, a total of 15 specimens and 5 different tests. The bars represent expanded measuring uncertainty of the hole calculated earlier in this section.
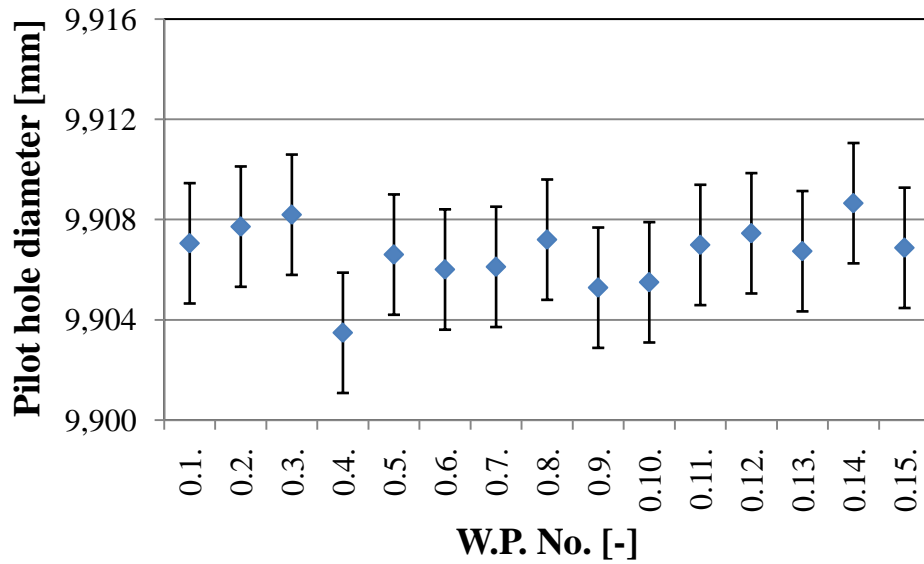
Fig. 7.2 – Pilot hole diameter results

From the results in figures Fig. 7.2, Fig. 7.3 and Fig. 7.4 one can observed a good reproducibity of measurement which is obvious looking at average values for all three measurands. When taking into account measuring uncertainties U_{Hole}^{P}, all values represent very consistent and reliable results which is based on a good repeatability of the CMM.
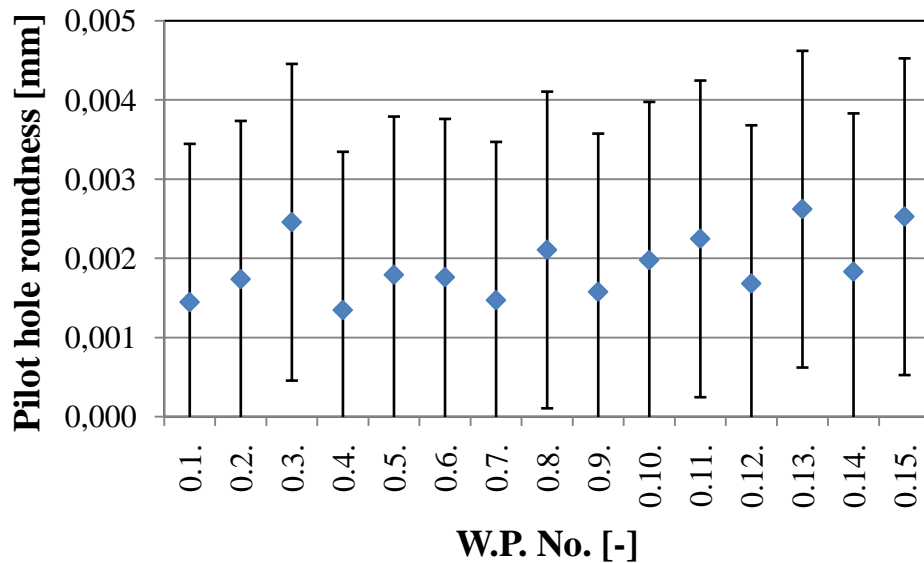

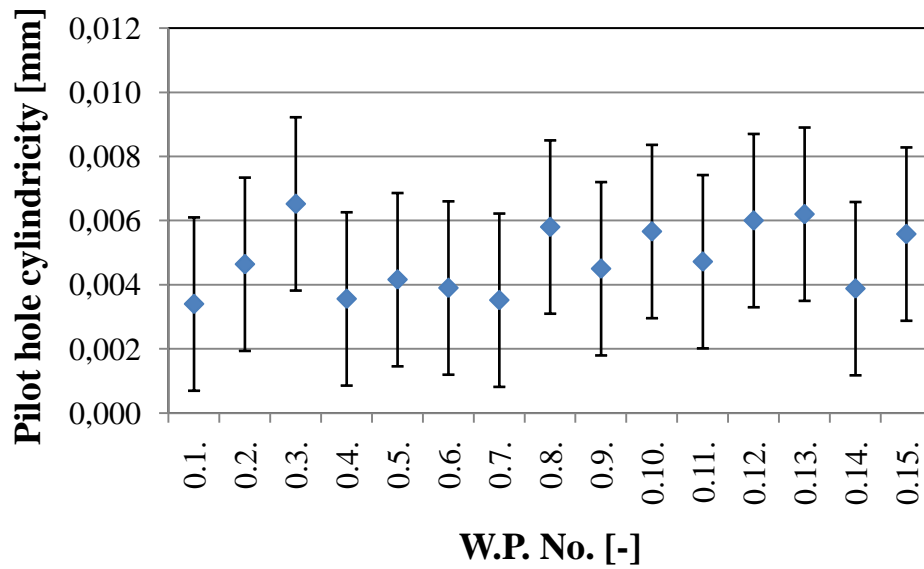Fig. 7.3 – Pilot hole roundness results

Fig. 7.4 – Pilot hole cylindricity results

When combining measurement uncertainty with an uncertainty resulting from the process, such uncertainty can be calculated as follows:

$$U_{total}^P = k \cdot \sqrt{u_{Hole}^P{}^2 + u_{process}^P{}^2} \qquad \text{Eq. 7.3}$$

Tab. 7.9 – Total uncertainty for pilot hole

	D	R	C
u_{Hole}^P	0.0012	0.0010	0.0013
$u_{process}^P$	0.0013	0.0004	0.0011
U_{total}^P	0.0035	0.0021	0.0034

Note: All values are in mm

From the results displayed both numericaly (Tab. 7.9) and graphically (Fig. 7.5) one can observe the reliability of the measurement and uncertainty with which the specimens are taken from the batch with corresponding hole quality.

The resutls also show that measured holes with calculated uncertainty fall within the tolerance of the hole taking randomly 15 specimens from the batch.
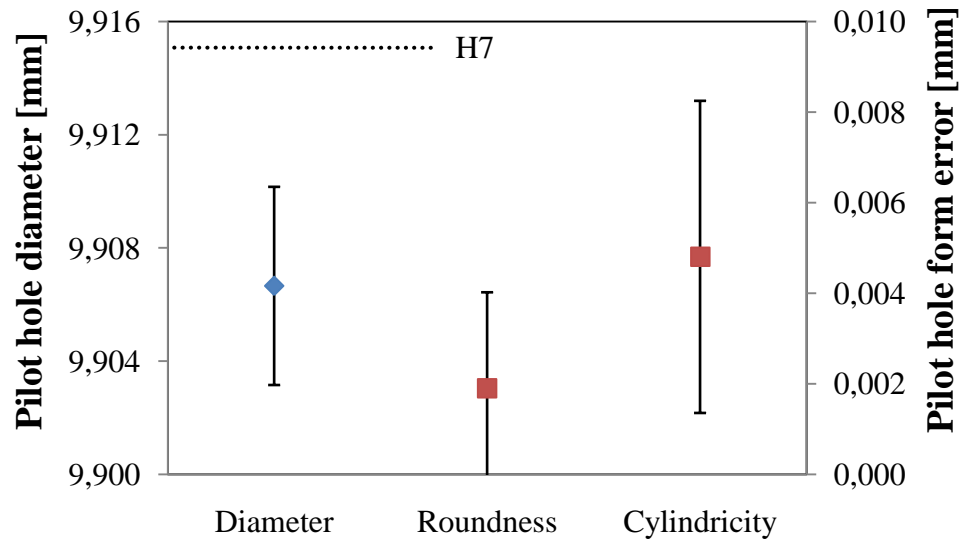
Fig. 7.5 – Pilot hole measurement results (process)

The general shape based on 4-level measurement can be seen in the following figure together with the concrete values of diameter. The highest difference in diameter can be observed to be 3.9 µm.
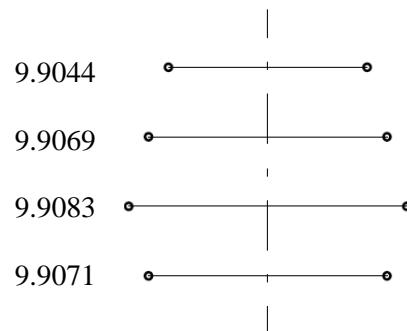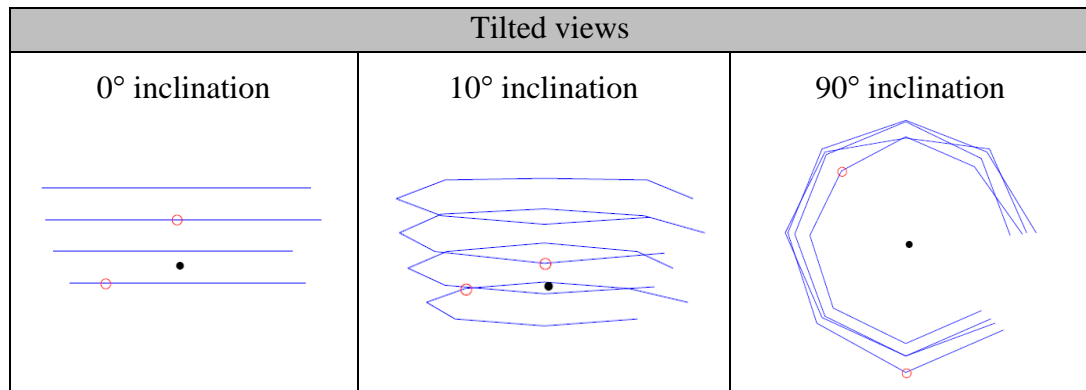

Fig. 7.6 – General shape of the pilot hole

Fig. 7.7 – Tilted views of workpiece profiles on CMM under different inclination angles

7.3   Surface topography

First of all, the stylus instrument is calibrated. This is done by measuring the background noise level of the stylus instrument. 12 measurements are performed using 10 µm measuring range and a cut-off 0.8 mm. Ra values were calculated during sampling of an ideally perfect plane optical glass plate WB 75/BL.

Using ISO type C standard [56] with the certified uncertainty U_n, a calibrated value and a measured surface roughness on reference standard at different locations, the correction factor (CF) is calculated as a ratio of Ra value from calibration certificate and average value of 15 measurements on different spots of reference standard (CF = 0.95). Using this CF, all measured values are multiplied by this value.

Measurements are performed following the proposed measuring strategy as described in section 6.4.

An uncertainty budget for surface roughness Ra is created calculating the uncertainty for pilot hole.

The formula for uncertainty budget of Ra for pilot hole is expressed in Eq. 7.4.

$$U^P_{Gen} = k \cdot \sqrt{u^2_{instr} + u^{P}_{Gen(abc)}{}^2} \qquad \text{Eq. 7.4}$$

7.3.1   Instrument uncertainty using ISO type C standard

The uncertainty budget consists of three components that are calculated from knowledge about: the reference artifact calibration uncertainty, the instrument repeatability and the background noise level. Formula for instrument uncertainty is expressed as follows:

$$U_{inst} = k \cdot \sqrt{u^2_n + u^2_r + u^2_b} \qquad \text{Eq. 7.5}$$

where

- $u_n = \frac{U_n}{2}$ uncertainty of the standard;
- $u_r = \frac{STD_r}{\sqrt{n}}$ uncertainty on the transfer of traceability (repeatability of the instrument). *N* is the number of measurements in the same track with standard deviation *STD*$_r$;
- $u_b = \frac{1}{2} \cdot \frac{Ra0}{\sqrt{3}}$ uncertainty caused by the background noise (*Ra0* is the measured background noise which is an average of measurements on the optical flat and assuming rectangular distribution).

Tab. 7.10 – Uncertainty components for surface roughness uncertainty assessment

Indication	Calculated value
u_n	0.006
u_r	0.001
u_b	0.004

Note: All values are in μm

7.3.2   Standard uncertainty due to roughness repeatability of the specimen

Standard uncertainty caused by variations in the roughness of the specimen at different locations $u_{Gen(abc)}^{P}$ is calculated as follows:

$$u_{Gen(abc)}^{P} = max(STD) \qquad\qquad \text{Eq. 7.6}$$

where *max(STD)* is a maximum value of standard deviation taking into account three following contributions:

(a) 15 specimens
(b) 3 repetitions at the same position on the specimen (measurements performed on the same specimen)
(c) 4 repetitions around the circumference (measurements performed on the same specimen)

7.3.3   Pilot hole roughness measurement results and discussion

Data from the measurement of surface roughness as well as profiles can be found in the Appendix F and Appendix H respectively placed on the CD attached to the report.

Several conclusions can be withdrawn (see Fig. 7.8):

- The surface roughness does not exceed 1 μm in any case, which results in well pre-manufactured hole quality.

- The uncertainties in Fig. 7.8 are those calculated as a maximum values taking into account an uncertainty of repeatable measurements on the same position and uncertainty of measurement around the circumference. The latter is an uncertainty contributor having the biggest influence on surface quality. However, when taking into consideration an uncertainty of the process itself, this has no influence on the uncertainty. This can be seen in Tab. 7.11 below.
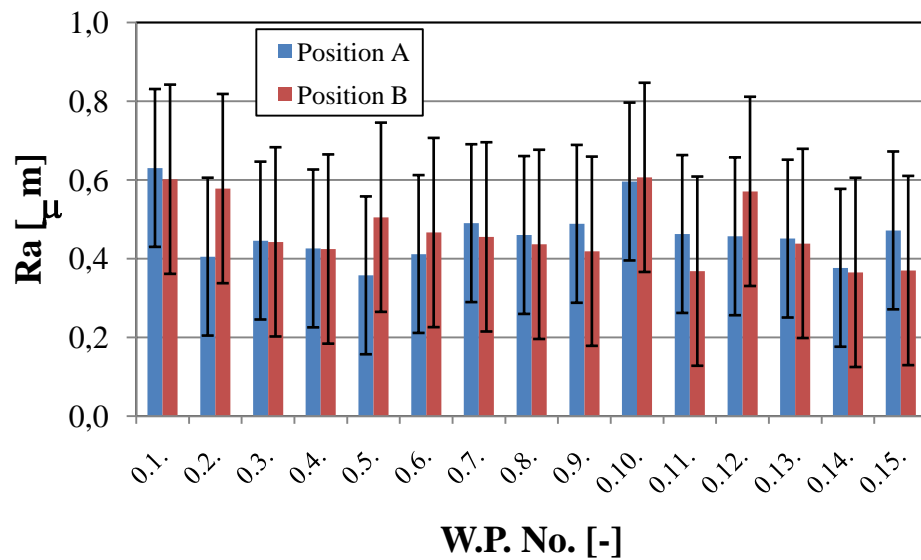

Fig. 7.8 – Surface roughness measurement results for pilot holes (without process)

Tab. 7.11 – Uncertainty budget for pilot hole measurement on stylus

No.	Uncertainty component category	Uncertainty component	Symbol	Standard uncertainty [µm]	
				A	B
1	Reference	Uncertainty of instrument calibration	u_{inst}	0.007	0.007
2	Procedure	Uncertainty of the process	$u_{Gen(a)}^{P}$	0.055	0.084
		Uncertainty of repeatable measurement on the same position	$u_{Gen(b)}^{P}$	0.031	0.045
		Uncertainty of measurement around the circumference	$u_{Gen(c)}^{P}$	0.088	0.120

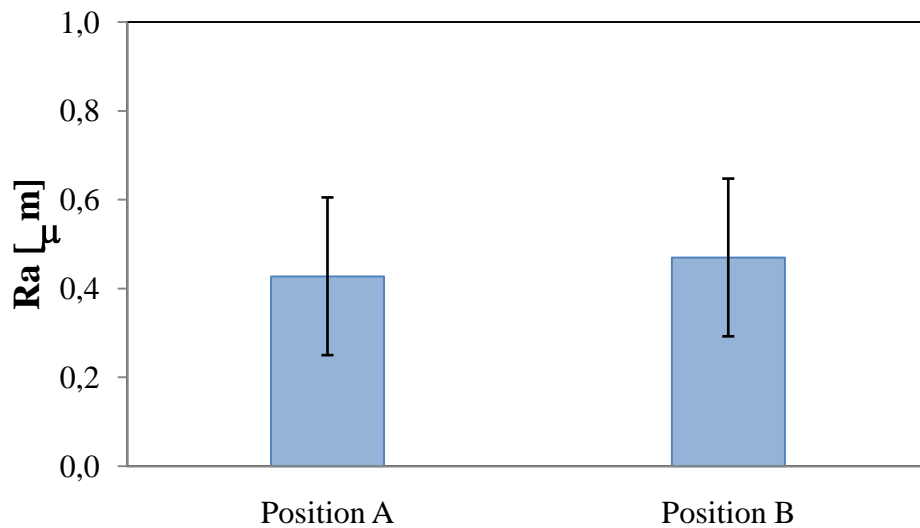|			
Standard combined uncertainty [µm]	u_{GEN}^{p}	0.09	0.12
Coverage factor (for a confidence level of 95%)	k	2	2
Expanded combined uncertainty[µm]	U_{GEN}^{p}	**0.18**	**0.24**

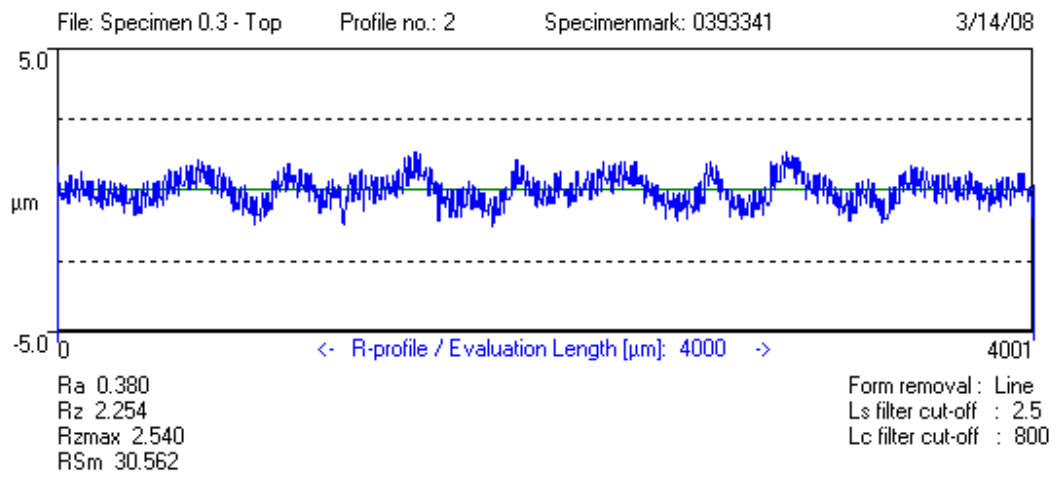Fig. 7.9 – Surface roughness measurement results for pilot holes (process)

Fig. 7.10 – Typical surface roughness profile of pilot hole

CHAPTER 8 - REAMING TESTS AND UNCERTAINTY BUDGET FOR REAMED HOLES

8.1 Introduction

This chapter contains the experimental results from cutting fluid performance evaluation in reaming for a stainless steel work material. The measurements and evaluation of reaming thrust and reaming torque are carried out as well as consequent hole quality evaluation that is influenced by all present factors when the cutting tool comes into contact with the workpiece. It has been stated in previous works that the cutting fluid performance has a significant effect on hole quality when higher cutting forces result during machining.

Six reaming test runs were carried out, characterized by different cutting conditions and setup.

8.2 Overview of the tests

The table below presents the sequence of reaming operations with varying cutting parameters. As an initial step of choosing cutting conditions for the first reaming operation (R1), the recommended process parameters set-up conditions from the tool manufacturer is employed.

Tab. 8.1 – Overview of the tests

Parameter	Symbol	Unit	Reaming operation					
			R1	R2	R3	R4	R5	R6
Reamer diameter	D_R	mm	10.1	10.1	10.1	10.0	10.1	10.1
Cutting speed	v_C	m/min	5	5	5	5	5	6
Revolutions	N	rev/min	158	158	158	159	158	189
Feed	f	mm/rev	0.315	0.315	0.21	0.21	0.21	0.21
Feed rate	v_f	mm/min	49.7	49.7	33.1	33.4	33.1	39.7
Type of feed rate			slow	rapid	rapid	rapid	rapid	rapid
Cutting time	t	sec	18.1	18.1	27.2	26.9	27.2	22.7
Temperature	T'	°C	26	28	28	25	28.5	28
Depth of cut	a_P	mm	0.1	0.1	0.1	0.05	0.1	0.1
Pressure	p	bar	6	6	6	6	6	6
Oil flow	Q	ml/h	50	60	55-60	50	55-60	
Nozzle positioning			TB	TB	TB	TB	TT	TB
Cutting fluid			C/Al Lenow Lube					

Note:

- Temperature is measured during the cutting operation and is found to be always ± 0.5°C.
- TB: Nozzle positioning from top and bottom, TT: Both nozzle positioned from top.
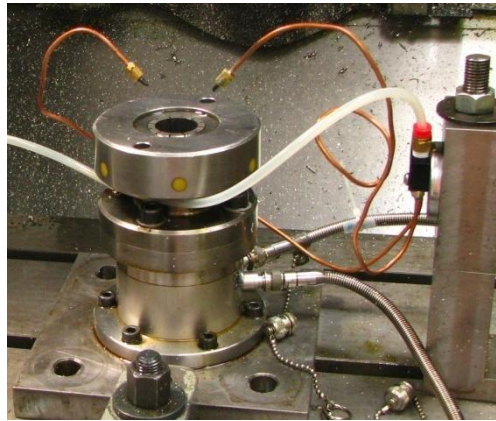

Fig. 8.1 – Reaming operation R5 with top nozzle positioning

All the tests are carried out using HSS-E COBALT reamers, 10.1 mm and 10.0 mm respectively, which dimensions are measured before every reaming operation using a micrometer. The results of the measurements can be seen in Tab. D.1 in the Appendix D. The positions where the reamer diameter is measured can be seen on Fig. 8.2. There is a slight inclination observed when measuring between two positions on the reamer. Bigger diameter of the reamer is found closer to the tool tip.
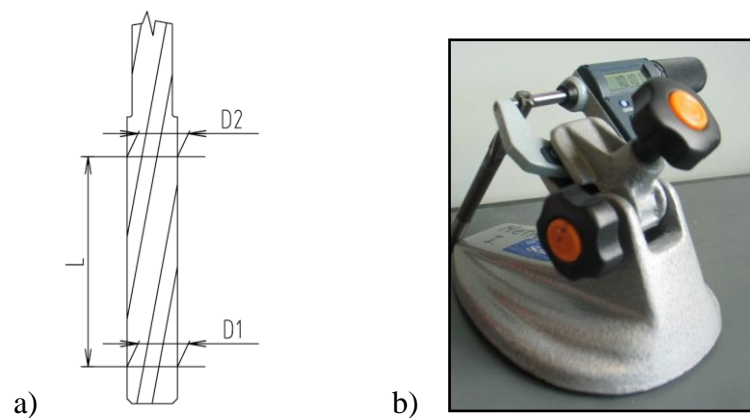

a)   b)

Fig. 8.2 – a) Measuring positions on the reamer (L=30 mm; b) Micrometer for reamer diameter measurement

MQL conditions are maintained constant throughout all reaming operations. The lubrication is turned off after each specimen is reamed. A fluid shut-off valve that is mounted to the unit enables the unit to maintain the system prime and provide instant lubrication.

Oil flow is always estimated based on the curve showing a dependence of oil flow on temperature. This can be observed in Fig. 5.8 in section 5.3.

8.3   CNC code for reaming operation

In order to run the reaming process, a CNC code is created on CNC machine, see following:

O5001
G 59 G90 G17 G0 G43 H2 X0 **Y**0 **Z5 S158 F33.18 M3**
G1 Z-25
G0 Z10
G28 Z0 M5
M30

From above mentioned CNC code one can observe (see Fig. 8.3) that the reamer starts working 5 mm above the workpiece zero point and goes 25 mm in $-z$ direction, i.e. 10 mm below the bottom face of the workpiece and then rapid traverse returns the tool to machine 0 point.
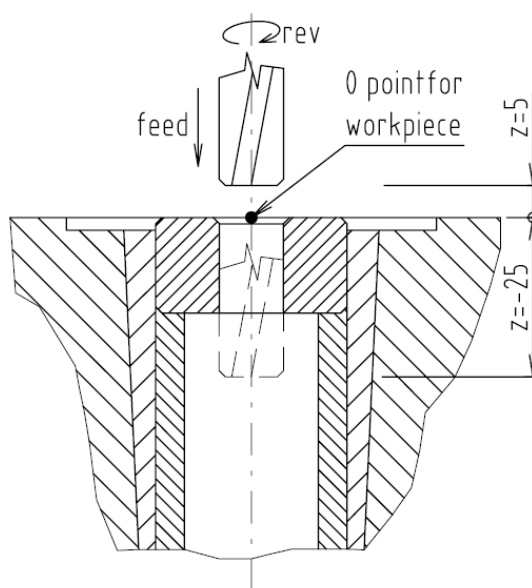

Fig. 8.3 – Reaming operation (CNC program)

P a g e | **83**

8.4   Reaming procedure

The general reaming test procedure is described below:

1) Warm up of the machine.
2) CNC program selection.
3) Reamer clamping into the tool holder.
4) Specimen clamping into the fixture and fastening.
5) Nozzles positioning.
6) MQL system start up in order to warm up and to reach constant conditions (oil flow).
7) Setup of the data acquisition system.
8) Start of the reaming operation.
9) After each reaming operation, the lubrication is turned off, the workpiece is re-leased from the fixture and replaced by a new one.
10) Repetition of the whole cycle for all 15 specimens.

8.5   Geometrical specifications of reamed holes

An uncertainty budget is created for geometrical specification of the reamed hole in-cluding uncertainty contributors related to the CMM machine.

Reamed hole measuring uncertainty:

The same procedure as for pilot hole measuring uncertainty using ISO 15530-3, de-scribed in section 7.2, is followed, i.e. Eq. 7.1 is used for reamed hole measuring un-certainty. The uncertainty contributors are discussed in the following sections.

8.5.1   Standard uncertainty of calibration u_{cal}

Standard uncertainty of calibration is calculated as in section 7.2.1.

8.5.2   Standard uncertainty u_p^R

Standard uncertainty u_p^R is divided into two uncertainty portions. A maximum value out of both portions is then taken into account for uncertainty calculation.

Standard uncertainty u_{p1}^R is calculated experimentally measuring RR and reamed hole. Four experiments are performed for both types of rings, based on measuring strategy as described in section 7.2.2. A randomly chosen workpiece out of 15 after reaming operation R3 is selected and used for the experiment.

Tab. 8.2 - Results of the influence of strategy and machine on RR and reamed hole

RR	1	2	3	4	$u_{strategy}$	1	2	3	4	$u_{machine}$
D	10.0005	10.0005	10.0007	10.0007	0.00011	0.00016	0.00025	0.00022	0.00019	0.00025
R	0.0010	0.0012	0.0012	0.0012	0.00009	0.00030	0.00035	0.00029	0.00021	0.00035
C	0.0011	0.0012	0.0012	0.0012	0.00005	0.00026	0.00035	0.00023	0.00020	0.00035
Reamed hole	1	2	3	4	$u_{strategy}$	1	2	3	4	$u_{machine}$
D	10.1073	10.1072	10.1074	10.1076	0.00018	0.00027	0.00020	0.00043	0.00030	0.00043
R	0.0039	0.0033	0.0043	0.0040	0.00043	0.00026	0.00040	0.00040	0.00030	0.00044
C	0.0077	0.0052	0.0076	0.0057	0.00130	0.00021	0.00039	0.00048	0.00032	0.00048

Note:
- All values are in mm
- 1 - *4L 8P*; 2 - *3L 8P*, 3- *4L 12P*, 4 - *3L 12P*

Individual measurement data of present investigation can be found in the Appendix A (Tab. A.1 and Tab. A.3).

It can be observed that strategy *3L 8P* would be the best for measurements from point of view of both number of levels and number of points probed around the circumference.

Maximum value $u_{p1}^R = $ max ($u_{strategy}$, $u_{machine}$) out of these uncertainty contributors for D, R, and C are taken into account for the uncertainty evaluation.

Standard uncertainty $u_{p2}^R = u_{p2}^P$ (see section 7.2.2). Data from this measurement can be found in the Appendix A (Tab. A.4.1 and Tab. A.4.2).

8.5.3   Standard uncertainty u_w^R

Standard uncertainty u_w^R takes into account temperature-related uncertainty and is calculated in the same way as described in 7.2.3.

Tab. 8.3 – Diameter variation due to temperature difference for standard uncertainty u_w^R assessment

	RR	Reamed
D	0.11000	0.16172
R	0.00001	0.00005
C	0.00002	0.00012

Note: All values are in μm

8.5.4 Systematic error b'

Systematic error is calculated in the same way as described in section 7.2.4.

8.5.5 Expanded combined uncertainty

Summarizing all above mentioned, one can calculate U_{Hole}^R uncertainty. An uncertainty budget including all uncertainty contributors can be seen in Tab. 8.4.

Tab. 8.4 – Uncertainty budget for reamed hole measurement on CMM

No.	Uncertainty component category	Uncertainty component	Symbol	Standard uncertainty [mm]		
				D	R	C
1	Reference	Uncertainty of calibration	u_{cal}	0.00049	0.00065	0.00080
2	Procedure	Uncertainty of strategy	u_p^R	0.00043	0.00044	0.00130
3	Environment	Temperature difference	u_w^R	1.6E-04	4.6E-08	1.2E-07
4	Systematic error		b'	0.00117	0.00043	0.00056

Standard combined uncertainty [mm]	u_{Hole}^R	0.00067	0.00078	0.00153
Coverage factor (for a confidence level of 95%)	k	2	2	2
Expanded combined uncertainty [mm]	$\boldsymbol{U_{Hole}^R}$	**0.0025**	**0.0020**	**0.0036**

8.5.6 Measuring uncertainty on reamer diameter

The measurement of reamer diameter is carried out before the reamer is used for each reaming operation. A 10 mm gauge block is used to check the validity of the measurement. All measuring results of reamer diameter and gauge block (GB) can be found in the Appendix D. The expanded combined uncertainty for a confidence level 95% is calculated in the following way:

$$U_{RD}^{Rn} = k \cdot \sqrt{u_{GB(cal)}^2 + u_{reamer}^2 + u_{res}^2 + u_{temp}^2} \qquad \text{Eq. 8.1}$$

where:

- $u_{GB(cal)}$ is the standard uncertainty related to the calibration of the gauge block is found to be 0.00012 mm.

- u_{reamer} is the standard uncertainty resulting from the measurement on the reamer diameter is standard deviation based on ten repeated measurements. This value is always found to be bigger than a standard deviation of measurements on GB taking also ten repeated measurements.

- u_{res} is the standard uncertainty resulting from the micrometer resolution is calculated assuming rectangular distribution.

- u_{temp} is the standard deviation resulting from temperature compensation between micrometer and reamer is calculated in the following way:

$$u_{temp} = \alpha \cdot \Delta T' \cdot D_R \cdot b''$$ Eq. 8.2

Note: D_R is an average measured reamer diameter based on 10 repeated measurements.

Tab. 8.5 – Uncertainty of reamer diameter measurements

No.	Uncertainty component category	Uncertainty component	Symbol	Standard uncertainty [μm]					
				R1	R2	R3	R4	R5	R6
1	Reference artifact	Uncertainty of GB calibration	$u_{GB(cal)}$	0.1	0.1	0.1	0.1	0.1	0.1
2	Procedure	Uncertainty of reamer diameter	u_{reamer}	1.1	1.2	1.1	1.1	1.2	1.0
3	Micrometer resolution	Uncertainty of micrometer resolution	u_{res}	2.9E-04	2.9E-04	2.9E-04	2.9E-04	2.9E-04	2.9E-04
4	Environment	Temperature compensation	u_{temp}	0.4	0.4	0.4	0.4	0.4	0.4

Standard combined uncertainty [μm]	u_{RD}^{Rn}	1.2	1.2	1.1	1.1	1.2	1.1
Coverage factor (for a confidence level of 95%)	k	2	2	2	2	2	2
Expanded combined uncertainty [μm]	U_{RD}^{Rn}	**2.4**	**2.5**	**2.3**	**2.3**	**2.5**	**2.1**

8.5.7   Reamed hole measurement results and discussion

Data from the measurement of hole diameter, roundness and cylindricity can be found in the Appendix E on the CD attached to the report.

When combining measurement uncertainty with an uncertainty resulting from the process, such uncertainty can be calculated as follows:

$$U^R_{total} = k \cdot \sqrt{{u^R_{Hole}}^2 + {u^R_{process}}^2} \qquad \text{Eq. 8.3}$$

Tab. 8.6 – Total uncertainty for reamed hole

	R1			R2			R3		
	D	R	C	D	R	C	D	R	C
u^R_{Hole}	0.0012	0.0010	0.0018	0.0012	0.0010	0.0018	0.0012	0.0010	0.0018
$u^R_{process}$	0.0008	0.0008	0.0014	0.0004	0.0006	0.0007	0.0003	0.0006	0.0006
U^R_{total}	**0.0030**	**0.0025**	**0.0046**	**0.0026**	**0.0024**	**0.0039**	**0.0026**	**0.0023**	**0.0038**
	R4			R5			R6		
	D	R	C	D	R	C	D	R	C
u^R_{Hole}	0.0012	0.0010	0.0018	0.0012	0.0010	0.0018	0.0012	0.0010	0.0018
$u^R_{process}$	0.0004	0.0004	0.0006	0.0008	0.0007	0.0007	0.0005	0.0008	0.0011
U^R_{total}	**0.0026**	**0.0021**	**0.0038**	**0.0029**	**0.0024**	**0.0039**	**0.0027**	**0.0026**	**0.0042**

Note: All values are in mm
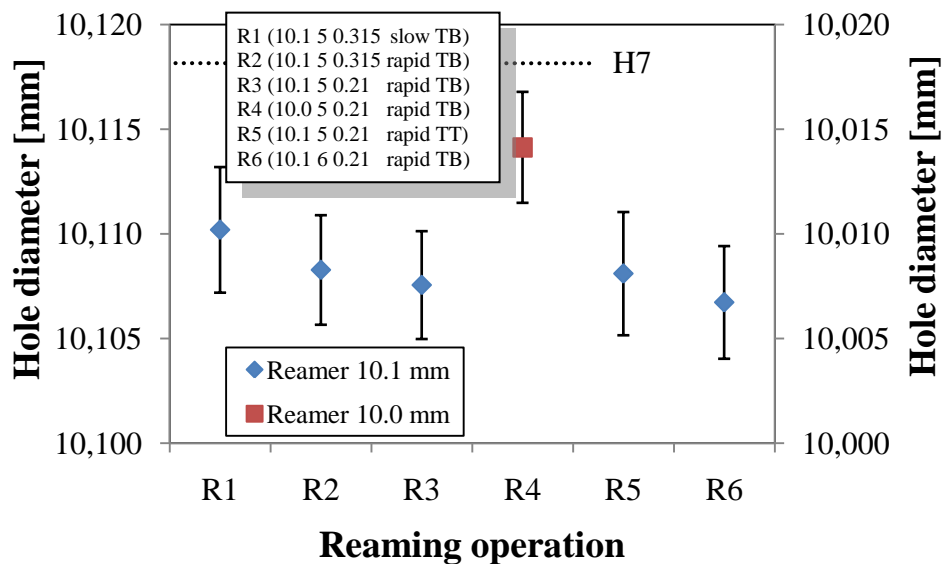
Fig. 8.4 – Reamed hole measurement results for diameter (process)

From the results displayed both numericaly (Tab. 8.6) and graphically (Fig. 8.4, Fig. 8.5 and Fig. 8.6) one can conclude several statements.

- First of all it has to be pointed out that all results of measured holes with calculated uncertainties fall within the tolerance of the hole taking 15 specimens into account, i.e the uncertainty of the manufacturing process is included.

- It is shown that individual reaming operations perform different results which is obvious when different cutting conditions and setups are used.

- First two reaming operations (R1 and R2, see Tab. 8.1) perform higher values for all three measurands. This is possibly caused due to significant change in feed rate, from 49.7 mm.min^{-1} (R1 and R2) to 33.1 mm.min^{-1} (R3), which prolongs the cutting time from 18.1 sec to 27.2 sec.

- Reaming operations R3 and R5 perform better and more consistent results than other reaming operations for all three measurands. Comparing these two reaming operations, reaming operation R5 is more convenient since the positioning of the nozzles is easier (both nozzles from the top).

- Reaming operation R4 performs larger diameter of the reamed hole which can be attributed to the small depth of cut.
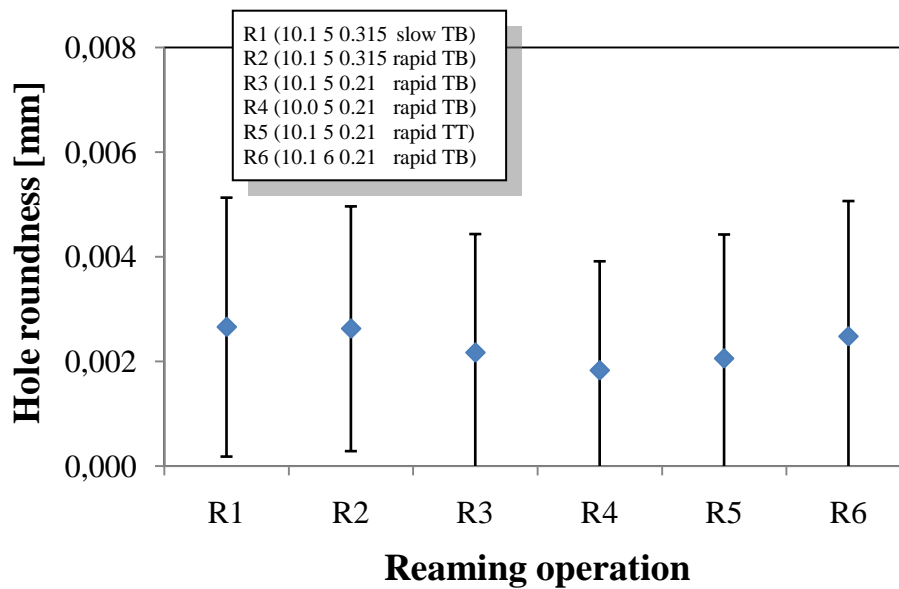
Fig. 8.5 – Reamed hole measurement results for roundness (process)
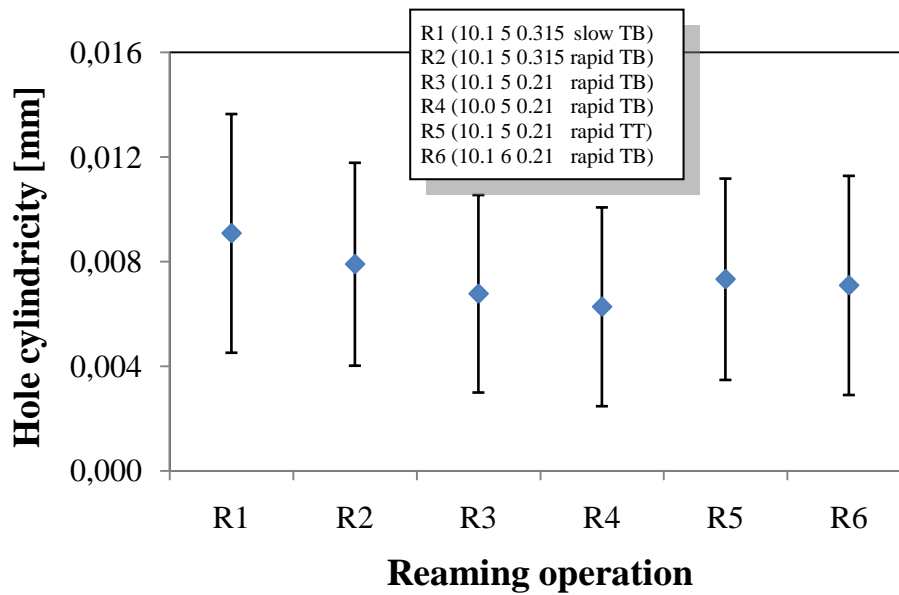
Fig. 8.6 – Reamed hole measurement results for cylindricity (process)

The general shape of reamed holes is as can be seen in Fig. 8.7. Such a shape can be explained by the fact that a material build-up is formed on the cutting edge and/or not sufficient chip evacuation from the cutting area.
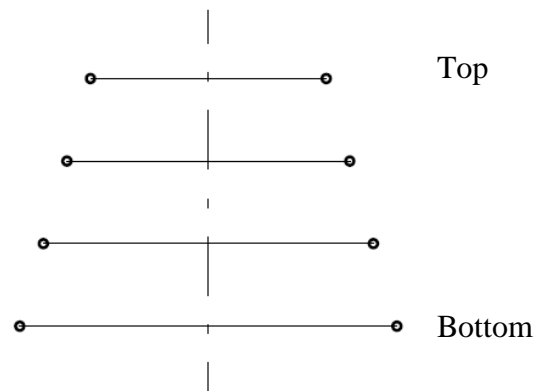
Fig. 8.7 – General shape of reamed holes

Graphs showing measurement results of diameter, roundness and cylindricity for individual reaming operations are shown in the Appendix A. The results are displayed together with their measuring uncertanties. It can be also found that some of the results perform outliers. All values for each reaming operation perform very good repeatability.

8.5.8 Conclusion

It can be concluded that every reaming operation brings along different behavior (see Fig. 8.5, Fig. 8.6, Fig. 8.7 and Fig. A.2 in the Appendix A where a detailed comparison between individual reaming operations is presented):

- However, all measured holes with calculated uncertainties fall within the tolerance of the hole taking 15 specimens into account, i.e taking into account the uncertainty due to the scatter of the manufacturing process.

- Not significant difference is observed among individual reaming operations since all the results are compatible within calculated uncertainties.

- The only reaming operation that performs a significantly larger diameter is R4. This is a result of a smaller radial depth of cut.

8.6　Surface roughness

All measurements are performed following the proposed measuring strategy as described in section 6.4.

An uncertainty budget for surface topography is created calculating the uncertainty for every reaming operation individually and consequently compared among each other.

The formula for uncertainty budget for reamed holes is expressed as follows:

$$U_{Gen}^R = k \cdot \sqrt{u_{instr}^2 + {u_{Gen(abc)}^R}^2} \qquad \text{Eq. 8.4}$$

Calculation of the instrument uncertainty is described in section 7.3.1.

8.6.1　Standard uncertainty caused by variations in the roughness of the specimen in different locations u_{Gen}^R

u_{Gen}^R is calculated as follows:

$$u_{Gen(abc)}^R = max(STD) \qquad \text{Eq. 8.5}$$

where *max(STD)* is a maximum value of standard deviation taking into account three following contributions:

(a) 15 specimens
(b) 3 repetitions at the same position on the specimen (measurements performed on the same specimen)

(c) 4 repetitions around the circumference (measurements performed on the same spe-
cimen)

8.6.2   Reamed hole roughness measurement results and discussion

Surface roughness at position A in average (see Fig. 8.7) is in all cases bigger than
when measuring at position B on the workpiece (only when calculating average values
since on single measurements the surface roughness at positions A and B performs
random behavior). This is caused due to possible material build up on the cutting edge
or unequal cutting oil delivery into tool/workpiece interface. The uncertainties in Fig.
B.1 in the Appendix B are those calculated as a maximum values taking into account
only uncertainty of repeatable measurements on the same position and uncertainty of
measurement around the circumference. However, when taking into consideration an
uncertainty of the process itself, this result in the uncertainty contributor having the
biggest influence on the result (see Tab. 8.7).

Tab. 8.7 – Uncertainty budget for reamed hole measurement on stylus

No.			1	2				Standard combined uncertainty [μm]	Coverage factor (for a c. l. of 95%)	Expanded combined uncertainty [μm]
Uncertainty component category			Reference	Procedure						
Uncertainty component			Uncertainty of instrument calibration	Uncertainty of the process	Uncertainty of repeatable measurement on the same position	Uncertainty of measurement around the circumference		Standard combined uncertainty [μm]	Coverage factor (for a c. l. of 95%)	Expanded combined uncertainty [μm]
Symbol			u_{inst}	$u_{Gen(a)}^{R}$	$u_{Gen(b)}^{R}$	$u_{Gen(c)}^{R}$		u_{GEN}^{R}	k	U_{GEN}^{R}
Reaming operation	R1	A	0.007	0.107	0.017	0.042		0.11	2	**0.21**
		B	0.007	0.073	0.014	0.057		0.07	2	**0.15**
	R2	A	0.007	0.097	0.017	0.048		0.10	2	**0.19**
		B	0.007	0.115	0.014	0.042		0.12	2	**0.23**
	R3	A	0.007	0.148	0.009	0.035		0.15	2	**0.30**
		B	0.007	0.126	0.015	0.045		0.13	2	**0.25**
	R4	A	0.007	0.163	0.019	0.064		0.16	2	**0.33**
		B	0.007	0.118	0.042	0.080		0.12	2	**0.24**
	R5	A	0.007	0.124	0.021	0.047		0.12	2	**0.25**
		B	0.007	0.120	0.033	0.070		0.12	2	**0.24**
	R6	A	0.007	0.154	0.014	0.046		0.15	2	**0.31**
		B	0.007	0.169	0.027	0.074		0.17	2	**0.34**
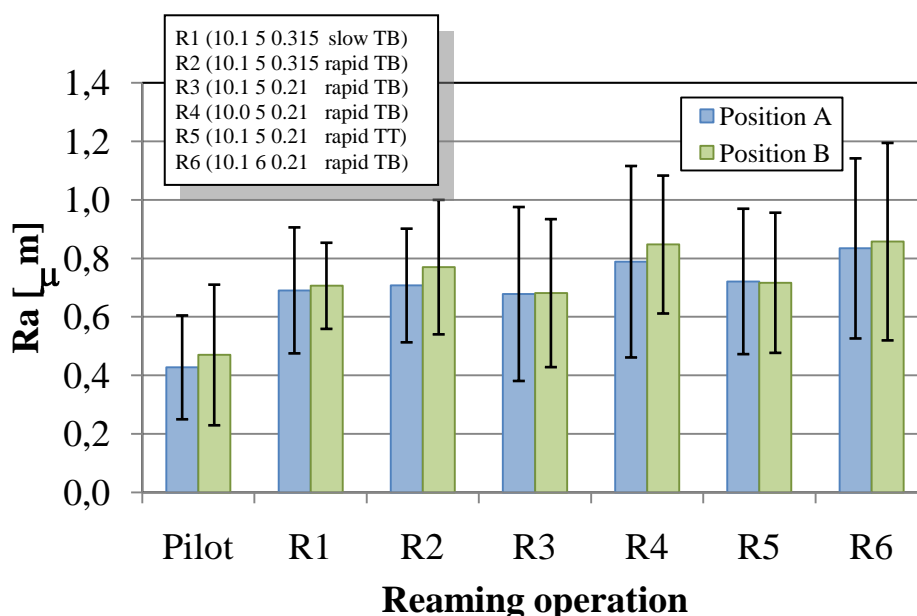
Fig. 8.8 – Surface roughness measurement results for pilot holes (process)

As result, the following is observed:

- When looking at the influence of reaming process, all reaming operations perform a stable behavior with uncertainties falling within the same range.

- First two reaming operations (R1 and R2) are compared to see whether there is any significant difference in surface topography when reaming operations differ on the reverse feed rate strategy (i.e. speed). When the same feed rate of the reamer when reaming in –z direction and when coming back in +z direction is used, there is no evidence on the workpiece to be scratched or somewhat damaged. While rapid feed rate is used, scratches on the workpiece are visible. However, difference in surface roughness no bigger than 4% can be observed when machining with rapid feed rate.

- Evident difference in surface topography (uneven surface profiles) can be observed when machining with a 10.0 mm diameter reamer (R4). The poor surface finish can be attributed to the relatively small amount of material removed and the consequent squeezing of the material by plastic deformation, instead of effective cutting action. Due to these facts the effect of the tool diameter with respect to test parameter is increased. Also when calculating the uncertainty proved that the results of reamed hole diameter are not within the tolerance with other reaming operations.

- Comparing R2 and R3 when the feed is lowered and therefore cutting time prolonged, no significant difference can be observed although better surface quality when using lower feeds is expected.

- Reaming operations R3 and R5 perform the most consistent results among all reaming operations. R5 results even with lower uncertainty and is therefore preferred to R3 since nozzle positioning in R5 is easier for the setup.
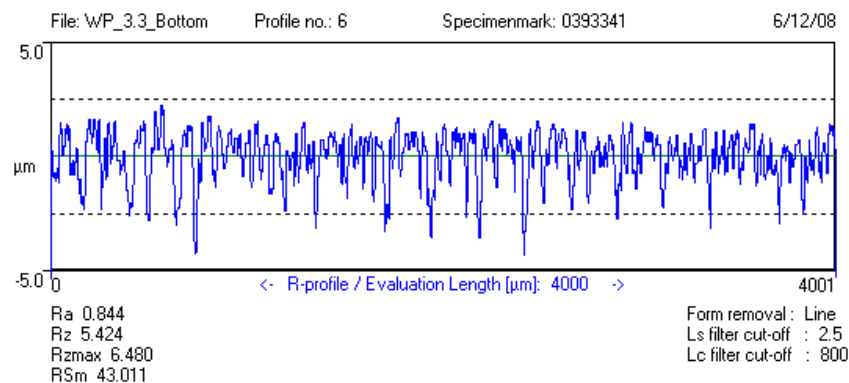
Fig. 8.9 – Typical surface roughness profile of reamed hole measured at the bottom
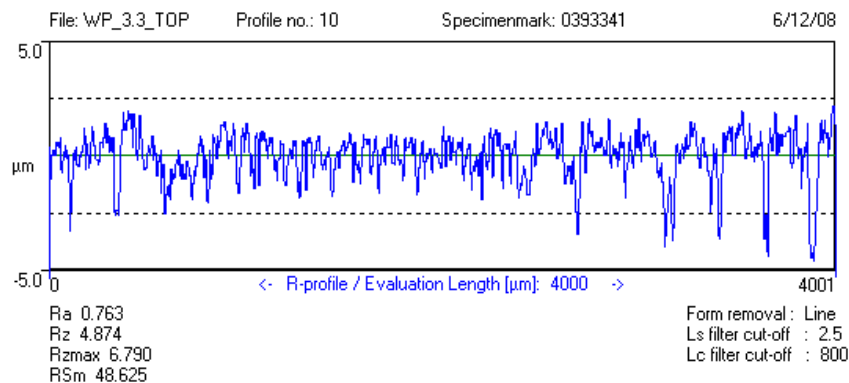
Fig. 8.10 – Typical surface roughness profile of reamed hole measured at the top

All graphs showing individual reaming operations together with their measuring uncertainties can be found in the Appendix B. Data from the measurement of surface roughness as well as profiles can be found in the Appendix F and Appendix H respectively placed on the CD attached to the report.

8.6.3   Conclusion

It can be concluded that every reaming operation brings along different behaviors (see Fig. 8.8 and Fig. B.2 in the Appendix B where a detailed comparison between individual reaming operations is presented):

- Reaming operations R1 and R2 perform the same surface roughness compatible within the stated uncertainties. Visible scratches after R2 can be observed on specimens which are results of rapid reverse feed rate.

- Both smaller depth of cut (R4) and higher cutting speed (R6) are subjected to worsened hole quality and result in big uncertainty.

- The best reaming operation can be considered R5 because it performs good surface roughness and lowest uncertainty, and it is of easier implementation due to nozzle positioning setup (both from the top).

8.7 Reaming thrust and reaming torque

Usually the measurements of cutting torque and cutting thrust are performed only considering the contribution of the experimental scatter, but this is generally not sufficient to account for measurement uncertainty. Therefore it is necessary to evaluate measurement uncertainty based on experimental scatter, as well as other process-related sources [11].

An uncertainty budget is created for reaming thrust and reaming torque including above mentioned uncertainty contributors. Uncertainty of both measurands ($U(Th)\ and\ U(To)$) is calculated based on their first derivation, following the GUM methodology [57]. Equations expressing reaming thrust (see Eq. 3.7) and reaming torque (see Eq. 3.10) are described in section 3.2.5. Equations for reaming thrust and reaming torque uncertainty calculation are expressed as follows:

$$U(Th) = k \cdot \sqrt{\sum_{i}^{n} \left(\frac{\partial Th}{\partial x_i} \cdot u(x_i) \right)^2} \qquad \text{Eq. 8.6}$$

$$U(To) = k \cdot \sqrt{\sum_{i}^{n} \left(\frac{\partial To}{\partial x_i} \cdot u(x_i) \right)^2} \qquad \text{Eq. 8.7}$$

The uncertainty contributors are discussed in the following.

8.7.1 Uncertainty of specific cutting force influence on thrust and torque $u(k_c)$

Calculation of specific cutting force is performed using following formula:

$$k_c = k_s \cdot \left(\frac{0.4}{f} \right)^{0.29} \qquad \text{Eq. 8.8}$$

k_s is an estimated value [39] for a work material similar to work material used in this master thesis. The uncertainty of this uncertainty contributor is calculated using the following formula:

$$U(k_c) = k \cdot \sqrt{\Sigma_i^n \left(\frac{\partial k_c}{\partial y_i} \cdot u(y_i) \right)^2}$$ Eq. 8.9

8.7.2   Uncertainty of feed influence on thrust and torque $u(f)$

This uncertainty is calculated using rectangular distribution for an estimated feed in-fluence on reaming torque ± 0.02 mm.rev^{-1}.

8.7.3   Uncertainty of reamer diameter influence on thrust and torque $u(D_R)$

This uncertainty is calculated in section 8.5.6 and brings along also an uncertainty of the form error and surface roughness.

8.7.4   Uncertainty of pilot hole influence on thrust and torque $u(d)$

This uncertainty is calculated in section 7.2.5 and brings along also an uncertainty of the form error and surface roughness.

8.7.5   Uncertainty of span definition window on thrust and torque $u(sdw)$

This uncertainty is calculated using rectangular distribution based on two different evaluating methods (window span definition A (wsd_A) and window span definition B (wsd_B)) for both reaming thrust and reaming torque. The window span definition can be seen in Fig. 8.11.

wsd_A: Half of the time that reamer interacts with the workpiece in the middle of the stable part of the curve.

wsd_B: Window span starts after 5 sec when reamer comes in contact with workpiece and takes 10 sec.

a) Evaluating method A   b) Evaluating method B
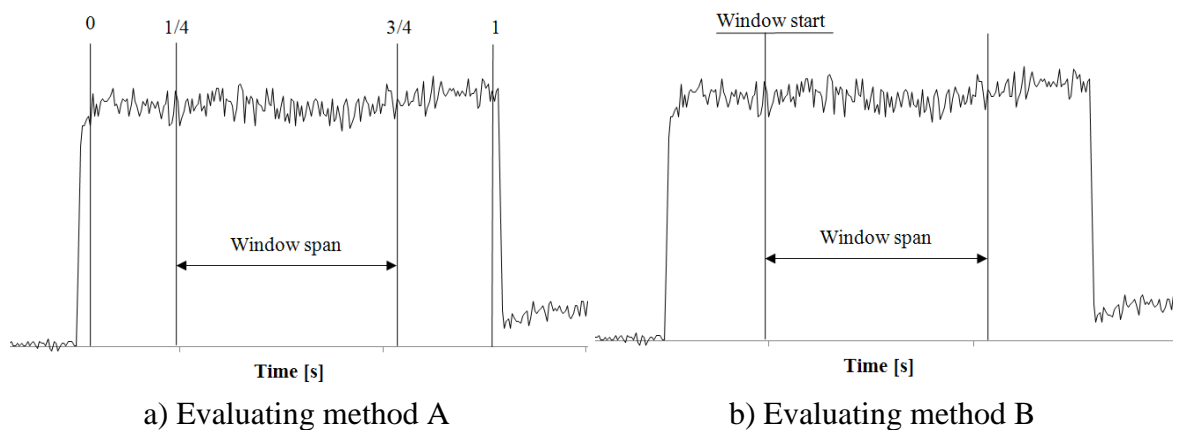
Fig. 8.11 – Window span definition for reaming thrust and reaming torque evaluation

8.7.6   Uncertainty of temperature influence on thrust and torque $u(Oil_t)$

Because the temperature in the workshop during the reaming process is not stable, the flow of the oil is changed (see section 5.3). The uncertainty related to this temperature change is calculated as follows:

$$u(Oil_t) = \frac{STD}{\sqrt{n}}$$
Eq. 8.9

where:

- STD is a standard deviation based on six independent measurements of oil flow. This uncertainty is assumed to be same for all reaming operations.

8.7.7   Uncertainty of acquisition system influence on thrust and torque $u(acq)$

This uncertainty is calculated using rectangular distribution for an estimated value ±10 Ncm.

8.7.8   Expanded combined uncertainty of thrust and torque measurements

Each machined specimen is analyzed in a reaming thrust and reaming torque vs. time diagram. Diagrams are evaluated in a given sampling window as described in section 6.5 evaluating reaming thrust and reaming torque on the stable part of the curve. Every point on the graph represents an average value calculated according to the proposed evaluating strategy. Graphs representing reaming thrust and reaming torque vs. time are shown in the Appendix G as well as data from individual machined workpiece which are placed in the Appendix G on the CD attached to the report.

Tab. 8.8 – Uncertainty budget for reaming operation R1 (reaming torque)

Reaming operation R1 – reaming torque						
No.	Uncertainty component	First derivative		Estimated uncertainty of the uncertainty component		
		$\frac{\partial To}{\partial x_i}$		$u_i(x_i)$		$\frac{\partial To}{\partial x_i} \cdot u_i(x_i)$
$u_1(k_c)$	Uncertainty of specific cutting force influence on torque	$\frac{\partial To}{\partial k_c}$	0.0255	$u(k_c)$	249	6.4
$u_2(f)$	Uncertainty of feed influence on torque	$\frac{\partial To}{\partial f}$	213	$u(f)$	0.012	2.5
$u_3(D_R)$	Uncertainty of reamer diameter influence on torque	$\frac{\partial To}{\partial D_R}$	-1343	$u(D_R)$	0.0024	-3.2
$u_4(d)$	Uncertainty of pilot hole influence on torque	$\frac{\partial To}{\partial d}$	1417	$u(d)$	0.0035	5.0
$u_5(wsd)$	Uncertainty of window span definition influence on torque			$u(wsd)$	9.1	9.1
$u_6(Oil_t)$	Uncertainty of oil temperature influence on torque			$u(Oil_t)$	1.6	1.6
$u_7(acq)$	Uncertainty of acquisition system influence on torque			$u(acq)$	5.8	5.8

Uncorrelated combined uncertainty [Nmm]	$u^{R1}(To)$	14.2
Coverage factor (for a c. l. of 95%)	k	2
Expanded combined uncertainty [Nmm]	$U^{R1}(To)$	28

Tables with uncertainty budget for reaming torque and reaming thrust of all remaining operations (e.g. R2, R3, R4, R5 and R6) are placed in the Appendix C. Figures showing reaming thrust and reaming torque for every reaming operation vs. time can be found in the Appendix C.

When combining measurement uncertainty with an uncertainty resulting from the process, such uncertainty can be calculated as follows:

$$U_{total}^{Th} = k \cdot \sqrt{u^{Rn}(Th)^2 + u_{process}^{Th}{}^2} \qquad \text{Eq. 8.10}$$

$$U_{total}^{To} = k \cdot \sqrt{u^{Rn}(To)^2 + {u_{process}^{To}}^2}$$ Eq. 8.11

where $u_{process}^{Rn}$ is an experimental standard deviation based on measurements of 15 specimens.

Tab. 8.9 – Total uncertainty for reamed hole (reaming thrust)

Thrust	R1	R2	R3	R4	R5	R6
$u^{Rn}(Th)$	3.4	3.5	2.8	2.6	2.9	2.8
$u_{process}^{Th}$	3.0	5.0	1.8	1.7	1.8	2.4
U_{total}^{Th}	**9**	**12**	**7**	**6**	**7**	**7**

Note: Values for thrust are in N.

Tab. 8.10 – Total uncertainty for reamed hole (reaming torque)

Torque	R1	R2	R3	R4	R5	R6
$u^{Rn}(To)$	14	11	10	8	10	9
$u_{process}^{To}$	79	46	46	57	36	59
U_{total}^{To}	**161**	**95**	**94**	**114**	**75**	**120**

Note: Values for torque are in Nmm.

It is obvious from Tab. 8.9 and Tab. 8.10 that reaming process is the biggest uncertainty contributor compared to other uncertainty contributors.

Tab. 8.11 – Number of evaluating points for different window span definition

	R1	R2	R3	R4	R5	R6
W.S.D. **A**	905	905	1360	1345	1360	1135
W.S.D. **B**	1000	1000	1000	1000	1000	1000

8.7.9 Reamed hole torque and thrust measurement results and discussion

- Reaming operations R1 and R2 are subjected to an experiment based on slow/rapid reverse feed rate of the spindle. Almost no difference can be observed in Fig. 8.12 between R1 and R2. This shows very good reproducibility of the machine since no influence on reaming thrust and torque is expected when different reverse feed rate is used.
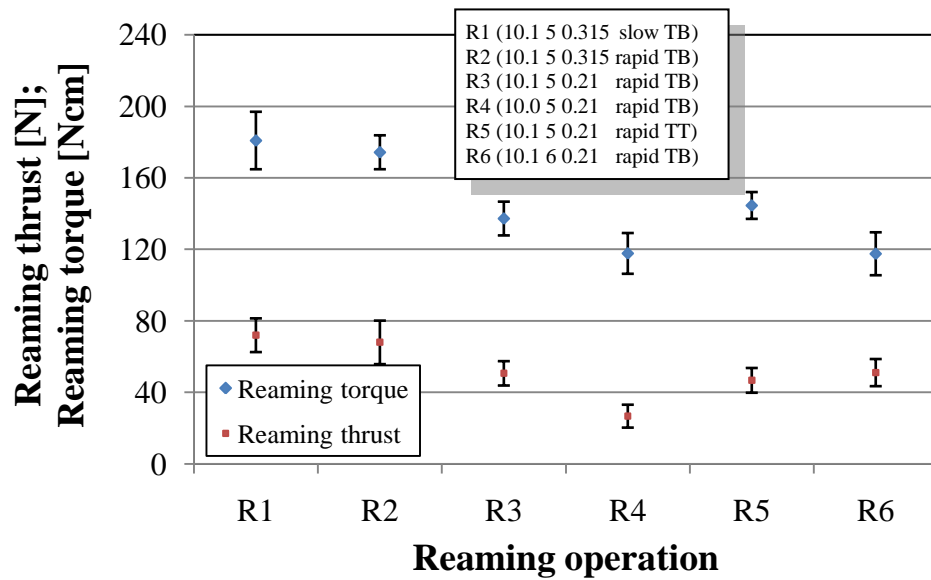
Fig. 8.12 – Reaming thrust and reaming torque results (process)
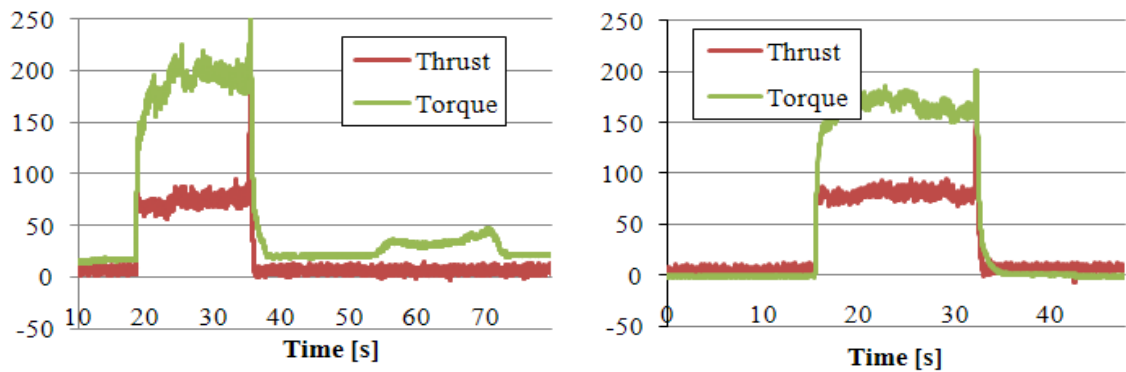
Fig. 8.13 – R1 and R2 reaming operations

- However, R2 performs better repeatability and therefore rapid reverse feed rate is used for further reaming operations. Fig. 8.13 shows that when using the same reverse feed rate as forward (slow), a reaming torque performs an increment in values when the tool is being removed from the work area. Results from surface roughness measurement show a slightly lower Ra values when the slow feed rate is used. The difference is small and can be therefore neglected. In practice a rapid feed rate is normally used.

- Reaming thrust and reaming torque are reduced significantly when lower feed is used. This behavior can be observed between R2 and R3. It is also shown that R3 represents very repeatable process.

- R4, when 10.0 mm diameter reamer is used, lowers reaming torque about 15% and reaming thrust about 50%, on the other hand this has a negative effect on surface quality as mentioned in section 8.6.2.

- The position of the nozzles does not play a big role since the results are fully compatible within the calculated uncertainties. A distance of the nozzles from the workpiece and the MQL setup play generally a paramount role since by changing these, the lubrication effect is changing as well.

- Increased cutting speed (R6) influences the process by lowering the reaming torque.

Note: All graphs showing the reaming process are shown in the Appendix C. Peaks at the end of the diagram represent burrs on the exit side of the specimen which were created during the initial hole making process.
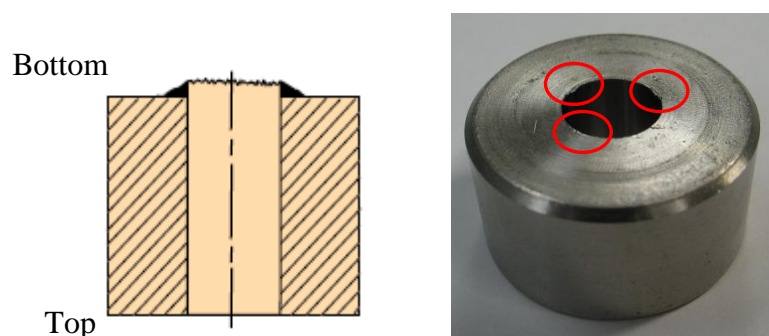
Fig. 8.14 – Burrs on the exit side

8.7.10   Conclusion

It can be concluded that every reaming operation brings along different behaviors which is clear looking at Fig. 8.12 and Fig. C.2 in the Appendix C where a detailed comparison between individual reaming operations is presented. In particular:

- Reaming operations R1 and R2 can be concluded to be not acceptable reaming operations since both reaming thrust and reaming torque perform much bigger values than the other reaming operations. Therefore a lower feed is preferred.

- The smaller material removal rate, the lower reaming thrust and reaming torque are expected. This however results in bigger uncertainty of the process since small material removal is more sensitive to the signal of reaming thrust and reaming torque measured on dynamometer.

- R5 is considered the best reaming operation set-up because it performs reasonably low values of reaming thrust and reaming torque, low uncertainty and easy nozzles positioning.

CHAPTER 9 – DISCUSSION: COMPARISON OF CUTTING FLUID PERFORMANCE TESTS AT DTU WITH RESULTS ACHIEVED IN PRESENT THESIS

A comparison between different cutting fluid performance tests carried out at DTU during previous years and the present work is carried out.

It is shown in [11] that reaming austenitic stainless steel and using different water based cutting fluids, different results of cutting fluid performance with respect to hole diameter, surface roughness, reaming thrust and reaming torque were achieved. The main difference compared to the present work is in coolant application. The specimens were immersed in a wrench. In this way, higher values of reaming thrust, reaming torque and diameter oversize as well as surface roughness were obtained. The cutting conditions were v_c=6 $m \cdot min^{-1}$, f=0.4 mm and a_p=0.2 mm. It can be also observed that higher a_p values increase the sensitivity to the fluid. Another difference in evaluation of the results can be encountered to the measuring methods and measuring strategies when uncertainty is calculated, i.e. only six repetitions were performed when uncertainty of reaming torque was performed which was 5%. Furthermore the strategy for pilot hole measuring uncertainty is not well defined which can misrepresent the total uncertainty.

The analysis of repeatability and resolution is carried out following [19] and [58]. The calculation of latter is performed for reaming forces (reaming thrust and reaming torque), hole geometry (hole diameter) and hole quality (surface roughness). The relative resolution of the test σ/ρ is introduced, where σ is defined as the ratio between the standard deviation of a measurand and the mean of the measurand, and where ρ is the range of variability of test results. Tab. 9.1 presents calculated values for above mentioned characteristics.

Tab. 9.1 – Relative resolution for reaming test

	σ [%]	ρ [%]	σ/ρ
Reaming torque	5-10	42	0.2
Reaming thrust	12-24	85	0.2
Surface roughness (A)	27-44	21	1.7
Surface roughness (B)	21-39	23	1.4
Hole diameter	0.03	0.03	0.8

Generally, reaming torque tests, according to [19], are connected with good repeatability and resolution and short time (typically half working day according to [19]) and therefore relatively lower costs than for other tests. This is also a case of this project where reaming torque performed very good repeatability as well as relative resolution.

In [9] it is shown that reaming austenitic stainless steel encourage for large experimental spread. During reaming with higher cutting depth ($a_p=0.2$ *mm*), the cutting fluid had a strong influence on the part accuracy which was reduced using smaller depth of cut ($a_p=0.05$ *mm*). This is not a case of this work because small depth of cut has a big influence on part accuracy and surface roughness. Cutting fluid application was the same as in [11]. The uncertainty of the reaming torque is based on six repetitions and lies in the range 5-30%, compared to the mean, depending on the performance of the fluid and on the accuracy of the specimen. The range of variation of the test is 40%. These results are fully comparable with results obtained during this project.

In [8] reaming austenitic stainless steel using water based cutting fluids is performed. The result of surface finish tests feature in high sensitivity to the choice of cutting fluid which accounts for repeatability of 5-60% and resolution of 0.3-0.4. The uncertainty combining the measurement and the process for surface roughness test is for the present work in the range 20-45% and the resolution is so high that surface roughness cannot be used as a reliable parameter to discriminate one test set-up being better than another. The main difference is again in the measurement strategy and the way how the uncertainty was evaluated.

CHAPTER 10 - CONCLUSION

10.1 Summary

This master thesis regards the development of a test procedure for cutting fluid performance in reaming and to apply the tests to MQL. In this project the performance of insoluble oil has been investigated by varying cutting conditions and experimental setup of the reaming process. The tests were carried out on austenitic stainless steels using HSS reamers with two different diameters. Individual reaming operations were compared with respect to a number of evaluating parameters such as hole diameter, roundness, cylindricity, surface roughness, reaming thrust and reaming torque. For all mentioned measurands the uncertainty budget was created so that the reaming process is fully under control. The calculated absolute and relative expanded uncertainties of all measurands are summarized in Tab. 10.1.

Tab. 10.1 – Absolute and relative expanded uncertainties

Measurand	Test uncertainty	Unit	Test uncertainty [%]
Diameter	3.0	μm	0.03-0.04
Roundness	2.6	μm	89-116
Cylindricity	4.6	μm	49-61
Surface roughness (position A)	0.31	μm	27-44
Surface roughness (position B)	0.34	μm	21-39
Reaming thrust	12	N	13-24
Reaming torque	12	Ncm	5-11

In this project a new unconventional method of MQL delivery was investigated. This was achieved by installing one of the external nozzles from bottom, i.e. nozzle positioned through the dynamometer and the fixture mounted to the dynamometer.

Based on present investigation several conclusions are drawn:

- Present tests can be applied not only in connection with reaming but also could be used for cutting fluid performance in drilling due to similarity of the process. Other cutting fluid can be taken into consideration since it would give bigger overview of the process and better quantification of the cutting fluid performance.

- Not only measurands used in the present work (hole diameter, roundness, cylindricity, surface roughness, reaming thrust and reaming torque) but also other (tool life, tool wear, microhardness, chip evacuation, cutting power) can be considered for cutting fluid performance evaluation.

- Care must be taken when evaluating the uncertainty since it contains both uncertainty of the measurement and uncertainty of the process itself. Moreover, it is associated with a loss of information regarding uncertainty contributors. For some measurands, uncertainty caused by the process variation plays the biggest role (i.e. reaming torque and surface roughness). The test parameters which could be used for cutting fluid evaluation were the reaming thrust and reaming torque. Results proved that measurements of reaming thrust and reaming torque are reliable, ensuring consistent characterization of the lubricating performance of cutting fluids. By measuring the hole geometry and hole quality, the corresponding measurands can be used in connection with quality control. Very good surface roughness, always found to be less than 1.2 μm, was achieved as well as hole cylindricity which did not exceed 14 μm taking into account both measurement and process variation.

- Reaming operations R6, for higher cutting speed and R4, for smaller depth of cut have the biggest influence on uncertainty of surface roughness and reaming torque. R1 and R2 do not perform consistent results when reaming thrust and reaming torque are considered although these two reaming operations should have the same effect on these measurands.

- There is no difference between MQL applications (R3 and R5) when taking into account all measurands. R5 is therefore preferred due to easier nozzle positioning.

- Comparing cutting fluid tests performed at DTU during last years, no significant difference was found. Uncertainty assessment was in most of the cases carried out by considering only the standard deviation from the process based on six repetitions. This can be biased since more influential parameters should be taken into consideration. This aspect was extensively investigated during the present research.

10.2   Future development of the present thesis

Based on the results achieved in the present M. Sc. Thesis, several suggestions on further research and development can be proposed.

Since the uncertainty budget phase has been quite time consuming, not many variations on the experimental setup and cutting conditions could be investigated. After this project, one will be able to continue with the following investigation:

a) Use of different tool materials on the same workpiece material. Cermet reamers could be an interesting alternative since smaller experimental spread in values is expected.

b) Use of different tool geometries.

c) Use of different reamer diameters to consider the effect of variations of depth of cut on the process and on the overall quality of the holes.

d) Test of different cutting fluids. Water based cutting fluids are good solution when reaming austenitic stainless steel and effective comparison with tests performed at DTU could be carried out.

e) Investigation on different cutting conditions.

f) Perform tests based on same cutting conditions and experimental setup as in the present thesis, but using conventional cooling and dry reaming. In this case a cermet reamer is recommended because of its good stability when high temperatures are developed.

Generally, when external MQL is applied, nozzle positioning plays a paramount role, therefore appropriate control on cutting fluid delivery into tool/workpiece interface should be complied.

Reaming operation R4 was found to differ from the theory that says that when material is removed, a hole oversize is expected (see section 8.5.7 and 8.6.2). Therefore a further research is needed to confirm this theory since an opposite behavior was experienced.

REFERENCES

[1] E. C. BIANCHI, R. E. CATAI, R.Y. FUSSE, T. V. FRANCE, P. R. AGUIAR, *Study on the Behavior of the MQL technique under different lubricating and cooling conditions when grinding ABNT 4340 steel*, Vol. XXVII, Issue no.2 (April-June 2005) pp.192-199.

[2] W. F. SALES, A. E. DINIZ, A. T. MACHALO, *Application of Cutting Fluids in Machining Processes*, J. Braz. Soc. Mech. Sci., Vol.23, Issue no.2, Rio de Janeiro, 2001.

[3] T. MAKIYAMA, *Advanced Near Dry Machining System*, Presentation for 4th Annual NCMS Fall Workshop Series, October 2000.

[4] K. WEINERT, I. INASAKI, J. W. SUTHERLAND, T. WAKABAYSHI, *Dry machining and Minimum Quantity Lubrication*, Annals CIRP, Vol.53, Issue no.2 (2004) pp.511-537.

[5] Sandvik Coromant, *Dry and MQL Machining*, Internal Presentation, 2005.

[6] Sandvik Coromant, *Drilling educational kit*, Internal Presentation, 2005.

[7] L. DE CHIFFRE, S. LASSEN, K.B. PEDERSEN, S. SKADE, *A reaming test for cutting fluid evaluation,* J. Synth. Lubr., Vol.11 (1994) pp.11-34.

[8] L. DE CHIFFRE, Z. ZENG, W. BELLUCO, *Parameter investigation in a reaming test for cutting fluid evaluation,* IPT, Technical University of Denmark, Publication no.MM99.71 (1999).

[9] W. BELLUCO, L. DE CHIFFRE, *Testing of Vegetable-Based cutting fluids in hole making operations,* Lubrication Engineering, Vol.57, Issue no.1 (2001) pp.12-16

[10] W. BELLUCO, Z. ZENG, L. DE CHIFFRE, *Evaluation of cutting fluids in multiple reaming of stainless steel,* Proceedings of PRIME 2001 Conference (Sestri Levante), 2001, pp.45-48.

[11] L. DE CHIFFRE, W. BELLUCO, Z. ZENG, *An investigation of reaming test parameters used for cutting fluid evaluation*, Lubr. Eng., Vol.57 (2001) pp.24-28.

[12] L. De CHIFFRE, *Mechanical testing and selection of cutting fluid,* Lubr. Eng., Vol.36 (1980) pp.33-39.

[13] L. DE CHIFFRE, *Mechanics of metal cutting and cutting fluid action,* Int. J. Mach. Tool Des. Res., Vol.17 (1977) pp.225-234.

[14] L. DE CHIFFRE, *Testing the overall performance of cutting fluids,* Lubr. Eng., Vol.34 (1978) pp.244-251.

[15] L. DE CHIFFRE, *Cutting fluid action, testing and selection,* Int. Yearbook of Tribology, W. J. Bartz (ed.), Expert Verlag, Grafenau, (1982) pp.769-773.

[16] L. DE CHIFFRE, *Laboratory testing of cutting fluid performance,* 3rd Int. Coll. Tribol., TAE Proceedings (1982) 74.1-74.5.

[17] L. DE CHIFFRE, *Function of cutting fluids in machining,* Lubr. Eng., Vol.44 (1988) pp.514-518.

[18] L. DE CHIFFRE, *Mechanical testing and selection of cutting fluids in laboratory and workshop,* Eurometalworking, Vol.92 (1992) pp.102-106.

[19] W. BELLUCO, L. DE CHIFFRE, *Comparison of methods for cutting fluid performance testing,* Annals of CIRP, Vol.49/1 (2000) pp.57-60.

[20] D. AXINTE, W. BELLUCO, L. DE CHIFFRE, *Reliable tool life measurements in turning – An application to cutting fluid efficiency evaluation*, Int. J. Mach. Tools Manufact., Vol.41 (2001) pp.1003-1014.

[21] L. DE CHIFFRE, W. BELLUCO, *Investigation on cutting fluid performance using different machining operations,* Lubr. Eng., Vol.58 (2002) pp.22-29.

[22] W. BELLUCO, L. DE CHIFFRE, *Surface integrity and part accuracy in reaming and tapping stainless steel with new vegetable based cutting oils,* Tribology International, Vol.35 (2002) pp.865-870.

[23] P. JERRY, I. BYERS, *Metalworking fluids,* 1994, ISBN 0-8247-9201-7, TJ1077.M457.

[24] K. KOCMAN, *Speciální technologie obrábění*, Vysoké učení technické v Brně, Fakulta strojního inženýrství, January 2004, ISBN: 80-214-2562-8.

[25] S. L. GAUTIER, *Metalworking Fluids: Oil Mist and Beyond*. 2003, pp.818–824, ISSN: 1047-322X print / 1521-0898 online, DOI 10.1080/10473220390237313.

[26] K., J. PROKOP, *Technologie obrábění,* Vysoké učení technické v Brně, Fakulta strojního inženýrství, December 2001, ISBN: 80-214-1996-2.

[27] *Metals handbook 9ᵗʰ edition*, Vol.16 Machining, ISBN: 0-87170-007-7.

[28] Dr. M. SCHACHT, Dr. CH. WOLFF, *40 % increase in production thanks to the resolute use of minimal quantity lubrication in production operations, the result of strategic planning*, Willy Vogel AG; March 2003.
http://www.vogel-lube.com/Products/NearDryMachining/MMS-Artikel_Feb_2003_US.pdf (September 2007).

[29] Sandvik Coromant, *Minimum Quantity Lubrication*, Internal Presentation, 2005.

[30] SKF website
http://www.skf.com/portal/skf_vog/home/faq?contentId=339411&langn   (October 2007).

[31] Lubrix website, http://www.lubrix.de/en/lubrix750.htm (January 2008).

[32] L. DE CHIFFRE, Lecture notes, Course 42216, Technical University of Denmark, 2006.

[33] J. BRULAND, *Fluid performance testing in cutting austenitic stainless steel,* Internal material, IPL, Technical University of Denmark, 1995.

[34] S. KALPAKJIAN, J. KARGER-KOCSIS, *Manufacturing Processes for Engineering Materials (2nd edition)*, 1999, ISSN 14658011.

[35] Union Butterfield website
http://www.unionbutterfield.com/tech/reamers/geometry.asp (June 2008).

[36] Super Tool, Inc. website
http://www.supertoolinc.com/tools/High-Speed-Steel (July 2008).

[37] Cutting tool central – American machinist website
http://www.cutting-tool.americanmachinist.com/guiEdits/Content/bdeee16/bdeee16_1.aspx (June 2008).

[38] A. HUMÁR, *Slinuté karbidy a řezná keramika pro obrábění, 1995, ISBN 80-85825-10-4.*

[39] A. HUMÁR, *Lecture material*, 2006.

[40] Sutton tools website
http://www.sutton.com.au/uploads/downloads/Literature/Product/499980268Reaming
_Brochure_lr.pdf (July 2008).

[41] http://books.google.com/books (June 2008).

[42] *Příručka obrábění*, Sandvik Coromant, 1997.

[43] Sandvik Coromant website
http://www2.coromant.sandvik.com/coromant/pdf/Metalworking_Products_061/tech_
e_1.pdf (May 2008).

[44] W. BELLUCO, *Performance testing of cutting fluids*, IPT, Technical University
of Denmark, PhD Thesis, December 2000, Publication no. IPT.198.00 (MM00.63).

[45] B. LEFFLER, *Stainless steels and their properties*
http://www.outokumpu.com/files/Group/HR/Documents/STAINLESS20.pdf (July
2008).

[46] British stainless steel association website
http://www.bssa.org.uk/topics.php?article=121 (July 2008).

[47] Dormer website
http://www.dormertools.com/sandvik/2531/internet/s003591.nsf?OpenDatabase (May
2008).

[48] Magafor website
www.obergverktoy.no/ez/index.php?/site/content/download/533/1904/file/4%20REA
MERS.pdf – (June 2008).

[49] ISO 4287:1997 Geometrical product specifications (GPS) -- Surface texture: Pro-
file method – Terms, definitions and surface texture parameters.

[50] Lubrix manual

[51] L. DE CHIFFRE, *Geometrical metrology and machine testing,* Lecture notes
(Course 42215), January 2005.

[52] ISO 1101:2004 Geometrical Product Specifications (GPS) -- Geometrical toler-
ancing -- Tolerances of form, orientation, location and run-out.

[53] Mahr website
http://www.mahr.com/index.php?NodeID=8718 (June 2008).

[54] ISO 11562:1996 Geometrical product specifications (GPS) -- Surface texture: Profile method – Metrological characteristics of phase correct filters.

[55] ISO/TS 15530-3:2004 - Geometrical Product Specifications (GPS) -- Coordinate measuring machines (CMM): Technique for determining the uncertainty of measurement -- Part 3: Use of calibrated workpieces or standards (2004).

[56] ISO 5436-2:2001 Geometrical Product Specifications (GPS) - Surface texture: Profile method; Measurement standards - Part 2: Software measurement standards (2001).

[57] ISO (International Organization for Standardization), GUM (Guide to the Expression of Uncertainty in Measurement) (1995).

[58] C. CARATOSSIDIS, *Analysis of cutting fluid tests with economical evaluation of machining tests*, 1998, M. Sc. Thesis, Publication nr. MM98.42, IPT, Technical University of Denmark.

NOMENCLATURE

a_P	[mm]	depth of cut
acq		acquisition system
A_C	[mm^2]	nominal chip cross-section
b	[mm]	nominal chip width
b'		systematic error
BUE		material build-up on cutting edge
b''		assumed U-distribution (b''=0.7)
C	[mm]	hole cylindricity
CMM		coordinate measuring machine
CT		carbide tipped
d	[mm]	diameter of pre-existing hole
D	[mm]	hole diameter
D_R	[mm]	reamer diameter
f	[mm]	feed/rev
f_Z	[mm]	feed/tooth
F_C	[N]	tangential force
F_{ci}	[N]	tangential force component
F_{fi}	[N]	feed force component
F_{pi}	[N]	passive force component
h	[mm]	nominal chip thickness
HSS		high speed steel
k		coverage factor for a confidence level of 95% $\rightarrow$ *k=2*
k_C	[N·mm^{-2}]	specific cutting force
k_S	[N·mm^{-2}]	specific cutting force (for a feed/rev *f=0.4* mm)
L	[mm]	cutting length
$\dot{m}$	[kg·s^{-1}]	mass flow
MQL		minimum quantity lubrication
n	[-]	number of measurements
N	[min^{-1}]	revolutions
p	[bar]	pressure
Q	[m^3·s^{-1}]	oil flow
r_A	[mm]	radius on which the tangential reaming force is acting
R	[mm]	hole roundness
Ra	[μm]	arithmetical mean roughness of a surface
RR		reference ring
$R1 - R6$	[-]	number of reaming operations

SC		solid carbide
t	[s]	time
T	[N·cm]	reaming torque
T'	[°C]	temperature
TB (T&B)		one nozzle positioned from top and one from bottom
TT (T&T)		two nozzle positioned from top
$u(f)$	[mm]	estimated uncertainty for cutting feed and is calculated using rectangular distribution
$u(k_s)$	[N·mm^{-2}]	estimated uncertainty for specific cutting force and is calculated using rectangular distribution
$u(Oil_t)$	[ml/hour]	uncertainty of oil temperature influence on thrust and torque
$u(x_i)$		estimated uncertainty of the uncertainty component
$u(y_i)$		estimated uncertainty of the uncertainty component
$U(Th)$	[N]	uncertainty derivation with respect to reaming thrust
$U(To)$	[N·mm]	uncertainty derivation with respect to reaming torque
$u^{Rn}(Th)$	[N]	uncorrelated combined uncertainty fro individual reaming operation of reaming thrust
$u^{Rn}(To)$	[N·mm]	uncorrelated combined uncertainty fro individual reaming operation of reaming torque
$u_1(k_c)$	[N·mm^{-2}]	uncertainty of specific cutting force influence on torque
$u_2(f)$	[mm]	uncertainty of feed influence on torque
$u_3(D_R)$	[mm]	uncertainty of reamer diameter influence on torque
$u_4(d)$	[mm]	uncertainty of pilot hole influence on torque
$u_5(wsd)$	[N·mm]	uncertainty of window span definition influence on torque
$u_6(Oil_t)$	[ml/hour]	uncertainty of oil temperature influence on torque
$u_7(acq)$	[N·mm]	uncertainty of acquisition system influence on torque
$u_1'(k_c)$	[N·mm^{-2}]	uncertainty of specific cutting force influence on thrust
$u_2'(f)$	[mm]	uncertainty of feed influence on thrust
$u_3'(D_R)$	[mm]	uncertainty of reamer diameter influence on thrust
$u_4'(d)$	[mm]	uncertainty of pilot hole influence on thrust
$u_5'(wsd)$	[N·mm]	uncertainty of window span definition influence on thrust
$u_6'(Oil_t)$	[ml/hour]	uncertainty of oil temperature influence on thrust
$u_7'(acq)$	[N·mm]	uncertainty of acquisition system influence on thrust
u_b	[μm]	uncertainty caused by the background noise
u_c	[mm]	standard uncertainty related to the calibration of the reference ring stated in the calibration certificate
u_{cal}	[mm]	standard uncertainty of calibration
$u_{GB(cal)}$	[μm]	standard uncertainty related to the calibration of the gauge

		block
u_{instr}	[μm]	standard uncertainty of the stylus instrument calibration
$u_{machine}$	[mm]	maximum value of standard deviations considering four measuring strategies
u_n	[μm]	uncertainty of the roughness standard
u_p	[mm]	standard uncertainty due to measuring process
u_r	[μm]	uncertainty on the transfer of traceability (repeatability of the instrument)
u_{reamer}	[μm]	standard uncertainty resulting from the measurement on reamer diameter
u_{res}	[μm]	standard uncertainty resulting from the micrometer resolution
$u_{strategy}$	[mm]	standard deviation of average measured values at different levels on the cylinder. Includes variation in number of levels together with number of points probed around the circumference
u_{temp}	[μm]	standard deviation resulting from temperature compensation
u_{Gen}^{R}	[μm]	standard uncertainty caused by variations in the roughness of the reamed hole in different locations
u_{Gen}^{P}	[μm]	standard uncertainty caused by variations in the roughness of the pilot hole in different locations
$u_{Gen(a)}^{P}$	[μm]	uncertainty of the process for surface roughness of pilot hole
$u_{Gen(b)}^{P}$	[μm]	uncertainty of repeatable measurement on the same position for surface roughness of pilot hole
$u_{Gen(c)}^{P}$	[μm]	uncertainty of measurement around the circumference for surface roughness of pilot hole
$u_{Gen(a)}^{R}$	[μm]	uncertainty of the process for surface roughness of reamed hole
$u_{Gen(b)}^{R}$	[μm]	uncertainty of repeatable measurement on the same position for surface roughness of reamed hole
$u_{Gen(c)}^{R}$	[μm]	uncertainty of measurement around the circumference for surface roughness of reamed hole
u_{Hole}^{P}	[mm]	standard combined pilot hole measuring uncertainty
u_p^{P}	[mm]	standard uncertainty resulting from the measurement procedure on CMM of the calibrated workpiece (pilot holes)
u_p^{R}	[mm]	standard uncertainty resulting from the measurement procedure on CMM of the calibrated workpiece (reamed holes)
u_{p1}^{P}	[mm]	maximum value of standard deviations of $u_{strategy}$ and $u_{machine}$ (pilot specimen)

$u_{p2}^{P} = u_{p2}^{R}$ [mm]		average value of standard deviations from measurements on five specimens positioned at three different positions in the fixture
u_{p1}^{R} [mm]		maximum value of standard deviations of $u_{strategy}$ and $u_{machine}$ (reamed specimen)
$u_{process}^{P}$ [mm]		experimental standard deviation for geometrical dimensions of pilot hole based on measurements of 15 specimens
$u_{process}^{R}$ [mm]		experimental standard deviation for geometrical dimensions of reamed hole based on measurements of 15 specimens
$u_{process}^{Th}$ [N]		experimental standard deviation for reaming thrust based on measurements of 15 specimens
$u_{process}^{To}$ [N·mm]		experimental standard deviation for reaming torque based on measurements of 15 specimens
u_{w}^{P} [mm]		standard uncertainty resulting from temperature deviation of pilot hole
u_{w}^{R} [mm]		standard uncertainty resulting from temperature deviation of reamed hole
U_{Gen}^{P} [μm]		expanded combined uncertainty for surface roughness of pilot hole
U_{Gen}^{R} [μm]		expanded combined uncertainty for surface roughness of reamed hole
U_{Hole}^{P}	[mm]	expanded combined pilot hole measuring uncertainty
$U_{Hole(C)}^{P}$	[mm]	pilot hole measuring uncertainty for cylindricity
$U_{Hole(D)}^{P}$	[mm]	pilot hole measuring uncertainty for diameter
$U_{Hole(R)}^{P}$	[mm]	pilot hole measuring uncertainty for roundness
U_{Hole}^{R}	[mm]	reamed hole measuring uncertainty
$U_{Hole(C)}^{R}$	[mm]	reamed hole measuring uncertainty for cylindricity
$U_{Hole(D)}^{R}$	[mm]	reamed hole measuring uncertainty for diameter
$U_{Hole(R)}^{R}$	[mm]	reamed hole measuring uncertainty for roundness
U_{RD}^{Rn}	[μm]	Measuring uncertainty on reamer diameter
U_{total}^{P} [mm]		total expanded uncertainty of the pilot hole measured on CMM
U_{total}^{R} [mm]		total expanded uncertainty of the reamed hole measured on CMM
U_{total}^{Th}	[N]	total expanded uncertainty of reaming thrust
U_{total}^{To}	[N·mm]	total expanded uncertainty of reaming torque
v_f	[mm·min^{-1}]	feed rate
wsp		window span definition

z	[-]	number of teeth
α	[10^{-6} m/m°C]	linear coefficient of thermal expansion
ΔT	[°C]	maximum possible change in temperature in accredited laboratory with controled temperature to be 20°C
$\Delta T'$	[°C]	temperature difference between micrometer and reamer
ρ	[kg·m^{-3}]	density
θ	[rad]	chamfer angle
$\frac{\partial k_c}{\partial y_i}$		first derivative of each component of the equation for specific cutting force
$\frac{\partial Th}{\partial x_i}$		first derivative of each component of the equation for reaming thrust
$\frac{\partial To}{\partial x_i}$		first derivative of each component of the equation for reaming torque

LIST OF APPENDICES

Appendix A:
1) Hole dimensions (Diameter, Roundness and Cylindricity) for every reaming operation.
2) Hole dimensional comparison (Diameter, Roundness and Cylindricity) for R1/R2, R2/R3, R3/R4, R3/R5 and R3/R6 reaming operations.
3) Experimental investigation on measuring strategy
4) Experimental investigation on space accuracy.

Appendix B:
1) Surface roughness for every reaming operation.
2) Surface roughness comparison for R1/R2, R2/R3, R3/R4, R3/R5 and R3/R6 reaming operations.

Appendix C:
1) Reaming thrust uncertainty calculation for every reaming operation.
2) Reaming torque uncertainty calculation for every reaming operation.
3) Reaming thrust and reaming torque for every reaming operation.
4) Reaming thrust and reaming torque comparison for R1/R2, R2/R3, R3/R4, R3/R5 and R3/R6 reaming operations.
5) Reaming thrust and reaming torque graphs for each reamed specimen and every reaming operation.

Appendix D:
1) Reamer diameter measurements

Appendix A - 1

Fig. A.1 - Hole dimensions (Diameter, Roundness and Cylindricity) for every reaming operation

Hole dimensions - Reaming operation R1
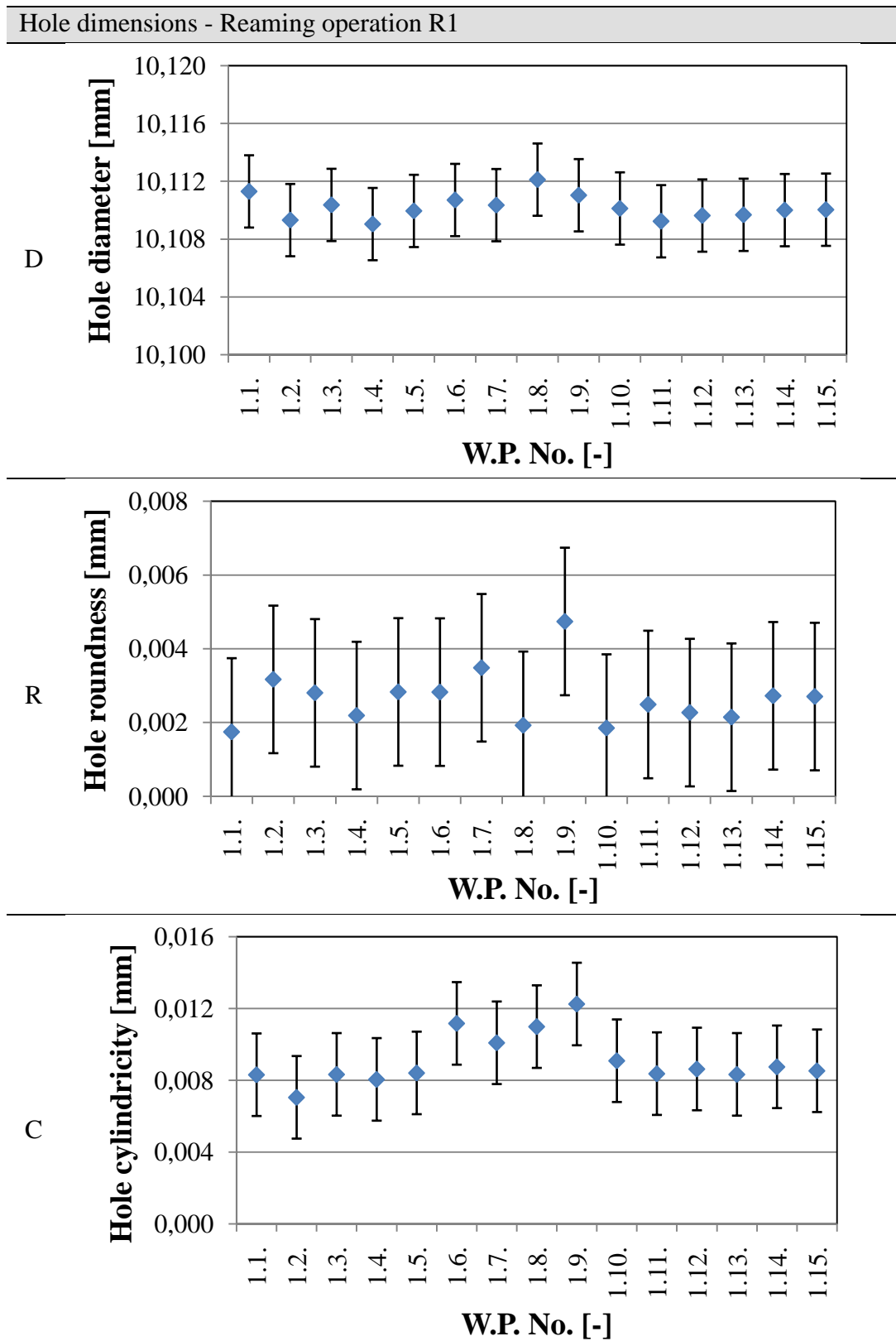
Hole dimensions - Reaming operation R2
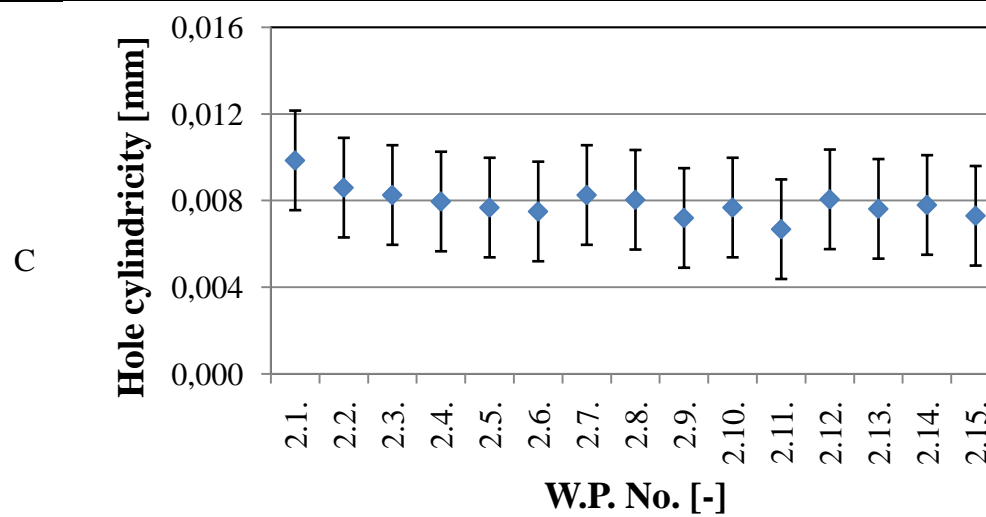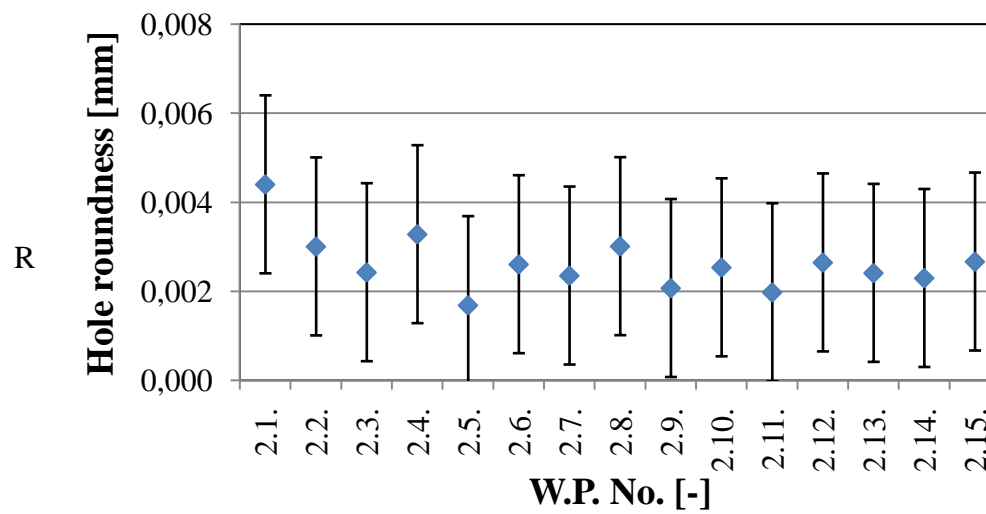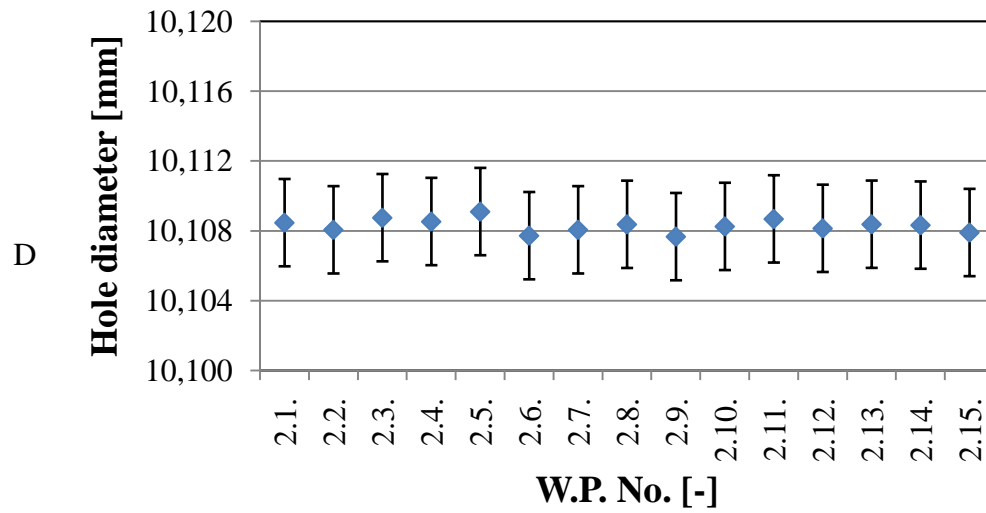
Hole dimensions - Reaming operation R3
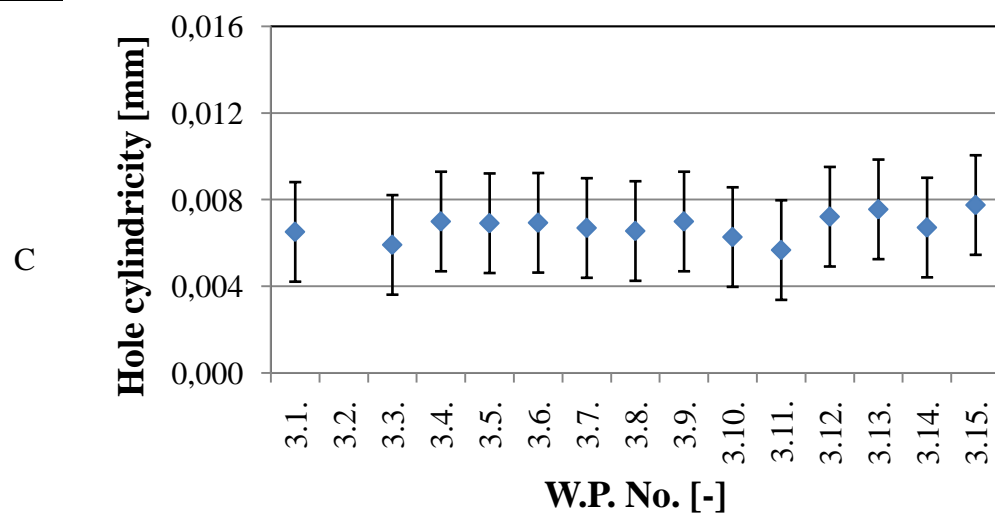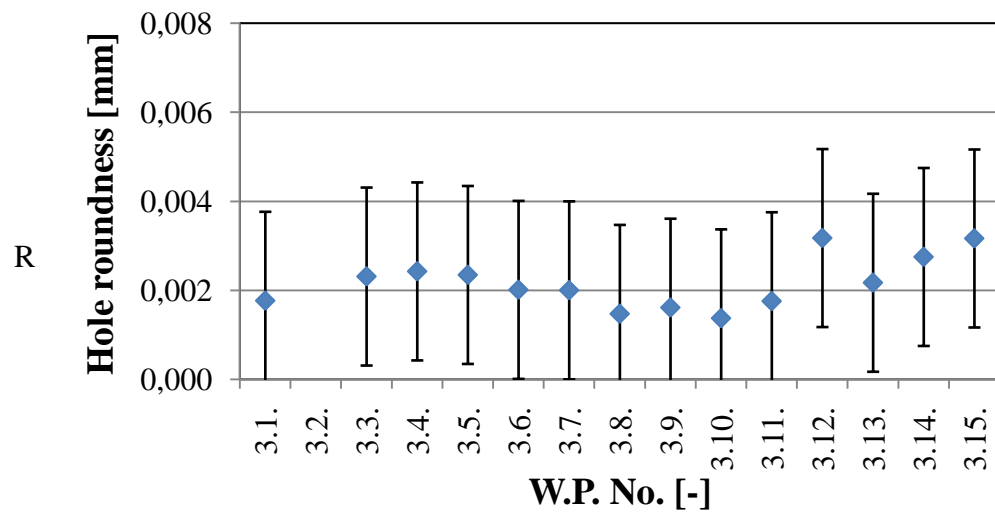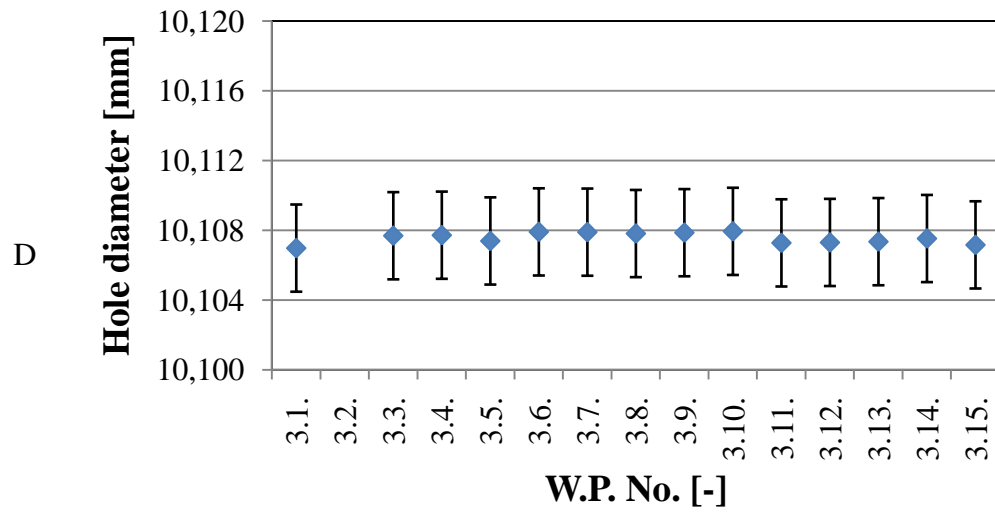
Hole dimensions - Reaming operation R4
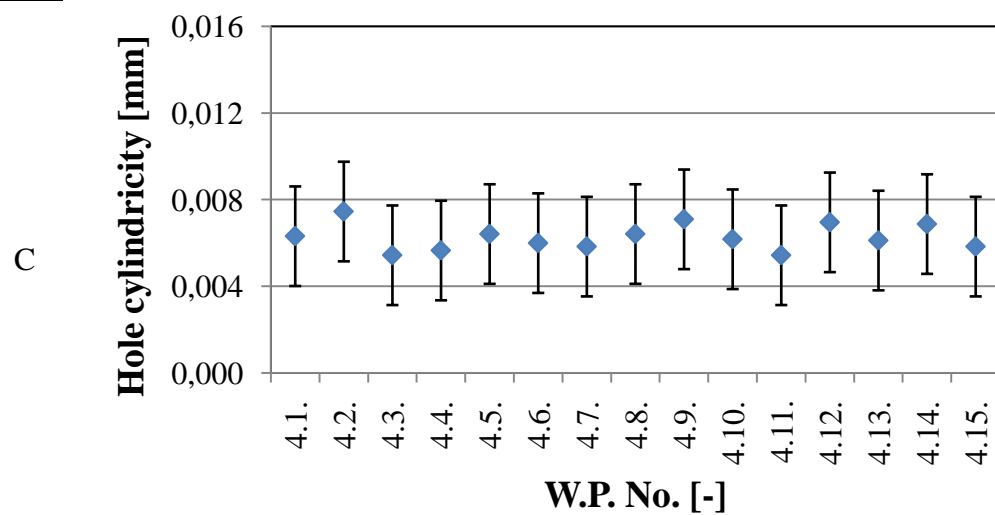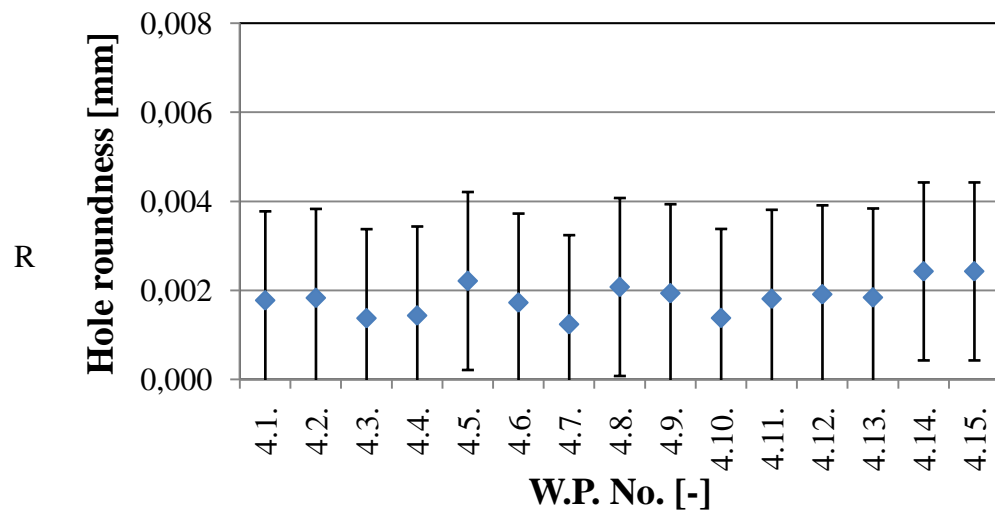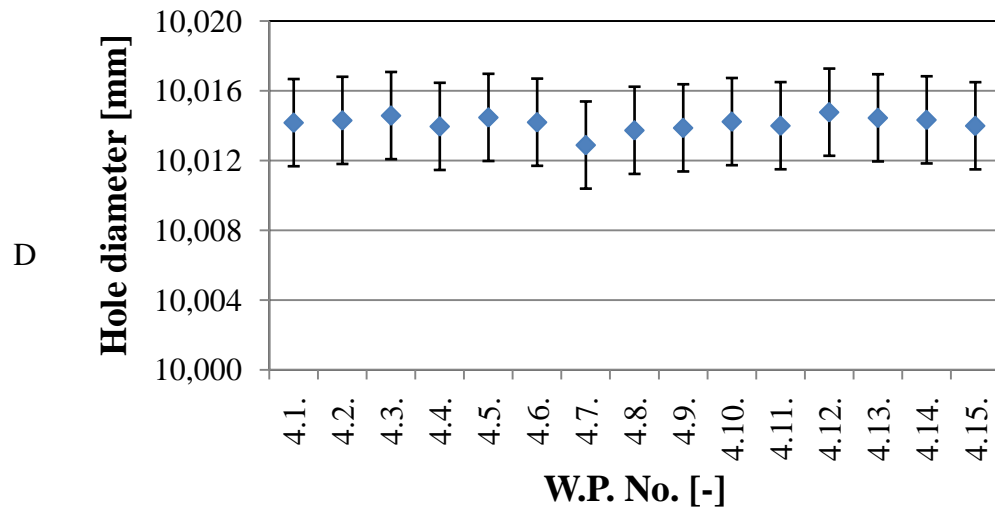
Hole dimensions - Reaming operation R5
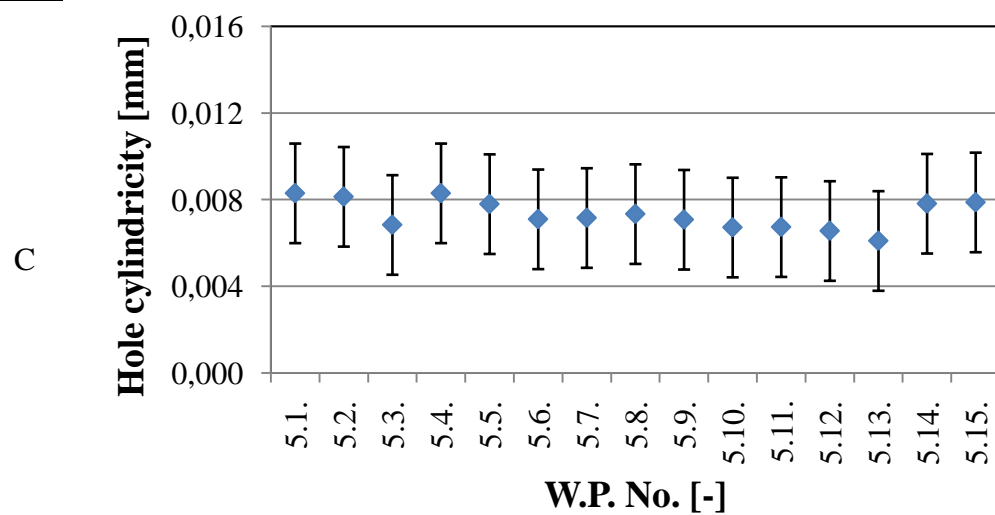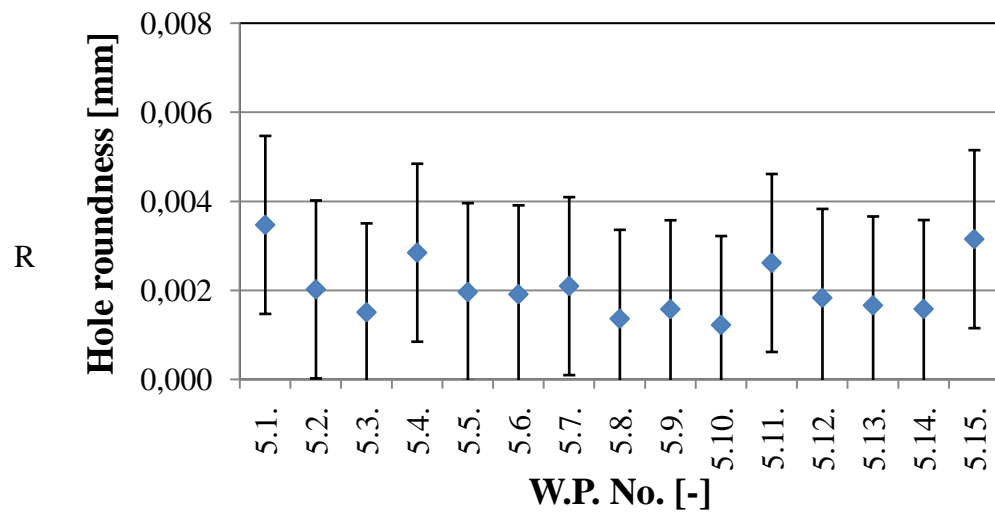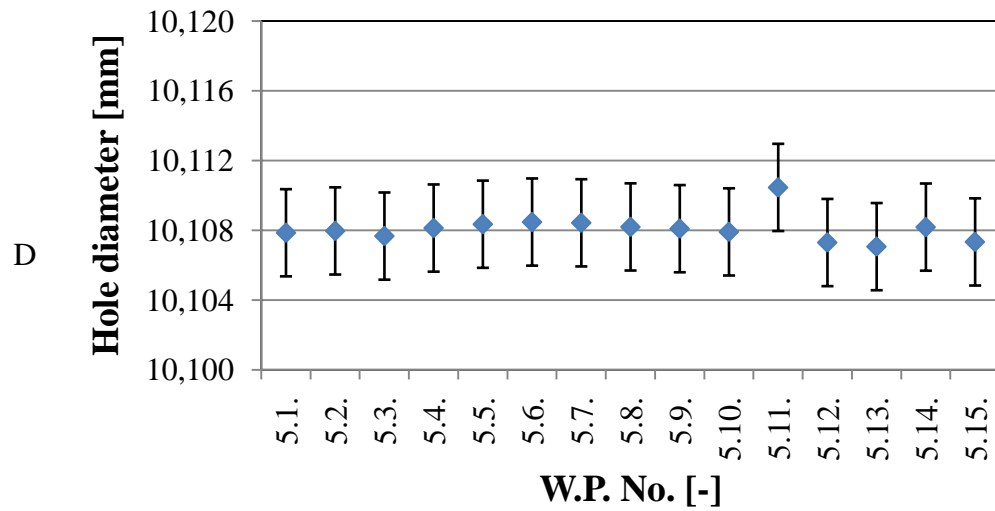
Hole dimensions - Reaming operation R6
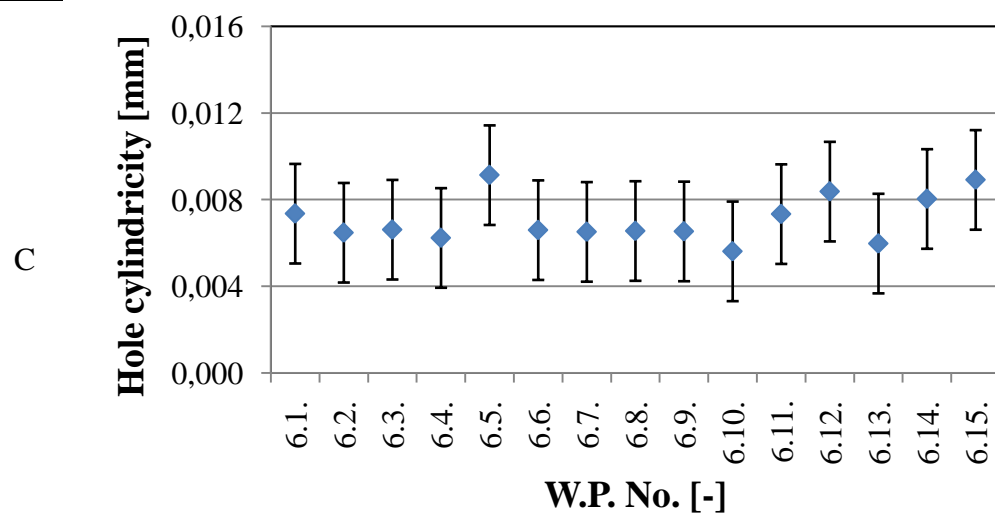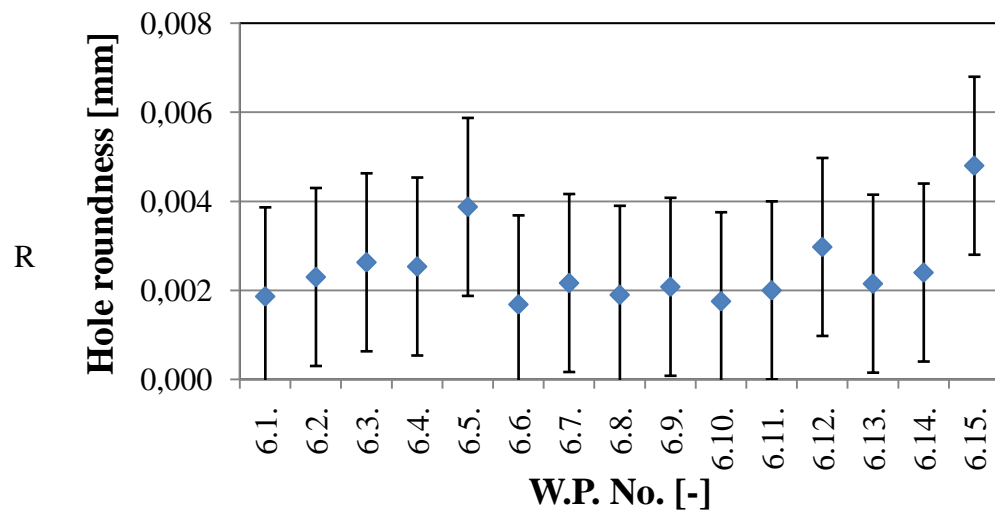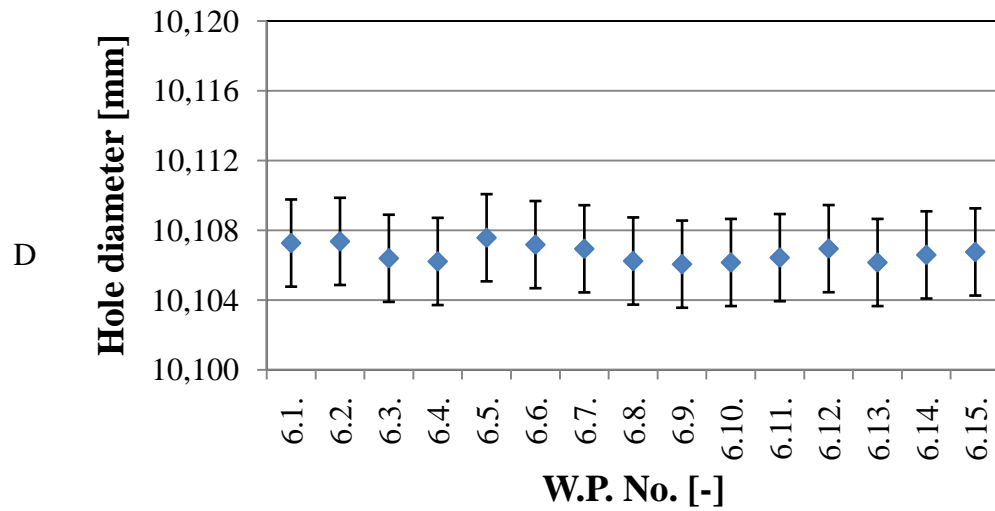
Appendix A - 2

Fig. A.2 - Hole dimensional comparison (Diameter, Roundness and Cylindricity) for R1/R2, R2/R3, R3/R4, R3/R5 and R3/R6 reaming operations

Hole dimensions comparison – R1/R2 (reverse feed rate)

Hole dimensions comparison – R2/R3 (feed)

Hole dimensions comparison – R3/R4 (depth of cut)
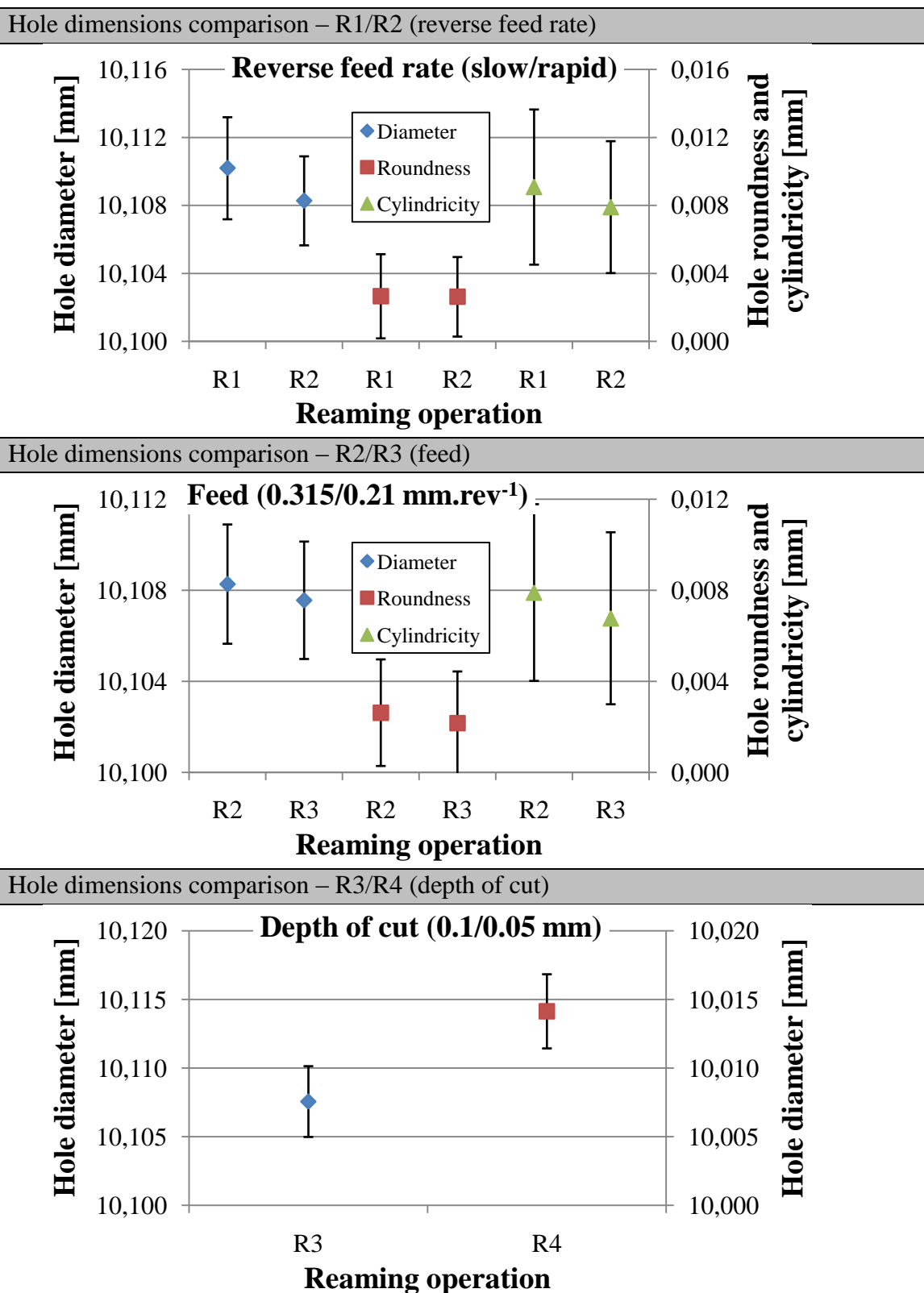
Hole dimensions comparison – R3/R4 (depth of cut)
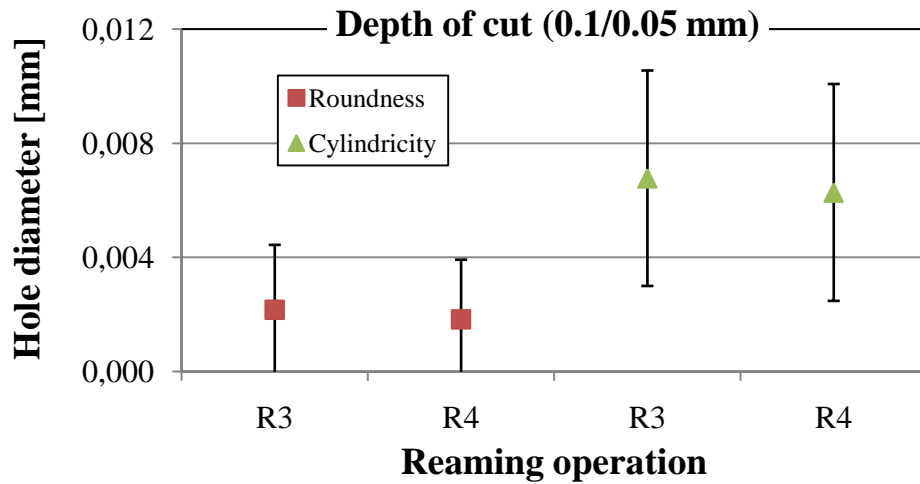
Hole dimensions comparison – R3/R5 (nozzle position)
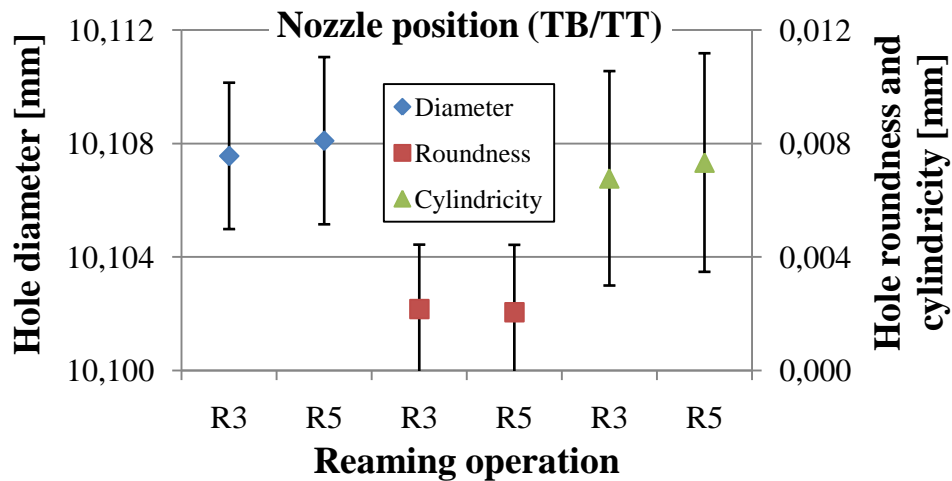
Hole dimensions comparison – R3/R6 (cutting speed)
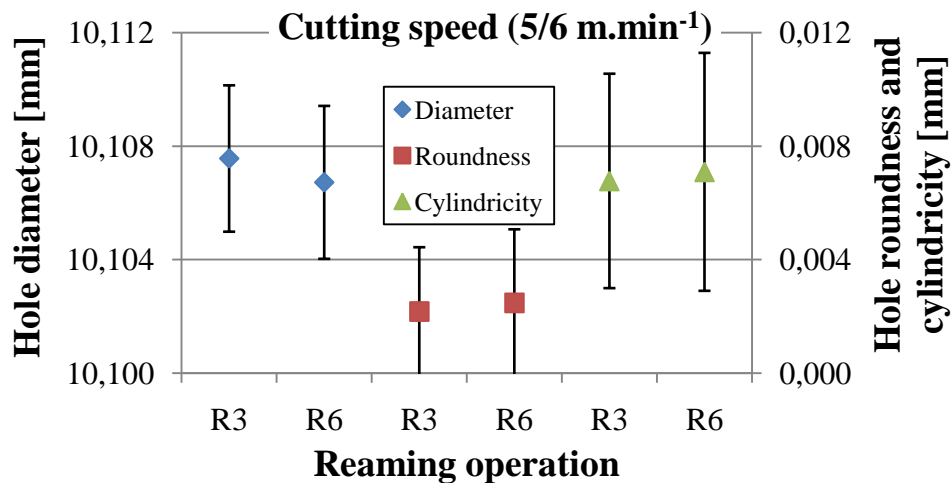
Appendix A - 3

Tab. A.1 - Experimental investigation on measuring strategy (RR)

Diameter

		Exp.No. 1 4L 8P			
Meas.No.	L 3	L 6	L 9	L 12	AVG
1	10.0005	10.0005	10.0005	10.0006	10.0005
2	10.0006	10.0004	10.0006	10.0006	10.0006
3	10.0003	10.0002	10.0005	10.0005	10.0004
4	10.0002	10.0005	10.0006	10.0005	10.0005
5	10.0000	10.0002	10.0010	10.0005	10.0004
AVG	10.0003	10.0004	10.0006	10.0005	10.0005
STD	0.0002	0.0002	0.0002	0.0001	0.0001

Diameter

		Exp.No. 2 3L 8P		
Meas.No.	L 4.5	L 7.5	L 10.5	AVG
1	10.0008	10.0007	10.0009	10.0008
2	10.0005	10.0003	10.0010	10.0006
3	10.0004	10.0001	10.0002	10.0002
4	10.0007	10.0004	10.0007	10.0006
5	10.0006	10.0001	10.0004	10.0004
AVG	10.0006	10.0003	10.0006	10.0005
STD	0.0002	0.0002	0.0003	0.0002

Diameter

		Exp.No. 3 4L 12P			
Meas.No.	L 3	L 6	L 9	L 12	AVG
1	10.0009	10.0009	10.0007	10.0012	10.0009
2	10.0006	10.0008	10.0007	10.0009	10.0008
3	10.0003	10.0008	10.0006	10.0005	10.0006
4	10.0006	10.0006	10.0007	10.0006	10.0006
5	10.0001	10.0004	10.0009	10.0009	10.0006
AVG	10.0005	10.0007	10.0007	10.0008	10.0007
STD	0.0003	0.0002	0.0001	0.0003	0.0002

Diameter

		Exp.No. 4 3L 12P		
Meas.No.	L 4.5	L 7.5	L 10.5	AVG
1	10.0006	10.0007	10.0009	10.0007
2	10.0007	10.0005	10.0009	10.0007
3	10.0005	10.0010	10.0008	10.0008
4	10.0006	10.0008	10.0007	10.0007
5	10.0001	10.0006	10.0006	10.0004
AVG	10.0005	10.0007	10.0008	10.0007
STD	0.0002	0.0002	0.0001	0.0001

Roundness

		Exp.No. 1 4L 8P			
Meas.No.	L 3	L 6	L 9	L 12	AVG
1	0.0009	0.0007	0.0003	0.0005	0.0006
2	0.0008	0.0008	0.0008	0.0007	0.0008
3	0.0004	0.0006	0.0003	0.0014	0.0007
4	0.0005	0.0005	0.0003	0.0007	0.0005
5	0.0014	0.0011	0.0005	0.0011	0.0010
AVG	0.0008	0.0007	0.0004	0.0009	0.0007
STD	0.0004	0.0002	0.0002	0.0004	0.0002

Roundness

		Exp.No. 2 3L 8P		
Meas.No.	L 4.5	L 7.5	L 10.5	AVG
1	0.0008	0.0012	0.0008	0.0009
2	0.0010	0.0010	0.0013	0.0011
3	0.0005	0.0005	0.0011	0.0007
4	0.0006	0.0004	0.0004	0.0005
5	0.0013	0.0012	0.0010	0.0012
AVG	0.0008	0.0009	0.0009	0.0009
STD	0.0003	0.0004	0.0003	0.0003

Roundness

		Exp.No. 3 4L 12P			
Meas.No.	L 3	L 6	L 9	L 12	AVG
1	0.0007	0.0007	0.0009	0.0007	0.0008
2	0.0011	0.0005	0.0006	0.0007	0.0007
3	0.0009	0.0009	0.0008	0.0010	0.0009
4	0.0010	0.0005	0.0001	0.0009	0.0006
5	0.0012	0.0012	0.0013	0.0012	0.0012
AVG	0.0010	0.0008	0.0007	0.0009	0.0008
STD	0.0002	0.0003	0.0004	0.0002	0.0002

Roundness

		Exp.No. 4 3L 12P		
Meas.No.	L 4.5	L 7.5	L 10.5	AVG
1	0.0008	0.0010	0.0006	0.0008
2	0.0009	0.0012	0.0009	0.0010
3	0.0009	0.0009	0.0008	0.0009
4	0.0012	0.0008	0.0012	0.0011
5	0.0012	0.0013	0.0011	0.0012
AVG	0.0010	0.0010	0.0009	0.0010
STD	0.0002	0.0002	0.0002	0.0002

Cylindricity

Meas.No.	1	2	3	4
1	0.0011	0.0014	0.0010	0.0010
2	0.0010	0.0016	0.0011	0.0013
3	0.0014	0.0011	0.0013	0.0010
4	0.0008	0.0007	0.0012	0.0014
5	0.0014	0.0014	0.0016	0.0014
AVG	0.0011	0.0012	0.0012	0.0012
STD	0.0003	0.0004	0.0002	0.0002

Tab. A.2 - Experimental investigation on measuring strategy (Pilot holes)

Diameter				
Exp.No. 1 4L 8P				
Meas.No.	L 3	L 6	L 9	L 12	AVG
1	9.9062	9.9065	9.9059	9.9038	9.9056
2	9.9064	9.9079	9.9060	9.9044	9.9062
3	9.9064	9.9074	9.9059	9.9042	9.9060
4	9.9060	9.9080	9.9059	9.9039	9.9060
5	9.9056	9.9078	9.9056	9.9043	9.9058
AVG	9.9061	9.9075	9.9059	9.9041	9.9059
STD	0.0003	0.0006	0.0002	0.0003	0.0002

Diameter				
Exp.No. 2 3L 8P				
Meas.No.	L 4.5	L 7.5	L 10.5	AVG
1	9.9070	9.9049	9.9042	9.9054
2	9.9072	9.9058	9.9044	9.9058
3	9.9070	9.9056	9.9053	9.9060
4	9.9071	9.9055	9.9047	9.9058
5	9.9067	9.9057	9.9043	9.9056
AVG	9.9070	9.9055	9.9046	9.9057
STD	0.0002	0.0004	0.0004	0.0002

Diameter				
Exp.No. 3 4L 12P				
Meas.No.	L 3	L 6	L 9	L 12	AVG
1	9.9060	9.9075	9.9054	9.9039	9.9057
2	9.9064	9.9081	9.9066	9.9041	9.9063
3	9.9063	9.9083	9.9060	9.9036	9.9061
4	9.9065	9.9076	9.9062	9.9043	9.9062
5	9.9061	9.9072	9.9058	9.9042	9.9058
AVG	9.9063	9.9077	9.9060	9.9040	9.9060
STD	0.0002	0.0005	0.0004	0.0003	0.0002

Diameter				
Exp.No. 4 3L 12P				
Meas.No.	L 4.5	L 7.5	L 10.5	AVG
1	9.9067	9.9061	9.9048	9.9059
2	9.9073	9.9057	9.9042	9.9057
3	9.9075	9.9056	9.9045	9.9059
4	9.9070	9.9061	9.9043	9.9058
5	9.9074	9.9059	9.9042	9.9058
AVG	9.9072	9.9059	9.9044	9.9058
STD	0.0003	0.0002	0.0003	0.0001

Roundness				
Exp.No. 1 4L 8P				
Meas.No.	L 3	L 6	L 9	L 12	AVG
1	0.0017	0.0022	0.0012	0.0017	0.0017
2	0.0019	0.0022	0.0018	0.0011	0.0018
3	0.0020	0.0021	0.0016	0.0013	0.0018
4	0.0019	0.0023	0.0014	0.0012	0.0017
5	0.0017	0.0020	0.0012	0.0008	0.0014
AVG	0.0018	0.0022	0.0014	0.0012	0.0017
STD	0.0001	0.0001	0.0003	0.0003	0.0001

Roundness				
Exp.No. 2 3L 8P				
Meas.No.	L 4.5	L 7.5	L 10.5	AVG
1	0.0017	0.0015	0.0020	0.0017
2	0.0011	0.0014	0.0016	0.0014
3	0.0012	0.0010	0.0016	0.0013
4	0.0021	0.0009	0.0009	0.0013
5	0.0010	0.0013	0.0009	0.0011
AVG	0.0014	0.0012	0.0014	0.0013
STD	0.0005	0.0003	0.0005	0.0002

Roundness				
Exp.No. 3 4L 12P				
Meas.No.	L 3	L 6	L 9	L 12	AVG
1	0.0011	0.0018	0.0022	0.0019	0.0018
2	0.0011	0.0017	0.0032	0.0021	0.0020
3	0.0009	0.0028	0.0019	0.0021	0.0019
4	0.0012	0.0016	0.0021	0.0018	0.0017
5	0.0014	0.0018	0.0013	0.0017	0.0016
AVG	0.0011	0.0019	0.0021	0.0019	0.0018
STD	0.0002	0.0005	0.0007	0.0002	0.0002

Roundness				
Exp.No. 4 3L 12P				
Meas.No.	L 4.5	L 7.5	L 10.5	AVG
1	0.0018	0.0018	0.0019	0.0018
2	0.0012	0.0014	0.0019	0.0015
3	0.0015	0.0019	0.0020	0.0018
4	0.0014	0.0015	0.0017	0.0015
5	0.0011	0.0018	0.0018	0.0016
AVG	0.0014	0.0017	0.0019	0.0016
STD	0.0003	0.0002	0.0001	0.0002

Cylindricity				
Meas.No.	1	2	3	4
1	0.0038	0.0033	0.0039	0.0033
2	0.0041	0.0025	0.0044	0.0031
3	0.0038	0.0022	0.0044	0.0032
4	0.0040	0.0025	0.0037	0.0031
5	0.0040	0.0024	0.0037	0.0034
AVG	0.0039	0.0026	0.0040	0.0032
STD	0.0001	0.0004	0.0004	0.0001

Tab. A.3 - Experimental investigation on measuring strategy (Reamed holes)

Diameter					
	Exp.No. 1 4L 8P				
Meas.No.	L 3	L 6	L 9	L 12	AVG
1	10.1125	10.1101	10.1062	10.1044	10.1083
2	10.1125	10.1074	10.1059	10.1036	10.1074
3	10.1121	10.1071	10.1061	10.1036	10.1072
4	10.1118	10.1073	10.1055	10.1035	10.1070
5	10.1123	10.1073	10.1056	10.1037	10.1072
AVG	10.1122	10.1078	10.1059	10.1038	10.1074
STD	0.0003	0.0013	0.0003	0.0004	0.0005

Diameter				
	Exp.No. 2 3L 8P			
Meas.No.	L 4.5	L 7.5	L 10.5	AVG
1	10.1093	10.1076	10.1053	10.1074
2	10.1093	10.1071	10.1052	10.1072
3	10.1094	10.1074	10.1050	10.1073
4	10.1091	10.1072	10.1048	10.1070
5	10.1092	10.1066	10.1050	10.1069
AVG	10.1093	10.1072	10.1051	10.1072
STD	0.0001	0.0004	0.0002	0.0002

Diameter					
	Exp.No. 3 4L 12P				
Meas.No.	L 3	L 6	L 9	L 12	AVG
1	10.1109	10.1082	10.1051	10.1039	10.1070
2	10.1111	10.1086	10.1062	10.1046	10.1076
3	10.1110	10.1078	10.1067	10.1050	10.1076
4	10.1105	10.1076	10.1067	10.1045	10.1073
5	10.1109	10.1081	10.1066	10.1048	10.1076
AVG	10.1109	10.1081	10.1063	10.1046	10.1074
STD	0.0002	0.0004	0.0007	0.0004	0.0003

Diameter				
	Exp.No. 4 3L 12P			
Meas.No.	L 4.5	L 7.5	L 10.5	AVG
1	10.1103	10.1078	10.1057	10.1079
2	10.1095	10.1072	10.1056	10.1074
3	10.1092	10.1074	10.1055	10.1074
4	10.1098	10.1072	10.1054	10.1075
5	10.1096	10.1074	10.1063	10.1078
AVG	10.1097	10.1074	10.1057	10.1076
STD	0.0004	0.0002	0.0004	0.0002

Roundness					
	Exp.No. 1 4L 8P				
Meas.No.	L 3	L 6	L 9	L 12	AVG
1	0.0057	0.0036	0.0030	0.0040	0.0041
2	0.0057	0.0032	0.0030	0.0025	0.0036
3	0.0065	0.0039	0.0030	0.0025	0.0040
4	0.0065	0.0043	0.0032	0.0024	0.0041
5	0.0064	0.0035	0.0030	0.0027	0.0039
AVG	0.0062	0.0037	0.0030	0.0028	0.0039
STD	0.0004	0.0004	0.0001	0.0007	0.0002

Roundness				
	Exp.No. 2 3L 8P			
Meas.No.	L 4.5	L 7.5	L 10.5	AVG
1	0.0034	0.0021	0.0022	0.0026
2	0.0045	0.0033	0.0028	0.0035
3	0.0042	0.0032	0.0028	0.0034
4	0.0049	0.0032	0.0028	0.0036
5	0.0046	0.0031	0.0026	0.0034
AVG	0.0043	0.0030	0.0026	0.0033
STD	0.0006	0.0005	0.0003	0.0004

Roundness					
	Exp.No. 3 4L 12P				
Meas.No.	L 3	L 6	L 9	L 12	AVG
1	0.0066	0.0042	0.0045	0.0037	0.0048
2	0.0057	0.0045	0.0035	0.0033	0.0043
3	0.0058	0.0041	0.0034	0.0037	0.0043
4	0.0066	0.0042	0.0036	0.0028	0.0043
5	0.0058	0.0038	0.0038	0.0028	0.0041
AVG	0.0061	0.0042	0.0038	0.0033	0.0043
STD	0.0005	0.0003	0.0004	0.0005	0.0003

Roundness				
	Exp.No. 4 3L 12P			
Meas.No.	L 4.5	L 7.5	L 10.5	AVG
1	0.0047	0.0046	0.0037	0.0043
2	0.0049	0.0037	0.0030	0.0039
3	0.0047	0.0039	0.0034	0.0040
4	0.0053	0.0037	0.0033	0.0041
5	0.0046	0.0040	0.0032	0.0039
AVG	0.0048	0.0040	0.0033	0.0040
STD	0.0003	0.0004	0.0003	0.0002

Cylindricity				
Meas.No.	1	2	3	4
1	0.0074	0.0046	0.0084	0.0060
2	0.0077	0.0054	0.0077	0.0055
3	0.0079	0.0054	0.0074	0.0055
4	0.0079	0.0056	0.0076	0.0061
5	0.0078	0.0051	0.0071	0.0054
AVG	0.0077	0.0052	0.0076	0.0057
STD	0.0002	0.0004	0.0005	0.0003

Appendix A - 4

Tab. A.4.1 - Experimental investigation on space accuracy (Diameter)

W.P.	Hole No.	D [mm]				
		(-3)	(-6)	(-9)	(-12)	AVG
1.3.	18	10.1168	10.1122	10.1082	10.1051	10.1106
	5	10.1163	10.1125	10.1087	10.1042	10.1104
	39	10.1172	10.1117	10.1081	10.1042	10.1103
AVG		10.1168	10.1121	10.1083	10.1045	10.1104
STD		0.0005	0.0004	0.0003	0.0005	0.0001
1.8.	7		10.1140	10.1085	10.1034	10.1086
	28		10.1143	10.1075	10.1036	10.1085
	1		10.1140	10.1081	*10.1035*	10.1085
AVG			10.1141	10.1080	10.1035	10.1085
STD			0.0002	0.0005	0.0001	0.0001
1.11.	36	10.1156	10.1110	10.1071	10.1033	10.1093
	1	10.1155	10.1115	10.1071	10.1033	10.1094
	19	10.1149	10.1107	10.1075	10.1032	10.1091
AVG		10.1153	10.1111	10.1072	10.1033	10.1092
STD		0.0004	0.0004	0.0002	0.0001	0.0001
1.12.	34	10.1166	10.1109	10.1076	10.1039	10.1098
	23	10.1158	10.1112	10.1072	10.1033	10.1094
	40	10.1180	10.1117	10.1079	10.1042	10.1105
AVG		10.1168	10.1113	10.1076	10.1038	10.1099
STD		0.0011	0.0004	0.0004	0.0005	0.0005
1.15.	1		10.1109	10.1076	10.1037	10.1074
	22		10.1115	10.1079	10.1034	10.1076
	14		10.1123	10.1082	10.1036	10.1080
AVG			10.1116	10.1079	10.1036	10.1077
STD			0.0007	0.0003	0.0002	0.0003
AVG						**0.00025**

Tab. A.4.2 - Experimental investigation on space accuracy (Roundness and cylindricity)

W.P.	Hole No.	R [mm]					C [mm]
		(-3)	(-6)	(-9)	(-12)	AVG	
1.3.	18	0.0032	0.0033	0.0024	0.0035	0.0031	0.0083
	5	0.0033	0.0029	0.0028	0.0023	0.0028	0.0085
	39	0.0027	0.0037	0.0019	0.0018	0.0025	0.0082
AVG		0.0031	0.0033	0.0024	0.0025	0.0028	0.0083
STD		0.0003	0.0004	0.0005	0.0009	0.0003	0.0002
1.8.	7	0.0023	0.0017	0.0023	0.0020	0.0021	0.0110
	28	0.0025	0.0021	0.0018	0.0018	0.0021	0.0114
	1	0.0020	0.0019	0.0026	0.0017	0.0021	0.0111
AVG		0.0023	0.0019	0.0022	0.0018	0.0021	0.0112
STD		0.0003	0.0002	0.0004	0.0002	0.00001	0.0002
1.11.	36	0.0031	0.0026	0.0026	0.0019	0.0026	0.0085
	1	0.0038	0.0031	0.0013	0.0014	0.0024	0.0085
	19	0.0045	0.0033	0.0013	0.0011	0.0026	0.0081
AVG		0.0038	0.0030	0.0017	0.0015	0.0025	0.0084
STD		0.0007	0.0004	0.0008	0.0004	0.0001	0.0002
1.12.	34	0.0041	0.0023	0.0013	0.0012	0.0022	0.0087
	23	0.0026	0.0017	0.0018	0.0020	0.0020	0.0083
	40	0.0043	0.0017	0.0014	0.0017	0.0023	0.0094
AVG		0.0037	0.0019	0.0015	0.0016	0.0022	0.0088
STD		0.0009	0.0003	0.0003	0.0004	0.0001	0.0006
1.15.	1	0.0043	0.0031	0.0031	0.0012	0.0029	0.0079
	22	0.0037	0.0022	0.0023	0.0019	0.0025	0.0081
	14	0.0052	0.0027	0.0032	0.0027	0.0035	
AVG		0.0044	0.0027	0.0029	0.0019	0.0030	0.0080
STD		0.0008	0.0005	0.0005	0.0008	0.0005	0.0001
AVG						**0.00020**	**0.00026**

Appendix B – 1

Fig. B.1 - Surface roughness for every reaming operation

Surface roughness – Reaming operation R1
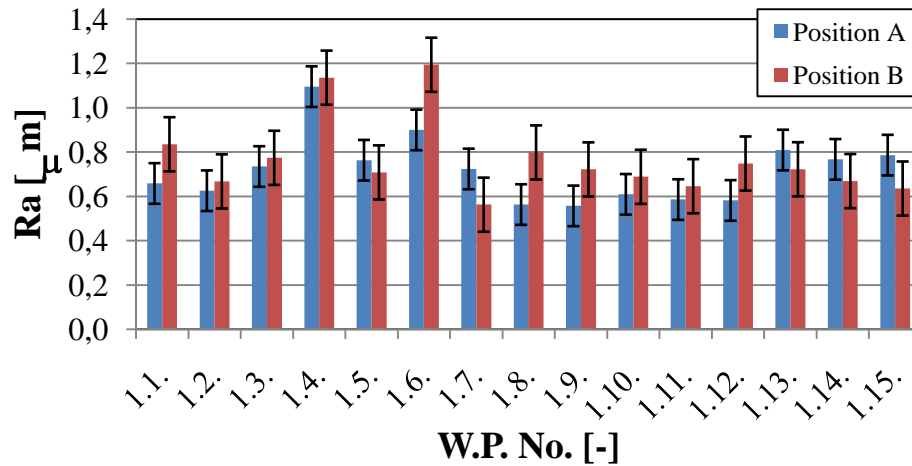
Surface roughness – Reaming operation R2
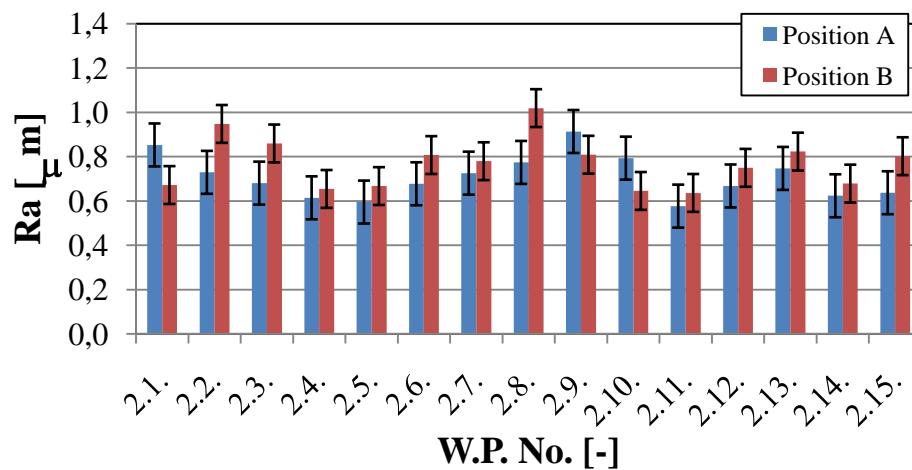
Surface roughness – Reaming operation R3
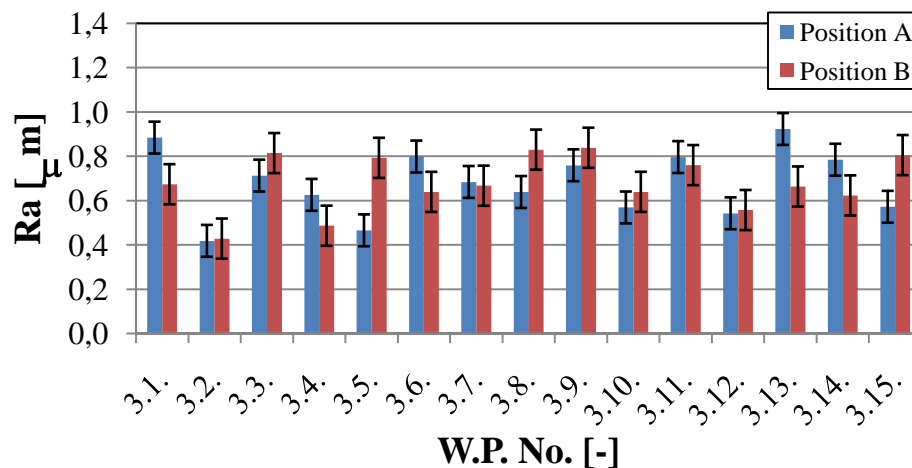
Surface roughness – Reaming operation R4
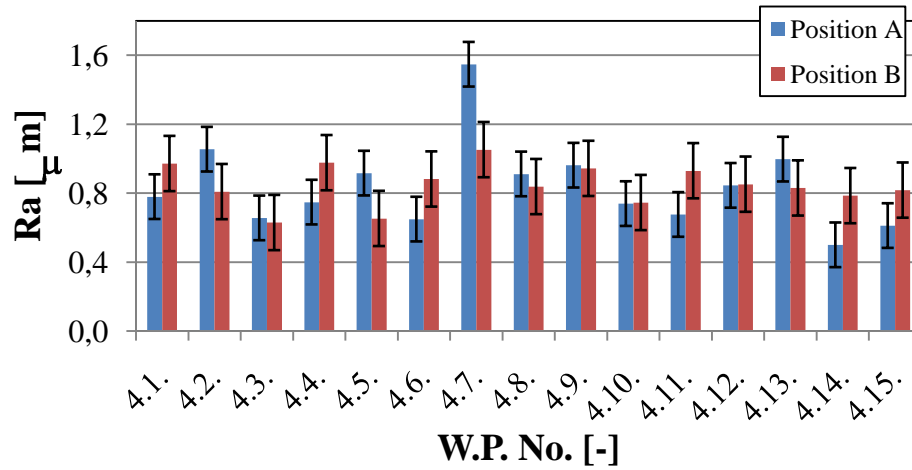
Surface roughness – Reaming operation R5
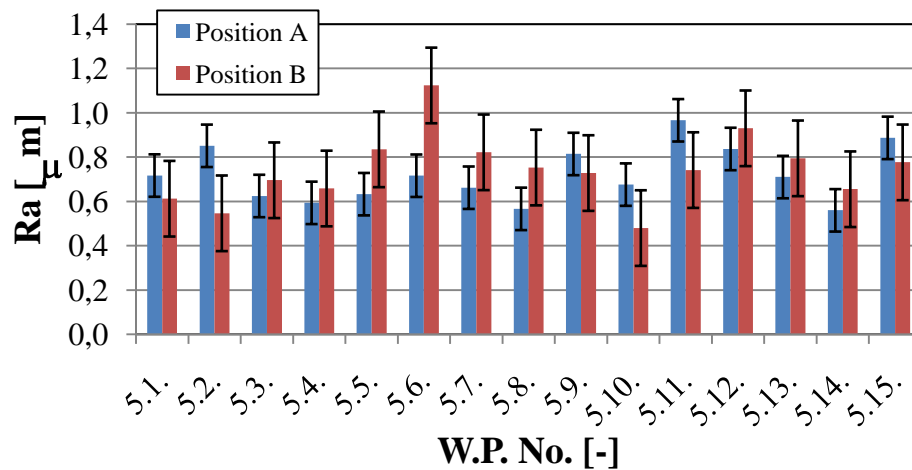
Surface roughness – Reaming operation R6
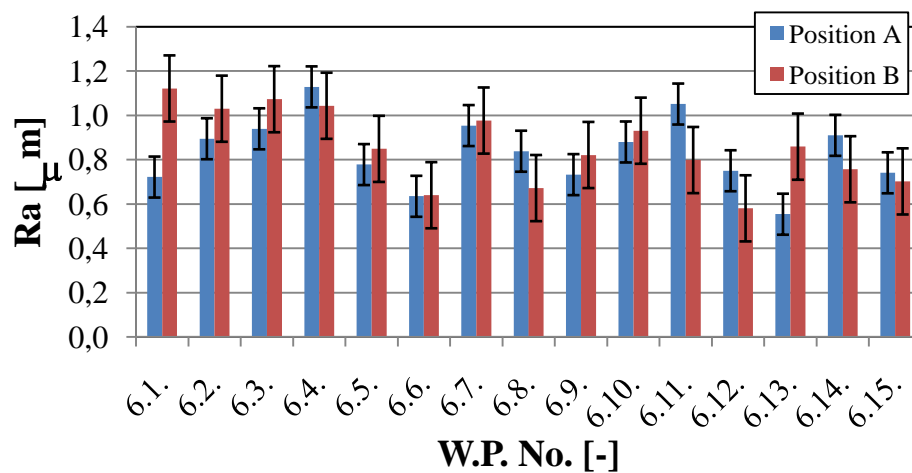
Appendix B - 2

Fig. B.2 - Surface roughness comparison for R1/R2, R2/R3, R3/R4, R3/R5 and R3/R6 reaming operations

Surface roughness comparison – R1/R2 (reverse feed rate)
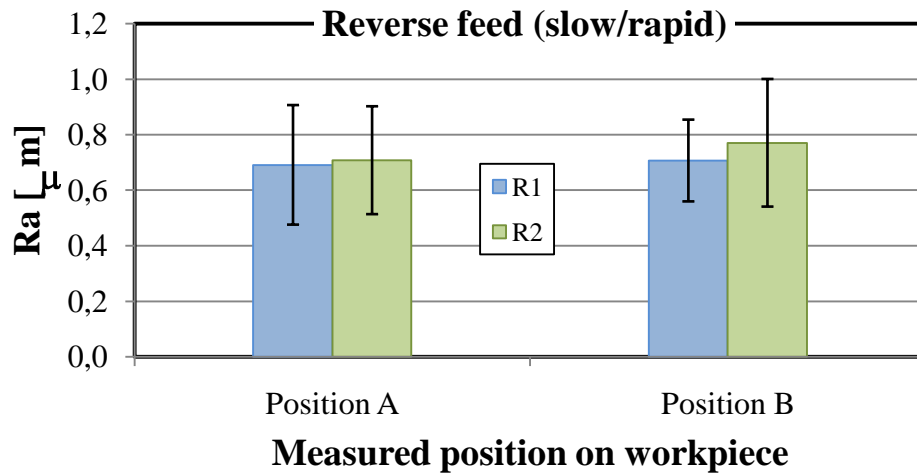
Surface roughness comparison – R2/R3 (feed)
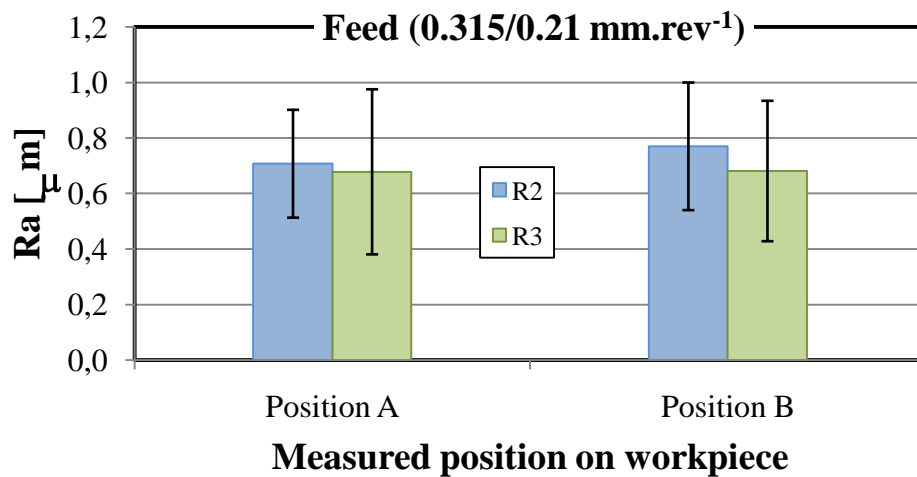
Surface roughness comparison – R3/R4 (depth of cut)
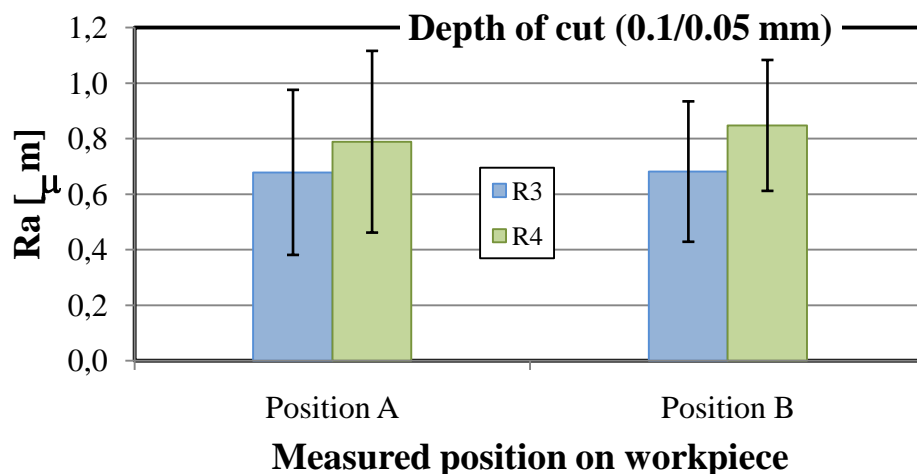
Surface roughness comparison – R3/R5 (nozzle position)

Nozzle postion (TB/TT)

Ra [_μm]

1,2 — 1,0 — 0,8 — 0,6 — 0,4 — 0,2 — 0,0

R3
R5

Position A   Position B

Measured position on workpiece

Surface roughness comparison – R3/R6 (cutting speed)

Cutting speed (5/6 m.min⁻¹)

Ra [_μm]

1,2 — 1,0 — 0,8 — 0,6 — 0,4 — 0,2 — 0,0

R3
R5

Position A   Position B

Measured position on workpiece
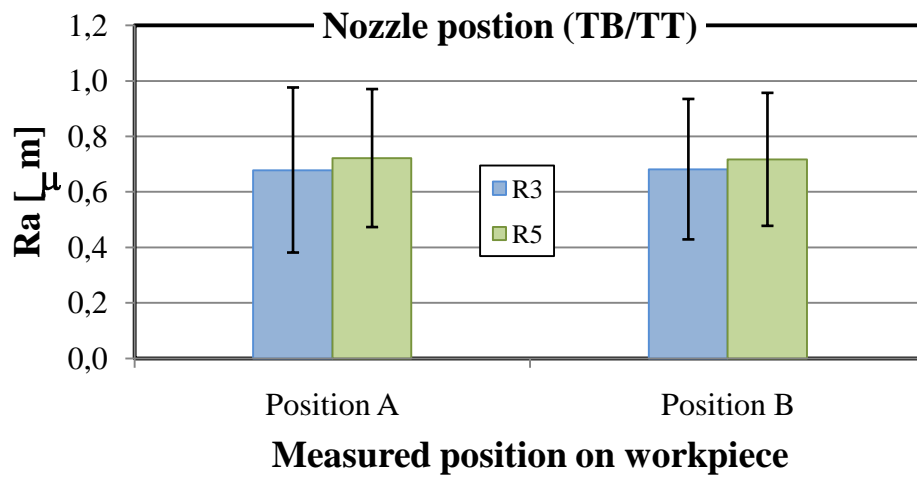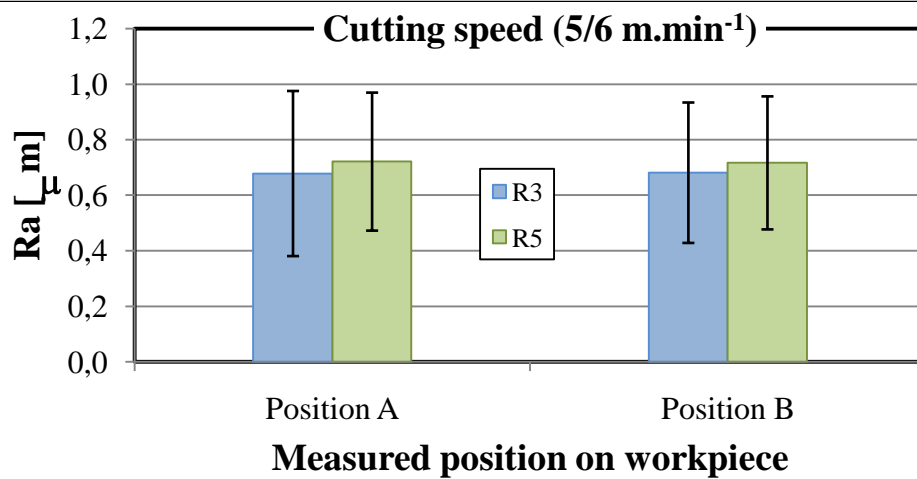
Appendix C - 1

Tab. C.1 - Reaming thrust uncertainty calculation

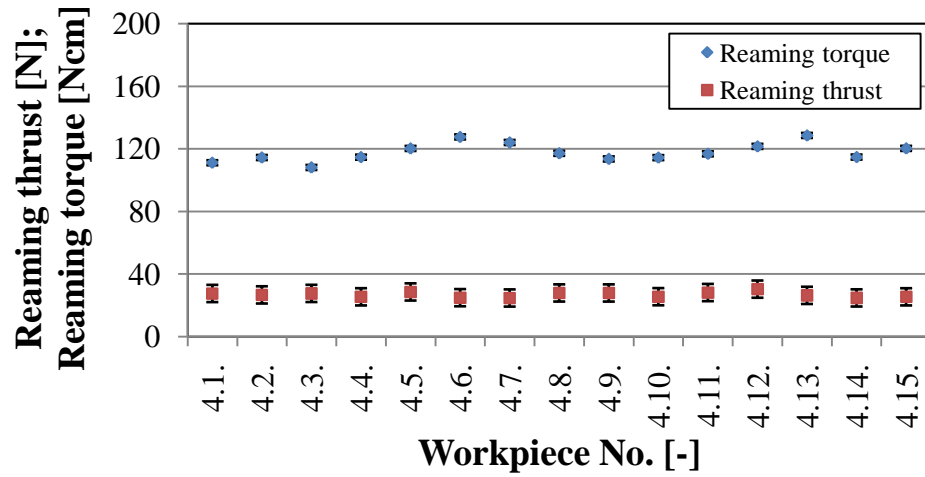| Reaming torque – Reaming operation R2						
No.	Uncertainty component	First derivative		Estimated uncertainty of the uncertainty component		
		$\frac{\partial To}{\partial x_i}$		$u_i(x_i)$		$\frac{\partial To}{\partial x_i} \cdot u_i(x_i)$
$u_1(k_c)$	Uncertainty of specific cutting force influence on torque	$\frac{\partial To}{\partial k_c}$	0.0255	$u(k_c)$	249	6.3
$u_2(f)$	Uncertainty of feed influence on torque	$\frac{\partial To}{\partial f}$	212	$u(f)$	0.012	2.5
$u_3(D_R)$	Uncertainty of reamer diameter influence on torque	$\frac{\partial To}{\partial D_R}$	-1343	$u(D_R)$	0.0025	-3.3
$u_4(d)$	Uncertainty of pilot hole influence on torque	$\frac{\partial To}{\partial d}$	1417	$u(d)$	0.0035	5.0
$u_5(wsd)$	Uncertainty of window span definition influence on torque			$u(wsd)$	2.7	2.7
$u_6(Oil_t)$	Uncertainty of oil temperature influence on torque			$u(Q_{oil})$	1.6	1.6
$u_7(acq)$	Uncertainty of acquisition system influence on torque			$u(acq)$	5.8	5.8

Uncorrelated combined uncertainty [Nmm]	$u^{R1}(To)$	47.3
Coverage factor (for a c. l. of 95%)	k	2
Expanded combined uncertainty [Nmm]	$U^{R1}(To)$	95

Reaming torque – Reaming operation R3						
No.	Uncertainty component	First derivative		Estimated uncertainty of the uncertainty component		
		$\dfrac{\partial To}{\partial x_i}$		$u_i(x_i)$		$\dfrac{\partial To}{\partial x_i} \cdot u_i(x_i)$
$u_1(k_c)$	Uncertainty of specific cutting force influence on torque	$\dfrac{\partial To}{\partial k_c}$	0.0169	$u(k_c)$	282	4.8
$u_2(f)$	Uncertainty of feed influence on torque	$\dfrac{\partial To}{\partial f}$	238	$u(f)$	0.012	2.7
$u_3(D_R)$	Uncertainty of reamer diameter influence on torque	$\dfrac{\partial To}{\partial D_R}$	-1007	$u(D_R)$	0.0023	-2.3
$u_4(d)$	Uncertainty of pilot hole influence on torque	$\dfrac{\partial To}{\partial d}$	1062	$u(d)$	0.0035	3.7
$u_5(wsd)$	Uncertainty of window span definition influence on torque			$u(wsd)$	4.7	4.7
$u_6(Oil_t)$	Uncertainty of oil temperature influence on torque			$u(Q_{oil})$	1.6	1.6
$u_7(acq)$	Uncertainty of acquisition system influence on torque			$u(acq)$	5.8	5.8

Uncorrelated combined uncertainty [Nmm]	$u^{R1}(To)$	10.3
Coverage factor (for a c. l. of 95%)	k	2
Expanded combined uncertainty [Nmm]	$U^{R1}(To)$	21

Reaming torque – Reaming operation R4						
No.	Uncertainty component	First derivative		Estimated uncertainty of the uncertainty component		
		$\dfrac{\partial To}{\partial x_i}$		$u_i(x_i)$		$\dfrac{\partial To}{\partial x_i} \cdot u_i(x_i)$
$u_1(k_c)$	Uncertainty of specific cutting force influence on torque	$\dfrac{\partial To}{\partial k_c}$	0.0082	$u(k_c)$	282	2.3
$u_2(f)$	Uncertainty of feed influence on torque	$\dfrac{\partial To}{\partial f}$	115	$u(f)$	0.012	1.3
$u_3(D_R)$	Uncertainty of reamer diameter influence on torque	$\dfrac{\partial To}{\partial D_R}$	-1010	$u(D_R)$	0.0023	-2.3
$u_4(d)$	Uncertainty of pilot hole influence on torque	$\dfrac{\partial To}{\partial d}$	1036	$u(d)$	0.0035	3.6
$u_5(wsd)$	Uncertainty of window span definition influence on torque			$u(wsd)$	0.5	0.5
$u_6(Oil_t)$	Uncertainty of oil temperature influence on torque			$u(Q_{oil})$	1.6	1.6
$u_7(acq)$	Uncertainty of acquisition system influence on torque			$u(acq)$	5.8	5.8

Uncorrelated combined uncertainty [Nmm]	$u^{R1}(To)$	7.9
Coverage factor (for a c. l. of 95%)	k	2
Expanded combined uncertainty [Nmm]	$U^{R1}(To)$	16

Reaming torque – Reaming operation R5					
No.	Uncertainty component	First derivative		Estimated uncertainty of the uncertainty component	
		$\frac{\partial To}{\partial x_i}$		$u_i(x_i)$	$\frac{\partial To}{\partial x_i} \cdot u_i(x_i)$
$u_1(k_c)$	Uncertainty of specific cutting force influence on torque	$\frac{\partial To}{\partial k_c}$	0.0170	$u(k_c)$	282	4.8
$u_2(f)$	Uncertainty of feed influence on torque	$\frac{\partial To}{\partial f}$	238	$u(f)$	0.012	2.8
$u_3(D_R)$	Uncertainty of reamer diameter influence on torque	$\frac{\partial To}{\partial D_R}$	-1007	$u(D_R)$	0.0025	-2.5
$u_4(d)$	Uncertainty of pilot hole influence on torque	$\frac{\partial To}{\partial d}$	1062	$u(d)$	0.0035	3.7
$u_5(wsd)$	Uncertainty of window span definition influence on torque			$u(wsd)$	2.1	2.1
$u_6(Oil_t)$	Uncertainty of oil temperature influence on torque			$u(Q_{oil})$	1.6	1.6
$u_7(acq)$	Uncertainty of acquisition system influence on torque			$u(acq)$	5.8	5.8

Uncorrelated combined uncertainty [Nmm]	$u^{R1}(To)$	9.5
Coverage factor (for a c. l. of 95%)	k	2
Expanded combined uncertainty [Nmm]	$U^{R1}(To)$	19

Reaming torque – Reaming operation R6						
No.	Uncertainty component	First derivative		Estimated uncertainty of the uncertainty component		
		$\frac{\partial To}{\partial x_i}$		$u_i(x_i)$		$\frac{\partial To}{\partial x_i} \cdot u_i(x_i)$
$u_1(k_c)$	Uncertainty of specific cutting force influence on torque	$\frac{\partial To}{\partial k_c}$	0.0169	$u(k_c)$	282	4.8
$u_2(f)$	Uncertainty of feed influence on torque	$\frac{\partial To}{\partial f}$	238	$u(f)$	0.012	2.7
$u_3(D_R)$	Uncertainty of reamer diameter influence on torque	$\frac{\partial To}{\partial D_R}$	-1007	$u(D_R)$	0.0021	-2.2
$u_4(d)$	Uncertainty of pilot hole influence on torque	$\frac{\partial To}{\partial d}$	1062	$u(d)$	0.0035	3.7
$u_5(wsd)$	Uncertainty of window span definition influence on torque			$u(wsd)$	1.2	1.2
$u_6(Oil_t)$	Uncertainty of oil temperature influence on torque			$u(Q_{oil})$	1.6	1.6
$u_7(acq)$	Uncertainty of acquisition system influence on torque			$u(acq)$	5.8	5.8

Uncorrelated combined uncertainty [Nmm]	$u^{R1}(To)$	9.3
Coverage factor (for a c. l. of 95%)	k	2
Expanded combined uncertainty [Nmm]	$U^{R1}(To)$	19

Appendix C - 2

Tab. C.2 - Reaming torque uncertainty calculation

No.	Uncertainty component	First derivative		Estimated uncertainty of the uncertainty component		
		$\frac{\partial Th}{\partial x_i}$		$u_i(x_i)$		$\frac{\partial Th}{\partial x_i} \cdot u_i(x_i)$
$u_1'(k_c)$	Uncertainty of specific cutting force influence on thrust	$\frac{\partial Th}{\partial k_c}$	0.0051	$u(k_c)$	249	1.3
$u_2'(f)$	Uncertainty of feed influence on thrust	$\frac{\partial Th}{\partial f}$	43	$u(f)$	0.012	0.5
$u_3'(D_R)$	Uncertainty of reamer diameter influence on thrust	$\frac{\partial Th}{D_R}$	-614	$u(D_R)$	0.0024	-1.5
$u_4'(d)$	Uncertainty of pilot hole influence on thrust	$\frac{\partial Th}{\partial d}$	627	$u(d)$	0.0035	2.2
$u_5'(wsd)$	Uncertainty of window span definition influence on thrust			$u(wsd)$	0.23	0.23
$u_6'(Oil_t)$	Uncertainty of oil temperature influence on thrust			$u(Q_{oil})$	1.6	1.6
$u_7'(acq)$	Uncertainty of acquisition system influence on thrust			$u(acq)$	0.6	0.6

Reaming thrust – Reaming operation R1

Uncorrelated combined uncertainty [N]	$u^{R1}(Th)$	3.4
Coverage factor (for a c. l. of 95%)	k	2
Expanded combined uncertainty [N]	$U^{R1}(Th)$	7

	Reaming thrust – Reaming operation R2					
No.	Uncertainty component	First derivative		Estimated uncertainty of the uncertainty component		
		$\frac{\partial Th}{\partial x_i}$		$u_i(x_i)$		$\frac{\partial Th}{\partial x_i} \cdot u_i(x_i)$
$u_1^{'}(k_c)$	Uncertainty of specific cutting force influence on thrust	$\frac{\partial Th}{\partial k_c}$	0.0051	$u(k_c)$	249	1.3
$u_2^{'}(f)$	Uncertainty of feed influence on thrust	$\frac{\partial Th}{\partial f}$	42	$u(f)$	0.012	0.5
$u_3^{'}(D_R)$	Uncertainty of reamer diameter influence on thrust	$\frac{\partial Th}{\partial D_R}$	-614	$u(D_R)$	0.0025	-1.5
$u_4^{'}(d)$	Uncertainty of pilot hole influence on thrust	$\frac{\partial Th}{\partial d}$	627	$u(d)$	0.0035	2.2
$u_5^{'}(wsd)$	Uncertainty of window span definition influence on thrust			$u(wsd)$	0.13	0.13
$u_6^{'}(Oil_t)$	Uncertainty of oil temperature influence on thrust			$u(Q_{oil})$	1.6	1.6
$u_7^{'}(acq)$	Uncertainty of acquisition system influence on thrust			$u(acq)$	0.6	0.6

Uncorrelated combined uncertainty [N]	$u^{R1}(Th)$	3.5
Coverage factor (for a c. l. of 95%)	k	2
Expanded combined uncertainty [N]	$U^{R1}(Th)$	7

Reaming thrust – Reaming operation R3						
No.	Uncertainty component	First derivative		Estimated uncertainty of the uncertainty component		
		$\frac{\partial Th}{\partial x_i}$		$u_i(x_i)$		$\frac{\partial Th}{\partial x_i} \cdot u_i(x_i)$
$u_1'(k_c)$	Uncertainty of specific cutting force influence on thrust	$\frac{\partial Th}{\partial k_c}$	0.0034	$u(k_c)$	282	1.0
$u_2'(f)$	Uncertainty of feed influence on thrust	$\frac{\partial Th}{\partial f}$	48	$u(f)$	0.012	0.5
$u_3'(D_R)$	Uncertainty of reamer diameter influence on thrust	$\frac{\partial Th}{\partial D_R}$	-460	$u(D_R)$	0.0023	-1.0
$u_4'(d)$	Uncertainty of pilot hole influence on thrust	$\frac{\partial Th}{\partial d}$	470	$u(d)$	0.0035	1.7
$u_5'(wsd)$	Uncertainty of window span definition influence on thrust			$u(wsd)$	0.03	0.03
$u_6'(Oil_t)$	Uncertainty of oil temperature influence on thrust			$u(Q_{oil})$	1.6	1.6
$u_7'(acq)$	Uncertainty of acquisition system influence on thrust			$u(acq)$	0.6	0.6

Uncorrelated combined uncertainty [N]	$u^{R1}(Th)$	2.8
Coverage factor (for a c. l. of 95%)	k	2
Expanded combined uncertainty [N]	$U^{R1}(Th)$	6

Reaming thrust – Reaming operation R4						
No.	Uncertainty component	First derivative		Estimated uncertainty of the uncertainty component		
		$\frac{\partial Th}{\partial x_i}$		$u_i(x_i)$		$\frac{\partial Th}{\partial x_i} \cdot u_i(x_i)$
$u_1'(k_c)$	Uncertainty of specific cutting force influence on thrust	$\frac{\partial Th}{\partial k_c}$	0.0016	$u(k_c)$	282	0.5
$u_2'(f)$	Uncertainty of feed influence on thrust	$\frac{\partial Th}{\partial f}$	23	$u(f)$	0.012	0.3
$u_3'(D_R)$	Uncertainty of reamer diameter influence on thrust	$\frac{\partial Th}{\partial D_R}$	-460	$u(D_R)$	0.0023	-1.1
$u_4'(d)$	Uncertainty of pilot hole influence on thrust	$\frac{\partial Th}{\partial d}$	465	$u(d)$	0.0035	1.6
$u_5'(wsd)$	Uncertainty of window span definition influence on thrust			$u(wsd)$	0.09	0.09
$u_6'(Oil_t)$	Uncertainty of oil temperature influence on thrust			$u(Q_{oil})$	1.6	1.6
$u_7'(acq)$	Uncertainty of acquisition system influence on thrust			$u(acq)$	0.6	0.6

Uncorrelated combined uncertainty [N]	$u^{R1}(Th)$	2.6
Coverage factor (for a c. l. of 95%)	k	2
Expanded combined uncertainty [N]	$U^{R1}(Th)$	5

Reaming thrust – Reaming operation R5						
No.	Uncertainty component	First derivative		Estimated uncertainty of the uncertainty component		
		$\frac{\partial Th}{\partial x_i}$		$u_i(x_i)$		$\frac{\partial Th}{\partial x_i} \cdot u_i(x_i)$
$u_1'(k_c)$	Uncertainty of specific cutting force influence on thrust	$\frac{\partial Th}{\partial k_c}$	0.0034	$u(k_c)$	282	1.0
$u_2'(f)$	Uncertainty of feed influence on thrust	$\frac{\partial Th}{\partial f}$	48	$u(f)$	0.012	0.6
$u_3'(D_R)$	Uncertainty of reamer diameter influence on thrust	$\frac{\partial Th}{\partial D}$	-460	$u(D)$	0.0025	-1.1
$u_4'(d)$	Uncertainty of pilot hole influence on thrust	$\frac{\partial Th}{\partial d}$	470	$u(d)$	0.0035	1.7
$u_5'(wsd)$	Uncertainty of window span definition influence on thrust			$u(wsd)$	0.06	0.06
$u_6'(Oil_t)$	Uncertainty of oil temperature influence on thrust			$u(Q_{oil})$	1.6	1.6
$u_7'(acq)$	Uncertainty of acquisition system influence on thrust			$u(acq)$	0.6	0.6

Uncorrelated combined uncertainty [N]	$u^{R1}(Th)$	2.9
Coverage factor (for a c. l. of 95%)	k	2
Expanded combined uncertainty [N]	$U^{R1}(Th)$	6

Reaming thrust – Reaming operation R6						
No.	Uncertainty component	First derivative		Estimated uncertainty of the uncertainty component		
		$\frac{\partial Th}{\partial x_i}$		$u_i(x_i)$		$\frac{\partial Th}{\partial x_i} \cdot u_i(x_i)$
$u'_1(k_c)$	Uncertainty of specific cutting force influence on thrust	$\frac{\partial Th}{\partial k_c}$	0.0034	$u(k_c)$	282	1.0
$u'_2(f)$	Uncertainty of feed influence on thrust	$\frac{\partial Th}{\partial f}$	48	$u(f)$	0.012	0.5
$u'_3(D_R)$	Uncertainty of reamer diameter influence on thrust	$\frac{\partial Th}{\partial D_R}$	-460	$u(D_R)$	0.0021	-1.0
$u'_4(d)$	Uncertainty of pilot hole influence on thrust	$\frac{\partial Th}{\partial d}$	470	$u(d)$	0.0035	1.7
$u'_5(wsd)$	Uncertainty of window span definition influence on thrust			$u(wsd)$	0.08	0.08
$u'_6(Oil_t)$	Uncertainty of oil temperature influence on thrust			$u(Q_{oil})$	1.6	1.6
$u'_7(acq)$	Uncertainty of acquisition system influence on thrust			$u(acq)$	0.6	0.6

Uncorrelated combined uncertainty [N]	$u^{R1}(Th)$	2.8
Coverage factor (for a c. l. of 95%)	k	2
Expanded combined uncertainty [N]	$U^{R1}(Th)$	6

Appendix C - 3

Fig. C.1 - Reaming thrust and reaming torque for every reaming operation

Reaming thrust and reaming torque – Reaming operation R1

Reaming thrust and reaming torque – Reaming operation R2

Reaming thrust and reaming torque – Reaming operation R3
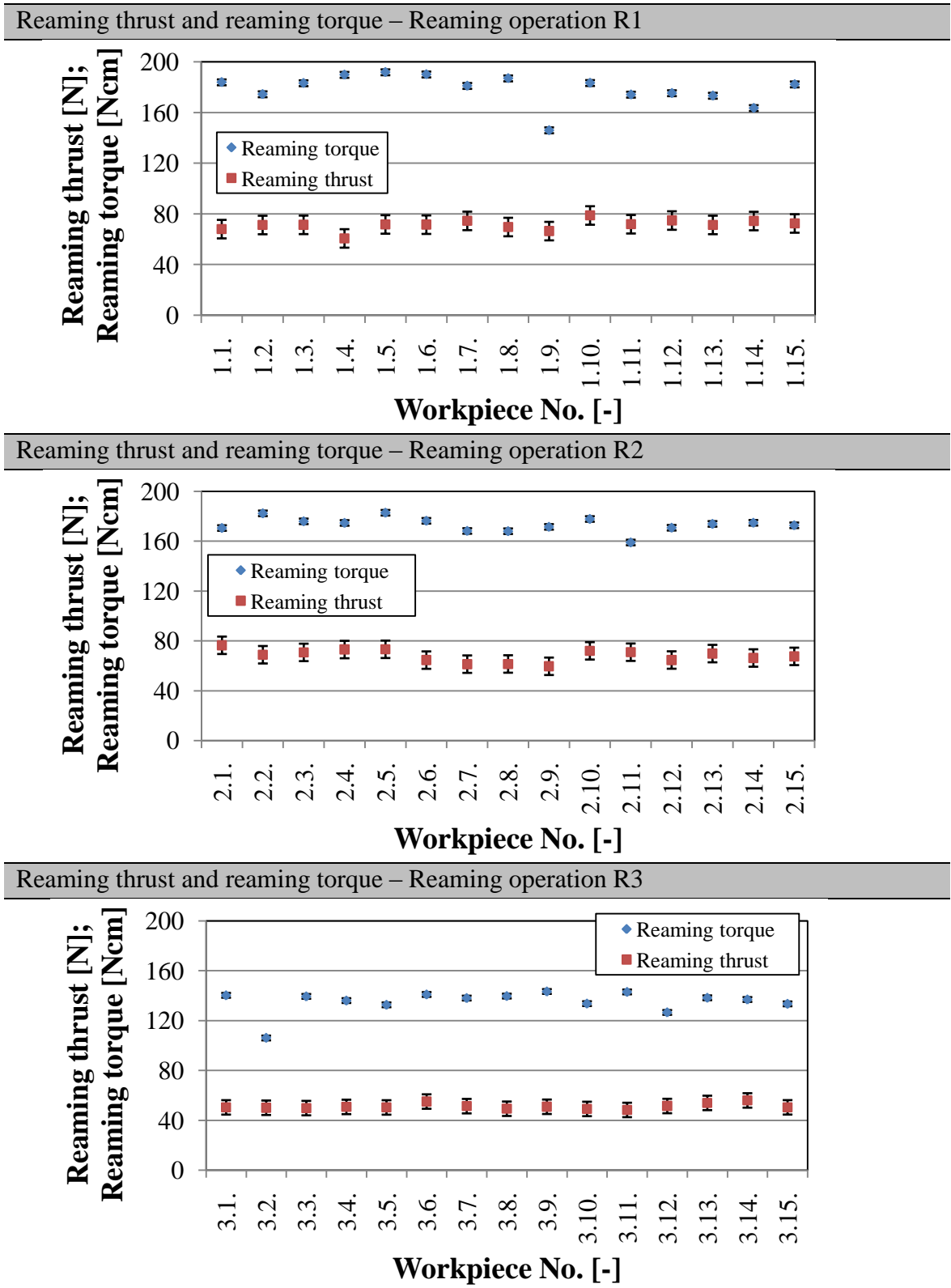
Reaming thrust and reaming torque – Reaming operation R4

Reaming thrust and reaming torque – Reaming operation R5
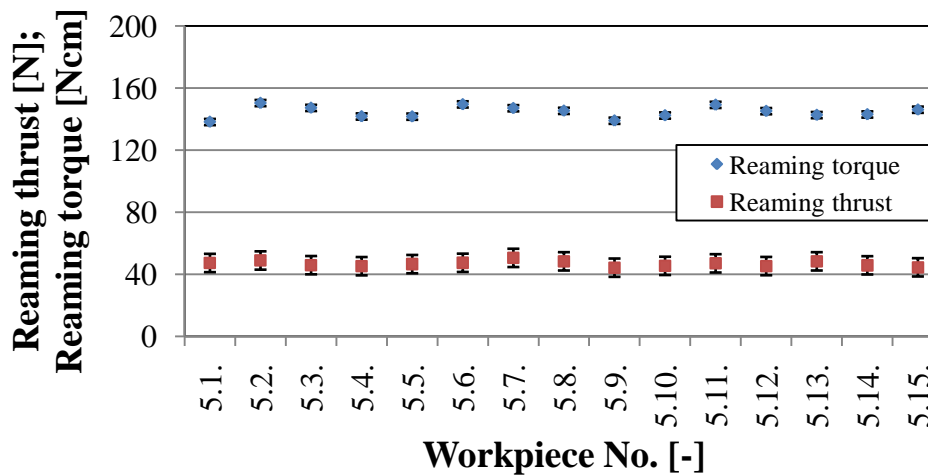
Reaming thrust and reaming torque – Reaming operation R6
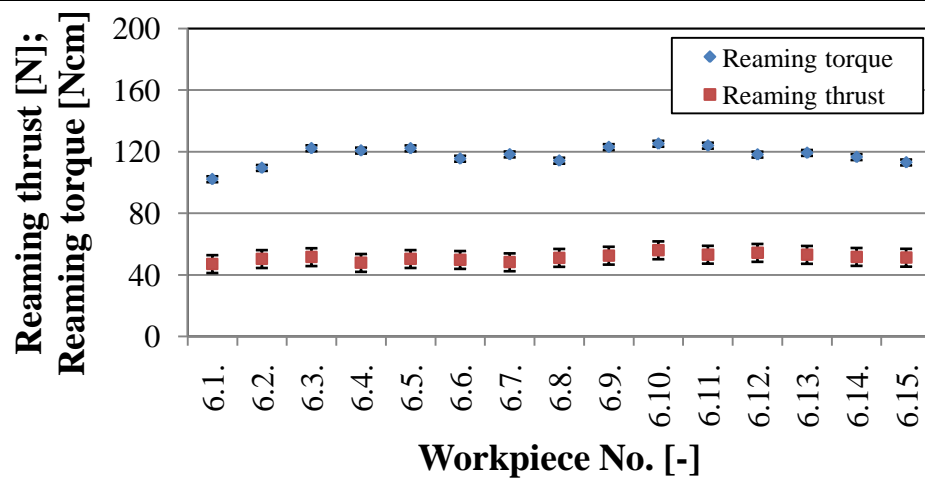
Appendix C - 4

Fig. C.2 - Reaming thrust and reaming torque comparison for R1/R2, R2/R3, R3/R4, R3/R5 and R3/R6 reaming operations
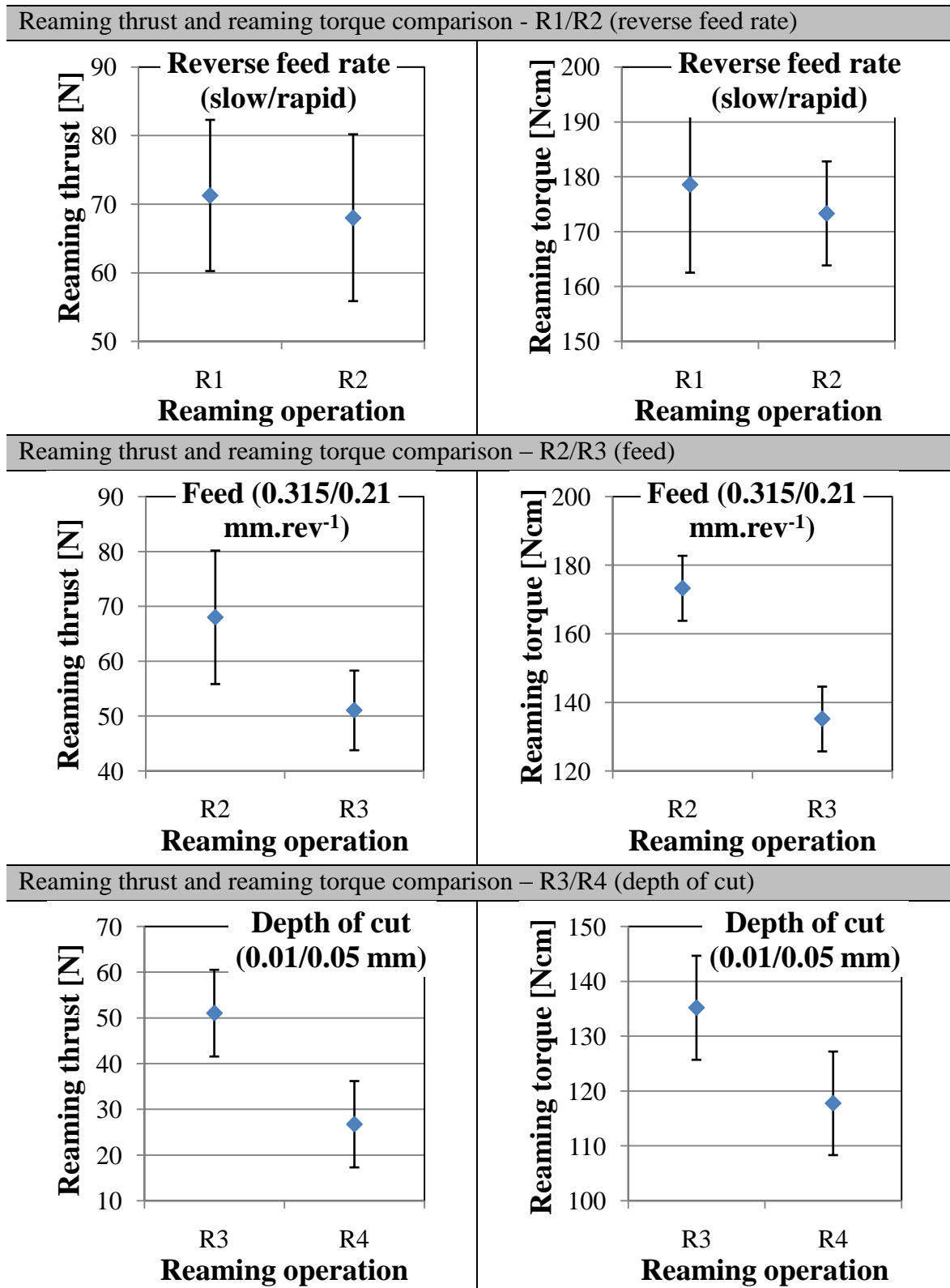
Reaming thrust and reaming torque comparison – R3/R5 (nozzle position)
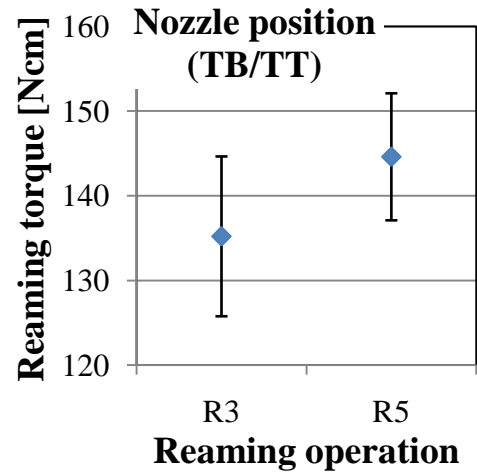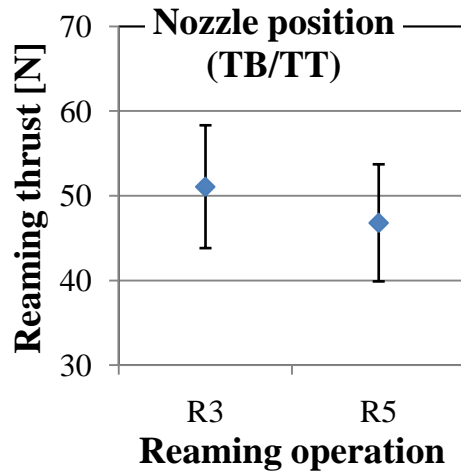
Reaming thrust and reaming torque comparison – R3/R6 (cutting speed)
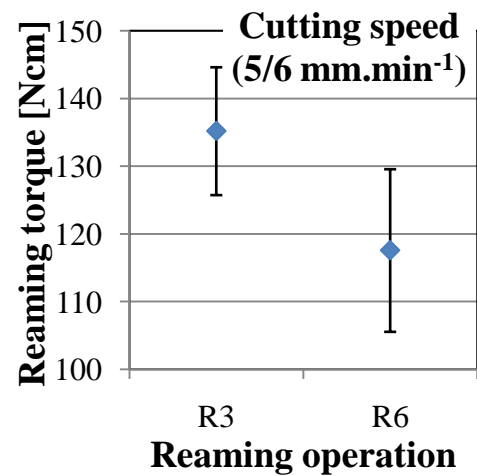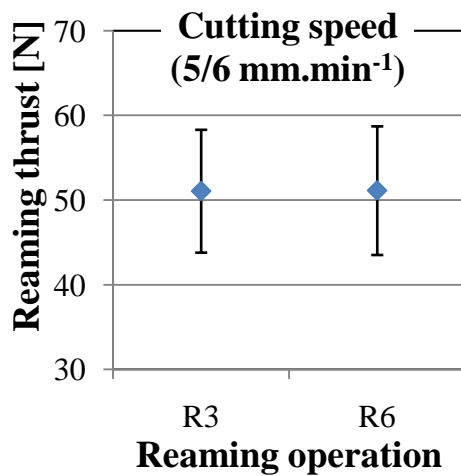
Appendix C - 5

Fig. C.3 - Reaming thrust and reaming torque graphs for each reamed specimen and every RO

Reaming operation R1

1.1.

1.2.

1.3.

1.4.

1.5.

1.6.

1.7.

1.8.

1.9.

1.10.

1.11.

1.12.
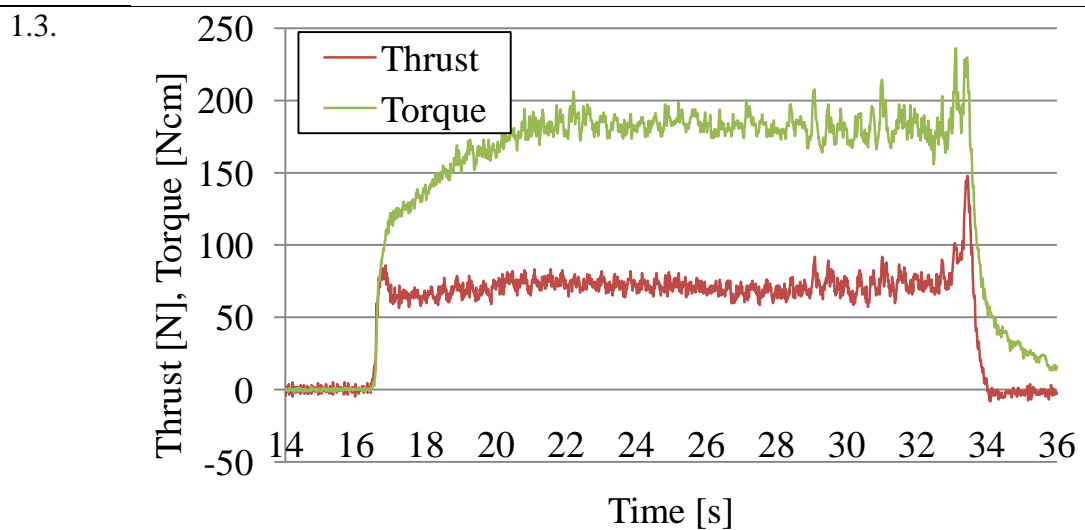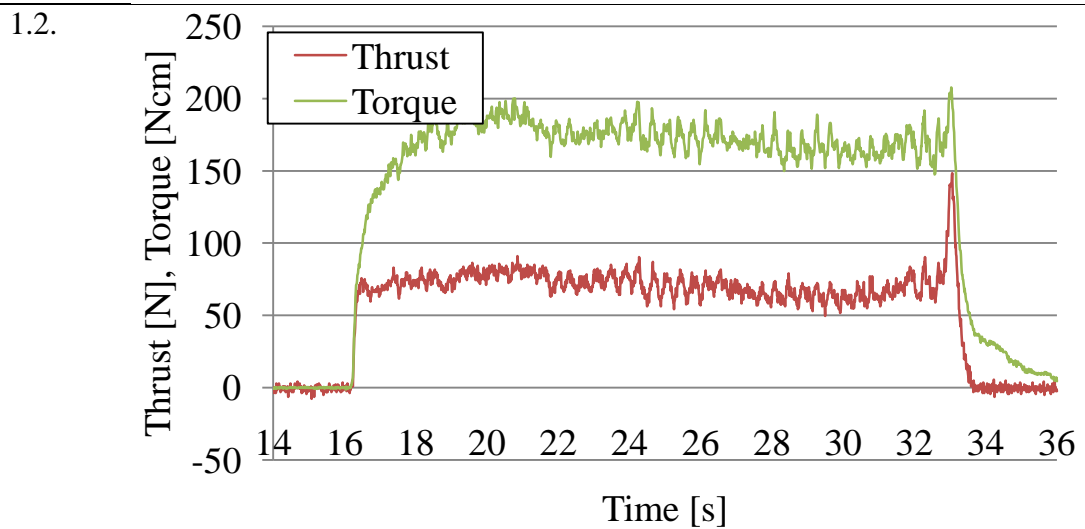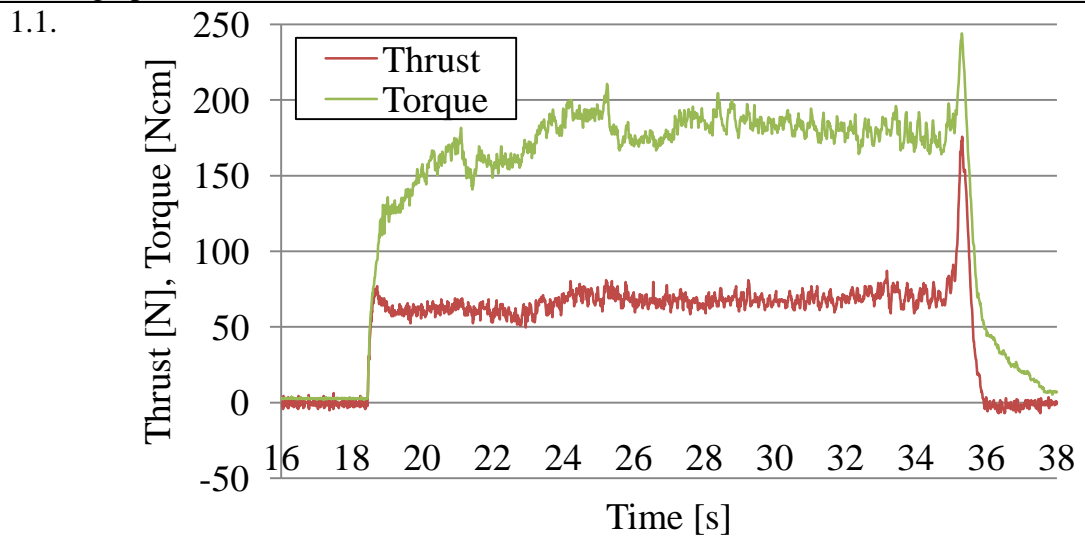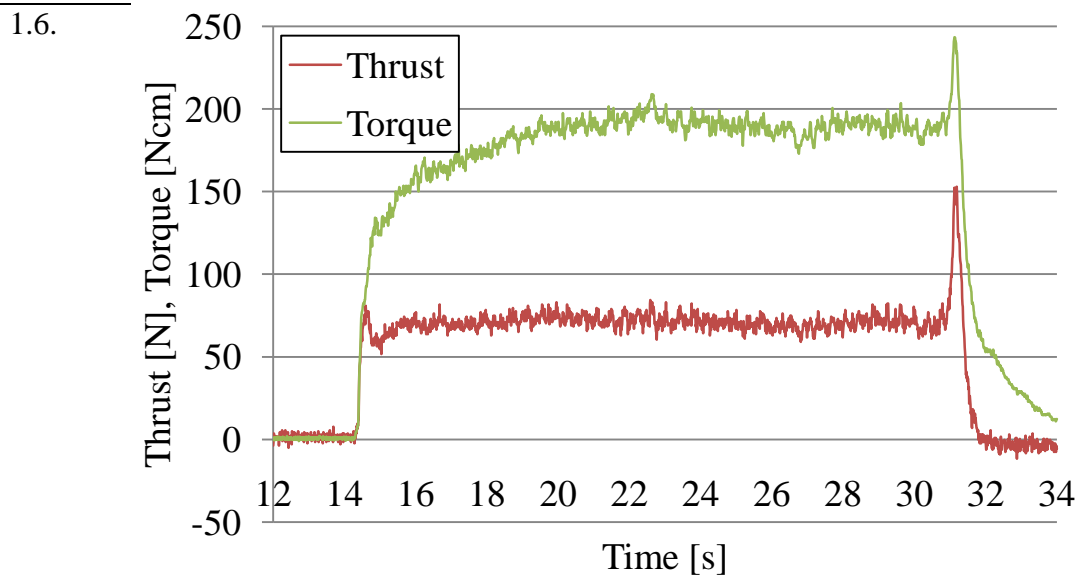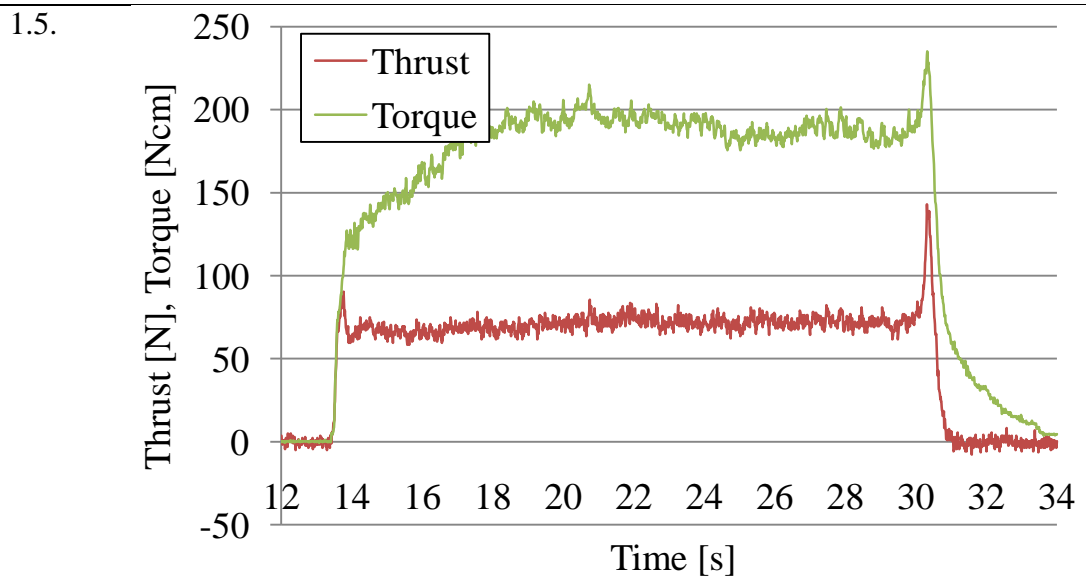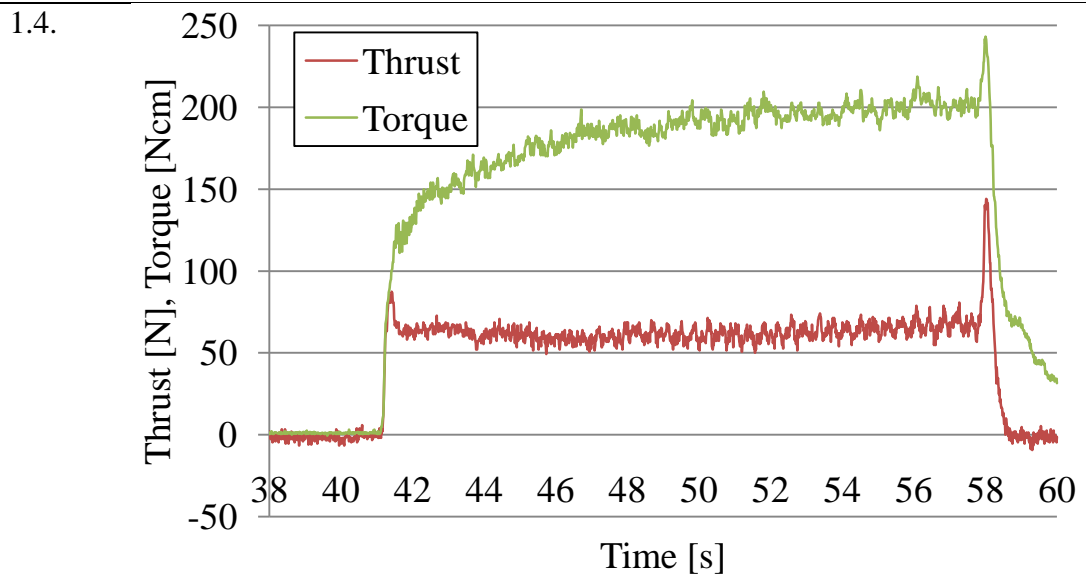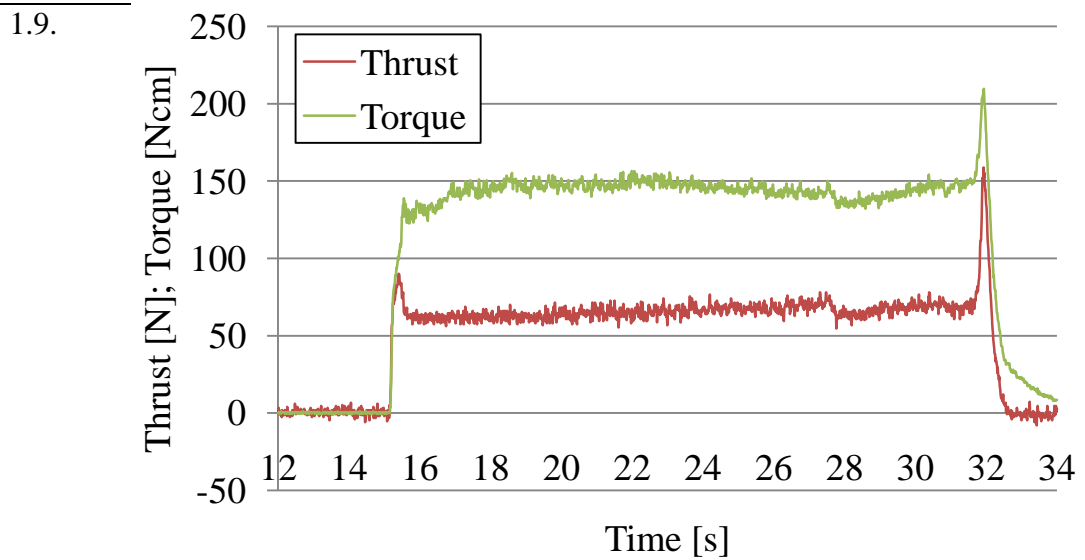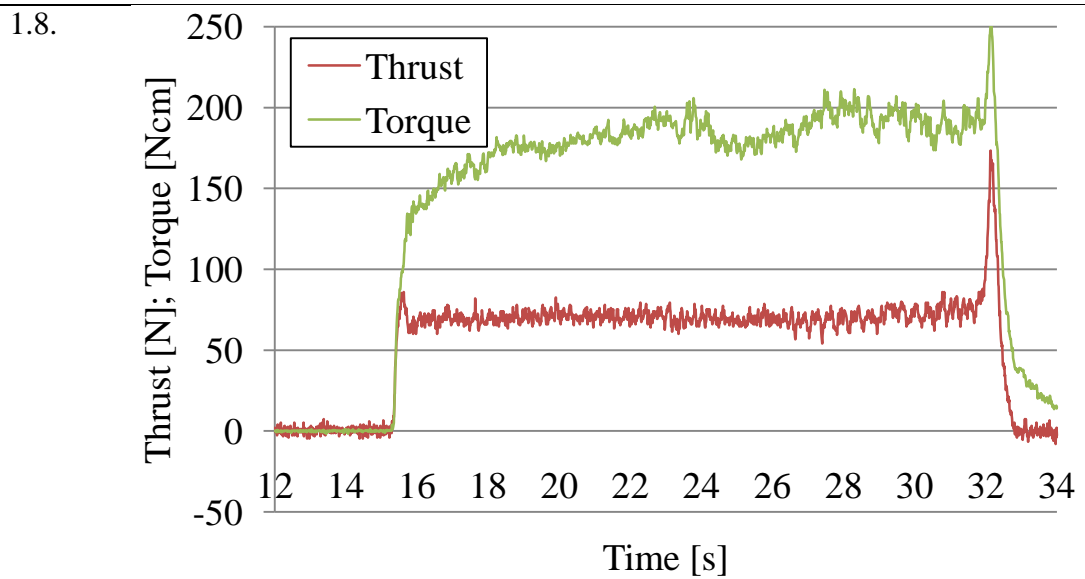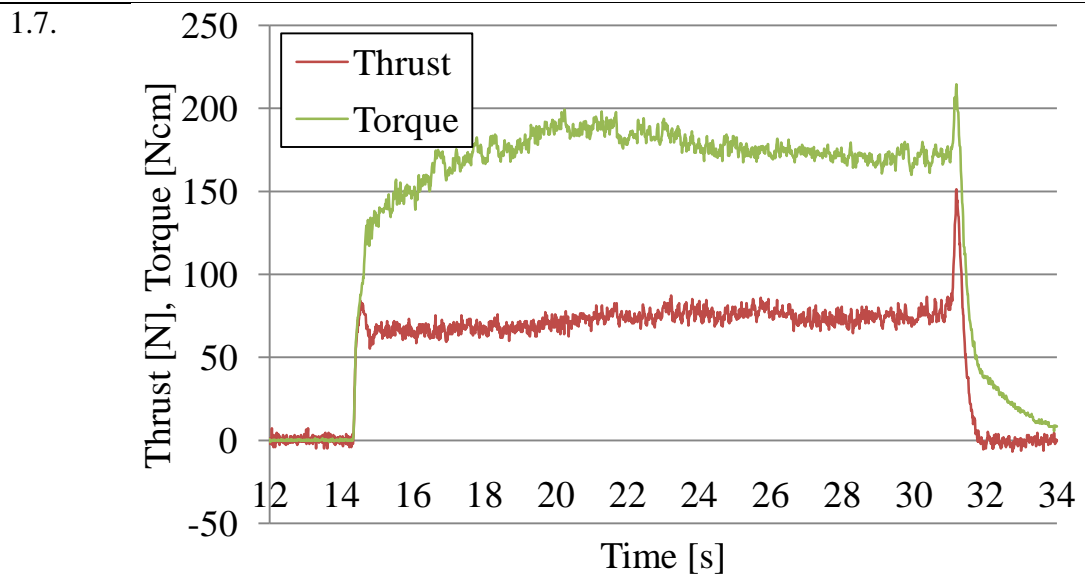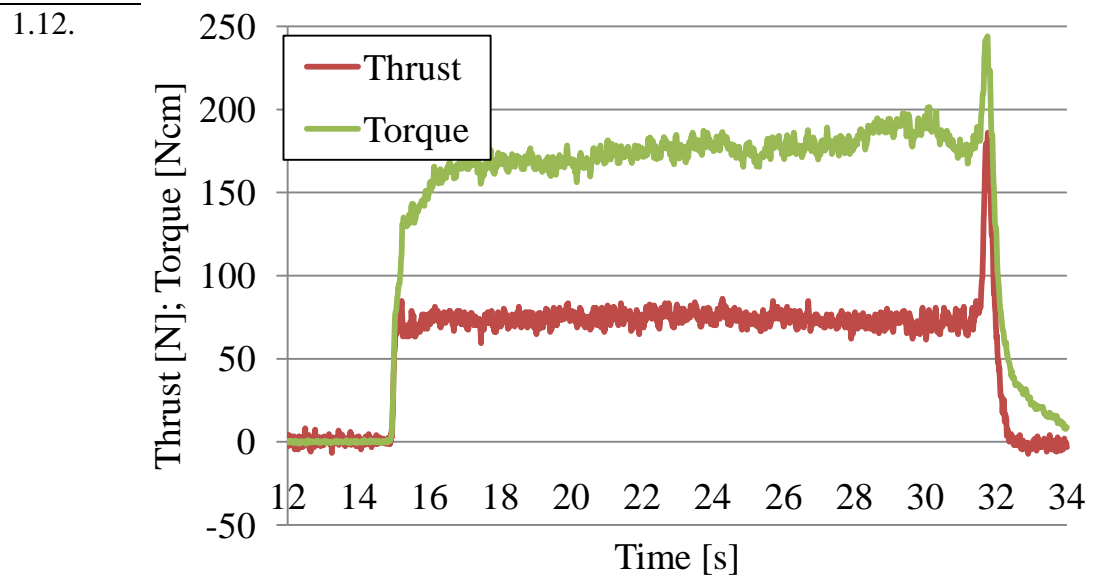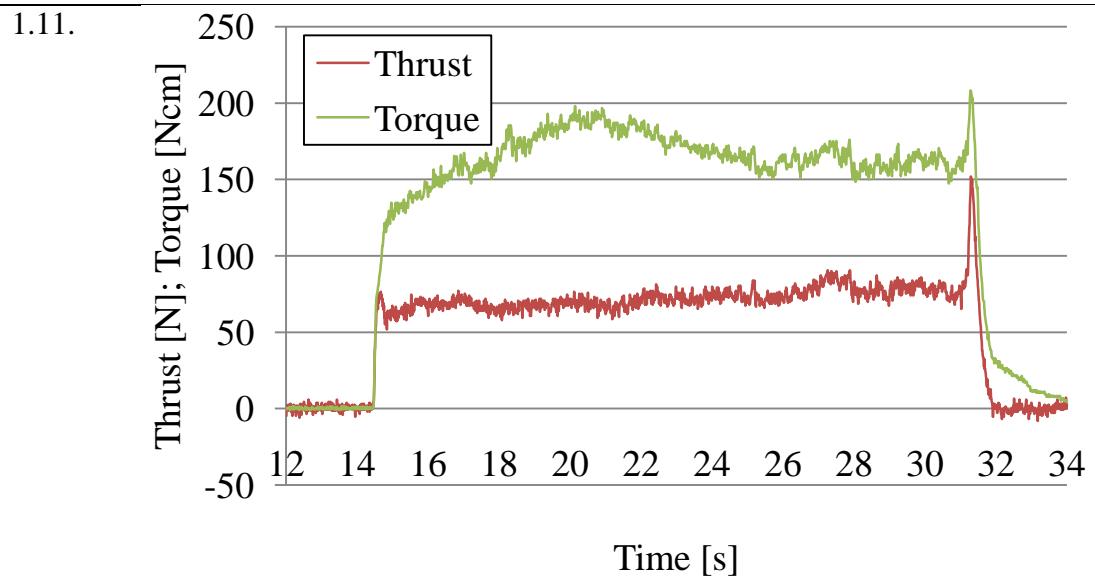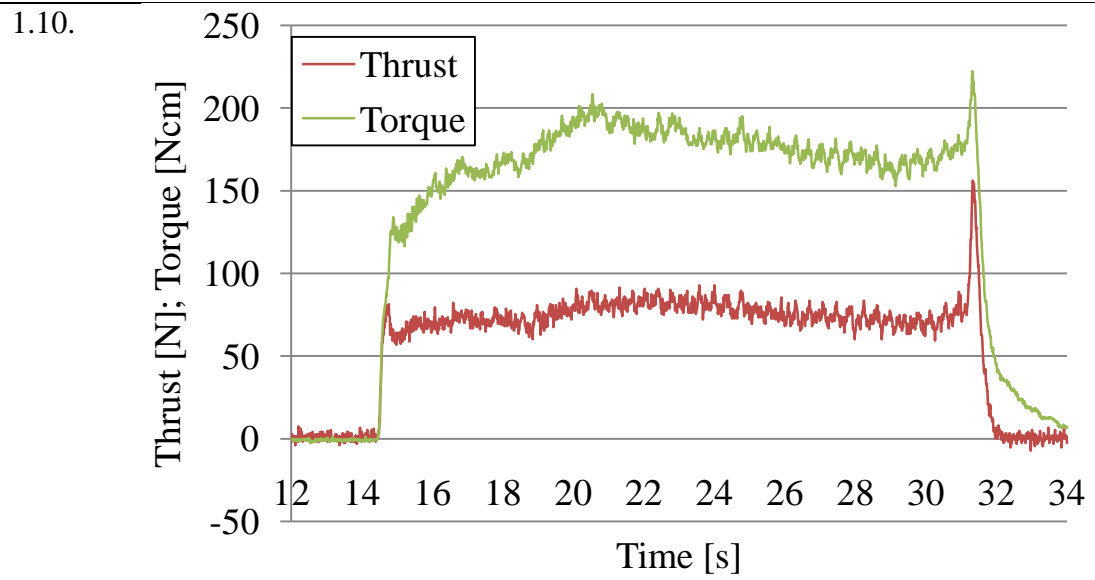
1.13.
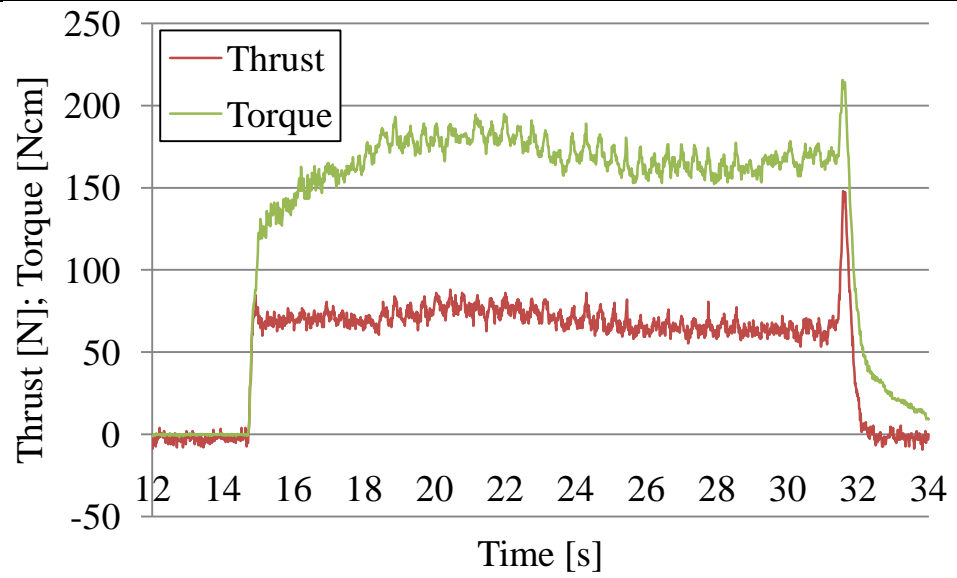
1.14.
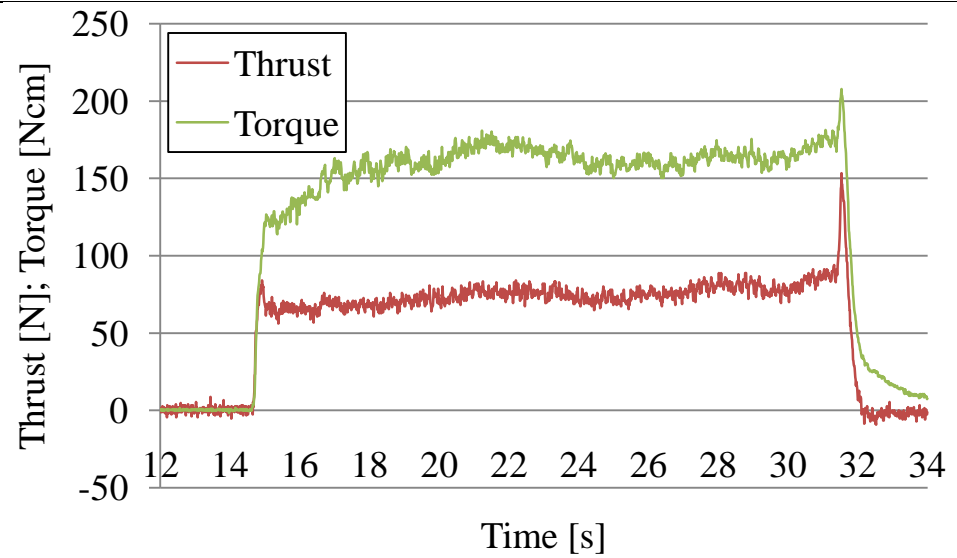
1.15.
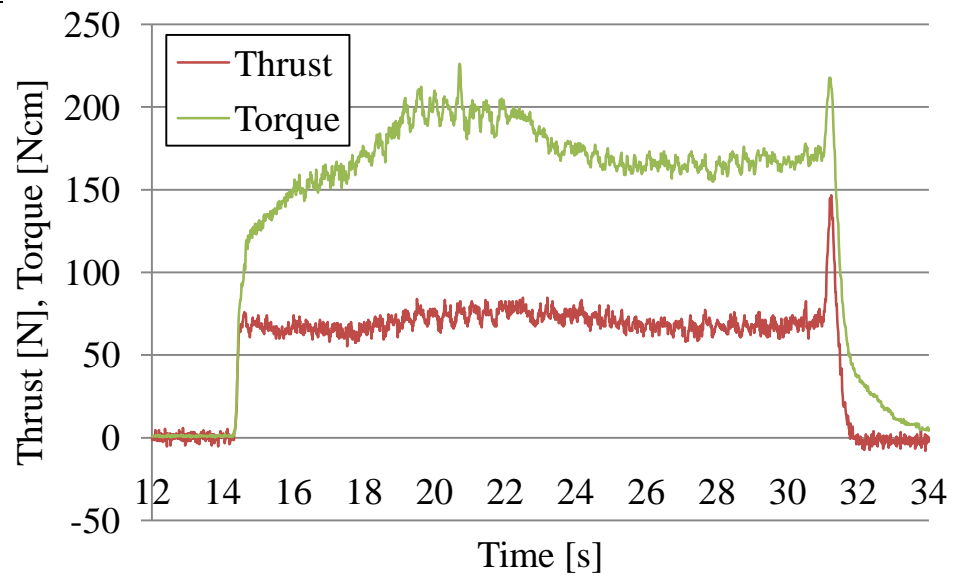
Reaming operation R2

2.1.

2.2.

2.3.

2.4.

2.5.

2.6.

2.7.

2.8.

2.9.

2.10.

2.11.

2.12.

2.13.

2.14.

2.15.
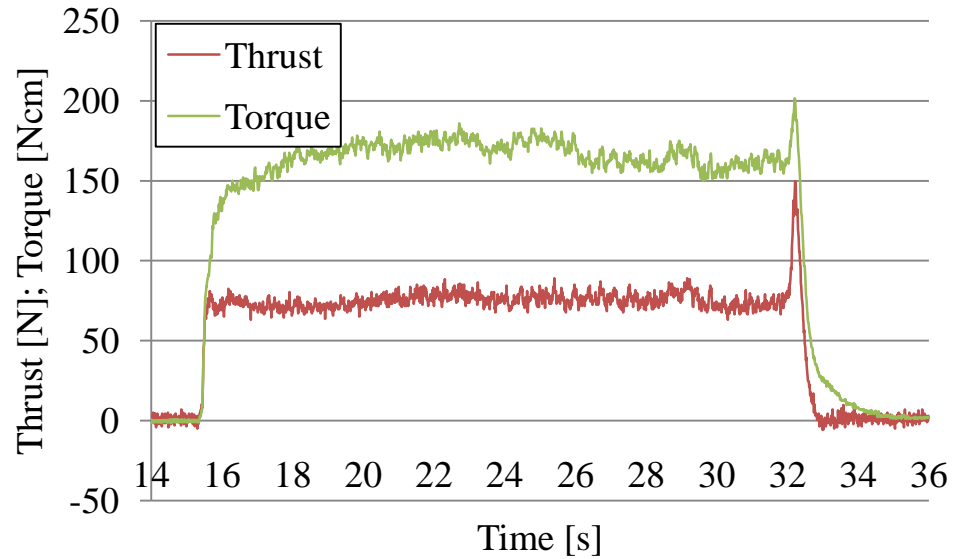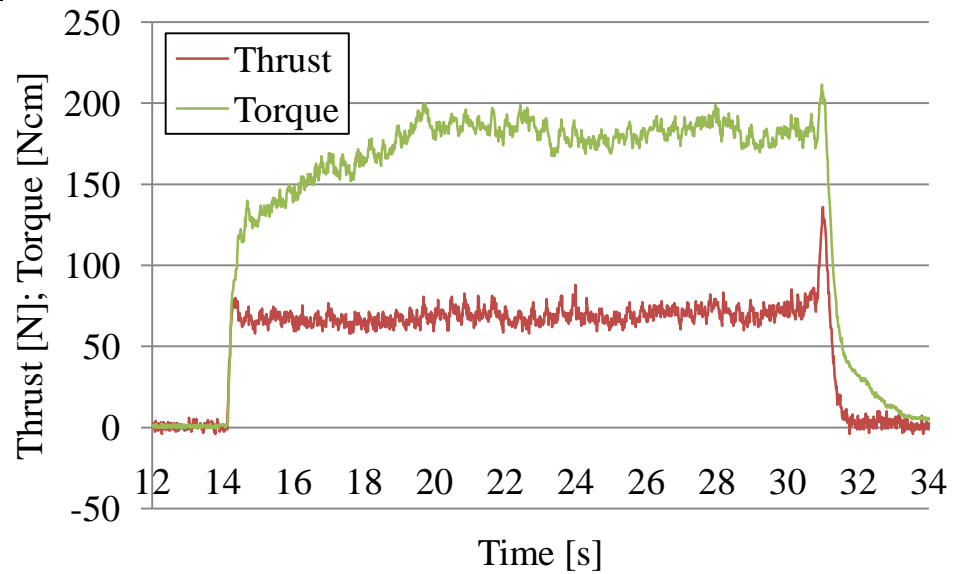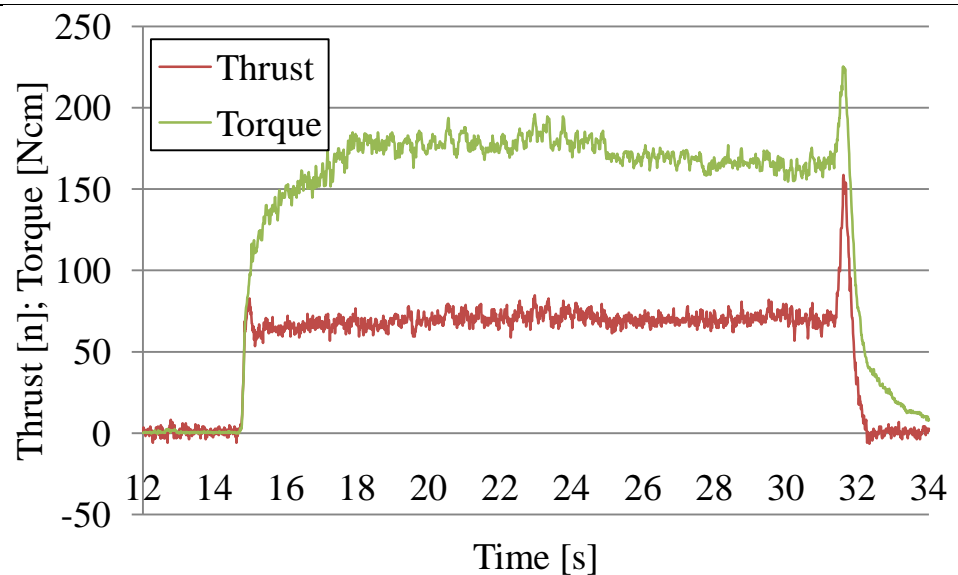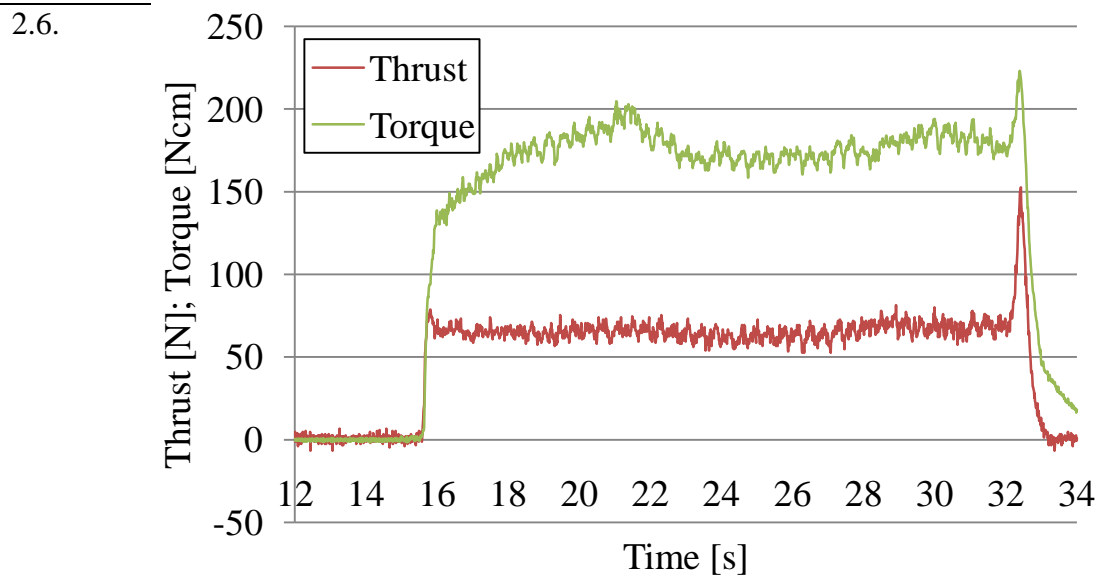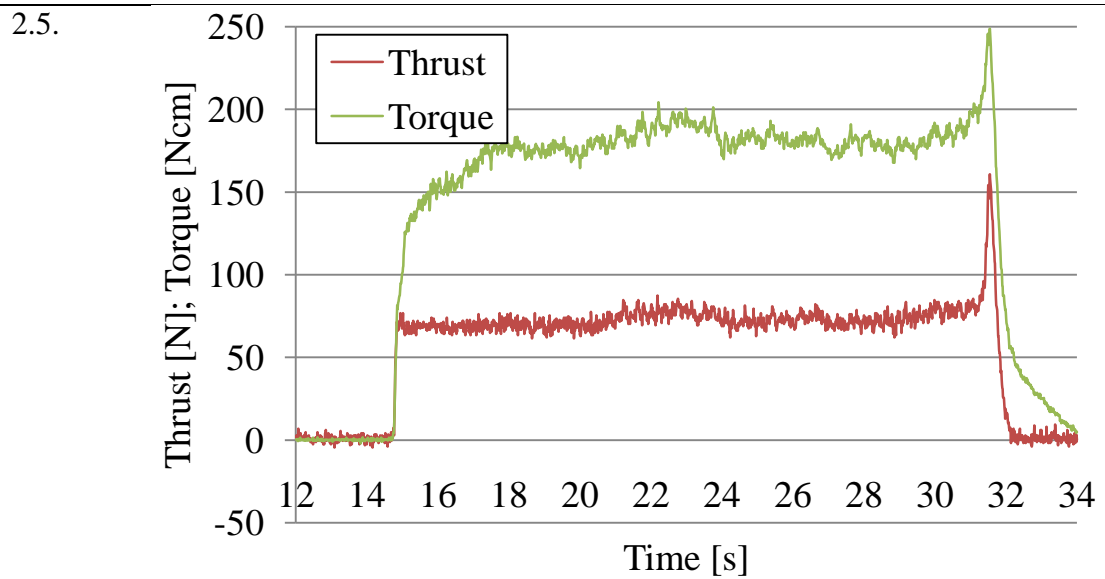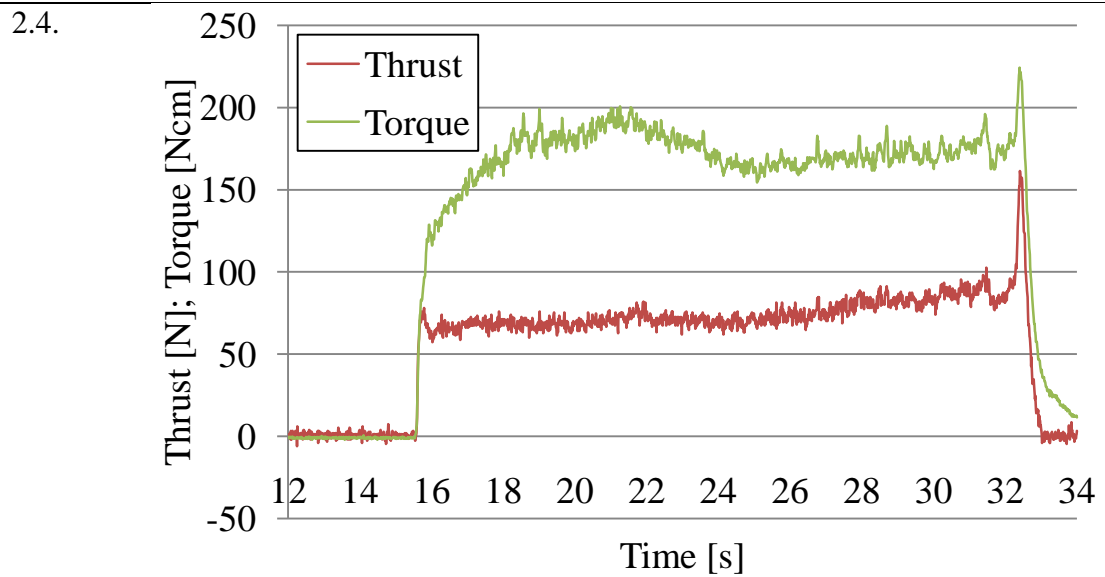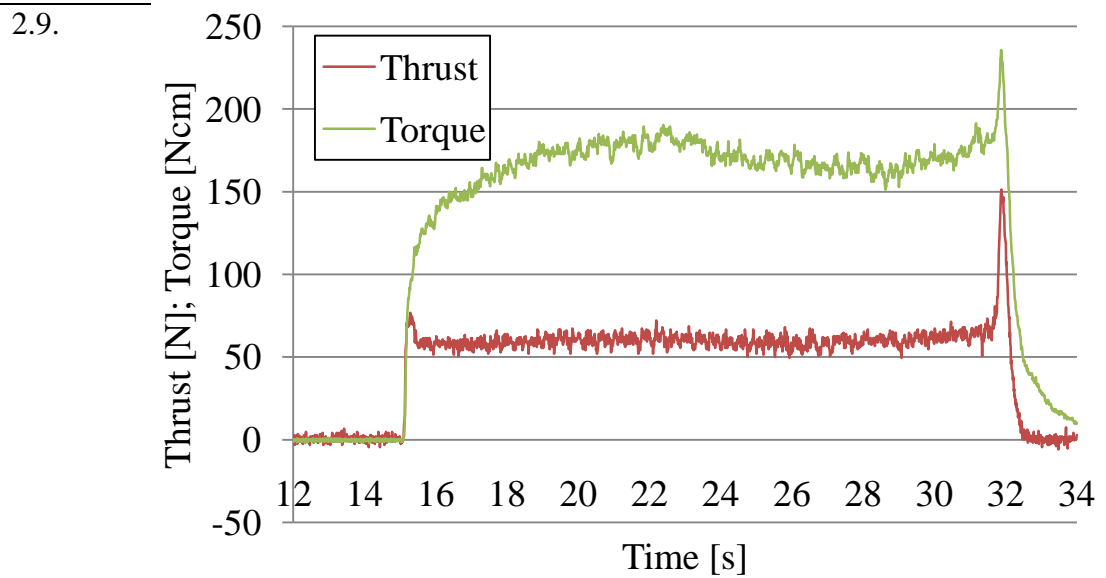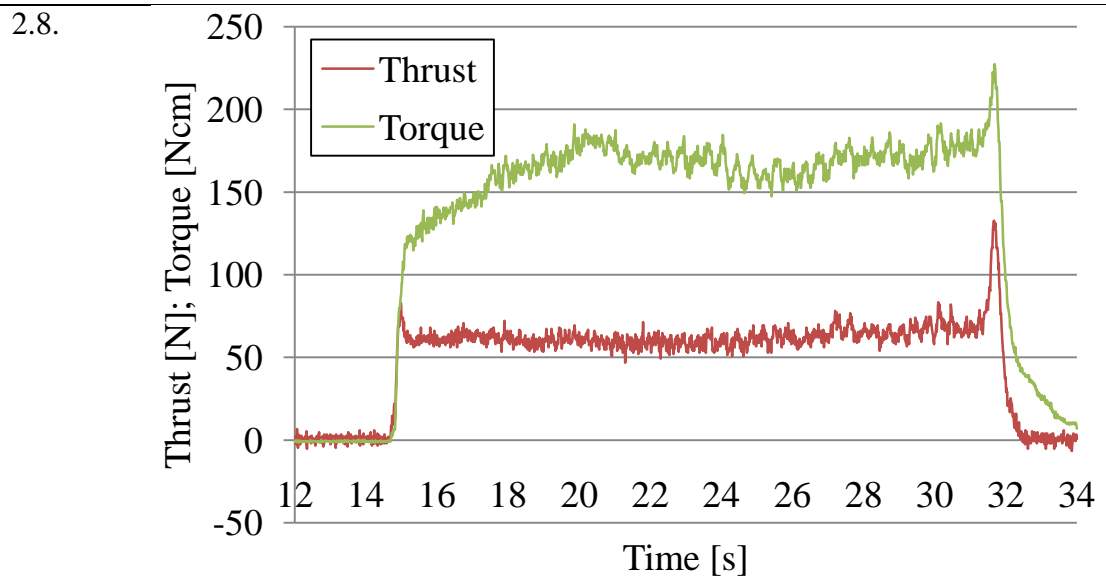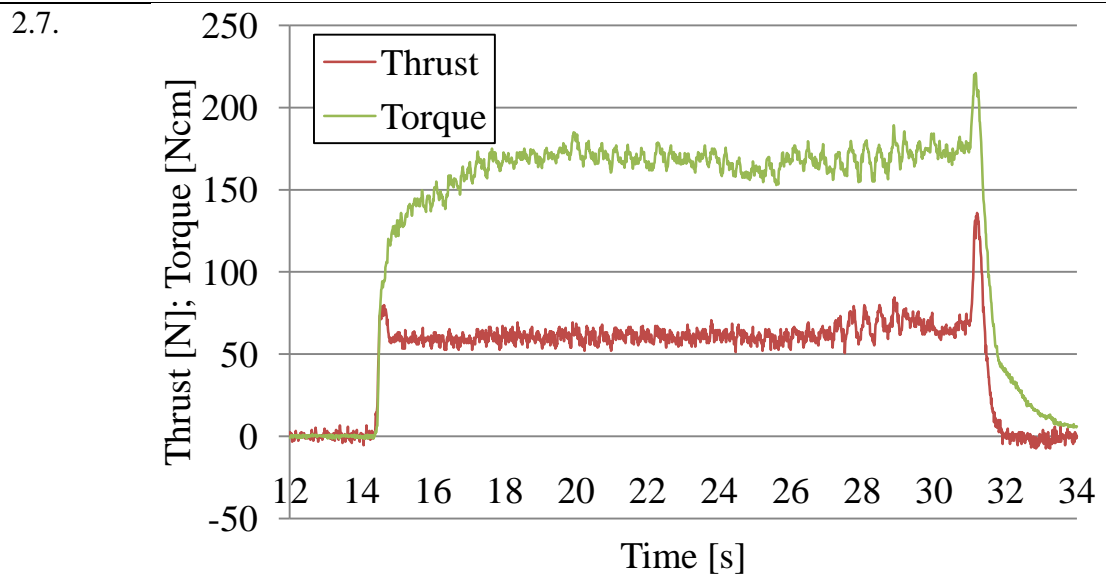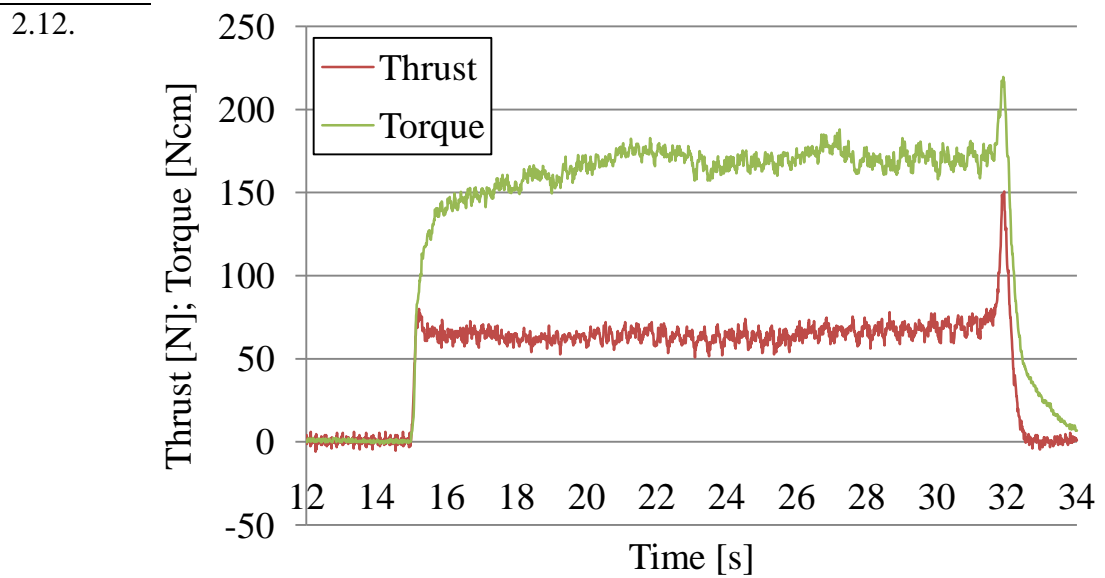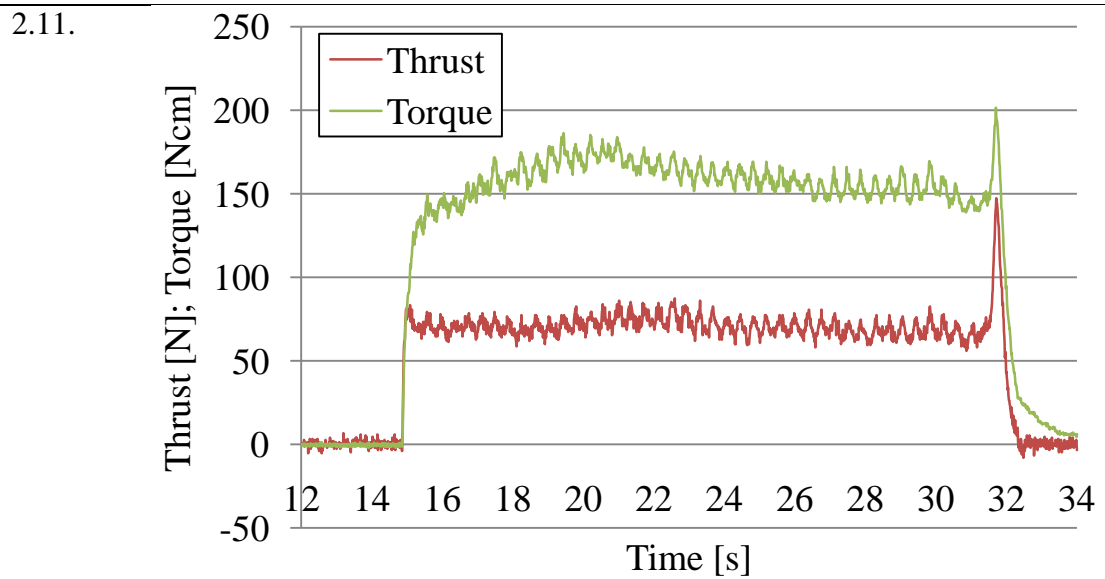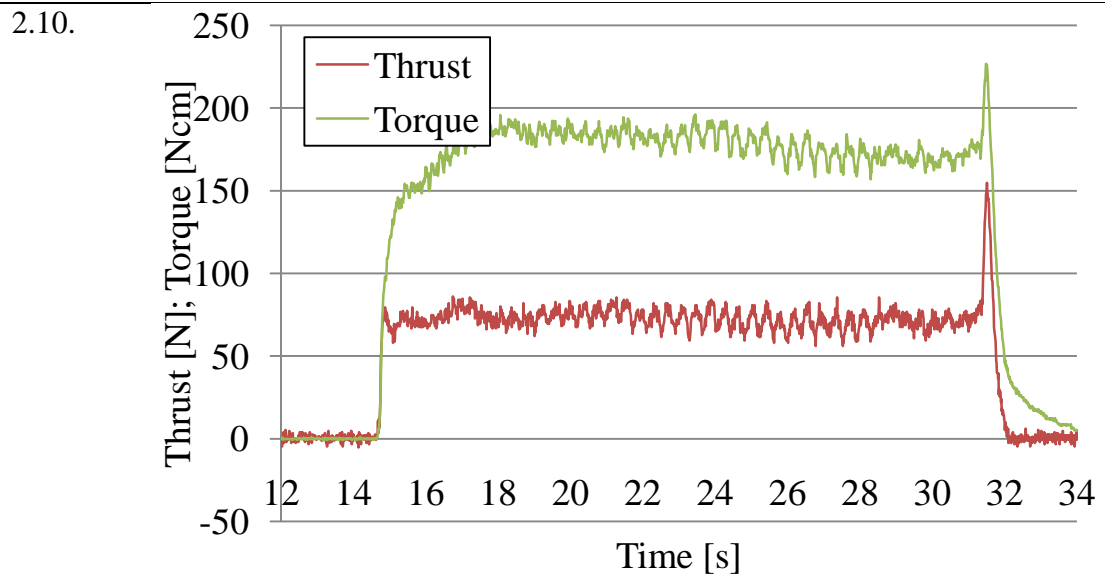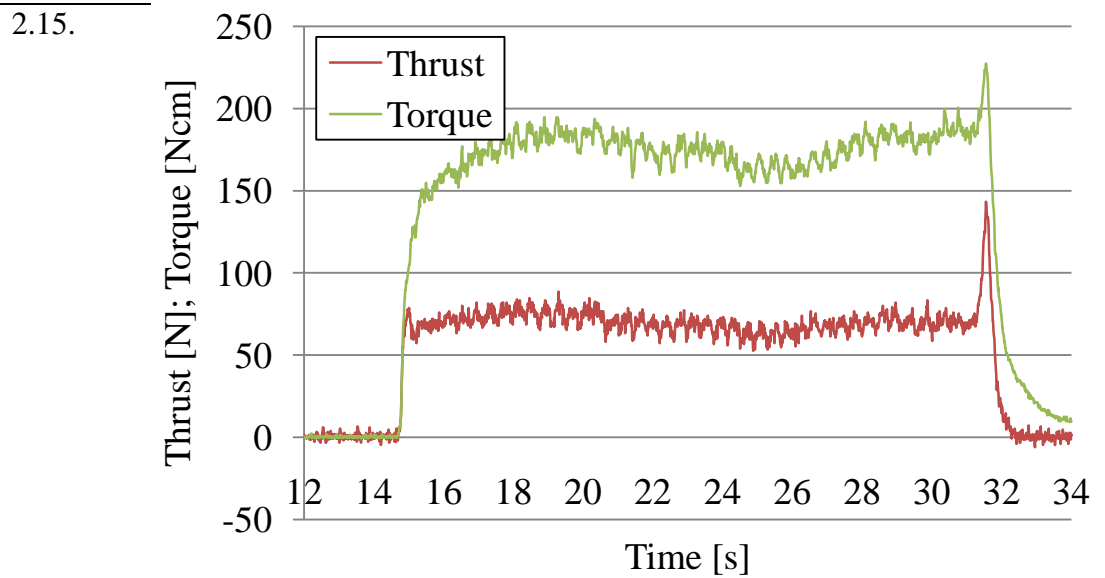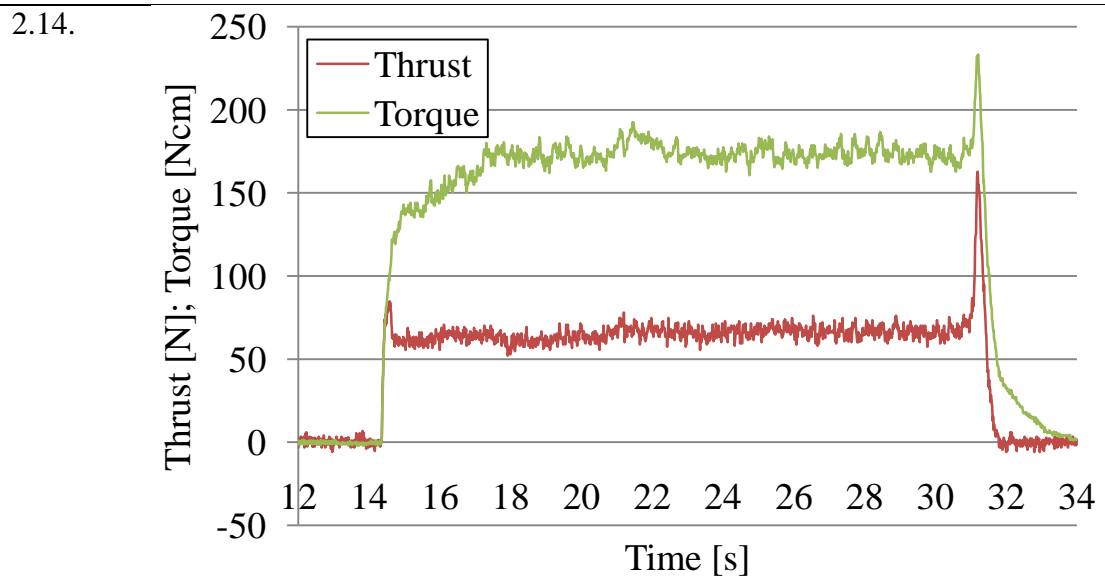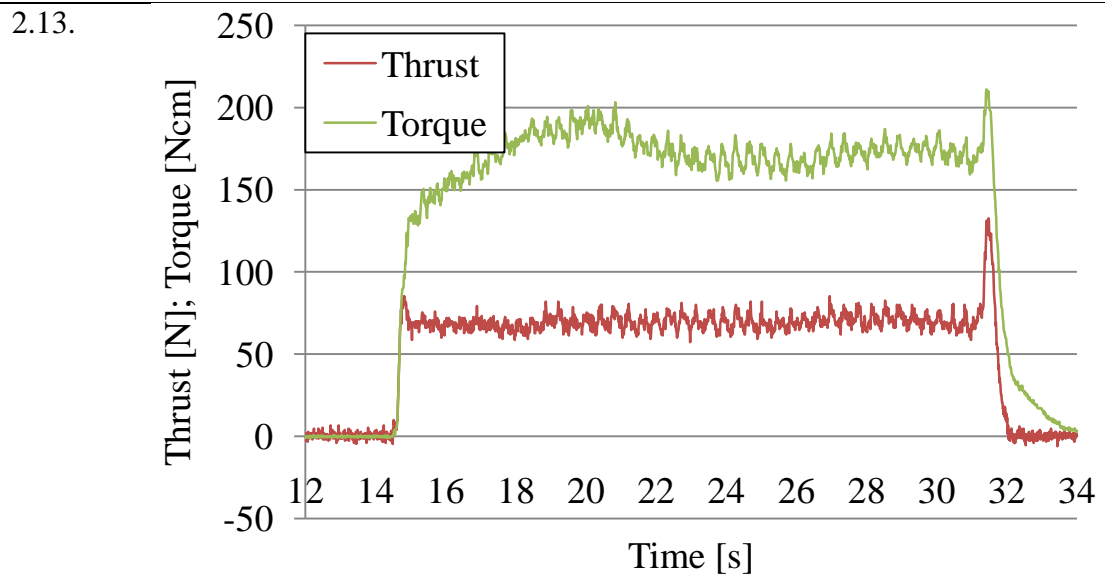
Reaming operation R3

3.1.
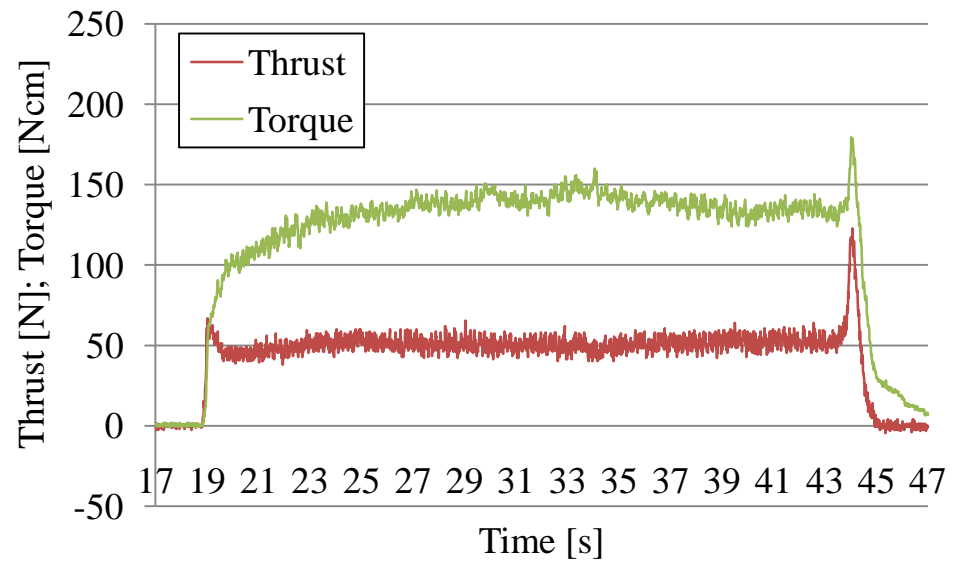
3.2.
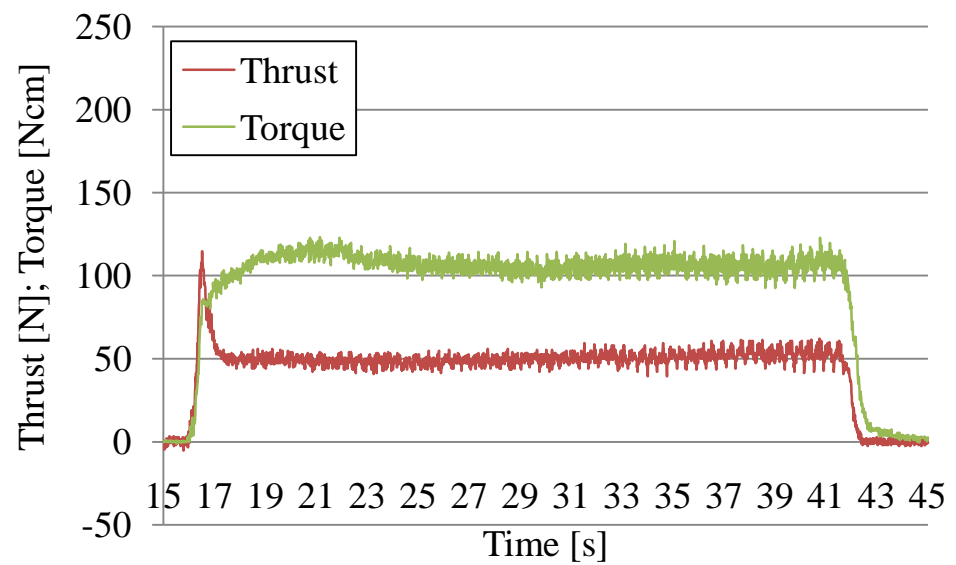
3.3.
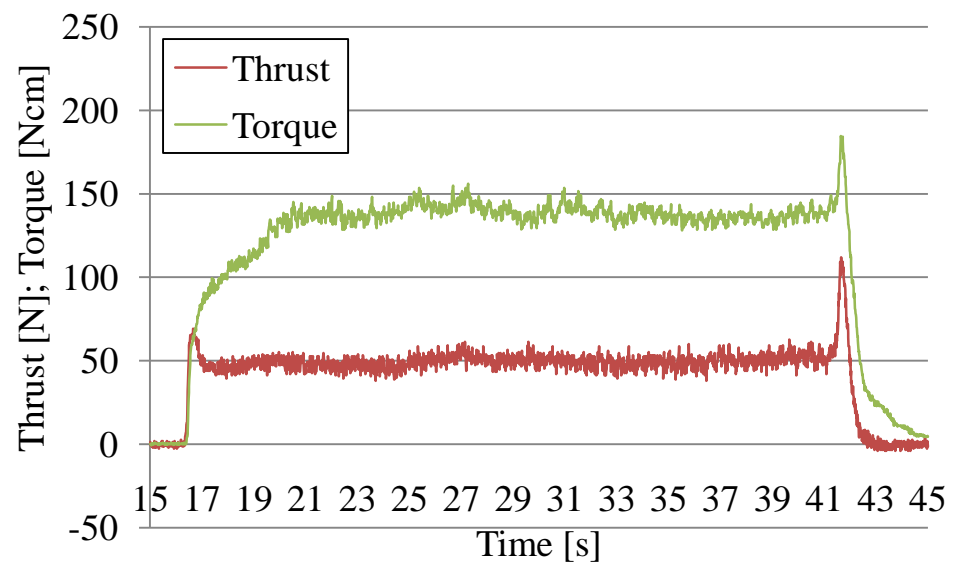
3.4.
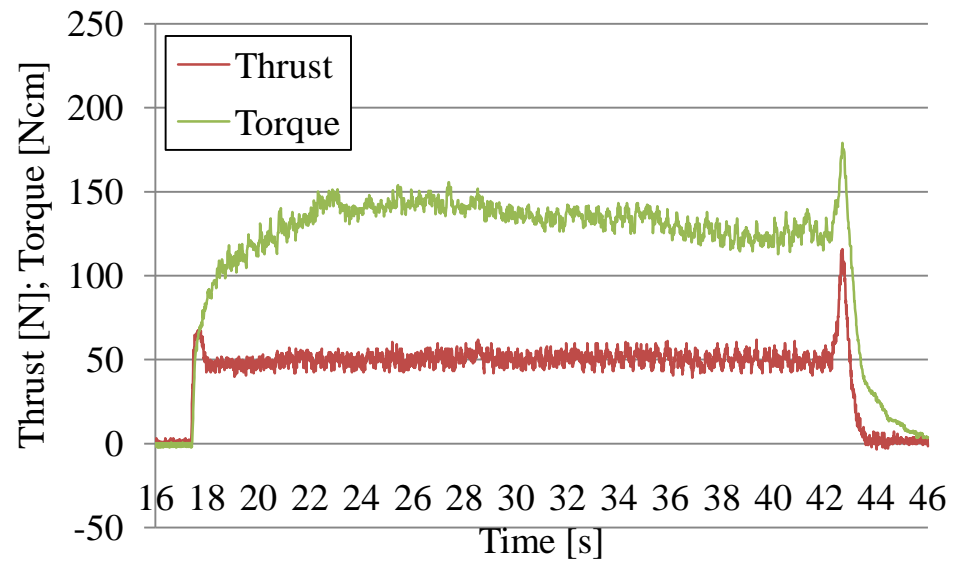
3.5.
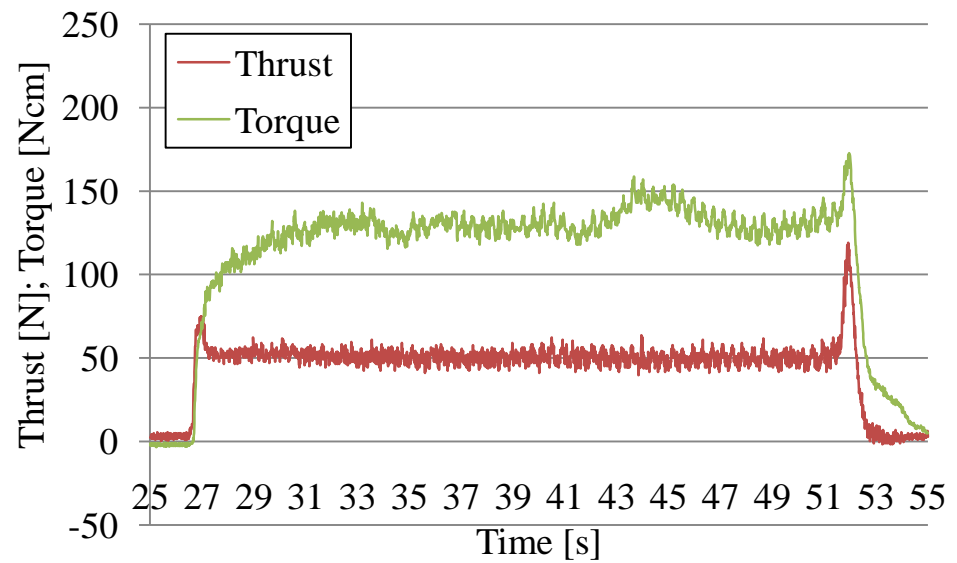
3.6.
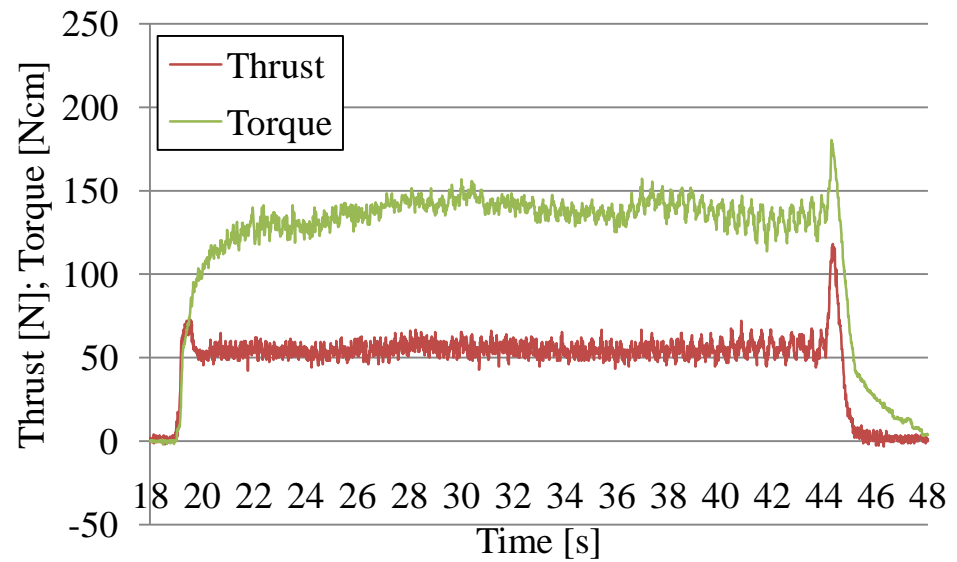
3.7.
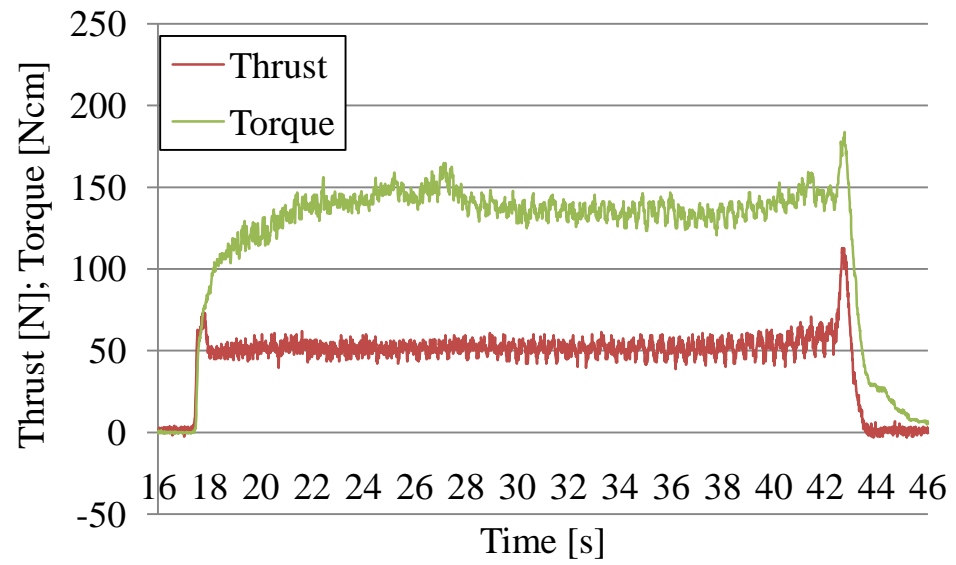
3.8.
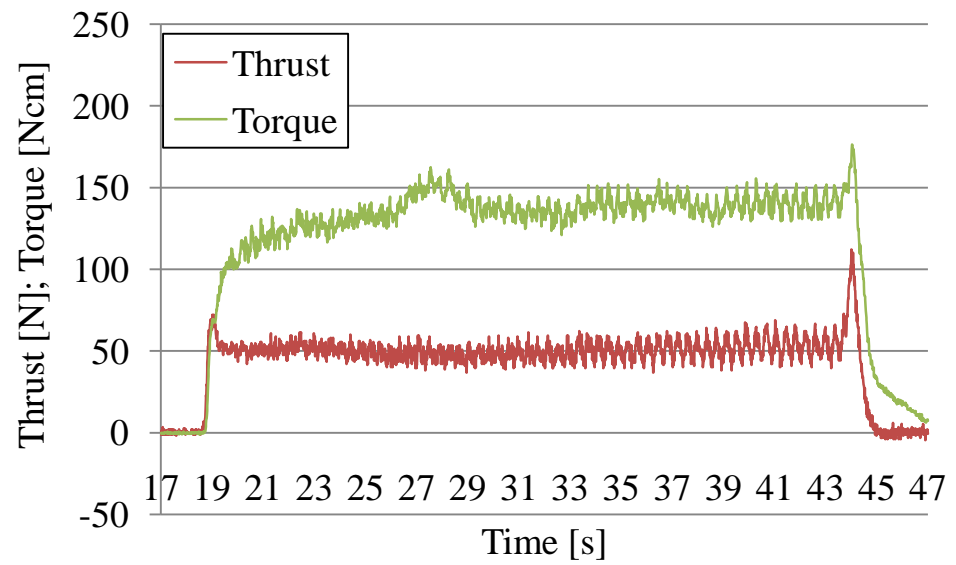
3.9.
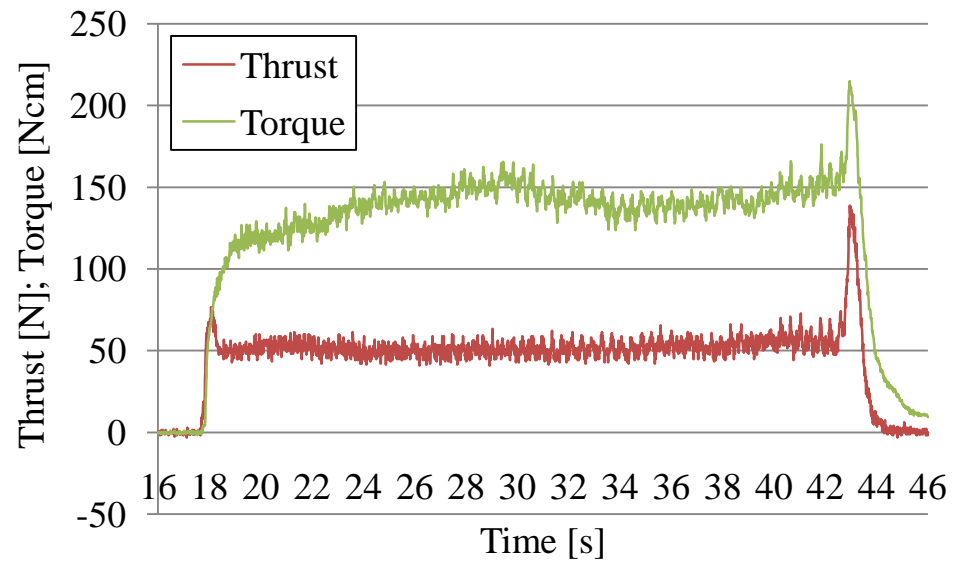
3.10.
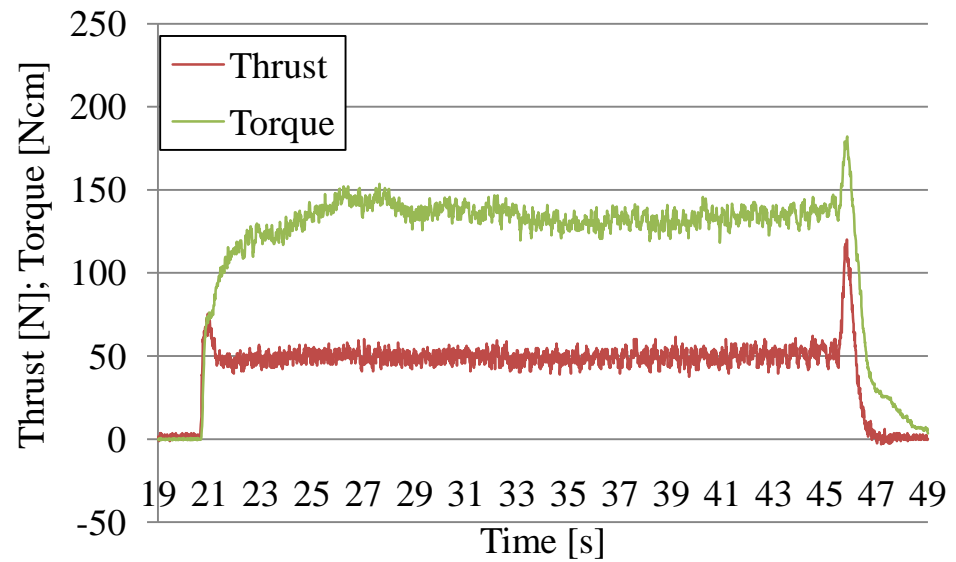
3.11.
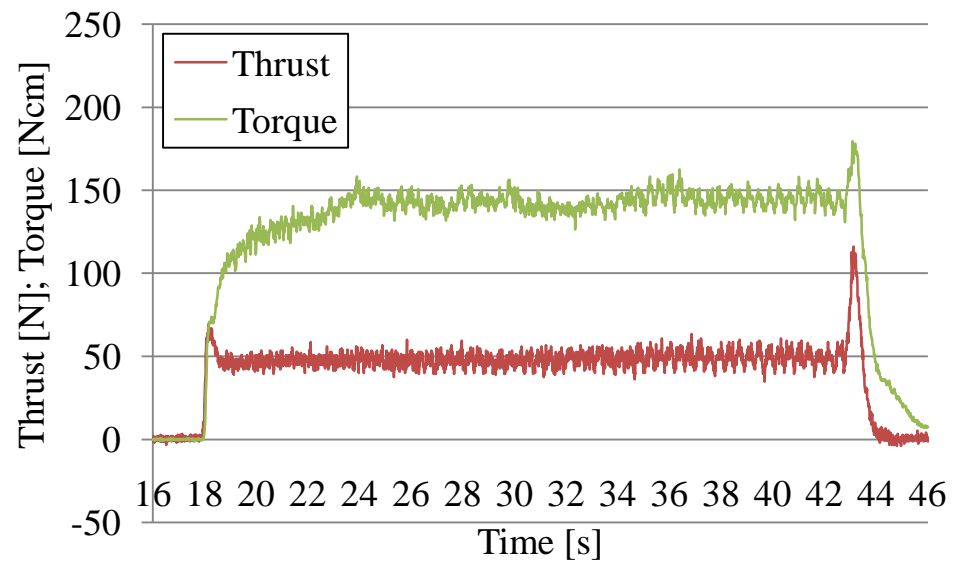
3.12.
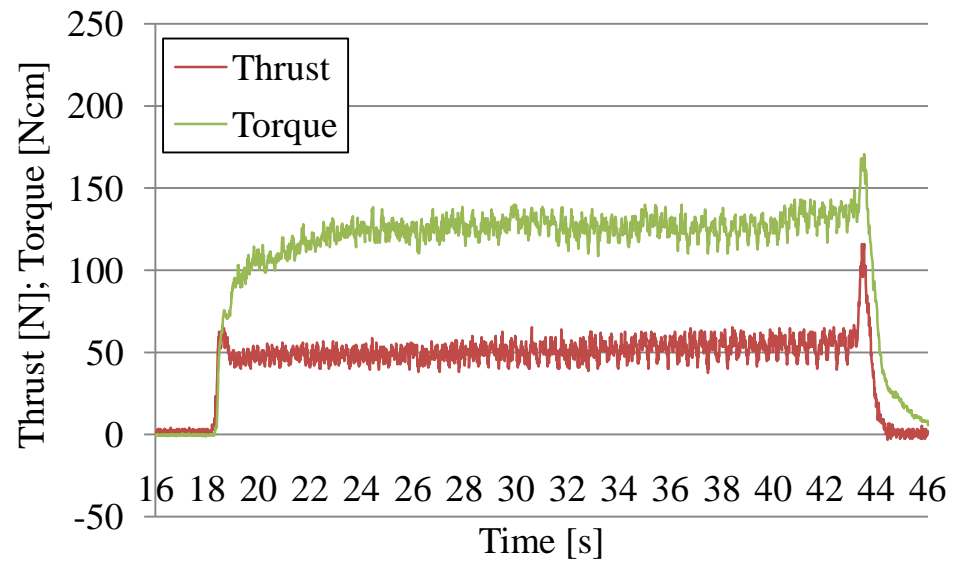
3.13.
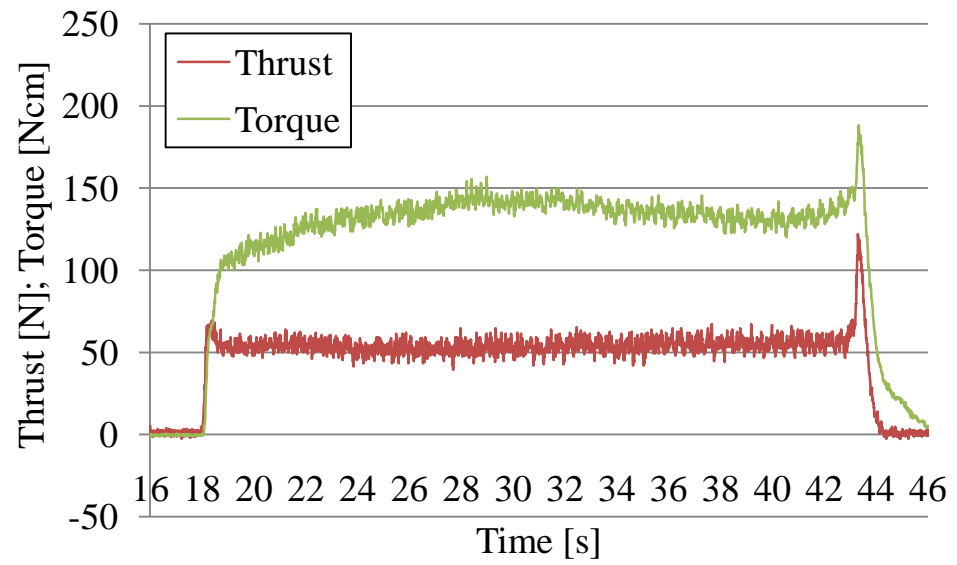
3.14.
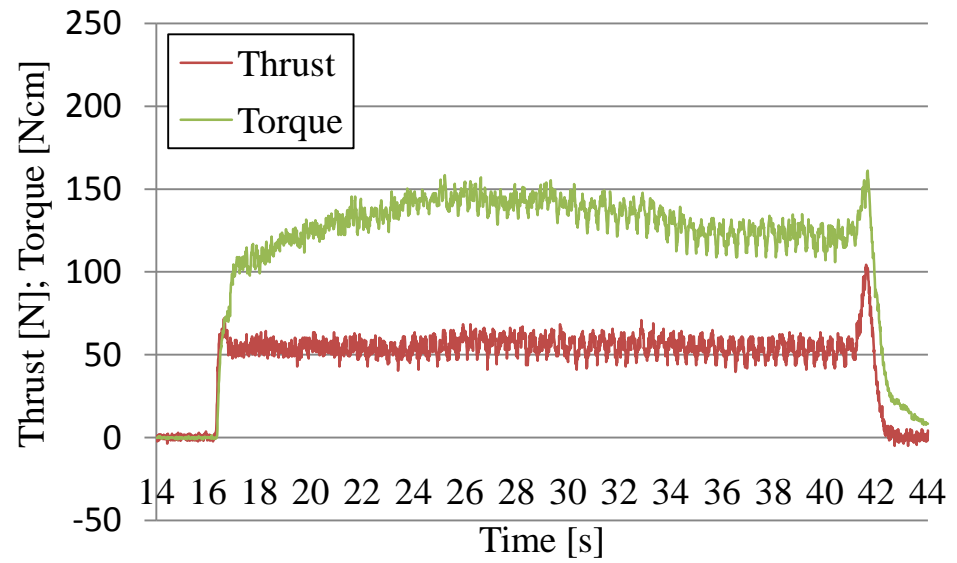
3.15.
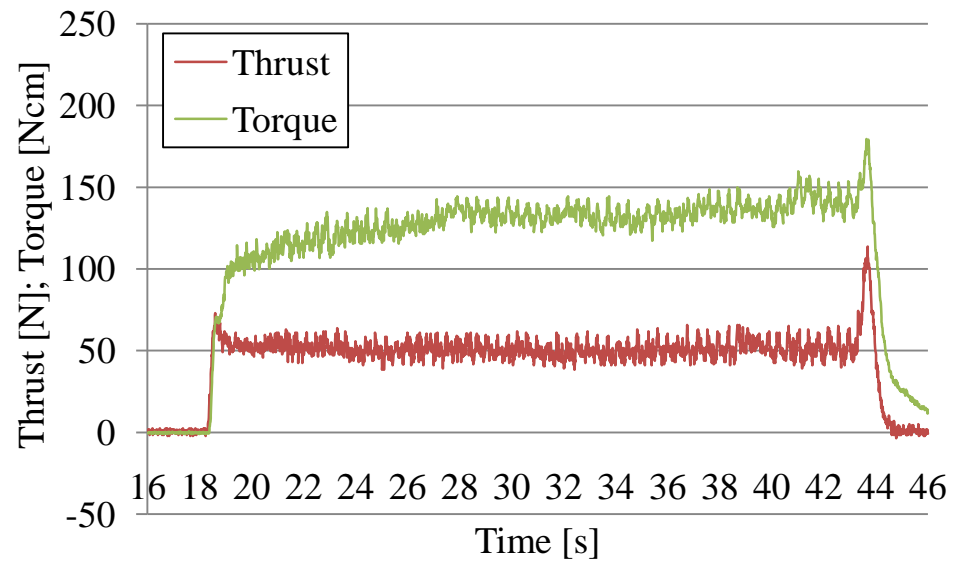
Reaming operation R4

4.1.
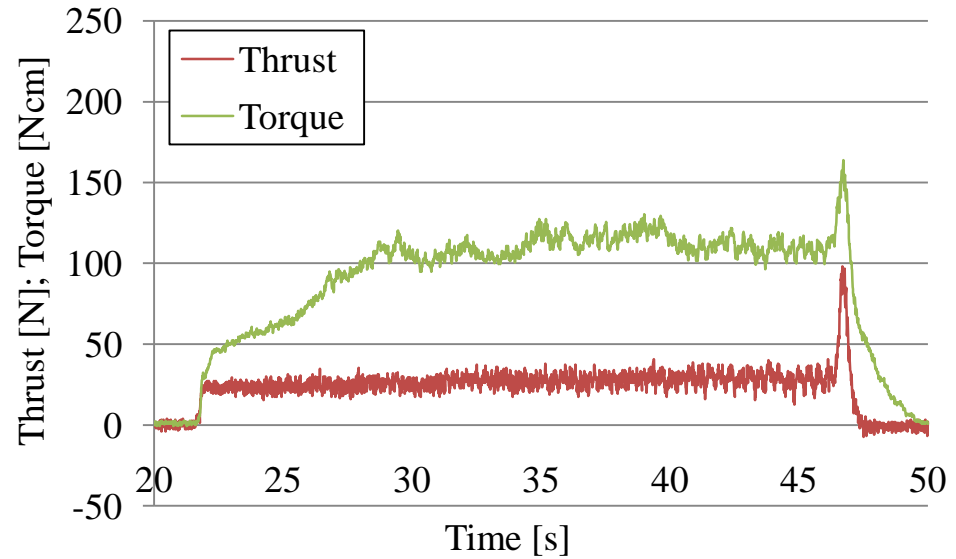
4.2.
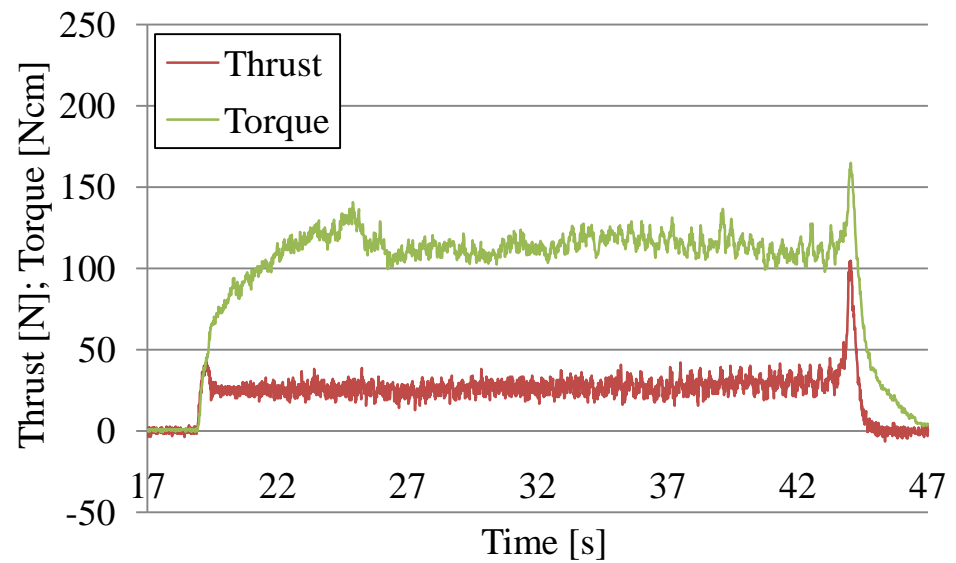
4.3.
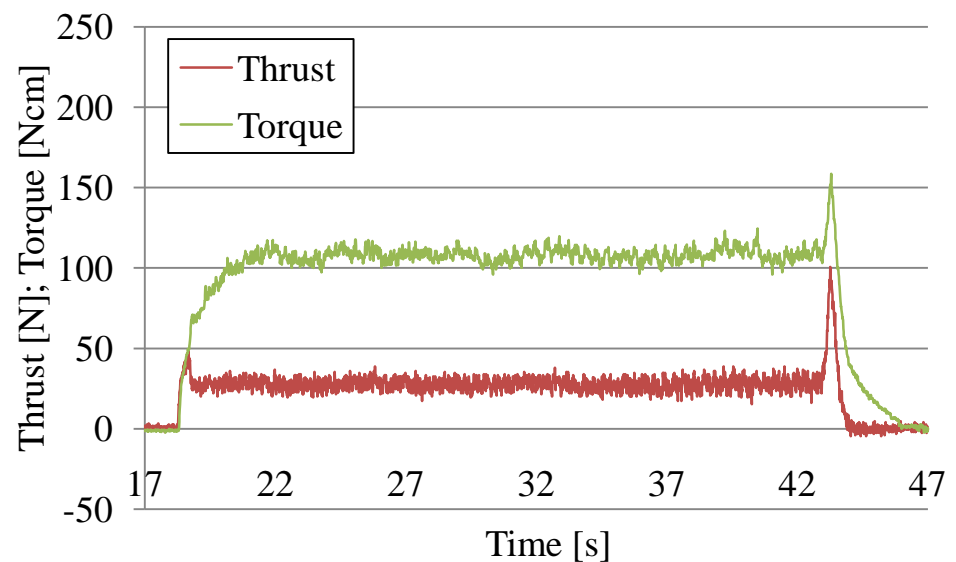
4.4.
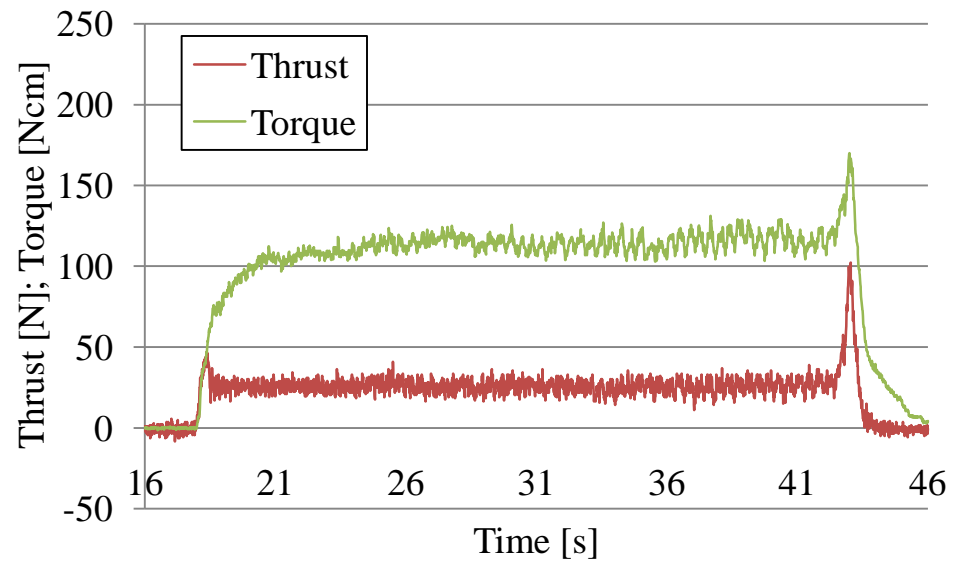
4.5.
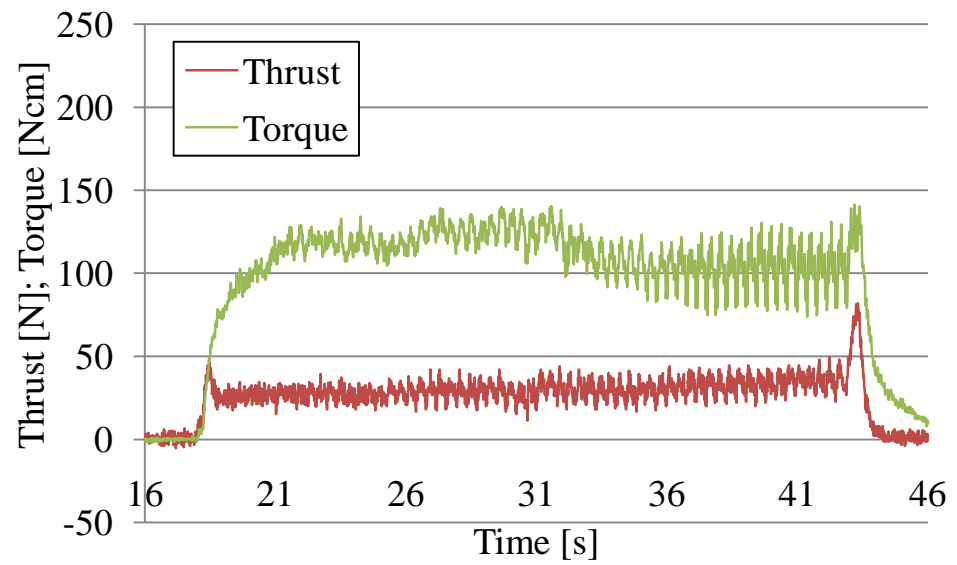
4.6.
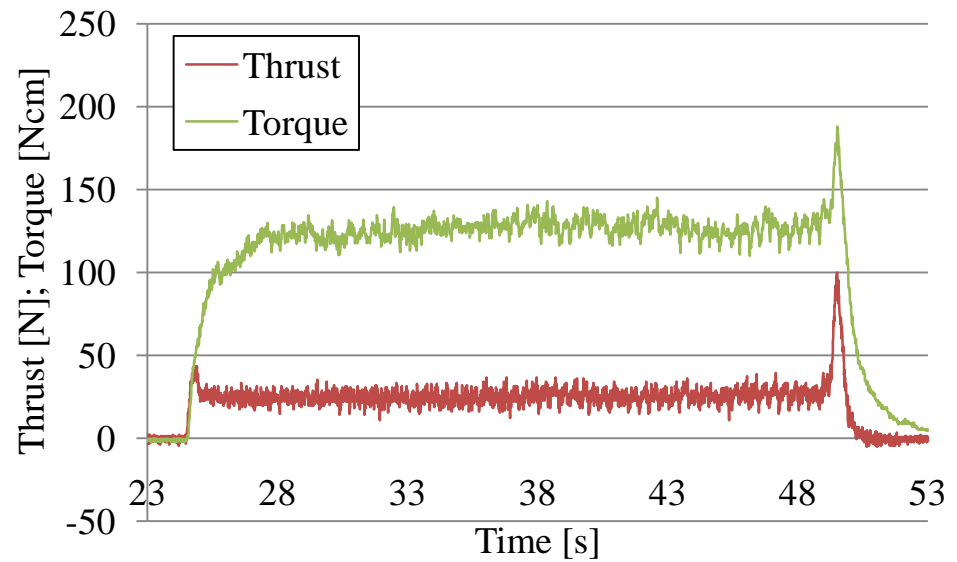
4.7.
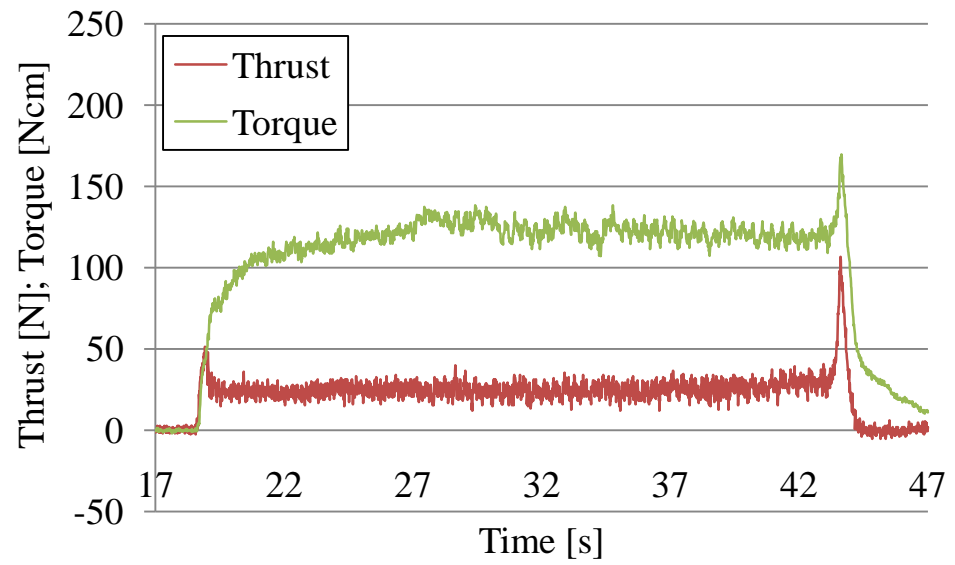
4.8.
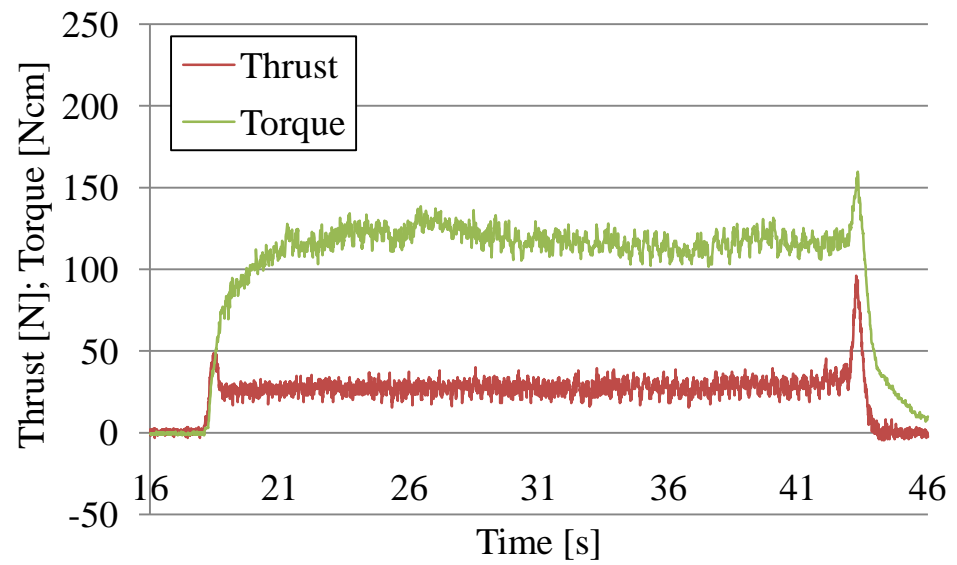
4.9.
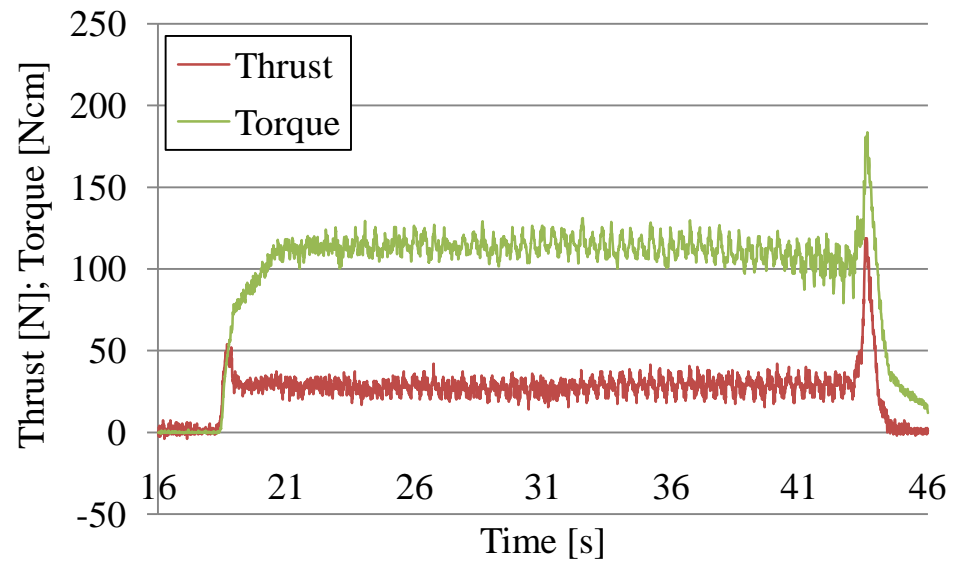
4.10.
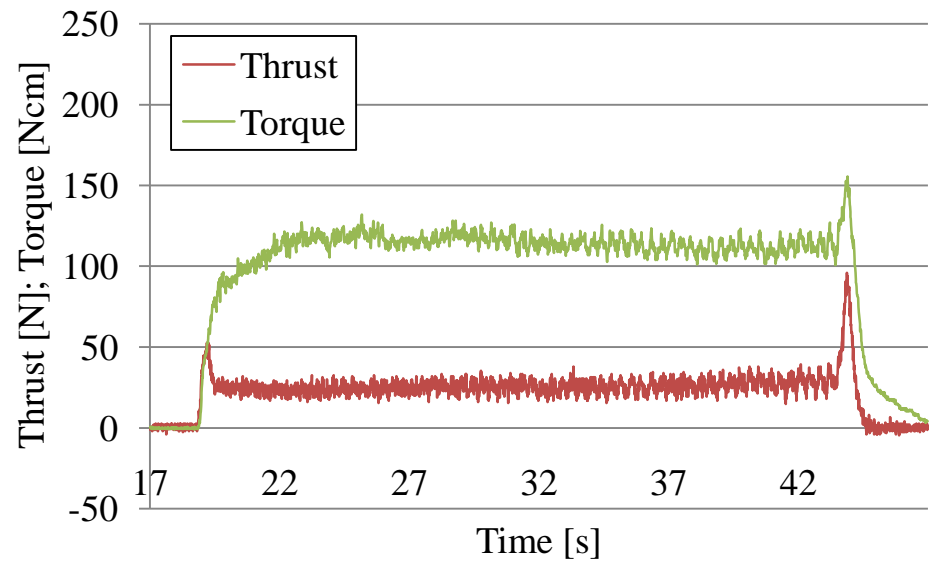
4.11.
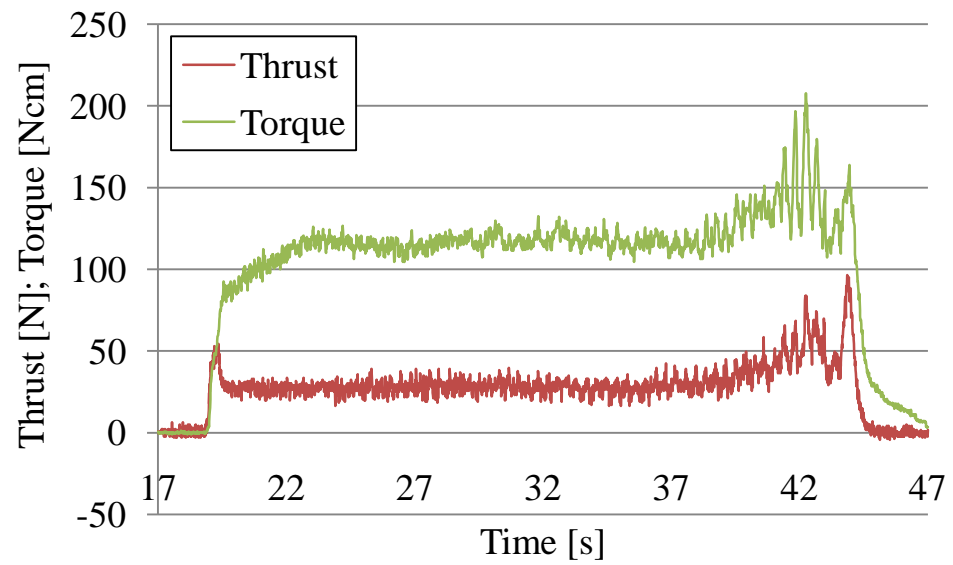
4.12.
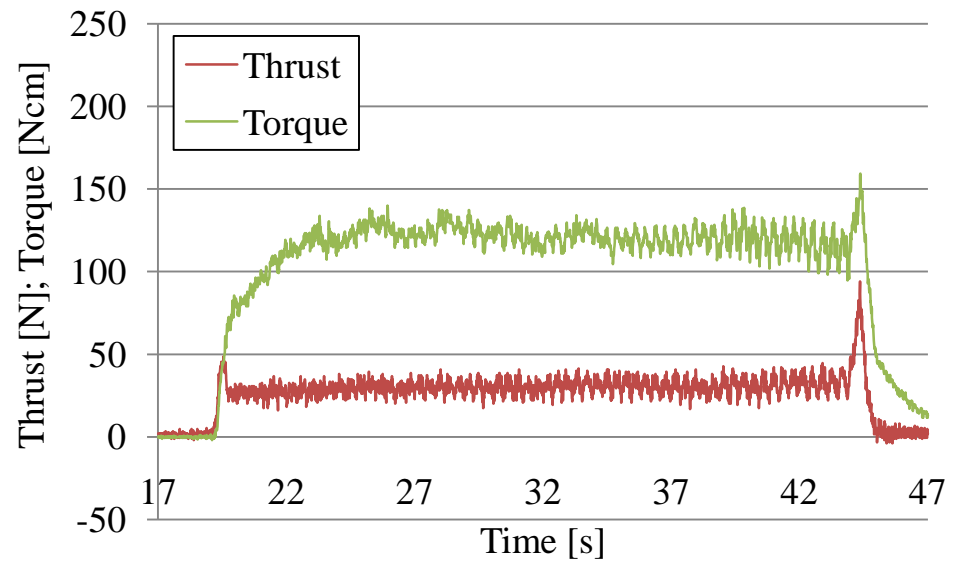
4.13.
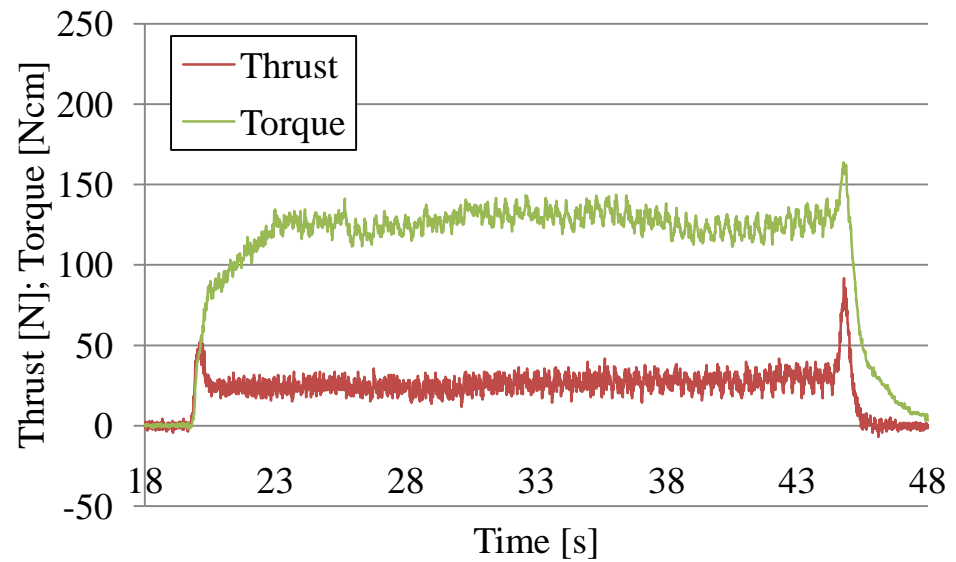
4.14.
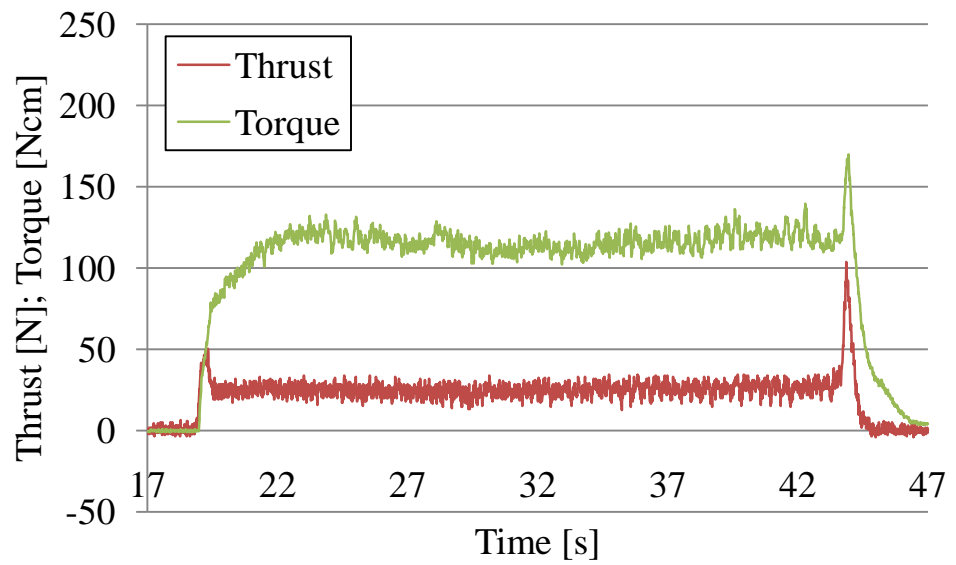
4.15.
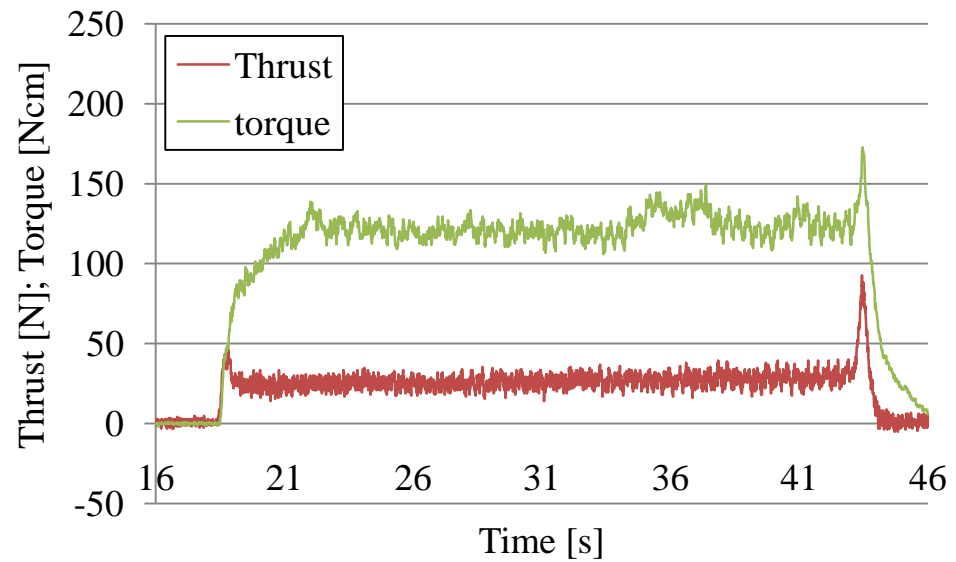
Reaming operation R5

5.1.
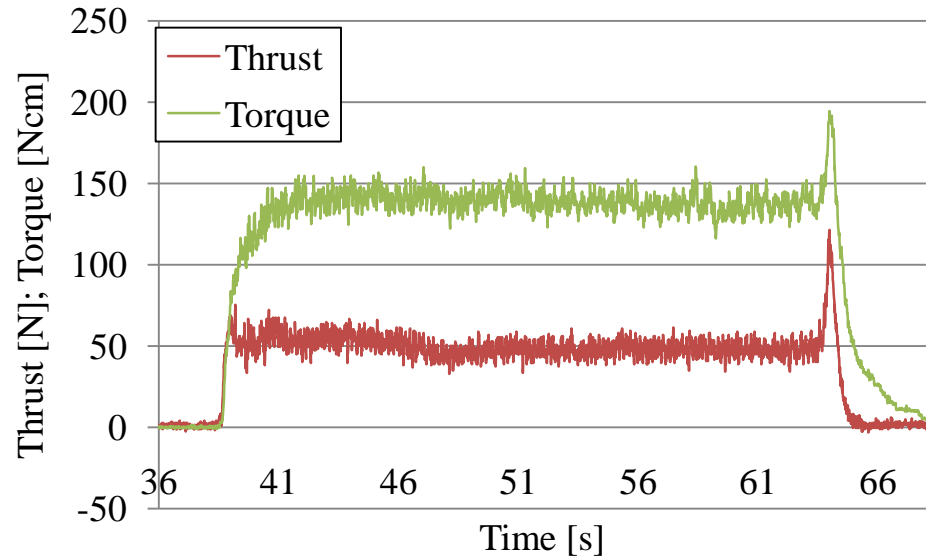
5.2.
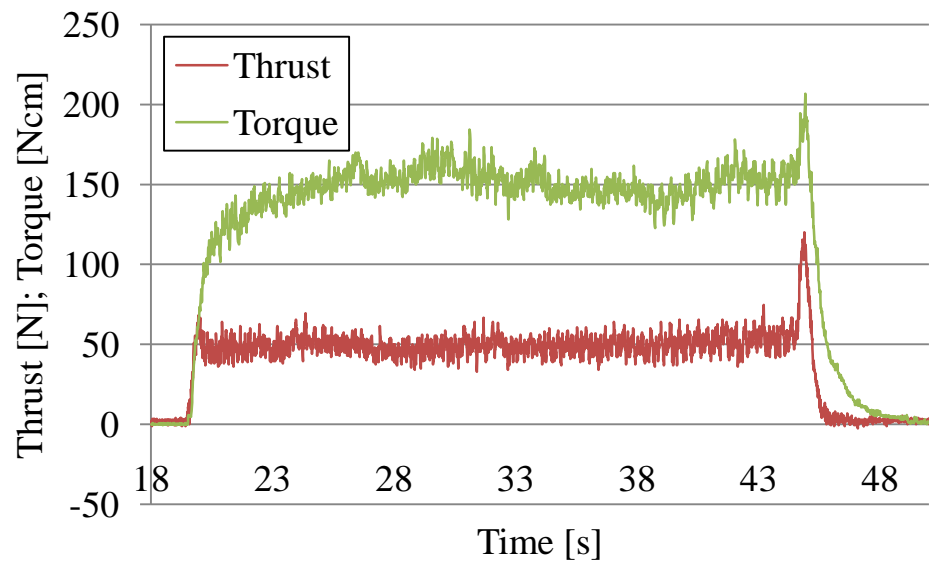
5.3.
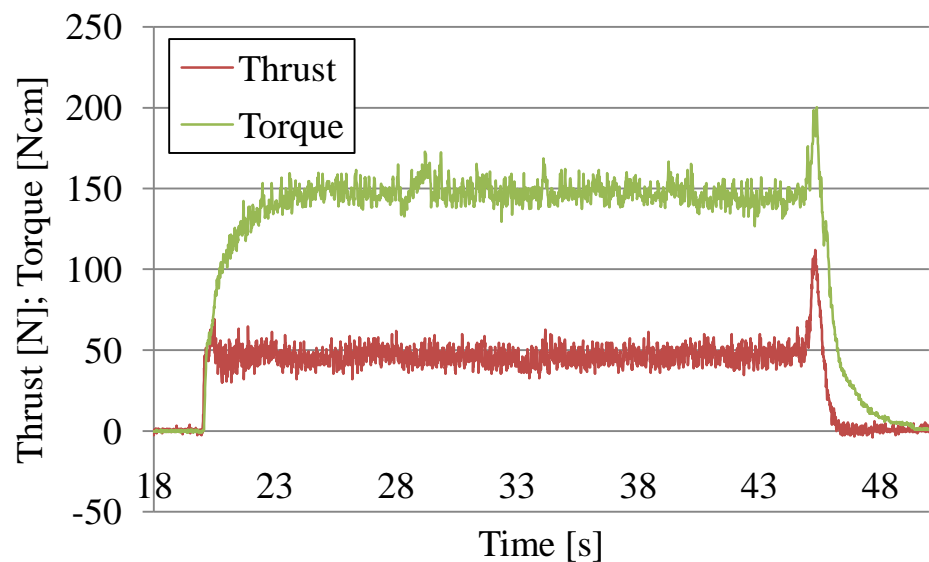
5.4.
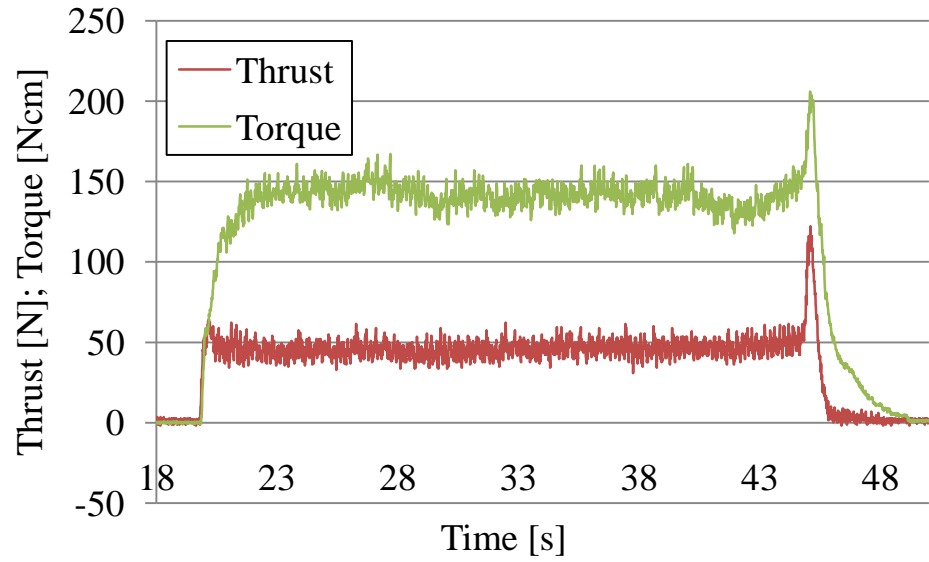
5.5.
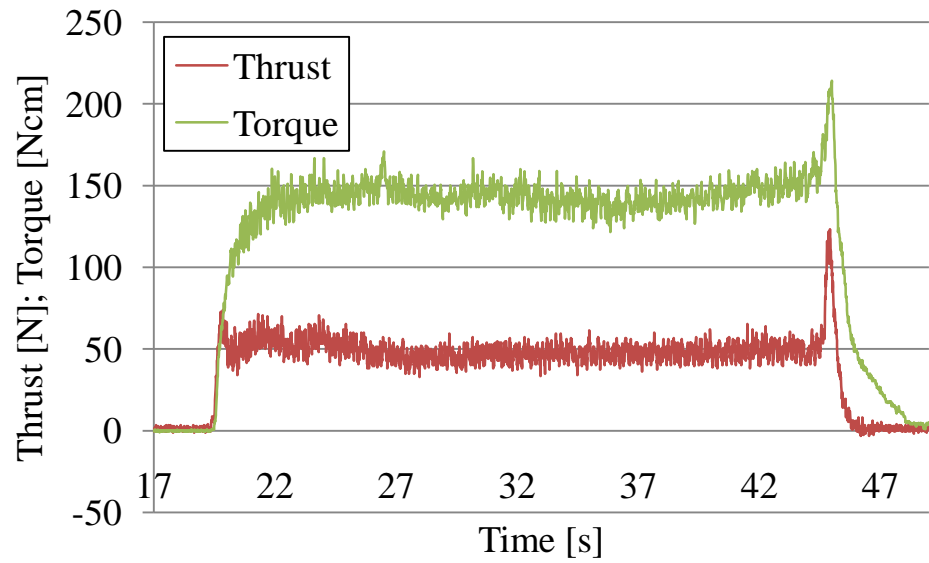
5.6.
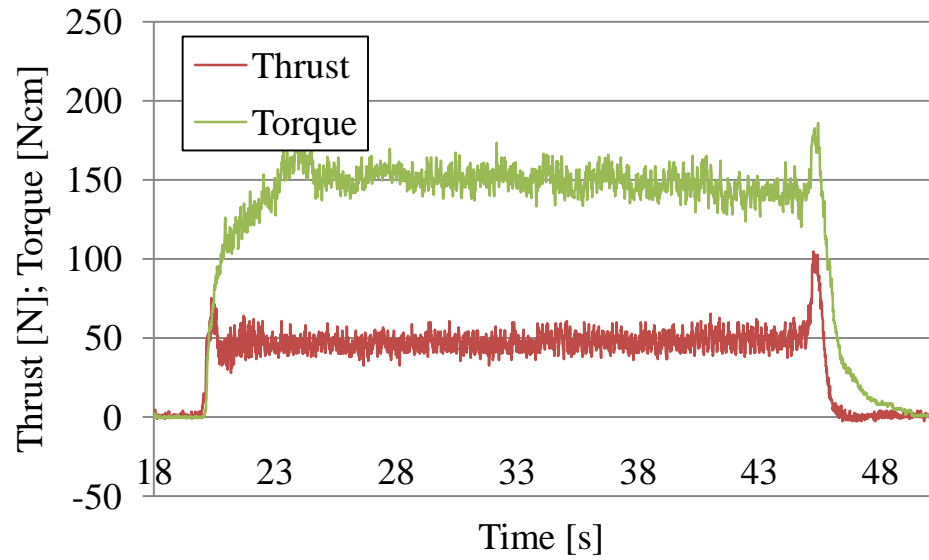
5.7.
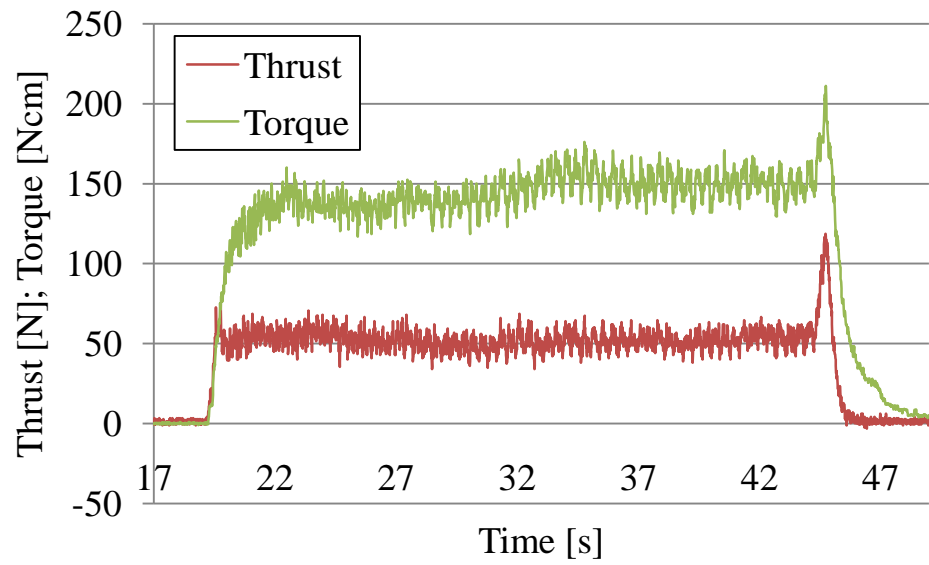
5.8.
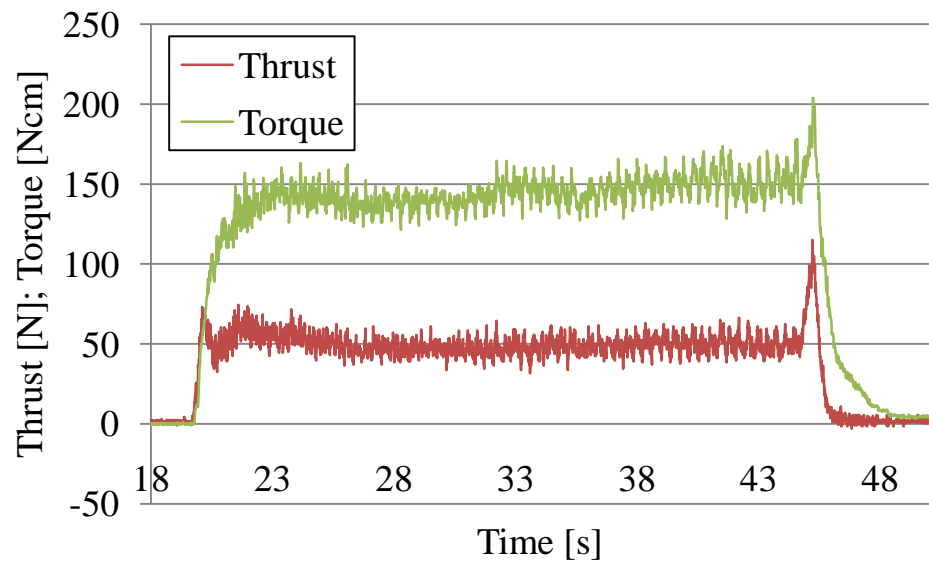
5.9.
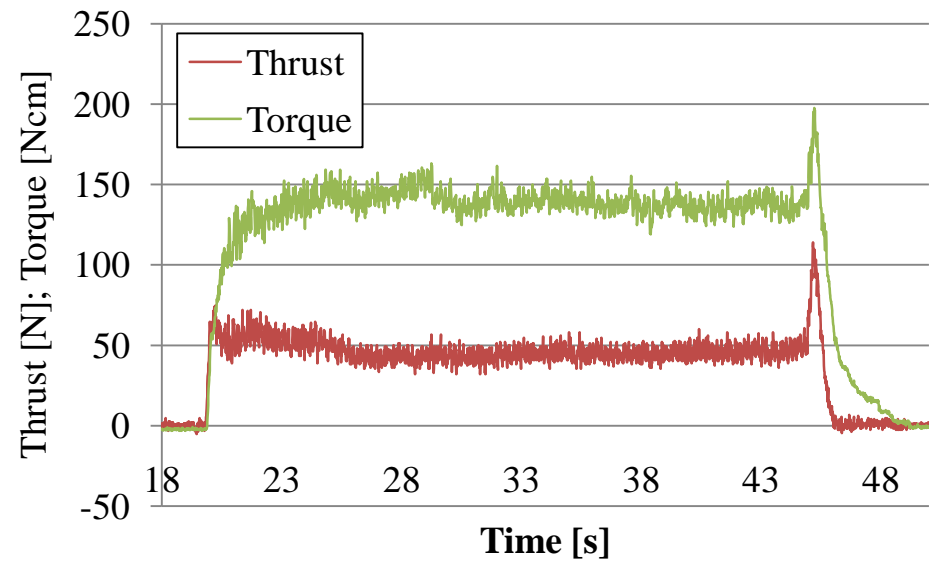
5.10.
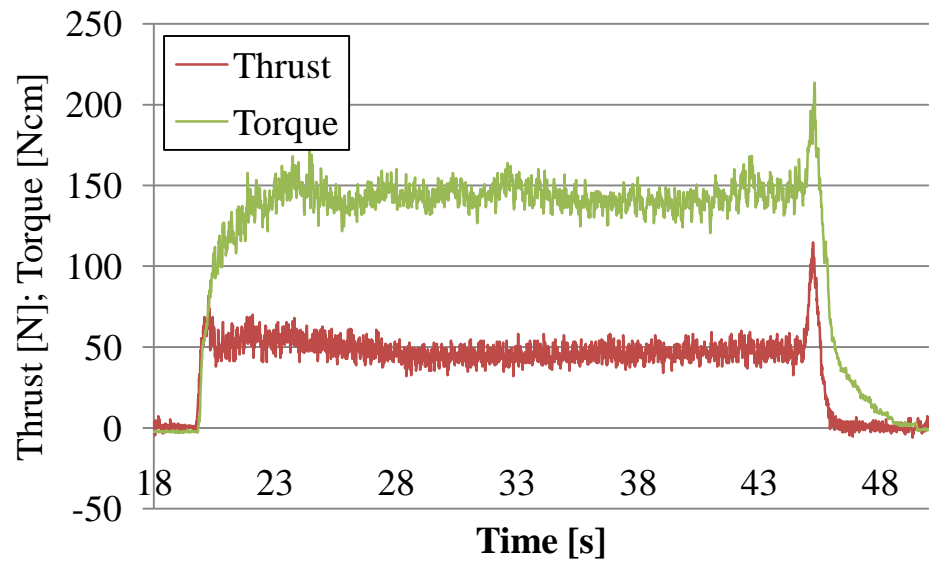
5.11.
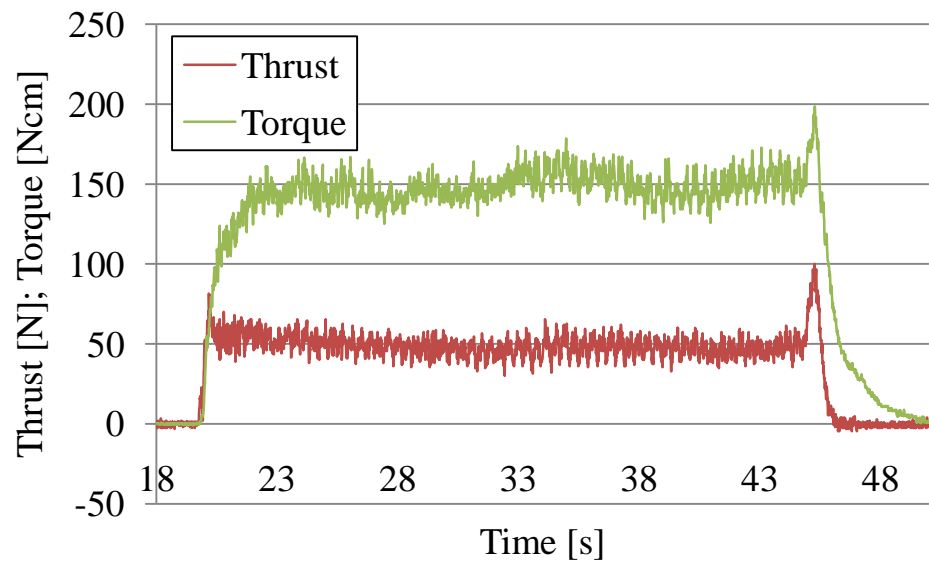
5.12.
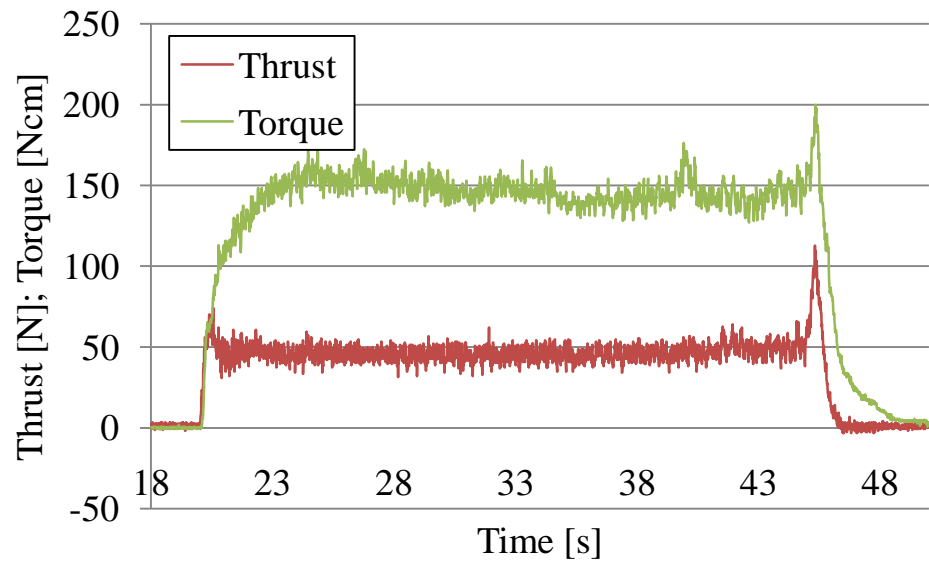
5.13.
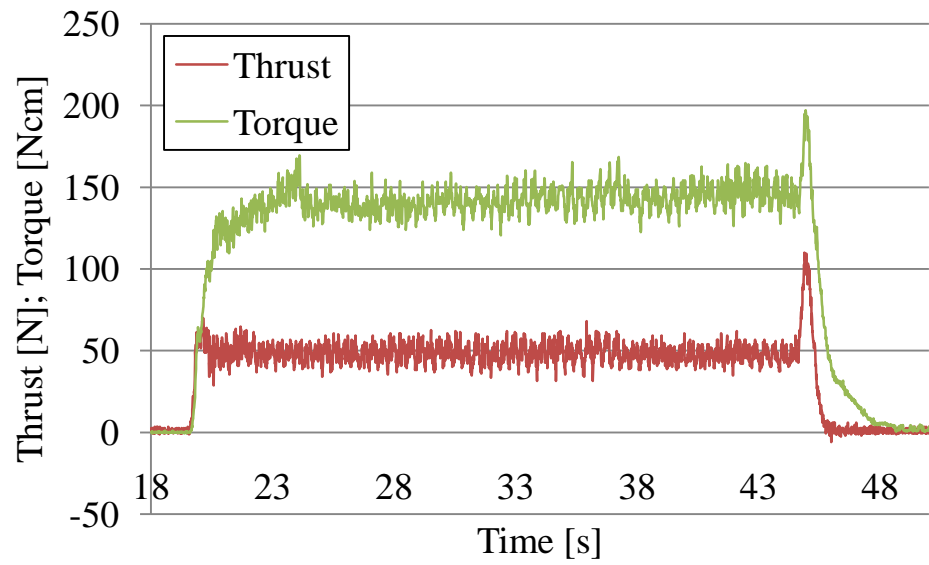
5.14.
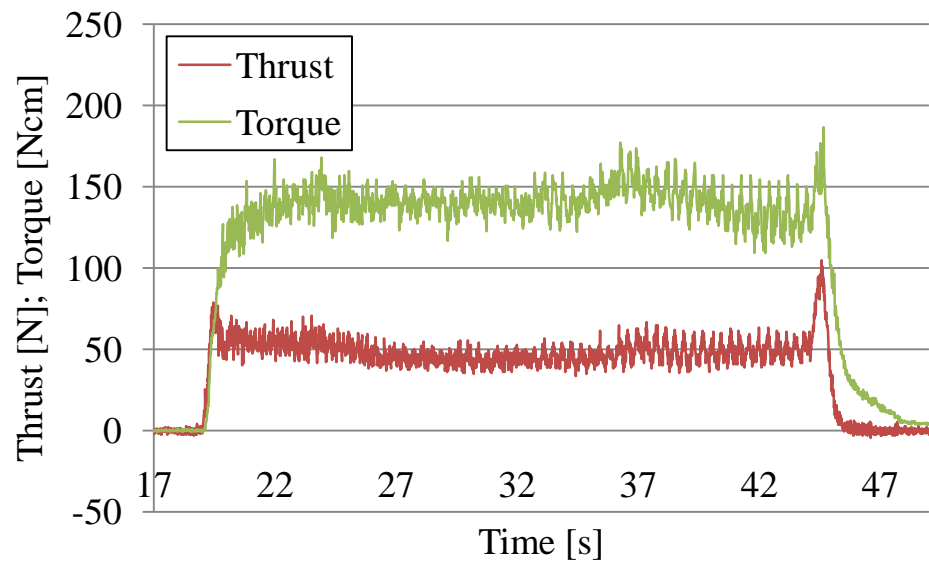
5.15.
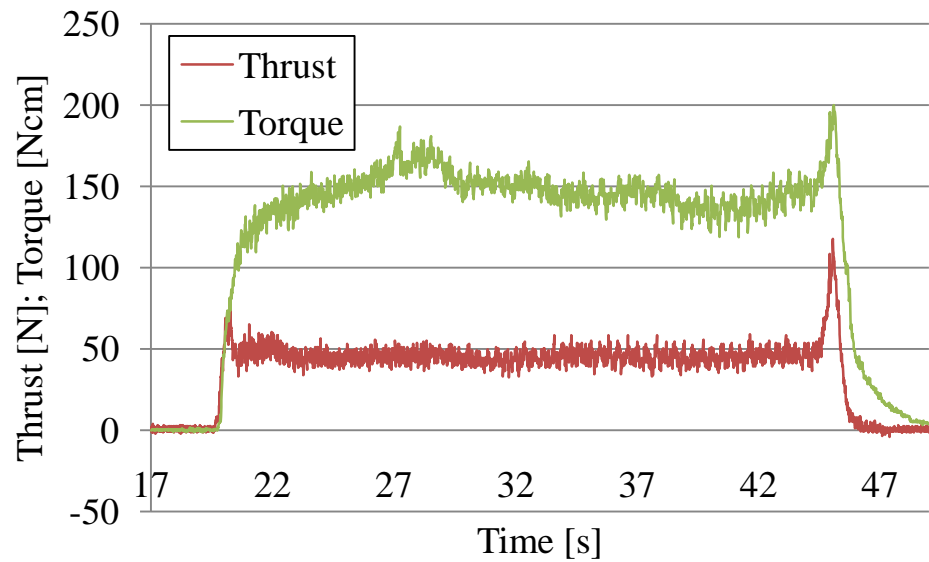
Reaming operation R6

6.1.
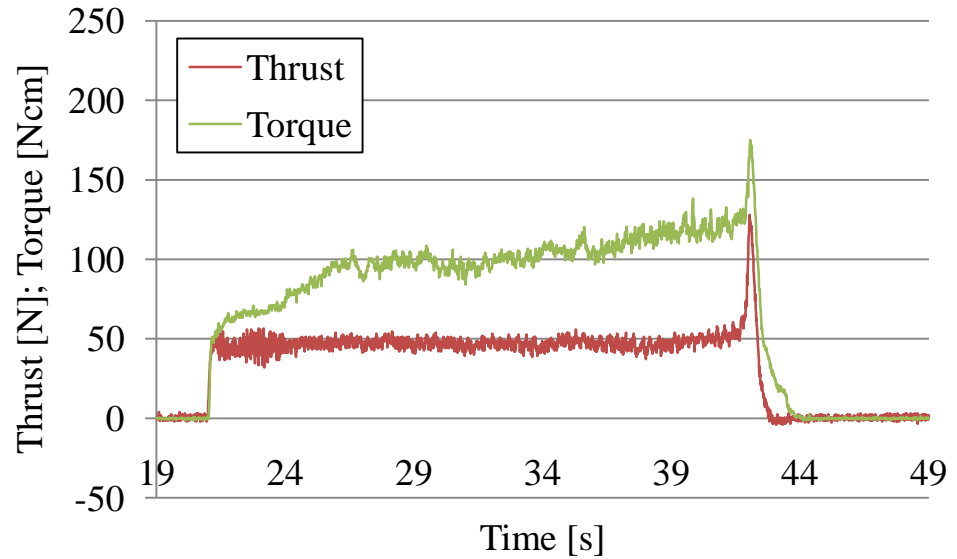
6.2.
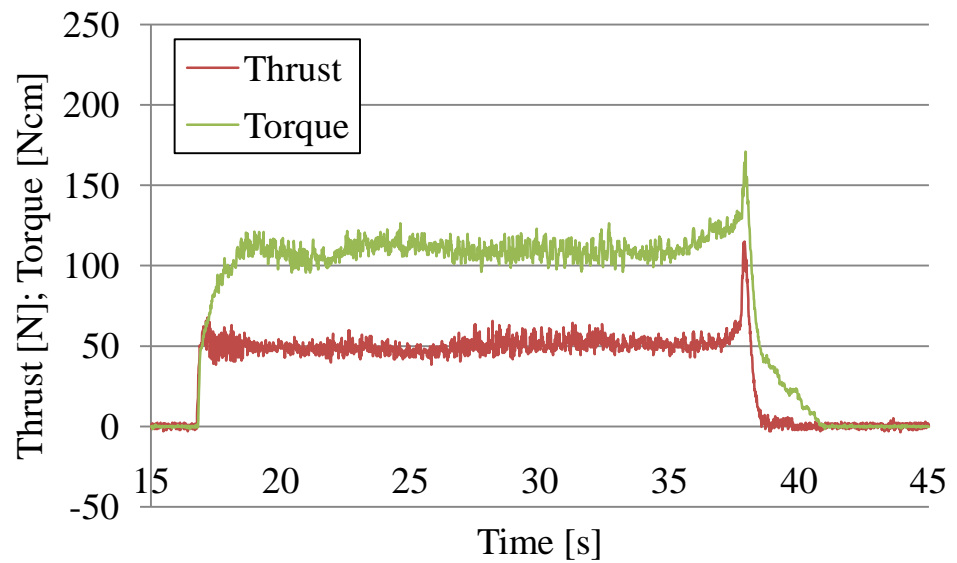
6.3.
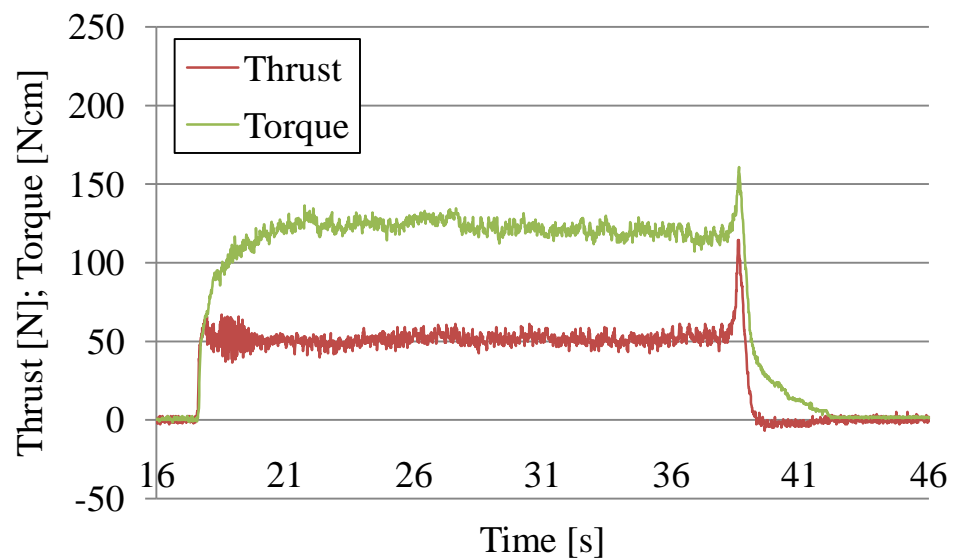
6.4.
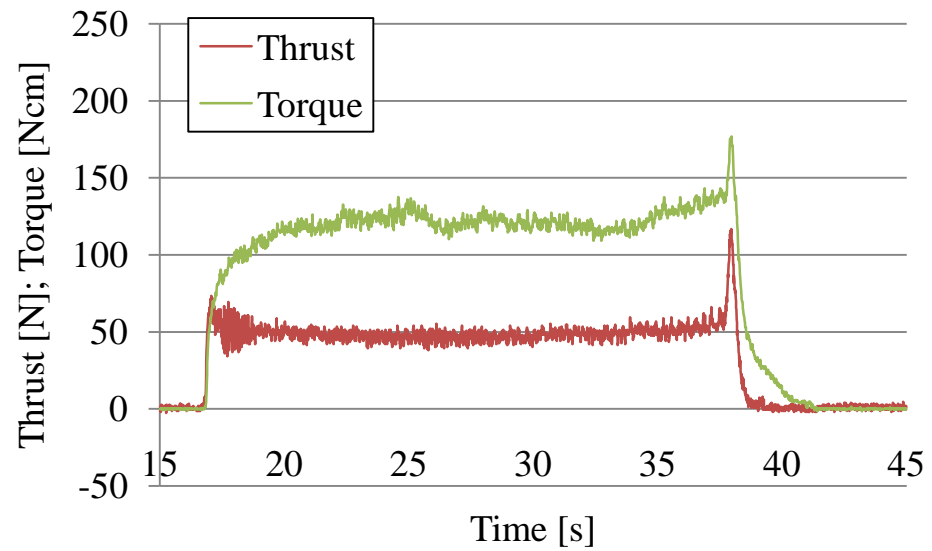
6.5.
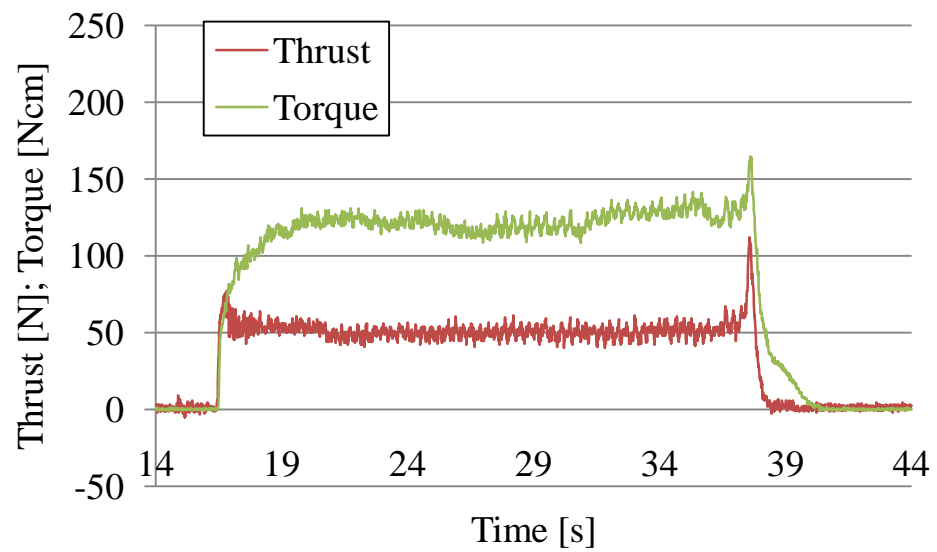
6.6.
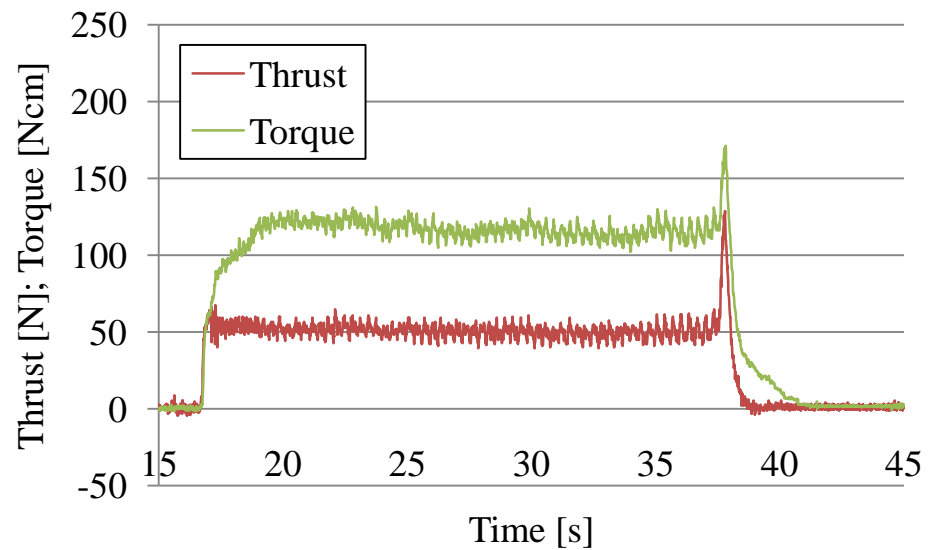
6.7.
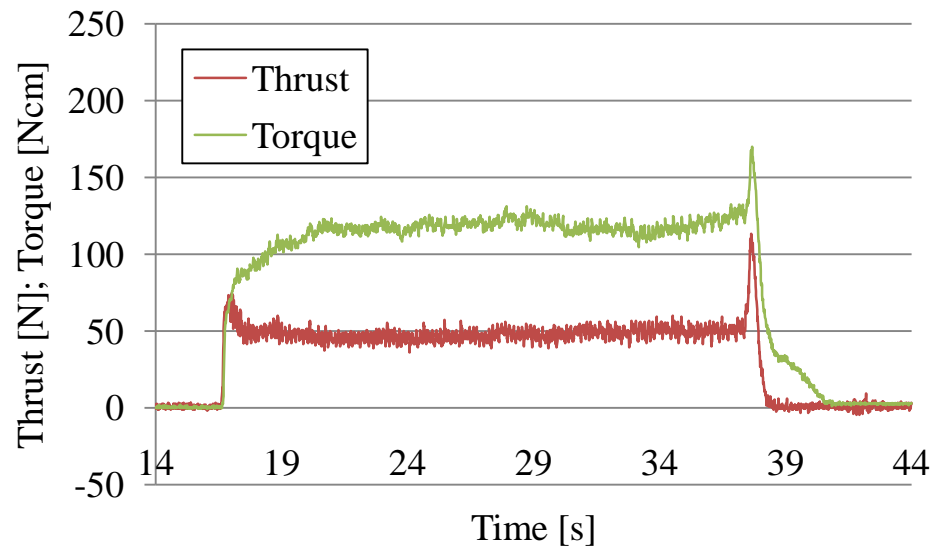
6.8.
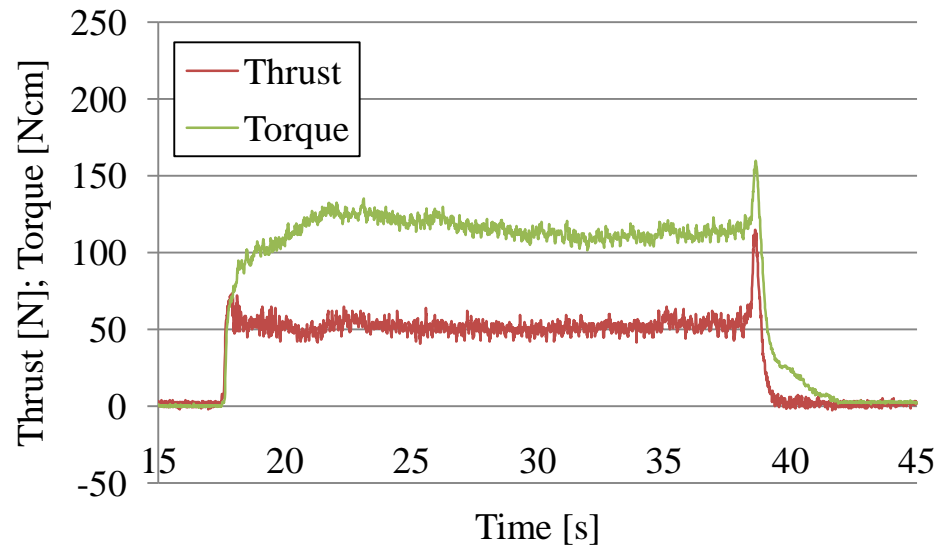
6.9.
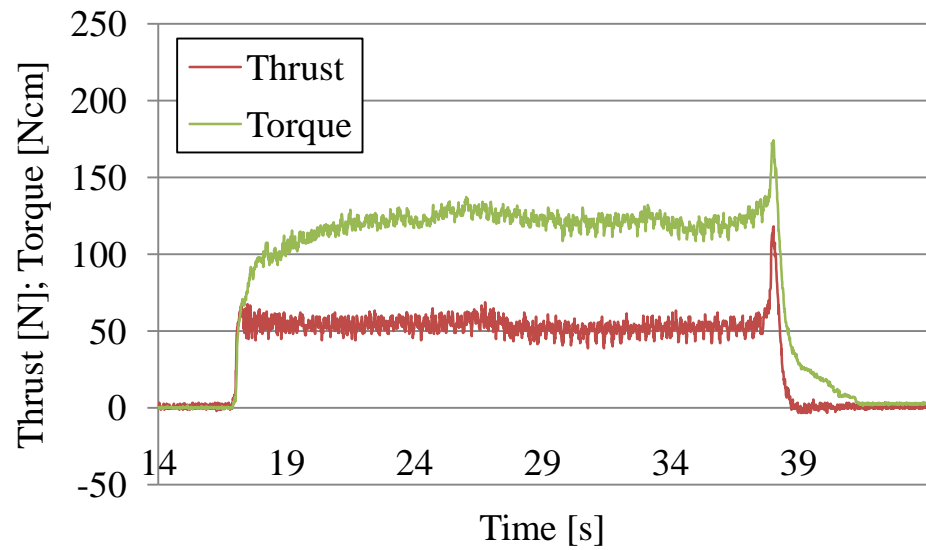
6.10.
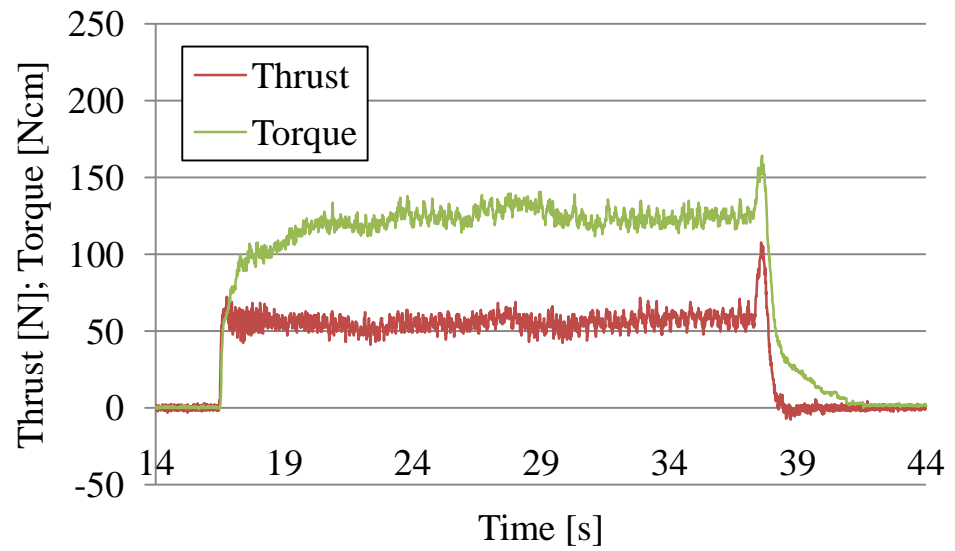
6.11.
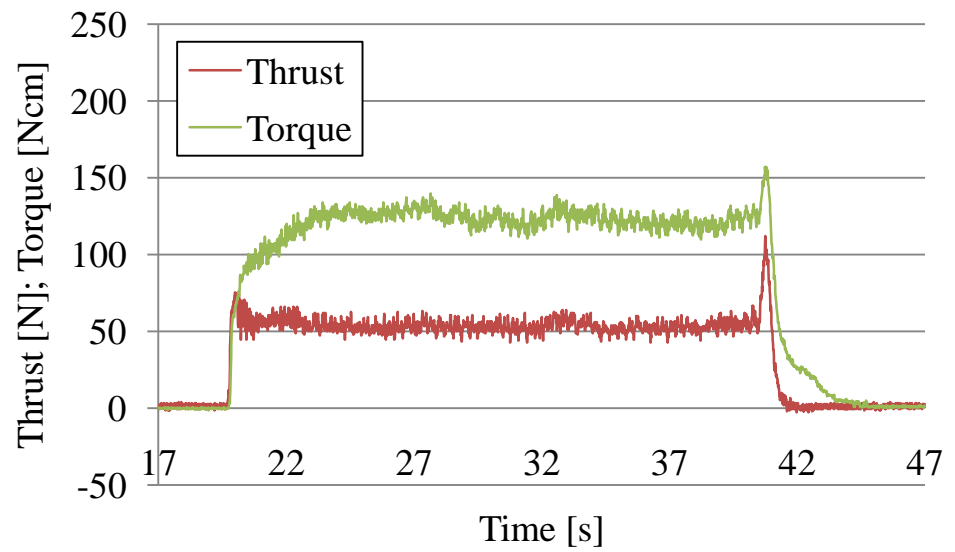
6.12.

6.13.
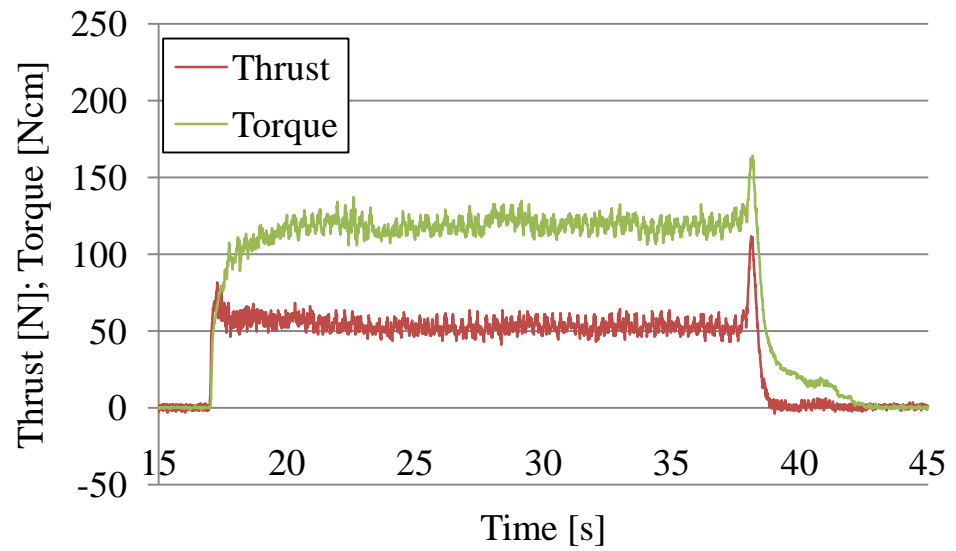
6.14.
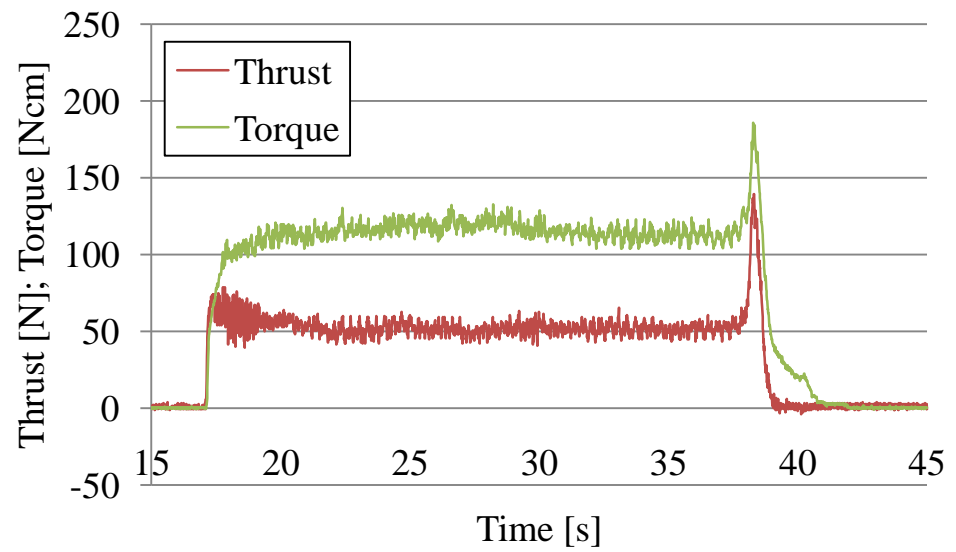
6.15.
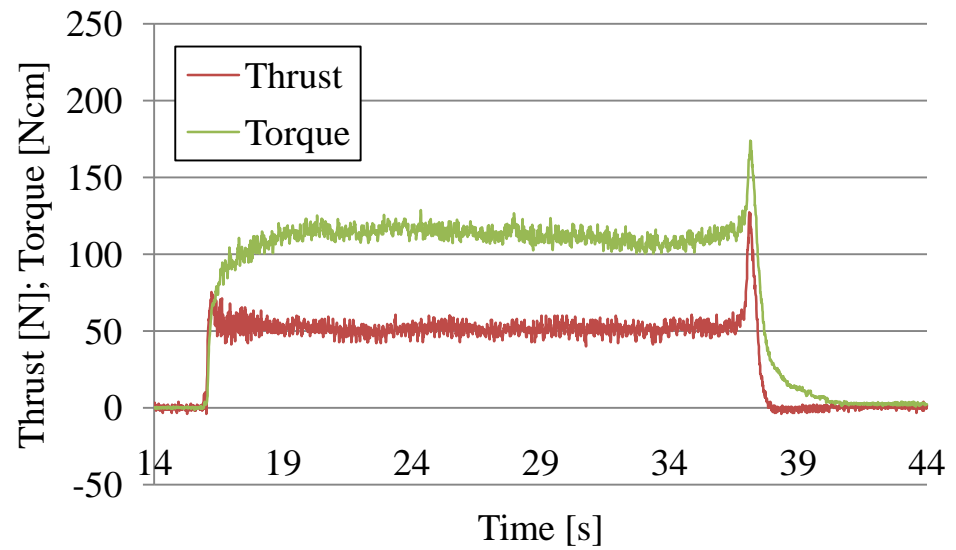
Appendix D - 1

Tab. D.1 – Reamer diameter measurements

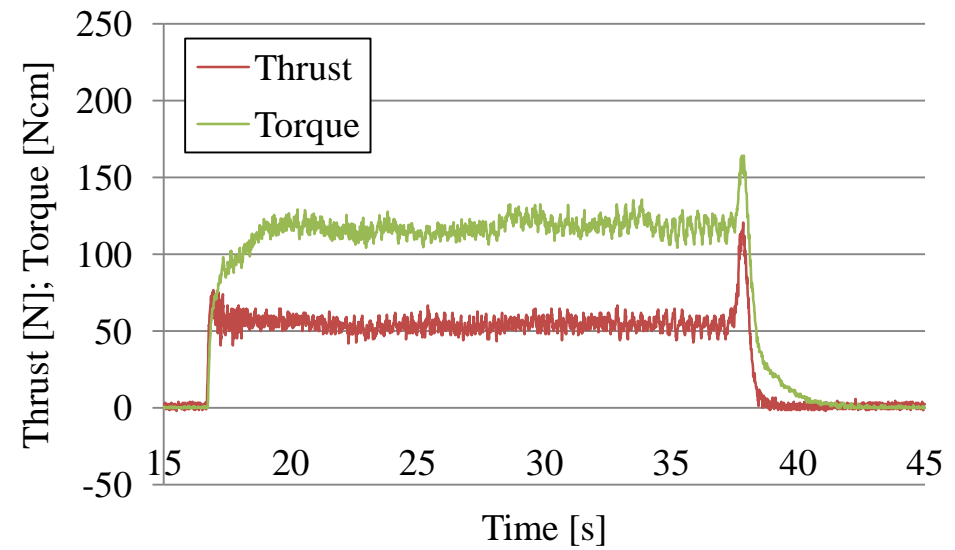| Meas.No.	R1		GB	R2		GB	R3		GB
	D1	D2	a	D1	D2	a	D1	D2	a
1	10.101	10.092	10.002	10.102	10.090	10.005	10.101	10.090	10.003
2	10.102	10.091	10.002	10.100	10.088	10.004	10.099	10.091	10.002
3	10.099	10.090	10.002	10.100	10.088	10.004	10.099	10.092	10.002
4	10.102	10.091	10.001	10.100	10.090	10.004	10.099	10.091	10.003
5	10.102	10.090	10.002	10.101	10.089	10.004	10.102	10.090	10.002
6	10.102	10.091	10.002	10.101	10.087	10.004	10.099	10.091	10.002
7	10.100	10.091	10.001	10.099	10.087	10.004	10.099	10.091	10.002
8	10.102	10.090	10.002	10.102	10.090	10.004	10.099	10.091	10.002
9	10.100	10.091	10.002	10.102	10.090	10.005	10.100	10.091	10.002
10	10.102	10.091	10.001	10.099	10.089	10.004	10.100	10.093	10.003
avg	10.101	10.091	10.002	10.101	10.089	10.004	10.100	10.091	10.002
std	0.0011	0.0006	0.0005	0.0012	0.0012	0.0004	0.0011	0.0009	0.0005

Reaming operation / 10 mm Gauge block (header spanning R1, R2, R3)

Meas.No.	R4		GB	R5		GB	R6		GB
	D1	D2	a	D1	D2	a	D1	D2	a
1	10.002	9.990	10.003	10.100	10.090	10.002	10.101	10.090	10.001
2	10.000	9.989	10.004	10.102	10.092	10.003	10.100	10.089	10.002
3	10.000	9.991	10.004	10.102	10.091	10.002	10.101	10.089	10.001
4	10.001	9.989	10.004	10.100	10.089	10.002	10.099	10.090	10.002
5	9.999	9.989	10.003	10.099	10.090	10.002	10.100	10.089	10.000
6	10.000	9.990	10.003	10.099	10.091	10.003	10.098	10.089	10.000
7	10.000	9.990	10.003	10.100	10.089	10.002	10.101	10.090	10.001
8	10.002	9.992	10.004	10.102	10.090	10.002	10.101	10.089	10.000
9	10.000	9.990	10.003	10.100	10.090	10.002	10.100	10.089	10.002
10	10.002	9.990	10.004	10.100	10.089	10.003	10.100	10.090	10.001
avg	10.001	9.990	10.004	10.100	10.090	10.002	10.100	10.089	10.001
std	0.0011	0.0009	0.0005	0.0012	0.0010	0.0005	0.0010	0.0005	0.0008

Reaming operation / 10 mm Gauge block (header spanning R4, R5, R6)